Performance Analysis of Diversity Combining Receivers Over Hoyt, $\eta - \mu$ and $\kappa - \mu$ Fading Channels

A

Thesis Submitted

in Partial Fulfillment of the Requirement

for the Degree of

DOCTOR OF PHILOSOPHY

By

RUPABAN SUBADAR

to the

DEPARTMENT OF ELECTRONICS AND COMMUNICATION ENGINEERING

INDIAN INSTITUTE OF TECHNOLOGY GUWAHATI

GUWAHATI - 781039, ASSAM, INDIA

January, 2011

Certificate

This is to certify that the thesis entitled "**Performance Analysis of Diversity Combining Receivers Over Hoyt, $\eta-\mu$ and $\kappa-\mu$ Fading Channels,**" submitted by **Rupaban Subadar** (07610210), a research scholar in the *Department of Electronics and Communication Engineering, Indian Institute of Technology Guwahati*, for the award of the degree of **Doctor of Philosophy**, is a record of an original research work carried out by him under my supervision and guidance. The thesis has fulfilled all requirements as per the regulations of the Institute and in my opinion has reached the standard needed for submission. The results embodied in this thesis have not been submitted to any other University or Institute for the award of any degree or diploma.

Dated:

Guwahati.

Pravas Ranjan Sahu

Associate Professor

Dept. of Electronics and Communication Engg.

Indian Institute of Technology Guwahati

Guwahati - 781039, Assam, India.

Acknowledgements

First and foremost, I feel it as a great privilege in expressing my deepest and most sincere gratitude to my supervisor Dr. Pravas Ranjan Sahu, for his excellent guidance. His kindness, dedication, friendly accessibility and attention to detail have been a great inspiration to me. My heartfelt thanks to my supervisor for the unlimited support and patience shown to me. I would particularly like to thank for all his help in patiently and carefully correcting all my manuscripts.

I am also very thankful to my doctoral committee members Prof. A. Mahanta, Dr. R. Bhattacharjee and Dr. A. Rajesh for sparing their precious time to evaluate the progress of my work. Their suggestions have been valuable. I would also like to thank other faculty members for their kind help carried out during my academic studies. I am grateful to all the members of the research and technical staff of the department without whose help I could not have completed this thesis. My special thanks to Mr. Sanjib Das, Mr. L. N. Sharma, Mr. Sidananda and Mrs. Jharna for maintaining an excellent computing facility and providing various resources useful for the research work.

Thanks go out to all my friends at ISPL Laboratory. They have always been around to provide useful suggestions, companionship and created a peaceful research environment.

My friends at IITG made my life joyful and were constant source of encouragement. Among my friends, I would like to extend my special thanks to Babusena, Ali, Himanshu, Dakua, Karthikeyan, Padam Priyal, Shyam and Utkal. My work in this remote place definitely would not be possible without their love and care that helped me to enjoy my new life in this IITG. Special thanks also go to Mr. Romesh Mishra, Mr. Bhaskar, Mrs. Amrita Ganguly, Mrs. G. Aruna and Mr. Mukesh Singh for their help during my stay.

I thank all my fellow research students for their cooperation. During these three years at IITG I have had several friends who have helped me in several ways, I would like to say a big thank you to all of them for their friendship and support.

My deepest gratitude goes to my family for their continuous love and support throughout my studies. The opportunities that they have given me and their unlimited sacrifices are the reasons where I am and what I have accomplished so far.

Finally, I believe this research experience will greatly benefit my career in the future.

Rupaban Subadar

This work is dedicated to

My parents,

Wife

and

Daughter Sruti

Abstract

Performance of diversity receivers over various slow and flat fading channels is analyzed. The classical PDF based approach has been followed to derive the performance measures of three basic diversity combiners namely Selection combining (SC), Equal gain combining (EGC) and Maximal ratio combining (MRC) receiver over Hoyt, $\eta-\mu$ and $\kappa-\mu$ fading channels. The analysis is carried out for both independent and correlated fading channels for various coherent and noncoherent modulation schemes. For independent diversity receivers the analysis has been carried out for arbitrary number of input branches. The effect of diversity order and fading parameters on performance measures is studied with the help of the numerical evaluation of the obtained expressions. For dual correlated receivers the analysis is carried out for arbitrary correlation, whereas for L diversity receivers it is for two most important practical correlation models, equal and exponential correlation. An equal correlation is observed in diversity reception by an array of three antennas placed on an equilateral triangle or by closely placed antennas (other than linear arrays) [1]. Exponential correlation is used to model the system when the receiving antennas are placed in a linear array [1, 2]. The effect of correlation on the receiver performance is studied for all the systems. To validate the derived expressions Monte carlo simulation is performed and also the obtained expressions are compared with the special case results available in the literature. For the expressions with infinite series the convergence is observed and where ever possible expressions for upper bound on truncation error have been provided.

Contents

List of Figures

List of Tables

List of Acronyms

ABER	Average bit error rate
ASER	Average symbol error rate
AWGN	Additive white Gaussian noise
ASEP	Average symbol error probability
AFD	Average fade duration
ASNR	Average **SNR**
ABEP	Average bit error probability
BER	Bit error rate
BDPSK	Binary differential phase-shift-keying
BFSK	Binary frequency-shift-keying
BPSK	Binary phase-shift-keying
CF	Characteristic function
CDF	Cumulative distribution function
CFSK	Coherent **FSK**
CPSK	Coherent **PSK**
DPSK	Differential phase-shift-keying
dB	Decibel
EGC	Equal gain combiner
FSK	Frequency-shift-keying

i. i. d.	Independent and identically distributed
LCR	Level crossing rate
LOS	Line of sight
L-**SC**	*L*- branch **SC**
L–**MRC**	*L*- branch **MRC**
L–**EGC**	*L*- branch **EGC**
ML	Maximum likelihood
MDPSK	M-ay **DPSK**
MPSK	M-ary **PSK**
MFSK	M-ary **FSK**
MQAM	M-ary **QAM**
MRC	Maximal ratio combiner
MGF	Moment generating function
MSK	Minimum-shift-keying
NCFSK	Non-coherent frequency-shift-keying
OSTBC	Orthogonal space time block coding
PDF	Probability density function
PSK	Phase-shift-keying
QAM	Quadrature amplitude modulation
RV	Random variable
RVs	Random variables
SEP	Symbol error probability
SC	Selection combiner
SNR	Signal-to-noise ratio

List of Symbols

$F_A\,(\cdot;\cdot;\cdot;\cdot)$	Appell hypergeometric function [4].
$\bar{(\cdot)}$	Statistical average
$\begin{pmatrix} a \\ n \end{pmatrix}$	Binomial coefficient.
$B(\cdot,\cdot)$	Beta function
${}_1F_1(\cdot,\cdot;\cdot)$	Confluent hypergeometric function [4].
$E[\cdot]$	Expectation operator.
$exp[\cdot]$	Exponential.
$\eta-\mu$	Eta-Mu fading channels.
$erf\,(\cdots)$	Error function.
$erfc\,(\cdots)$	Complementary error function.
$\forall$	For all.
${}_2F_1(\cdot,\cdot;\cdot;\cdot)$	Hypergeometric function.
$\Gamma(\cdot)$	Gamma function.
$G(\cdot)$	Meijers G-function.
$g(a,x)=\int\limits_0^x t^{a-1}e^{-t}dt$	Lower incomplete gamma function
$\Gamma(a,x)=\int\limits_x^\infty t^{a-1}e^{-t}dt$	Upper incomplete gamma function

${}_rF_s\left[\begin{matrix} a_1 & a_2 & \ldots & a_r & z \\ b_1 & b_2 & \ldots & b_s & \end{matrix}\right] = \sum_{n=0}^{\infty} \frac{(a_1)_n(a_2)_n\ldots(a_r)_n}{(b_1)_n(b_2)_n\ldots(b_s)_n} z^n$	Generalized hypergeometric function.
γ_{sc}	Output SNR of SC receiver.
γ_{egc}	Output SNR of EGC receiver.
γ_{mrc}	Output SNR of MRC receiver.
$I_0(\cdot)$	Modified Bessel function of first kind order zero.
$I_v(\cdot)$	Modified Bessel function of first kind order v.
$\in$	Set membership.
$\Im\{\cdot\}$	Operator of imaginary part.
$\kappa-\mu$	Kappa-Mu fading channels.
$K_v(\cdot)$	v^{th} order modified Bessel function of the second kind.
$\ln(\cdot)$	Natural log.
$\log_{10}(\cdot)$	Logarithm with base 10.
$\lvert\cdot\rvert$	Absolute value or modulus.
$\mathrm{Max}(\cdot,\cdot,\ldots,\cdot)$	Maximum.
$Q_M[\cdot]$	Marcum Q function.
$\prod_{i=1}^{n}$	Product.
$(x)_n$	Pochhammer's symbol [5, (6.1.22)].
$Q(\cdot)$	Q function
$\Re\{\cdot\}$	Real-part operator.
$\sum_{i=0}^{n}$	Summation.

$\sum_{k_1,k_2,\ldots,k_n=0}^{\infty}$	$\sum_{k_1=0}^{\infty}\sum_{k_2=0}^{\infty}\cdots\sum_{k_n=0}^{\infty}$.
$\sum_{k_i\|_1^n=0}^{\infty}$	$\sum_{k_1=0}^{\infty}\sum_{k_2=0}^{\infty}\cdots\sum_{k_n=0}^{\infty}$.
t	Time
$var[\cdot]$	Variance.

Chapter 1

Introduction

Propagation of a signal in mobile wireless channels results in a received signal with time varying strength, a phenomena known as fading. It occurs as multiple copies of the transmitted signal travel through different paths as a result of being scattered and redirected several times from various man-made and natural objects before getting combined with different attenuations and unequal propagation delays, at the destination. This effect is also attributed as the time-varying impulse response of the wireless channel. The time varying signal at a desired receiver affects its various performance measures among which signal-to-noise ratio (SNR) and average bit error rate (ABER) are prominent. The penalty in receiver performance varies with the severity of fading which may change with the location of the mobile and may be highly unpredictable due to irregular environment structure.

A known effective counter measure which can alter derogatory effects of fading on the receiver performance is the Diversity Combining. Multiple copies of non-identically, attenuated and time delayed received signals, when weighted suitably and equiphased before combining is likely to decay the rate of variation and hence would be able to defy the fading effects. In principle, diversity combining can be explained as the effect of reducing the probability of error p of a system when a single copy of the signal is received, to p^L when L independent fading copies of the same signal are present. Certainly, the probability of error reduces significantly since $p \leq 1$ [2].

1.1 Diversity Combining

Diversity combining is a well known approach to mitigate the effect of fading in wireless channels. A diversity combining operation improves the receiver performance by processing preferably a number of statistically independent copies of the same information-bearing signal over two or more fading channels and combining these multiple replicas efficiently. The intuition behind this concept is to exploit the low probability of concurrence of deep fades in all the diversity channels at the same time, hence reduce the probability of error or outage. The possible ways by which independent fading signals can be obtained are enumerated below.

1. Spatial Diversity: By receiving signals from a source by different antennas placed sufficiently apart statistically independent fading signals can be received [2, 6, 7]. The minimum antenna spacing for a mobile unit can be at least half wavelength [6]. For a base station, which is stationary with elevated antennas, the required antenna spacing to receive independent faded signals can be much wider than the mobile unit antenna spacings [6]. An experimental value of 30 to 50 wavelength for stationary receivers can restrict the correlation below 0.3 between faded signals is also reported in [7].

2. Frequency Diversity: Signal may be transmitted through different modulation frequencies which are sufficiently apart to induce independent fading channels. The minimum frequency separation should be at least the coherence bandwidth of the channel [8, 9].

3. Time Diversity: The same information signal transmitted at different time intervals can be received as independent fading signals. The minimum time interval should exceed the coherence time of the channel [8, 9].

4. Polarization Diversity: Independent fading path may also be realized by simultaneous horizontal and vertical polarizations transmission of signals [8,9].

5. Angle Diversity: Angle of arrival in case of beam forming antennas can also be used to generates independent fading channels [8,9].

6. Multipath Diversity: By resolving multipath components at different delays by using direct sequence spread spectrum signaling along with a RAKE receiver [6,8,9].

1.2 Multipath Fading Models

The multipath fading also known as small scale fading occurs due to multipath propagation of the signal in a wireless channel [2,6,10]. Depending on the signal and channel characteristics the fading can be modeled as flat or frequency non-selective, frequency selective, fast and slow fadings. The frequency selectivity is the characteristic of the multipath time delay spread whereas fast or slow fading is related to the Doppler spread of the channel.

It is difficult to have an accurate mathematical model of fading because of the complexity involved. However, in last few decades, extensive work has been carried out to model this complicated effects statistically and as a result a number of mathematical models have been evolved for fading channels.

In different environments multipath fading can be modeled with different statistical distributions. It is as described below.

Rayleigh

Rayleigh distribution is used to model the multipath fading when independent scatterers are sufficiently large with approximately identical energy and no line of sight component is received by the receiver. In this case the probability density function (PDF) of channel fading amplitude α can be given as [2]

$$p_\alpha(\alpha) = \frac{2\alpha}{\Omega}\exp(-\frac{\alpha^2}{\Omega}), \quad \alpha \geq 0, \tag{1.1}$$

where $\Omega = E\alpha^2$ and $E(\cdot)$ is the expectation operator. A Rayleigh RV α can be modeled as $\alpha = |Z| = |X + jY|$, where X and Y are independent Gaussian RVs with zero mean and equal variances.

Nakagami Fading

1. *Nakagami-m:* The Nakagami-m distribution often gives the best fit to land-mobile and indoor-mobile multipath propagation, as well as scintillation of ionospheric radio links [2]. Also, the Nakagami-m distribution is widely used to model the urban environment and the PDF of the envelop is given by [2]

$$p_\alpha(\alpha) = \frac{2m^m\alpha^{2m-1}}{\Omega^m\Gamma(m)}\exp\left(-\frac{m\alpha^2}{\Omega}\right), \quad \alpha \geq 0, \tag{1.2}$$

   where $m \geq 0.5$ is the parameter which determines the severity of fading. For $m = 1$, the PDF of Nakagami-m distribution simplifies to Rayleigh distribution and for $m = 0.5$, it becomes the one-sided Gaussian distribution.

2. *Nakagami-q (Hoyt):* The Nakagami-q distribution [11] or the Hoyt distribution is commonly observed in satellite links subject to strong ionospheric scintillation and in a heavily shadowed environments [2,12]. It includes the Rayleigh ($q = 1$) and one sided Gaussian ($q = 0$) as special cases. The PDF can be given as [2]

$$p_\alpha(\alpha) = \frac{(1+q^2)\alpha}{q\Omega}\exp\left(-\frac{(1+q^2)^2\alpha^2}{4q^2\Omega}\right) I_0\left(\frac{(1-q^4)\alpha^2}{4q^2\Omega}\right), \quad \alpha \geq 0, \tag{1.3}$$

   where q is the fading parameter and $I_0(\cdot)$ is the modified Bessel function of first kind and zero order. A useful complex Gaussian modeling of Hoyt RV is given in [13] and is reproduced in Section A.1 in Appendix.

3. *Nakagami-n (Rice):* The Nakagami-n distribution is also known as the Rice distribution. It is used to model propagation paths consisting of one strong direct line-of-sight (LOS) component and many multipath components. The PDF of α is given as [2]

$$p_{\alpha}(\alpha) = \frac{2(1+n^2)e^{-n^2}\alpha}{\Omega}\exp\left(-\frac{(1+n^2)\alpha^2}{\Omega}\right) I_0\left(2n\alpha\sqrt{\frac{1+n^2}{\Omega}}\right), \quad \alpha \geq 0, \tag{1.4}$$

where n is the rice fading parameter. A Rice RV α can be modeled as $\alpha = |Z| = |X + jY|$, where X and Y are independent Gaussian RVs with non-zero mean μ and variances σ^2.

Weibull Fading

The Weibull distribution is another mathematical description of a probability model for characterizing amplitude fading in a multipath environment associated with mobile radio systems operating in the 800/900 MHz frequency range. The Weibull PDF is given by [2]

$$p_{\alpha}(\alpha) = c\left(\frac{\Gamma\left(1+\frac{2}{c}\right)}{\Omega}\right)^{c/2}\alpha^{c-1}\exp\left[-\left(\frac{\alpha^2}{\Omega}\Gamma\left(1+\frac{2}{c}\right)\right)^{c/2}\right], \quad \alpha \geq 0, \tag{1.5}$$

where c is the Weibull fading parameter.

$\eta - \mu$ Fading

The η-μ fading model is suitable for modeling small scale fading channels without LOS components [14], [15]. Non-homogeneous physical characteristics of the surroundings is taken into account in the mathematical modeling of this channel. It best fits to the practical scenario and experimental data. Commonly used fading models such as Rayleigh, Hoyt, Nakagami-m etc., can be realized as special cases of this channel model [14]. The PDF of the η-μ distribution can be given as [14]

$$p_{\alpha_l}(\alpha_l) = \frac{4\sqrt{\pi}\mu^{\mu+\frac{1}{2}}h^{\mu}\alpha_l^{2\mu}}{\Gamma(\mu)H^{\mu-\frac{1}{2}}\Omega_l^{\mu+\frac{1}{2}}}e^{-\frac{2\mu h}{\Omega_l}\alpha_l^2}I_{\mu-\frac{1}{2}}\left[\frac{2\mu H}{\Omega_l}\alpha_l^2\right], \tag{1.6}$$

where the parameters h and H are function of η. The parameter μ (>0) is defined as

$$\mu = \frac{E^2(\alpha_l^2)}{2V(\alpha_l^2)}\left[1+\left(\frac{H}{h}\right)^2\right], \tag{1.7}$$

where $V(\cdot)$ represents the variance operator. There are two formats available for η-μ fading channels, which represent two distinct physical models. In Format1, $0<\eta<\infty$ is the scattered-wave power ratio between the in-phase and quadrature phase components of each cluster of multipath. In such case $h=\frac{2+\eta^{-1}+\eta}{4}$ and $H=\frac{\eta^{-1}-\eta}{4}$. In Format2, $-1<\eta<1$ is the correlation coefficient between the scattered-wave in-phase and quadrature phase components of each cluster of multipath. In such a case, $h=\frac{1}{1-\eta^2}$ and $H=\frac{\eta}{1-\eta^2}$. However, mathematically, one format is related to the another by the formula, $\eta_{Format2}=\frac{1-\eta_{Format1}}{1+\eta_{Format1}}$.

$\kappa-\mu$ Fading

The κ-μ models have been found to be suitable for modeling small scale fading in mobile radio channels with LOS components [14], [16]. Non-homogeneous physical modeling has been considered in the mathematical modeling of this channel, hence best fits to the practical scenario and experimental data. Also, commonly used fading models Rayleigh, Nakagami-m, Nakagami-n (Rice) etc., can be realized as special cases of this fading model [14]. The PDF of the κ-μ distribution is given as [14]

$$p_{\alpha_l}(\alpha_l) = \frac{2\mu(1+\kappa)^{\frac{\mu+1}{2}}\alpha_l^{\mu}e^{-\frac{\mu(1+\kappa)}{\Omega_l}\alpha_l^2}}{\kappa^{\frac{\mu-1}{2}}\exp(\mu\kappa)\Omega_l^{\frac{\mu+1}{2}}} I_{\mu-1}\left[2\mu\sqrt{\frac{\kappa(1+\kappa)}{\Omega_l}}\alpha_l\right], \tag{1.8}$$

where the parameter κ is defined as the ratio between the total power of the dominant component and the total power of the scattered waves and the parameter $\mu=\frac{1}{V(\alpha_l^2)}\frac{1+2\kappa}{(1+\kappa)^2}$ denotes the number of multipath clusters and $I_v(\cdot)$ is the modified Bessel function of the first kind and v^{th} order.

1.3 Literature Survey

Performance of diversity receivers over independent Hoyt fading channels are discussed in [17–26]. ABER performance of EGC receivers are analyzed in [17] and [18], where ABER expressions for coherent and noncoherent modulations are presented. Binary modulations are employed in [17] using the PDF based approach whereas in [18] analysis is for MFSK modulation. ABER expressions, for coherent and non-coherent modulations for a conventional receiver (i.e. without diversity combining) are derived in [19]. ABER performance of a MRC receiver for continuous phase modulation scheme is presented in [20] and exact ASEP expressions for MPSK and MQAM modulation schemes are obtained in [21]. A direct approach is used in [20] whereas [21] uses the MGF based approach. Further, the obtained final ABER expression in [20] is in the form of an integral with finite limits. Channel capacity of MRC receivers over Hoyt fading channels are analyzed in [22] and [23]. Error performance of orthogonal space time block coding (OSTBC) schemes, theoretically equivalent to MRC, are studied for M-ary modulations in [24–26]. Average BER expression is derived in [24] and in [25] capacity analysis is presented besides ABER performance. In [26], exact closed-form symbol error rate expressions for coherent and noncoherent M-ary modulations are presented.

The performance of a SC receiver is analyzed for Rayleigh, Nakagami and Weibull fading channels using either the PDF or the MGF based approaches for both independent and correlated fading cases in [27–31]. Closed-form expression for the average signal-to-noise ratio (ASNR) for a dual-SC receiver over correlated Nakagami-m fading channels is presented in [27] using the MGF based approach. A number of performance measures such as PDF, CDF, moments, outage and ABER for coherent and non-coherent M-ary modulations of a dual-SC receiver over correlated Weibull fading channels are obtained in [28]. In [29], outage and ABER performance over equally correlated Nakagami-m fading channels is derived whereas an analysis for a three branch SC receiver over correlated Rayleigh fading channels is presented in [30]. In [31], outage and ABER performance of a dual-SC receiver over correlated Nakagami-m fading channels are presented for non-identical fading parameters.

For dual correlated Hoyt fading channels, the second order statistical properties such as level crossing rate (LCR) and average fade duration (AFD) are derived for different diversity systems in [32–34]. The outage probability performance of a dual-SC receiver over correlated Hoyt fading channels is studied in [35] and for MRC and EGC receivers are presented in [36]. Analysis of diversity combining receivers with arbitrary number of branches over correlated fading channels is challenging and may not be always possible as because obtaining an expression for the joint PDF of multivariate faded signals in a suitable form is not easy. Thus, three correlated models of practical importance namely equal or constant correlation, circular correlation and exponential correlation have been suggested in [1,2,37] which are also convenient from the analysis point of view. Performance analysis of MRC receiver for constant and exponential correlations over Nakagami-m fading channels is presented in [1]. For equal and circular correlation models, PDF of the combiner output SNR, outage, ABER performance for binary coherent modulations and channel capacity measures are given in [37]. Recently, [38] also presented closed-form expressions for ASER of a dual-MRC receiver over correlated Hoyt fading channels for a number of coherent and non-coherent modulations using a novel decorrelation transformation technique.

For independent $\eta-\mu$ and $\kappa-\mu$ fading channels, performance studies are presented in [39–47]. Outage and ASEP performance of a multi-branch MRC receiver for coherent and noncoherent digital modulation schemes over $\kappa-\mu$ fading channels are given in [39] whereas ASEP expressions only for noncoherent modulations are presented in [40]. In [41], closed-form expressions for the ASEP of a multi-branch MRC are presented for $\eta-\mu$ fading channels for both coherent and non-coherent modulations including asymptotic expressions. LCR and AFD over $\eta-\mu$ fading channels are presented in [42–44] of which [42] addresses a conventional receiver. LCR and AFD for SC, EGC and MRC receivers are presented in [43] whereas it is only for MRC and EGC receivers in [44] which further provides an expression for phase crossing rate. For a multi-branch EGC receiver, outage and ABEP for differential binary coherent modulations is derived in [45]. Performance of receivers in $\eta-\mu$ and $\kappa-\mu$ channels without employing diversity are treated in [46, 47], using the MGF based approach. In [46], ASER expressions for QAM modulation is presented and in [47] it is given for the BPSK modulation. Recently, [48] also presented closed-form expressions for outage probability of a MRC receiver over $\eta-\mu$ fading channels for a number of coherent and non-coherent modulations.

1.4 Motivation

In the literature survey, we noticed that for independent Hoyt fading channels, performance studies are available for MRC and EGC receivers, but the SC receiver has not received enough attention. For correlated Hoyt fading channels, analysis is available only for outage probability of dual diversity receivers [35, 36, 38]. For $\eta-\mu$ and $\kappa-\mu$ fading channels, performance analysis is known for MRC and EGC receivers with arbitrary number of independent branches but an analysis is not available for SC receiver. To the best of our knowledge, performance analysis of diversity receivers over correlated $\eta-\mu$ or $\kappa-\mu$ channels are not reported in the literature.

1.5 Problem Formulation

Based on the discussion presented in the previous section, we feel that analysis of diversity receivers over correlated Hoyt fading channels for arbitrary number of branches can be a potential area of research. Further, analysis of SC receivers is due for independent and correlated Hoyt fading channels. For $\eta-\mu$ and $\kappa-\mu$ fading channels, analysis of SC receiver for independent channels needs to be investigated. Again, analysis for all diversity receivers for correlated $\eta-\mu$ and $\kappa-\mu$ channels can be of interest to the research community. Hence, in this report, we consider the following problems for analysis, as stated below.

1. For independent and correlated Hoyt fading channels, performance analysis of MRC, EGC

and SC receiver for arbitrary number of branches.

2. For $\eta-\mu$ and $\kappa-\mu$ fading channels,

   (a) performance of SC receiver over both independent and correlated fading channels with arbitrary number of branches.

   (b) performance of MRC and EGC receiver over correlated fading channels, with arbitrary number of branches.

For the above stated problem, we focus on the mathematical analysis of the diversity receivers. To be specific we stress in obtaining expressions for various performance measures of these receivers, mathematically in the best possible compact form.

1.6 Thesis Contributions

The important contributions of the thesis are stated below:

1. For Hoyt fading channels:

   (a) L-SC and L-MRC receivers are analyzed over independent channels. Mathematical expressions for average output SNR, outage probability and ASER are obtained.

   (b) Mathematical expressions for outage probability and ABER for are obtained for dual correlated SC, MRC and EGC receivers.

   (c) For the MRC receiver, the analysis in (b) is extended to arbitrary number of branches with equal and exponential correlation models.

2. For $\eta-\mu$ and $\kappa-\mu$ fading channels:

   (a) Analytical expressions for average output SNR and ABER have been obtained for a L-SC receiver with independent branches.

(b) Outage probability of L-SC receiver has been derived for $\eta - \mu$ fading channels with exponential correlation among fading branches.

(c) For L-MRC receiver, mathematical expressions are derived for average output SNR, outage probability, and ASER, for equally correlated $\eta - \mu$ channels.

1.7 Organization

There are six chapters in the thesis. Brief description about the contents of each chapter is given below.

Chapter 2 gives an overview of the diversity combining systems. It describes the system model, apprises receiver performance measures and analysis techniques of diversity combiners, and provides definitions of some useful notations to be used in subsequent chapters.

Chapter 3 presents performance analysis of diversity receivers over Hoyt fading channels. It is divided into two sections under the headings 'Independent' and 'Correlated' channels. In the 'Independent' section, the performance analysis of SC and MRC receiver with arbitrary diversity order are presented. In 'Correlated' section performance of dual correlated SC, EGC and MRC receivers and L correlated MRC receiver are obtained followed by numerical and simulation results are presented.

Chapter 4 presents performance of the diversity receiver over $\eta - \mu$ fading channels. The chapter is divided in two sections under the headings 'Independent' and 'Correlated' channels. Performance of L-SC receiver is presented in the 'Independent' section. In 'Correlated' section, the performance analysis of L-MRC receiver for equal correlation and L-SC for exponential correlation model is presented followed by numerical and simulation results and discussion.

Chapter 5 presents performance of L-SC receiver over independent $\kappa - \mu$ fading channels. In the result section, the effect of diversity order and the fading parameter on system performance have been discussed in details.

Chapter 6 presents the conclusion of the thesis with a brief summary of the work presented. Besides, it introduces some research problems for future work.

Chapter 2

Performance Analysis Overview

Analytical ABER performance analysis approach of a diversity combining receiver depends primarily on three important factors such as the combining technique, the fading model and the modulation scheme. For each diversity combining type the analytical approach can be different since principles of operation of combiners are different. The approach changes with fading channel types since a particular fading model may impose some restriction on the analysis. For a given fading model, approaches may not be same for all parameter values of the model too. For example, for the Nakagami-m fading model, analytical approaches may be different for integer and real values of m. For independent and correlated fading channels, analyses are different which is relatively less complex for independent fading compared to correlated case. The approach also depends on the order of diversity and the complexity of analysis goes up with the order. In literature, there are many presentations which analyze only for the dual diversity receivers as because an analysis for arbitrary order of diversity involves huge complexity. The approach is different for coherent and non coherent modulations.

There are some known approaches used in the literature for the ABER performance analysis of diversity receivers such as the PDF based approach, the characteristic function (CF) based approach and the moment generating function (MGF) based approach. The PDF based approach is the straightforward one and can be applied if the PDF of the combiner output SNR is known [2]. The MGF and CF based approaches are used when the either the MGF or CF of the combiner output SNR is known. The Gil Palaez Lemma based approach, a CF based approach, is applicable to coherent receivers only [49]. Another CF based approach is available using Parseval's theorem can be applied for both coherent and non coherent modulations as well as independent and correlated channels [3]. MGF based approach can be applied to all types of systems and modulation schemes and requires the MGF of the combiner output SNR and parameters of modulation schemes [2]. This approach has been widely applied in the ABER analysis of diversity communication systems.

2.1 System Model

A diversity combining receiver as shown in the Figure 2.1 is considered for analysis. The combiner may be either a SC or EGC or a MRC combiner with L receiving antennas. The antenna spacing although should be sufficient enough to receive independent fading signals in some situations it is close enough to violate the independent assumption. Under mutipath propagation of a modulated signal $s(t)$, the received faded signals in an additive white Gaussian (AWGN) channel are $\{r_l(t)\}_{l=1}^{L}$. The combiner can be a predetection or a post detection type [6]. The combiner is followed by a detector which employs detection rules as per the modulation scheme used in $s(t)$. A standard operation in a receiver assumes that a demodulated signal should be fed to the detector [8, 9]. To meet this requirement it is assumed that the demodulation operation is performed in the combiner itself.

Let the the energy of the signal $s(t)$ over a symbol or bit duration T_s (or T_b) be E_s (orE_b) which can be chosen depending on whether the modulation scheme is a M-ary or binary. We Assume a slow and flat fading channel throughout this presentation. The received complex baseband signal at the l^{th} received antenna of the combiner can be expressed as

$$r_l(t) = \alpha_l e^{j\varphi_l} s(t) + n_l(t), \qquad 0 \le t \le T_s, \tag{2.1}$$

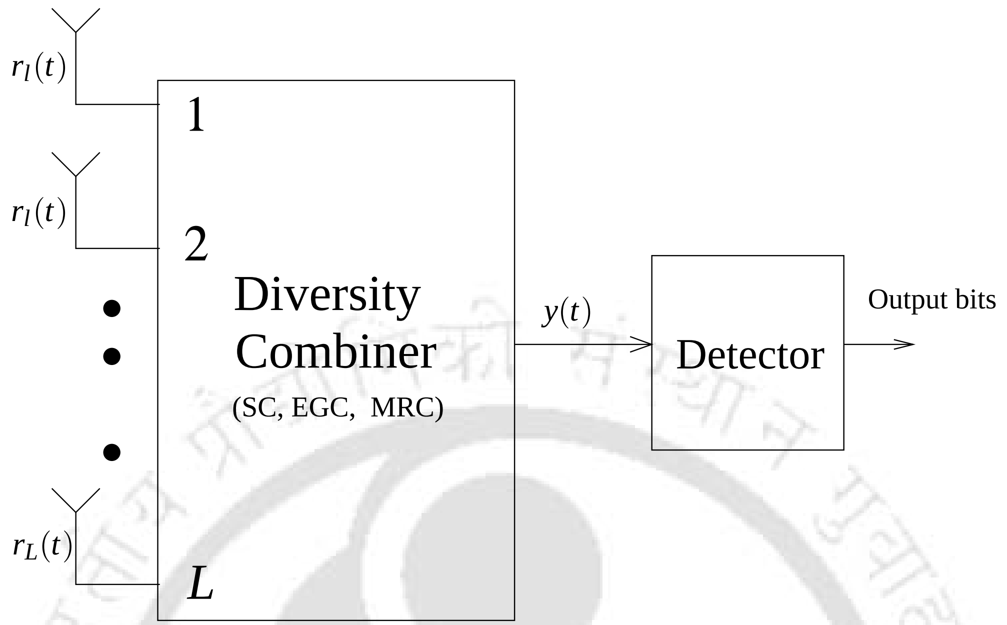

Figure 2.1: Block diagram of a diversity receiver system

where α_l is the fading amplitude, φ_l is the phase, $n_l(t)$ is the complex Gaussian noise with zero mean and two sided power spectral density $2N_0$. The statistical distribution of the α_l and phase φ_l depends on the nature of the radio propagation environment. Some distributions such as Rayleigh, Nakagami, Weibull etc., which are observed in wireless channels are presented in Section 1.2. From Equation 2.1 the instantaneous and average value of the received SNR at the l^{th} antenna can be given as $\gamma_l = \frac{\alpha_l^2 E_b}{N_0}$ and $\bar{\gamma}_l = E[\gamma_l] = \frac{E_b}{N_0} E[\alpha_l^2]$, respectively.

The output of the combiner $y(t)$, can be mathematically expressed from the principle of operation of the combiner. For linear diversity combining, a general expression for $y(t)$ can be given as [7]

$$y(t) = a_1 r_1(t) + a_2 r_2(t) + \ldots + a_L r_L(t) = \sum_{l=1}^{L} a_l r_l(t), \tag{2.2}$$

where the combining coefficients a_ls, assume values corresponding to the combining rule employed. Below we discuss basic combining techniques in detail.

2.1.1 Selection Combining

For a SC combiner, a_ls in Equation 2.2 can be given as

$$a_l = \begin{cases} 1, \text{for}\, l = k \\ 0, \text{for}\, l \neq k \end{cases}. \tag{2.3}$$

Thus, at any point of time only one signal out of L available signals is selected for processing which is the the signal with the highest SNR, among all L. From the implementation point of view this is the simplest of all diversity combiners. The block diagram is shown in Figure. 2.2. Assuming identical noise power in all the received branches, the output of the combiner can be given by

$$y(t) = \alpha e^{j\theta} s(t) + z(t), \tag{2.4}$$

where $\alpha = \max\{\alpha_1, \alpha_2, \ldots, \alpha_L\}$. The combiner output SNR can be given as

$$\gamma = \frac{\alpha^2 E_b}{N_0} = \max\{\gamma_1, \gamma_2, \ldots, \gamma_L\}. \tag{2.5}$$

With uncorrelated fading at the input receiving antennas, the cumulative distribution function (CDF) of the combiner output $P_\gamma(\gamma_{sc})$ can be expressed as

$$P_\gamma(\gamma_{sc}) = Pr\{\gamma < \gamma_{sc}\} = \prod_{l=1}^{L} P_{\gamma_l}(\gamma_{sc}), \tag{2.6}$$

where $P_{\gamma_l}(\gamma_{sc})$ is the CDF of the received signal at the l^{th} antenna. For i. i. d. receiving branches, the joint CDF can be given as $P_\gamma(\gamma_{sc}) = [P_{\gamma_1}(\gamma_{sc})]^L$. Thus, the PDF can be given as

$$f_{\gamma_{sc}}(\gamma_{sc}) = L f_{\gamma_1}(\gamma_l)[P_{\gamma_1}(\gamma_{sc})]^{L-1}. \tag{2.7}$$

Another version of SC combiner is the Switching and Stay combining. In this scheme once a branch is selected it remains connected to the output for demodulation processing until its SNR falls below a predefined threshold. The performance observed for this combiner is close to that of the selection combiner where as the required switching among the branches reduces significantly compared to that of SC.

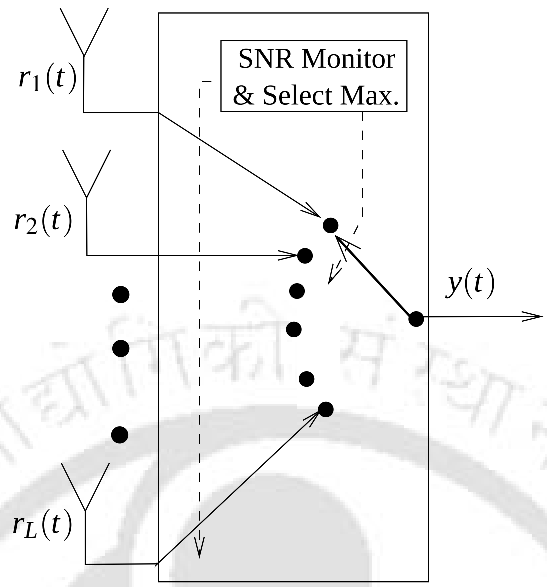

Figure 2.2: Block diagram showing principle of operation of the Selection Combiner

2.1.2 Maximal Ratio Combining

In MRC combiner all the received signals are co-phased and then multiplied by a weight factor proportional to the branch SNR before summing up to form the combiner output. A block diagram of the MRC combiner is shown in Figure 2.3. The combiner output is given by $y(t) = \sum_{i=1}^{L} \alpha_i r_i(t)$. Weights to be the conjugate of channel gain [must be estimated]

$$\begin{aligned} y(t) &= \sum_{i=1}^{L} \alpha_i e^{-j\theta_i} r_i(t) = \sum_{i=1}^{L} \alpha_i e^{-j\theta_i} [\alpha_i e^{j\theta_i} s(t) + n_i(t)] \\ &= \left(\sum_{i=1}^{L} \alpha_i^2 \right) s(t) + \sum_{i=1}^{L} \alpha_i e^{-j\theta_i} n_i(t) \end{aligned} \tag{2.8}$$

The SNR of the combined signal is

$$\gamma = \frac{\sum_{i=1}^{L} \alpha_i^2 E_b}{N_0} = \sum_{i=1}^{L} \gamma_i \tag{2.9}$$

Maximal ratio combiner provides optimum performance and needs all channel fading information at the receiver. Thus, complexity of a communication receiver with MRC combining is high.

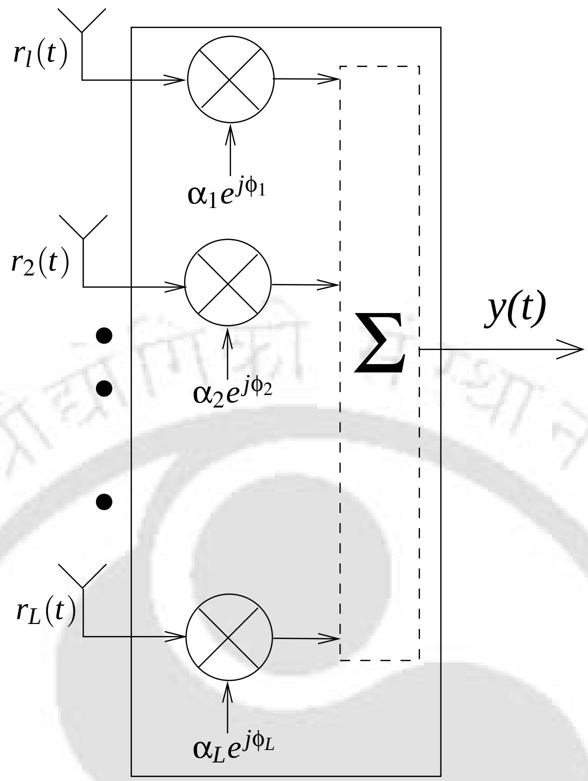

Figure 2.3: Block diagram showing principle of operation of a Maximal Ratio combiner

2.1.3 Equal Gain Combining

In an EGC combiner, received signals from all L receiving antennas are co-phased and multiplied by an unit weight factor before being added together to form the output signal of the combiner. For an EGC combiner, the combining coefficients a_ls in Equation 2.2 can be given as

$$a_l = 1, \forall l = 1, 2, \ldots, L. \tag{2.10}$$

The combiner output signal can be mathematically expressed as

$$y(t) = \sum_{i=1}^{L} e^{-j\theta_i} r_i(t) = \left(\sum_{i=1}^{L} \alpha_i\right) s(t) + \sum_{i=1}^{L} e^{-j\theta_i} n_i(t). \tag{2.11}$$

The SNR at the EGC output can be given as

$$\gamma = \left(\sum_{i=1}^{L} \alpha_i\right)^2 \frac{E_b}{LN_0}. \tag{2.12}$$

The performance of a EGC is very close to MRC, whereas the complexity is less. So in the communication system EGC is widely used.

The combiner output is fed as input to a detector to decide which one of the symbol from the transmitter signal set was transmitted. Thus, the complexity of the detector depends on the modulation scheme used. For example, for a BPSK modulation scheme which has only two symbols in its signal set, the detector has to decide whether a '$1'$' or '$0'$' was transmitted. Hence, the detection rule is the threshold value in the middle of the signal constellation for ML detector [2].

2.2 Correlated Fading Models

Diversity receivers having independent fading channels as input give the best performance. However, in practical scenario obtaining an independent fading channels are difficult due to space constrain of mobile portable devices [1,2]. The analysis for L correlated diversity receivers is not handy as an expression for the joint PDF of multivariate fading RVs is not possible to obtain in each case. Hence, the analysis is carried out for two useful correlation models namely equal correlation and exponential correlation. Below these two correlation models are described.

Equal Correlation

Equal or constant correlation model is one in which the correlation coefficient is defined as [1,2]

$$\rho_{i,j} = \rho, \forall i \neq j, 1 \leq i, j \leq L, \tag{2.13}$$

where $\rho_{i,j}$ is the correlation coefficient between the fading signals received at the i^{th} and the j^{th} receiving antennas. In practice, this correlation model is observed in diversity reception by an array of three antennas placed on an equilateral triangle or by a closely spaced set of antennas [50].

Exponential Correlation

In exponential correlation model the correlation coefficient between i^{th} and j^{th} received received fading signals is defined as [1, 2, 51]

$$\rho_{i,j} = \rho^{|i-j|}, \, i, j = 1, 2, \ldots, L \tag{2.14}$$

The exponential correlation is observed when the receiving antennas are placed in a linear array.

2.3 Analytical Methods for System Performance Evaluation

There are some standard methods used in literature to analyze various performance of a diversity receiver. These methods are discussed below.

2.3.1 Probability Density Function Based Approach

The PDF based approach is a straightforward approach for performance analysis which requires the knowledge of the PDF of the combiner output SNR. Formulas for obtaining various performance measures are mentioned below.

1. **Average output SNR:** Average output SNR can be obtained by averaging the instantaneous SNR over its PDF. It can be given as

$$\bar{\gamma} = \int_0^\infty \gamma f_\gamma(\gamma) d\gamma \tag{2.15}$$

   where, $\bar{\gamma}$ is the average SNR and $f_\gamma(\gamma)$ is the PDF of γ.

2. **Outage Probability:** Outage probability is an important performance measure of any communication receiver. For the output SNR, it is defined as the probability that the output SNR

γ, falls below a certain threshold value γ_{th} [2]. Mathematically, it can be given as

$$P_{\text{out}}(\gamma_{th}) = \int_{0}^{\gamma_{th}} f_\gamma(\gamma) d\gamma. \tag{2.16}$$

3. **Average Bit Error Rate:** The average bit error rate (ABER) of a digital communication system for various modulations can be obtained by averaging the conditional BER (conditioned on SNR) corresponding to the modulation scheme over the PDF of the receiver output SNR [2]. Mathematically, it can be given as

$$P_e(\overline{\gamma}) = \int_{0}^{\infty} p_e(\varepsilon|\gamma) f_\gamma(\gamma) d\gamma, \tag{2.17}$$

where $p_e(\varepsilon|\gamma)$ is the conditional BER corresponding to the modulation scheme used.

4. **Amount of fading:** Amount of fading is an important statistical characteristic of the fading channel, also known as the *fading figure*. It is generally associated with the PDF of the fading [2]. It can be mathematically obtained from the first and second moments of the SNR as

$$AF = \frac{var[\gamma]}{(E[\gamma])^2} = \frac{E(\gamma^2) - (E[\gamma])^2}{(E[\gamma])^2}, \tag{2.18}$$

where $var[\cdot]$ represents the variance and $E[\cdot]$ is the expectation operator.

2.3.2 Moment Generating Function Based Approach

In a number of cases it is not possible to obtain the PDF of the combiner output SNR in a suitable mathematical form. MGF method is an alternative method for a large number of such cases [2]. It requires an expression for the MGF of the combiner output SNR. Performance measures using the MGF of the combiner output SNR can be obtained as below.

1. **Average output SNR**: The average output SNR of a diversity combiner can be given by

$$\overline{\gamma} = \frac{d}{ds}\left[M_\gamma(s)\right]|_{s=0} \tag{2.19}$$

where, $M_\gamma(s)$ is the MGF of the combiner output SNR and $\frac{d}{dt}[\cdot]$ is the differential operator.

2. **Outage probability:** The outage probability can be given by [2]

$$P_{\text{out}}(\gamma_{th}) = \frac{1}{2\pi j}\int_{\sigma-j\infty}^{\sigma+j\infty} \frac{M_\gamma(-s)}{s} e^{\gamma_{th}s} ds, \tag{2.20}$$

where σ is chosen in the region of convergence of the integral in the complex s-plane.

3. **Average BER:** The formula for the average BER in MGF approach is given by [2]

$$P_e(\bar{\gamma}) = \frac{1}{2\pi j}\int_{\sigma-j\infty}^{\sigma+j\infty} \frac{M_D(-s)}{s} ds. \tag{2.21}$$

2.3.3 Characteristic Function Based Approach

In this approach characteristic function (CF) of some of the variables of the receiver is used to obtain performance measures. This approach is discussed below.

1. **Coherent Receivers:** For a coherent receiver with BPSK modulation, the ABER can be obtained using the following formula (Gil-Palaez lemma) [49]

$$P_e(\bar{\gamma}) = \Pr(D_1 < 0) = \frac{1}{2} - \frac{1}{2\pi}\int_{-\infty}^{\infty} \frac{\Im\{\Phi_{D_1}(j\omega)\}}{\omega} d\omega, \tag{2.22}$$

where Φ_{D_1} is the characteristic function of the receiver output decision variable D_1 assuming a '1' was transmitted.

2. **Non-coherent Receivers:** For receivers with noncoherent modulations, the CF based formula for ABER can be given as (using Parseval's theorem) [3]

$$P_e(\bar{\gamma}) = \frac{1}{\pi}\int_{0}^{\infty} \Re\{G^*(s)\Phi_\alpha(s)\} ds, \tag{2.23}$$

where $\Phi_\alpha(s)$ is the CF of the combiner output instantaneous amplitude, $G(s)$ the Fourier transform of the conditional error probability and $*$ is the complex conjugate operator. This

Table 2.1: Conditional BER of coherent and noncoherent modulation schemes with instantaneous SNR γ [3]

Modulation	Conditional BER
MPSK	$\frac{1}{\pi}\int_{0}^{\pi-\frac{\pi}{M}} exp\left(\frac{-\gamma \sin^2\left(\pi/M\right)}{Sin^2\theta}\right)d\theta$
MDPSK	$\frac{1}{\pi}\int_{0}^{\pi-\frac{\pi}{M}} Exp\left(\frac{-\gamma Sin^2\left(\pi/M\right)}{1+Cos\left(\pi/M\right)}\right)d\theta$
NCMFSK	$\frac{M-1}{2}Exp(\frac{-\gamma}{2})$
MSK	$erf\left(\sqrt{\gamma/2}\right)-0.25erfc^2\left(\sqrt{\gamma/2}\right)$
$\frac{\pi}{4}$ DQPSK with gray coding	$\frac{1}{2\pi}\int_{0}^{\infty} exp\left(\sqrt{\frac{-2\gamma}{2-\sqrt{2}Cos\theta}}\right)d\theta$
Square QAM	$2qerfc\left(\sqrt{p\gamma}\right)-q^2erfc^2\left(\sqrt{p\gamma}\right)$ $q=1-\frac{1}{\sqrt{M}}$ and $p=\frac{1.5}{M-1}$

method has been found to be appropriate for ABER performance of EGC receiver. Since, the Equation 2.23 requires only the combiner output CF, this formula can be safely used both for coherent and noncoherent modulation schemes. Besides, it can also be used to analyze combiners with both independent and correlated fading branches.

The conditional BER for different modulation schemes are listed in Table 2.1. For coherent binary signaling, the expression for the conditional BER can be given by putting $M=2$ for the entry for MPSK in the table which can be simplified as

$$p_{e,\text{coh}}(\varepsilon|\gamma)=Q\left(\sqrt{2a\gamma}\right), \tag{2.24}$$

where $a=0.5,1$ for CFSK and CPSK modulations. For noncoherent modulations, the simplified form of conditional BER can be given as

$$p_{e,\text{ncoh}}(\varepsilon|\gamma)=\frac{1}{2}\exp(-a\gamma), \tag{2.25}$$

with $a=0.5,1$ for NCFSK and DPSK modulations.

Chapter 3

Performance Analysis in Hoyt Fading Channels

Performance analysis related research works on diversity receivers in Hoyt fading channels are available in [17, 18, 20, 22–26]. These analyses provide studies on the performance of MRC and EGC receivers over independent fading channels. Apart from issues covered in these presentations many other useful performance measures also need attention. Performance analysis of SC receiver over Hoyt fading channels is not available in literature. Selection combiner having the least complexity among known diversity combiners can be of interest from the implementation point view. As it is well known that practical diversity receivers have to operate in correlated fading environments [1], analysis of diversity receivers for correlated fading channels can provide actual performance of these systems.

In this chapter, analysis of SC, MRC and EGC receivers are presented for Hoyt fading channels. For SC receiver the analysis is provided for independent channels. Available analysis for MRC receiver over independent fading channels are extended further to obtain performance measures such as outage probability and amount of fading. For correlated Hoyt fading channels, the analysis are presented for dual diversity combiners. Further, performance of correlated MRC receiver results are extended to arbitrary order of diversity.

3.1 Selection Combining in Independent Fading Channels

Analysis of the SC receiver using the PDF based approach as discussed in Section 2.3.1 requires an expression for the PDF of the combiner output SNR. For independent Hoyt fading channels we derive an expression for this PDF $f_{\gamma_{sc}}(\gamma_{sc})$ and use it further to obtain moments expression for the combiner output SNR, outage probability and ABER for binary, coherent and noncoherent modulation schemes.

3.1.1 PDF of Combiner Output Signal-to-Noise Ratio

As discussed in Section 2.1, the combiner has L independent input faded signals whose SNRs are given as $\gamma_l = \frac{E_b}{N_0}\alpha_l^2, l = 1, 2, \ldots, L$. The RVs α_ls are Hoyt distributed having a PDF expression given in Equation 1.3. For the convenience of analysis Equation 1.3 can be expressed in another form as shown in Equation A.2 of Appendix A.1 and is reproduced below.

$$f_{\alpha_l}(\alpha_l) = \frac{\alpha_l e^{-\frac{1}{2q^2}\alpha_l^2}}{q} {}_1F_1\left(\tfrac{1}{2}; 1; \tfrac{1-q^2}{2q^2}\alpha_l^2\right). \tag{3.1}$$

Since, α_ls are independent RVs an expression for the joint PDF of fading envelopes at the combiner input can be given by the product of L PDFs as

$$f_{\alpha_1,\alpha_2,\ldots,\alpha_L}(\alpha_1, \alpha_2, \ldots, \alpha_L) = \frac{1}{q^L}\prod_{i=1}^{L} \alpha_i e^{-\frac{1}{2q^2}\alpha_i^2} {}_1F_1\left(\frac{1}{2}; 1; \frac{1-q^2}{2q^2}\alpha_i^2\right). \tag{3.2}$$

The combiner output envelope α depends on the input envelopes as per the switching rule of the SC combiner discussed in Section 2.1.1. An expression for the CDF of output envelop α can be obtained by integrating Equation 3.2 w. r. t. α_ls as

$$F_\alpha(\alpha) = \frac{1}{q^L}\prod_{l=1}^{L}\left\{\int_0^\alpha \alpha_l e^{-\frac{1}{2q^2}\alpha_l^2}\,{}_1F_1\left(\frac{1}{2};1;\frac{1-q^2}{2q^2}\alpha_l^2\right)d\alpha_l\right\}. \tag{3.3}$$

The integral in Equation 3.3 can be solved by expressing ${}_1F_1(\cdot;\cdot;\cdot)$ in infinite series applying [4, 9.14.1] (reproduced in Equation B.11) and then solving the resulting integral using [4, (3.381.1)] (reproduced in Equation B.6). The final expression after integration can be obtained as

$$F_\alpha(\alpha) = \frac{1}{2^{L-1}q^{L-2}}\left[\sum_{k=0}^{\infty}\frac{\left(\frac{1}{2}\right)_k}{(k!)^2}\left(1-q^2\right)^k g\left(k+1,\frac{\alpha^2}{2q^2}\right)\right]^L. \tag{3.4}$$

The PDF of α can be obtained by differentiating Equation 3.4 w.r.t. α, which after simplification can be given as

$$f_\alpha(\alpha) = Lq^{L-2}\sum_{\substack{k_j=0\\ j=1,2,\ldots,L}}^{\infty}\frac{(1-q^2)^{\sum_{i=1}^{L}k_i}\alpha^{2k_L+1}e^{-\frac{\alpha^2}{2q^2}}}{\left(\sqrt{2}q\right)^{2k_L}}\left\{\prod_{i=1}^{L}\frac{\left(\frac{1}{2}\right)_{k_i}}{k_i!^2}\right\}\left\{\prod_{i=1}^{L-1}g\left(k_i+1,\frac{\alpha^2}{2q^2}\right)\right\} \tag{3.5}$$

The instantaneous output SNR of the combiner is $\gamma_{sc} = \alpha^2 E_b/N_0$ and its average values is $\bar{\gamma} = (1+q^2)E_b/N_0$ (from Equation A.3). Applying the concept of the transformation of RVs, the PDF of γ_{sc} can be obtained from Equation 3.5 as

$$\begin{aligned} f_{\gamma_{sc}}(\gamma_{sc}) &= L\left(\frac{1+q^2}{2\bar{\gamma}q}\right)^L \gamma_{sc}^{L-1}e^{-\frac{L(1+q^2)}{2\bar{\gamma}q^2}\gamma_{sc}}\sum_{\substack{k_j=0\\ j=1,2,\ldots,L}}^{\infty}\left\{\prod_{i=1}^{L}\frac{\left(\frac{1}{2}\right)_{k_i}}{(k_i!)^2}\right\}\left(\frac{1-q^4}{2\bar{\gamma}q^2}\gamma_{sc}\right)^{\sum_{i=1}^{L}k_i} \\ &\times\left\{\prod_{i=1}^{L-1}\frac{{}_1F_1\left(1;k_i+2;\frac{1+q^2}{2\bar{\gamma}q^2}\gamma_{sc}\right)}{k_i+1}\right\}. \end{aligned} \tag{3.6}$$

The expression in Equation 3.6 can be verified for Rayleigh fading channels which is a special case of Hoyt fading ($q = 1$). Substituting $q = 1$ followed by some algebraic manipulations it can be shown that Equation 3.6 reduces to

$$f_{\gamma_{sc}}(\gamma_{sc}) = \frac{L}{\bar{\gamma}}e^{\frac{-\gamma_{sc}}{\bar{\gamma}}}\left(1-e^{-\frac{\gamma_{sc}}{\bar{\gamma}}}\right)^{L-1}, \tag{3.7}$$

which is the same as [10, (7.60)].

Upper Bound on Truncation Error

It can be observed that Equation 3.6 consists of L number of infinite series. In the numerical evaluation of these series we take a finite number of terms of each infinite series, ensuring a desired accuracy, in the sum. This results in a truncation error of the expression. Considering equal number of terms 'K' for each infinite series in the evaluation, it can be shown that the truncation error has an upper bound. A derivation of an expression for this upper bound is shown in A.10.1 of Appendix and can be given as

$$E_K \leq Le^{-\frac{L(1+q^2)}{2\bar{\gamma}q^2}\gamma_{sc}} \left[\frac{(1-q^4)^{K+1}}{(1-q^2)q^{2K+1}}\right]^L {}_2F_2\left[\begin{array}{ccc} 1 & \frac{1}{2}+K & \frac{(1-q^4)\gamma_{sc}}{2\bar{\gamma}q^2} \\ K+1 & K+1 & \end{array}\right]$$
$$\times \left\{ {}_1F_1\left(1;K+2;\frac{1+q^2}{2\bar{\gamma}q^2}\gamma_{sc}\right) {}_3F_3\left[\begin{array}{cccc} 1 & \frac{1}{2}+K & K+1 & \frac{(1-q^4)\gamma_{sc}}{2\bar{\gamma}q^2} \\ K+1 & K+1 & K+2 & \end{array}\right]\right\}^{L-1}. \quad (3.8)$$

3.1.2 Moments of Combiner Output Signal-to-Noise Ratio

The N^{th} order moment associated with the combiner output instantaneous SNR γ_{sc} can be given, mathematically, as

$$E[\gamma_{sc}^N] = \int_0^\infty \gamma_{sc}^N f_{\gamma_{sc}}(\gamma_{sc})d\gamma_{sc}, \quad (3.9)$$

Putting $f_{\gamma_{sc}}(\gamma_{sc})$ from Equation 3.6, Equation 3.9 can be rewritten as

$$E[\gamma_{sc}^N] = L\left(\frac{1+q^2}{2\bar{\gamma}q}\right)^L \sum_{\substack{k_j=0 \\ j=1,2,\dots,L}}^{\infty} \left\{\prod_{i=1}^{L-1} \frac{\left(\frac{1}{2}\right)_{k_i}}{k_i!^2(k_i+1)}\right\} \frac{\left(\frac{1}{2}\right)_{k_L}}{k_L!^2} \left(\frac{1-q^4}{2\bar{\gamma}q^2}\right)^{\sum_{i=1}^{L} k_i}$$
$$\times \int_0^\infty \gamma_{sc}^{L+N+\sum_{i=1}^{L} k_i - 1} e^{-\frac{L(1+q^2)}{2\bar{\gamma}q^2}\gamma_{sc}} \left\{\prod_{i=1}^{L-1} {}_1F_1\left(1;k_i+2;\frac{1+q^2}{2\bar{\gamma}q^2}\gamma_{sc}\right)\right\} d\gamma_{sc}. \quad (3.10)$$

The integral in Equation 3.10 can be solved by applying the identity [3, (C.1)], (reproduced in Equation B.15). After integration the moment expression can be given as

$$E[\gamma_{sc}^N] = \frac{q^{L+2N}}{L^{L+N-1}}\left(\frac{2\bar{\gamma}}{1+q^2}\right)^N \sum_{\substack{k_j=0\\ j=1,2,\ldots,L}}^{\infty} \frac{\Gamma(L+N+\sum_{i=1}^{L} k_i)}{\left\{\prod_{i=1}^{L-1}(k_i+1)\right\}} \left\{\prod_{i=1}^{L}\frac{(\frac{1}{2})_{k_i}}{(k_i!)^2}\right\}\left(\frac{1-q^2}{L}\right)^{\sum_{i=1}^{L} k_i}$$
$$\times F_A\left(L+N+\sum_{i=1}^{L}k_i;\ \underbrace{1,1,\ldots,1;}_{(L-1),\text{numbers}}\ k_1+2,k_2+2,\ldots,k_{L-1}+2;\ \underbrace{\tfrac{1}{L},\tfrac{1}{L},\ldots,\tfrac{1}{L}}_{(L-1)\text{numbers}}\right). \quad (3.11)$$

The average output SNR of the SC combiner $\bar{\gamma}_{sc}$, can be obtained by putting $N=1$ in Equation 3.11 and can be given as

$$\bar{\gamma}_{sc} = \frac{q^{L+2}}{L^{L}}\left(\frac{2\bar{\gamma}}{1+q^2}\right) \sum_{\substack{k_j=0\\ j=1,2,\ldots,L}}^{\infty} \frac{\Gamma(L+1+\sum_{i=1}^{L} k_i)}{\left\{\prod_{i=1}^{L-1}(k_i+1)\right\}} \left\{\prod_{i=1}^{L}\frac{(\frac{1}{2})_{k_i}}{(k_i!)^2}\right\}\left(\frac{1-q^2}{L}\right)^{\sum_{i=1}^{L} k_i}$$
$$\times F_A\left(L+1+\sum_{i=1}^{L}k_i;\ \underbrace{1,1,\ldots,1;}_{(L-1),\text{numbers}}\ k_1+2,k_2+2,\ldots,k_{L-1}+2;\ \underbrace{\tfrac{1}{L},\tfrac{1}{L},\ldots,\tfrac{1}{L}}_{(L-1)\text{numbers}}\right). \quad (3.12)$$

For the case of Rayleigh fading which is a special case of Hoyt fading ($q=1$), the average output SNR of a dual-SC combiner can be obtained by substituting $q=1$ and $L=2$ in Equation 3.11 as $\bar{\gamma}_{sc} = \frac{3}{2}\bar{\gamma}$, which is same as the expression in [31, (12)].

3.1.3 Outage Probability of Combiner

The outage probability $P_{\text{out}}(\gamma_{th})$ of a combiner is defined in Section 2.3 and a mathematical expression for the same is given in Equation 2.16. Putting the expression for the PDF of γ_{sc} from Equation 3.6 into Equation 2.16 and expressing the involved hypergeometric function in infinite series [4, 9.14.1] (reproduced in Equation B.11) and rearranging the terms, an expression for the outage probability can be given as

$$P_{\text{out}}(\gamma_{th}) = L\left(\frac{1+q^2}{2\bar{\gamma}q}\right)^L \sum_{\substack{k_j=0\\ j=1,2,\ldots,L}}^{\infty} \left\{\prod_{i=1}^{L}\frac{\left(\frac{1}{2}\right)_{k_i}}{k_i!^2}\right\} \frac{\left(\frac{1-q^4}{2\bar{\gamma}q^2}\right)^{\sum_{i=1}^{L}k_i}}{\left\{\prod_{i=1}^{L-1}(k_i+1)\right\}} \sum_{\substack{t_p=0\\ j=1,2,\ldots,L-1}}^{\infty} \frac{\left(\frac{1+q^2}{2\bar{\gamma}q^2}\right)^{\sum_{i=1}^{L-1}t_i}}{\left\{\prod_{i=1}^{L-1}(k_i+2)_{t_i}\right\}}$$
$$\times\int_0^{\gamma_{th}} \gamma_{sc}^{\,L+\sum_{i=1}^{L}k_i+\sum_{j=1}^{L-1}t_j-1} e^{-\frac{L(1+q^2)}{2\bar{\gamma}q^2}\gamma_{sc}}\,d\gamma_{sc}. \tag{3.13}$$

The integral in Equation 3.13 can be solved by applying the identity [4, (3.381.1)], (reproduced in Equation B.6). For the convenience of presentation, which is used very often in the related literature, defining a new variable i.e., *Normalized Average Branch SNR* as $\bar{\gamma}_N \triangleq \frac{\bar{\gamma}}{\gamma_{th}}$, an expression for $P_{\text{out}}(\gamma_{th})$ as a function of $\bar{\gamma}_N$ can be given as

$$P_{\text{out}}(\bar{\gamma}_N) = \frac{q^L}{L^{L-1}} \sum_{\substack{k_j=0\\ j=1,2,\ldots,L}}^{\infty} \left\{\prod_{i=1}^{L}\frac{\left(\frac{1}{2}\right)_{k_i}}{(k_i!)^2}\right\} \frac{\left(\frac{1-q^2}{L}\right)^{\sum_{i=1}^{L}k_i}}{\left\{\prod_{i=1}^{L-1}(k_i+1)\right\}} \sum_{\substack{t_p=0\\ p=1,2,\ldots,L-1}}^{\infty} \frac{g\left(L+k_L+\sum_{i=1}^{L-1}(k_i+t_i), \frac{L(1+q^2)}{2\bar{\gamma}_N q^2}\right)}{L^{\sum_{j=1}^{L-1}t_j}\left\{\prod_{i=1}^{L-1}(k_i+2)_{t_i}\right\}}. \tag{3.14}$$

3.1.4 Average Bit Error Rate

ABER performance of diversity communication systems is defined in Section 2.3 and a general mathematical expression for ABER, as a function of conditional BER for modulation scheme and the PDF of received SNR, is given in Equation 2.17. To obtain an expression for ABER of a SC receiver in Hoyt fading channels, the obtained expression for the PDF of the output SNR γ_{sc} in Equation 3.6 and an expression for the conditional BER $p_{e,\text{coh}}(\varepsilon|\gamma)$ corresponding to the employed modulation scheme is required. Expressions for the conditional BER of a communication system for different digital modulation schemes are listed in Table 2.1. Thus, ABER expressions for binary, coherent and noncoherent modulations can be obtained as discussed below.

Binary Coherent Modulations

For binary coherent modulations (CPSK or BPSK and CFSK or BFSK), an expression for $p_{e,\text{coh}}(\varepsilon|\gamma)$ can be obtained by evaluating the entries for MPSK and MFSK modulations for $M = 2$ in Table 2.1. A simplified combined expression for conditional BERs is also given in Equation 2.24. Thus, putting $p_{e,\text{coh}}(\varepsilon|\gamma)$ from Equation 2.24 and $f_{\gamma_{sc}}(\gamma_{sc})$ from Equation 3.6 into Equation 2.17, binary coherent ABER expression can be written as

$$P_{e,ch}(\bar{\gamma}) = L\left(\frac{1+q^2}{2\bar{\gamma}q}\right)^L \sum_{\substack{k_j=0 \\ j=1,2,\ldots,L}}^{\infty} \left\{\prod_{i=1}^{L} \frac{\left(\frac{1}{2}\right)_{k_i}}{k_i!^2}\right\} \frac{\left(\frac{1-q^4}{2\bar{\gamma}q^2}\right)^{\sum_{i=1}^{L} k_i}}{\left\{\prod_{i=1}^{L-1}(k_i+1)\right\}}$$
$$\times \int_0^{\infty} Q\left(\sqrt{2a\gamma_{sc}}\right) \gamma_{sc}^{L+\sum_{i=1}^{L} k_i - 1} e^{-\frac{L(1+q^2)}{2\bar{\gamma}q^2}\gamma_{sc}} \left\{\prod_{i=1}^{L-1} {}_1F_1\left(1; k_i+2; \frac{1+q^2}{2\bar{\gamma}q^2}\gamma_{sc}\right)\right\} d\gamma_{sc}. \quad (3.15)$$

The $Q(\cdot)$ function in the Equation 3.15 can be expressed using incomplete gamma function applying the identity [1, A-(8a)] (reproduced in Equation B.14). Also, the hypergeometric function can be written in series form using [4, 9.14.1] (reproduced in Equation B.11). After these modifications the obtained integral can be solved using the identity [1, A-(6)]) (reproduced in Equation B.13) and an expression for ABER can be obtained as

$$P_{e,ch}(\bar{\gamma}) = L(q\eta_1)^{L+1} \sqrt{\frac{a\bar{\gamma}}{2\pi(1+q^2)}} \sum_{\substack{k_j=0 \\ j=1,2,\ldots,L}}^{\infty} \left\{\prod_{i=1}^{L} \frac{\left(\frac{1}{2}\right)_{k_i}}{(k_i!)^2}\right\} \frac{[(1-q^2)\eta_1]^{\sum_{i=1}^{L} k_i}}{\prod_{i=1}^{L-1}(k_i+1)} \sum_{\substack{t_p=0 \\ p=1,2,\ldots,L-1}}^{\infty} \eta_1^{\sum_{j=1}^{L-1} t_j}$$
$$\times \frac{\Gamma\left(L+\frac{1}{2}+\sum_{i=1}^{L} k_i + \sum_{j=1}^{L-1} t_j\right)}{\left\{\prod_{j=1}^{L-1}(k_j+2)_{t_j}\right\}\left(L+\sum_{i=1}^{L} k_i + \sum_{j=1}^{L-1} t_j\right)} {}_2F_1\left(1, L+\frac{1}{2}+\sum_{i=1}^{L} k_i + \sum_{j=1}^{L-1} t_j;\right.$$
$$\left. L+1+\sum_{i=1}^{L} k_i + \sum_{j=1}^{L-1} t_j; L\eta_1\right), \quad (3.16)$$

where $\eta_1 \triangleq \frac{1+q^2}{L(1+q^2)+2a\bar{\gamma}q^2}$.

Binary Non-coherent Modulations

Noncoherent binary modulation includes BDPSK and BFSK schemes. For these modulations, expressions for conditional BERs can be obtained by evaluating the entries in Table 2.1 for MDPSK and NCFSK, for $M = 2$. A simplified combined expression for both the modulations is given in Equation 2.25. Putting $p_{e,\text{ncoh}}(\varepsilon|\gamma)$ from Equation 2.25 and $f_{\gamma_{sc}}(\gamma_{sc})$ from Equation 3.6 into Equation 2.17, an expression for noncoherent ABER can be written as

$$P_{e,nch}(\bar{\gamma}) = \frac{L}{2}\left(\frac{1+q^2}{2\bar{\gamma}q}\right)^L \sum_{\substack{k_j=0 \\ j=1,2,\dots,L}}^{\infty} \left\{\prod_{i=1}^{L} \frac{\left(\frac{1}{2}\right)_{k_i}}{k_i!^2}\right\} \frac{\left(\frac{1-q^4}{2\bar{\gamma}q^2}\right)^{\sum_{i=1}^{L} k_i}}{\left\{\prod_{i=1}^{L-1}(k_i+1)\right\}} \times \int_0^{\infty} \gamma_{sc}^{L+\sum_{i=1}^{L} k_i - 1} e^{-\frac{L(1+q^2)+2a\bar{\gamma}q^2}{2\bar{\gamma}q^2}\gamma_{sc}} \left\{\prod_{i=1}^{L-1} {}_1F_1\left(1; k_i+2; \frac{1+q^2}{2\bar{\gamma}q^2}\gamma_{sc}\right)\right\} d\gamma_{sc}. \quad (3.17)$$

The integral in Equation 3.17 can be solved using identity [3, (C.1)] (reproduced in Equation B.15). Thus, an expression for the ABER for binary non-coherent modulations can be obtained as

$$P_{e,nch}(\bar{\gamma}) = \frac{L}{2}(q\eta_1)^L \sum_{\substack{k_j=0 \\ j=1,2,\dots,L}}^{\infty} \left\{\prod_{i=1}^{L} \frac{\left(\frac{1}{2}\right)_{k_i}}{(k_i!)^2}\right\} \frac{\Gamma\left(L+\sum_{i=1}^{L} k_i\right)}{\left\{\prod_{i=1}^{L-1}(k_i+1)\right\}} \left[\left(1-q^2\right)\eta_1\right]^{\sum_{i=1}^{L} k_i} \times F_A\left(L+\sum_{i=1}^{L} k_i; \underbrace{1,1,\dots,1}_{(L-1)\text{numbers}}; k_1+2, k_2+2, \dots, k_{L-1}+2; \underbrace{\eta_1,\eta_1,\dots,\eta_1}_{(L-1)\text{numbers}}\right). \quad (3.18)$$

It can be verified that for the case of Rayleigh fading, which is a particular case of Hoyt fading (for $q = 1$), it can be shown that Equation 3.18 reduces to $P_{e,nch}(\bar{\gamma}) = \frac{1}{(2+a\bar{\gamma})(1+a\bar{\gamma})}$, for $L = 2$ which is same as [52, (13)].

3.1.5 Results and Discussion

The outage probability expression obtained in Equation 3.14 is numerically evaluated and curves are plotted for $P_{\text{out}}(\bar{\gamma}_N)$ vs. $\bar{\gamma}_N$ in Figure 3.1 for different values of L and q. In this figure, it can be observed that for a given value of γ_{th} (or $\bar{\gamma}_N$) and L, with the decrease in q the outage increases. It is because the decrease in q indicates an increase in severity of fading resulting in an increase the probability of outage. It can also be seen in the figure that an increase in L reduced the probability of outage at the cost of increase in complexity of the diversity receiver. From the figure it can be observed that the plot for $L = 3$ and $q = 0.2$ is almost overlapping the curve for $L = 2$ and $q = 1$, which is counter intuitive. This indicates that the performance benefit expected from $L = 3$ over $L = 2$ is nullified due to severity of the fadings i.e., $q = 0.2$ over $q = 1$. For binary, coherent and non-coherent modulations, the expressions in Equations 3.16 and 3.18 are numerically evaluated and curves for ABER vs. $\bar{\gamma}$ per branch are shown in Figures 3.2 and 3.3, as a function of L. In these figures it can be observed that fading severity conditions cause increase in the ABER. ABER of the receiver decreases with the increase in L, as the combiner receives the signal from more number of redundant input antennas. To further investigate the effect of L on the performance, we plotted the magnitude of gain in output SNR vs. L in Figure 3.4 for an ABER of 10^{-4}, for CPSK and DPSK modulations. From this figure it can be observed that the gain in SNR is maximum for $L = 2$ and decreases relatively with every increase in L. It can also be noticed that over modulation schemes, the gain in output SNR per increase in L is small.

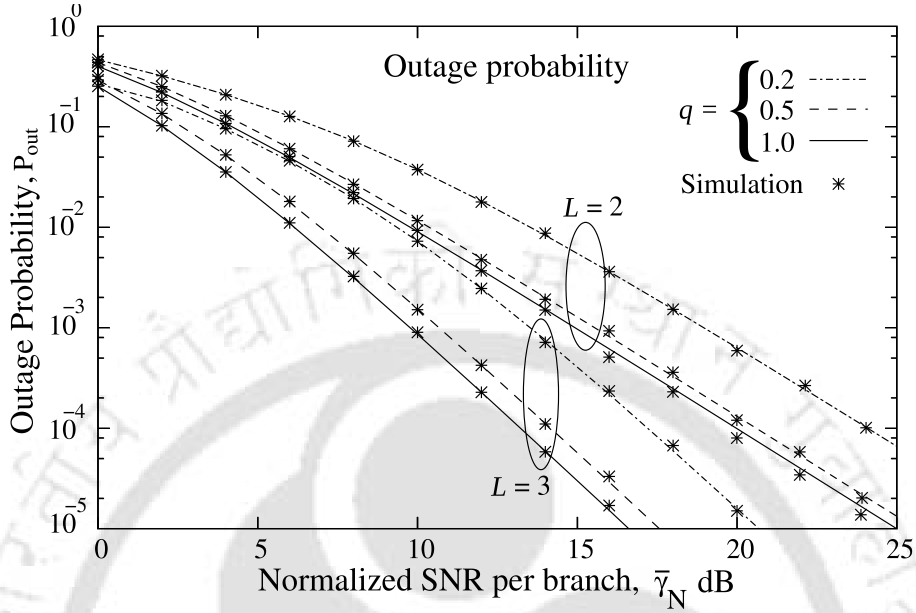

Figure 3.1: Outage probability of L independent SC receiver.

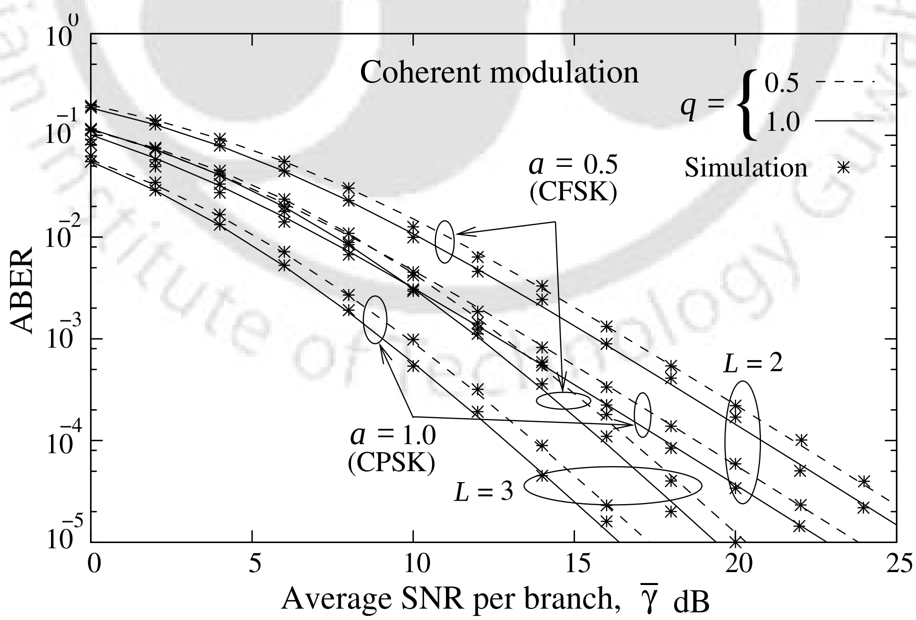

Figure 3.2: ABER of L-independent SC receiver for CPSK and CFSK modulations.

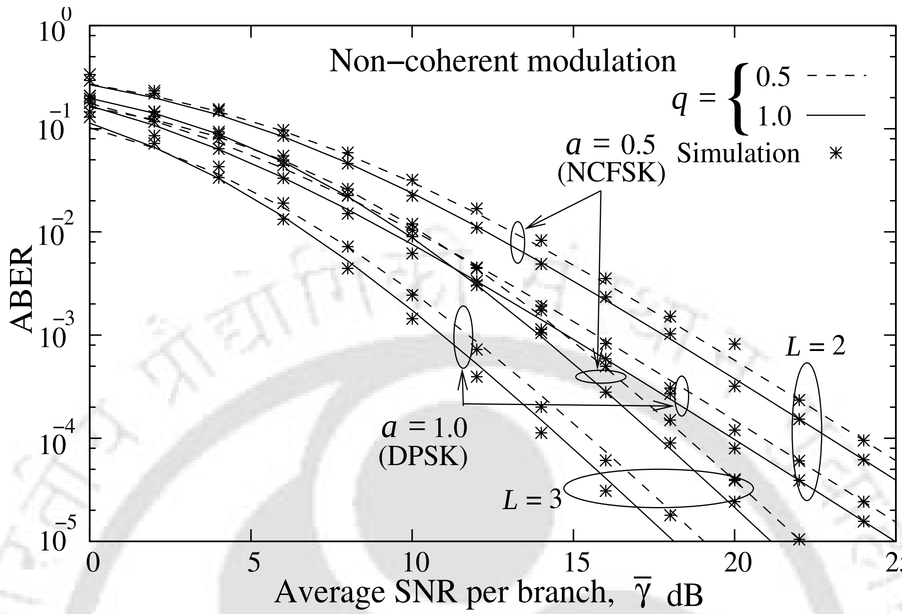

Figure 3.3: ABER of L-independent SC receiver for NCFSK and DPSK modulations.

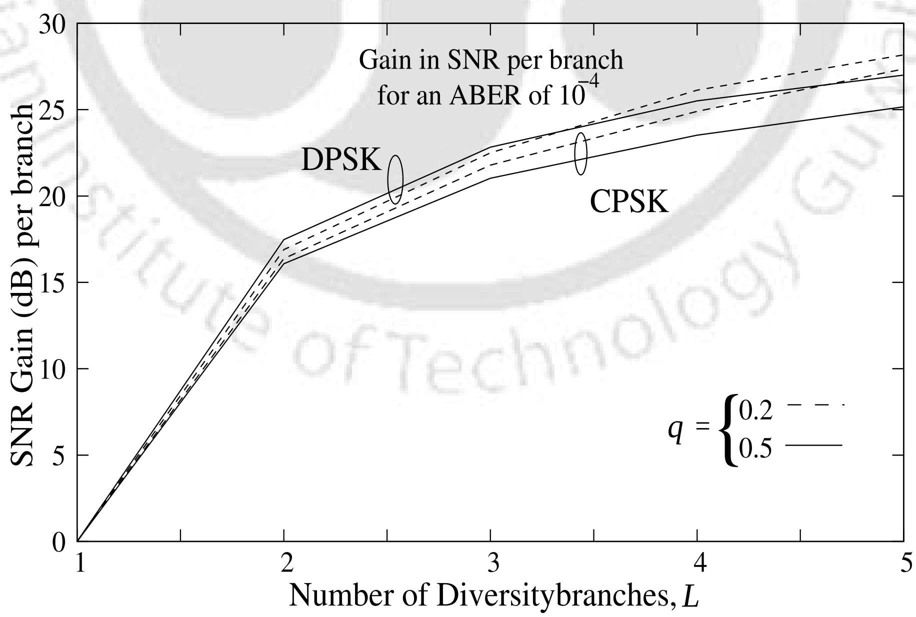

Figure 3.4: SNR gain per branch vs. L for CPSK and DPSK modulations as a function of q.

3.2 Maximal Ratio Combining in Independent and Identical Fading Channels

An expression for the output SNR γ_{mrc} of a MRC receiver is given in Equation 2.9. It is the sum of the received branch SNRs γ_ls. Using the definition of branch SNRs i.e., $\gamma_l = \frac{E_b}{N_0}\alpha_l^2$, γ_{mrc} can be expressed, mathematically, as

$$\gamma_{mrc} = \frac{E_b}{N_0}\left(\alpha_1^2 + \alpha_2^2 + \ldots + \alpha_L^2\right) = \frac{E_b}{N_0}\alpha^2, \tag{3.19}$$

where $\alpha^2 = \alpha_1^2 + \alpha_2^2 + \ldots + \alpha_L^2$. Thus, the PDF of γ_{mrc} can be obtained from the PDF of the RV α^2.

3.2.1 PDF of Combiner Output Signal-to-Noise Ratio

From Equation 3.19, it can be noticed that an expression for the PDF of γ_{mrc} can be derived from the PDF of α^2. The PDF of α^2, under the assumption of independent α_ls can be given mathematically as the L fold convolution of the PDFs of RVs $\alpha_1^2, \alpha_2^2, \ldots, \alpha_L^2$s. But, using this method it is not possible to obtain a compact expression for this PDF and the complexity of the numerical evaluation increases exponentially with increase in L [53]. However, by using the complex Gaussian model for a Hoyt distributed RV discussed in section A.1 [13], it is possible to obtain an expression for this PDF. Using this model, an expression for the PDF of α^2 is obtained as below.

Using the model for Hoyt distribution in [13], an expression for the CF of the sum of Hoyt square RV is derived in Appendix A.2 and is given in Equation A.11. For convenience, it is reproduced below.

$$\Phi_{\alpha_1^2,\alpha_2^2,\ldots,\alpha_L^2}(j\omega_1, j\omega_2, \ldots, j\omega_L) = \frac{1}{(2\sigma_x\sigma_y)^L}\prod_{i=1}^{L}\frac{1}{\sqrt{\left(\frac{1}{2\sigma_x^2} + j\omega_i\right)\left(\frac{1}{2\sigma_y^2} + j\omega_i\right)}}, \tag{3.20}$$

where σ_x^2 and σ_y^2 are variances of the inphase and quadrature phase components of the α in the Hoyt model described in [13]. An expression for the PDF of α^2 can be obtained by putting $\omega_1 = \omega_2 =$

$\ldots = \omega_L = \omega$ in Equation A.11 and subsequently applying inverse Fourier transform to the resulting expression. This expression can be given as

$$f_{\alpha^2}(\alpha^2) = \frac{1}{2^{L+1}\pi(\sigma_x\sigma_y)^L}\int_{-\infty}^{\infty}\frac{e^{j\omega\alpha}}{\left[\left(\frac{1}{2\sigma_y^2}+j\omega\right)\left(\frac{1}{2\sigma_x^2}+j\omega\right)\right]^{\frac{L}{2}}}d\omega. \tag{3.21}$$

Solving the integration in Equation 3.21 (using [4, 3.384.8], reproduced in Equation B.8), an expression for $f_{\alpha^2}(\alpha^2)$ can be obtained as

$$f_{\alpha^2}(\alpha^2) = \frac{\alpha^{L-1}e^{-\frac{1}{2\sigma_y^2}\alpha}}{(2\sigma_x\sigma_y)^L\,\Gamma(L)}\,{}_1F_1\left[\frac{L}{2};L;\frac{1}{2}\left(\frac{1}{\sigma_y^2}-\frac{1}{\sigma_x^2}\right)\alpha\right]. \tag{3.22}$$

Performing a transformation of RV on α^2 corresponding to the multiplying factor E_b/N_0 and substituting $E_b/N_0 = \bar{\gamma}/(1+q^2)$ from Equation A.3, an expression for the PDF of γ_{mrc} can be obtained as

$$f_{\gamma_{mrc}}(\gamma_{mrc}) = \frac{1}{(L-1)!}\left(\frac{1+q^2}{2\bar{\gamma}q}\right)^L \gamma_{mrc}^{L-1}e^{-\frac{1+q^2}{2\bar{\gamma}q^2}\gamma_{mrc}}\,{}_1F_1\left(\frac{L}{2};L;\frac{1-q^4}{2\bar{\gamma}q^2}\gamma_{mrc}\right). \tag{3.23}$$

3.2.2 Average Output Signal-to-Noise Ratio

Average output SNR of MRC receiver can be obtained from Equation 3.23 as

$$E[\gamma_{mrc}] = \bar{\gamma}_{mrc} = \frac{1}{(L-1)!}\left(\frac{1+q^2}{2\bar{\gamma}q}\right)^L\int_0^{\infty}\gamma_{mrc}^{L}e^{-\frac{1+q^2}{2\bar{\gamma}q^2}\gamma_{mrc}}\,{}_1F_1\left(\frac{L}{2};L;\frac{1-q^4}{2\bar{\gamma}q^2}\gamma_{mrc}\right)d\gamma_{mrc}, \tag{3.24}$$

The above integral can be solved using the identity [4, (7.621.4)] (reproduced in Equation B.10). After simplification $\bar{\gamma}_{mrc}$ can be obtained as

$$\bar{\gamma}_{mrc} = \frac{2L\bar{\gamma}q^{L+2}}{1+q^2}\,{}_2F_1\left(\tfrac{L}{2},L+1;L;1-q^2\right) = L\bar{\gamma}. \tag{3.25}$$

In the above equation the hypergeometric function is eliminated using the expression given in [54] (reproduced in Equation B.17 in Appendix). This result is obvious from the definition of average output SNR of the MRC combiner given in Equation 2.9 and hence is a verification of the correctness of Equation 3.23.

3.2.3 Outage Probability of Combiner Output Signal-to-Noise Ratio

Outage probability of the MRC output SNR can be obtained putting $f_{\gamma_{mrc}}(\gamma_{mrc})$ from Equation 3.23 into Equation 2.16 as given below.

$$P_{\text{out}}(\gamma_{th}) = \frac{1}{\Gamma(L)}\left(\frac{1+q^2}{2\bar{\gamma}q}\right)^L \int_0^{\gamma_{th}} \gamma_{mrc}^{L-1} e^{-\frac{1+q^2}{2\bar{\gamma}q^2}\gamma_{mrc}} \, {}_1F_1\left(\frac{L}{2}; L; \frac{1-q^4}{2\bar{\gamma}q^2}\gamma_{mrc}\right) d\gamma_{mrc}. \tag{3.26}$$

The confluent hypergeometric function in the above expression can be expressed in infinite series (using [4, 9.14.1], reproduced in Equation B.11) resulting in the expression

$$P_{\text{out}}(\gamma_{th}) = \frac{1}{\Gamma(L)}\left(\frac{1+q^2}{2\bar{\gamma}q}\right)^L \sum_{k=0}^{\infty} \frac{\left(\frac{L}{2}\right)_k}{(L)_k k!}\left(\frac{1-q^4}{2\bar{\gamma}q^2}\right)^k \int_0^{\gamma_{th}} \gamma_{mrc}^{L+k-1} e^{-\frac{1+q^2}{2\bar{\gamma}q^2}\gamma_{mrc}} d\gamma_{mrc}. \tag{3.27}$$

This integral can be solved applying [4, (3.381.1)] (reproduced in Equation B.6) and a final expression can be given as a function of $\bar{\gamma}_N$ (defined in Section 3.1.3), as

$$P_{\text{out}}(\bar{\gamma}_N) = q^L \sum_{k=0}^{\infty} \frac{\left(\frac{L}{2}\right)_k \left(1-q^2\right)^k}{k!\Gamma(L+k)} g\left(L+k, \frac{1+q^2}{2\bar{\gamma}_N q^2}\right). \tag{3.28}$$

It can be verified that for $q = 1$, which is the Rayleigh fading case, Equation 3.28 reduces to

$$P_{\text{out}}(\gamma_{th}) = \frac{g\left(L, \frac{\gamma_{th}}{\bar{\gamma}}\right)}{\Gamma(L)}, \tag{3.29}$$

which is same as the expression [1, (40), for $m = 1$]. The infinite series involved in Equation 3.28 can be upper bounded on truncation error as shown in Section 3.2.6.

3.2.4 Amount of Fading of Combiner Output Signal

The amount of fading of a combiner is defined in Section 2.3 and a mathematical expression for the same is given in Equation 2.18 which needs expressions for the first and second order moments of γ_{mrc} for evaluation. First order moment is given in Equation 3.25. An expression for the second order moment can be obtained as below.

$$\begin{aligned} E\left[\gamma_{mrc}^2\right] &= \frac{1}{\Gamma(L)}\left(\frac{1+q^2}{2\bar{\gamma}q}\right)^L \int_0^\infty \gamma_{mrc}^{L+1} e^{-\frac{1+q^2}{2\bar{\gamma}q^2}\gamma_{mrc}} {}_1F_1\left(\frac{L}{2};L;\frac{1-q^4}{2\bar{\gamma}q^2}\gamma_{mrc}\right) d\gamma_{mrc} \\ &= \frac{L(L+2)(1+q^4)+2Lq^2}{(1+q^2)^2}\bar{\gamma}^2, \end{aligned} \tag{3.30}$$

where we solved the integral in the above equation using the identity [4, 7.621.4] (reproduced in Equation B.10). Thus, putting $E[\gamma_{mrc}]$ from Equation 3.25 and $E[\gamma_{mrc}^2]$ from Equation 3.30, in Equation 2.18 and simplifying the resulting expression, AF can be obtained as

$$AF = \frac{2\left(1+q^4\right)}{L\left(1+q^2\right)^2}. \tag{3.31}$$

The amount of fading expression in Equation 3.31 can be verified for $L = 1$ $\left(AF = \frac{2(1+q^4)}{(1+q^2)^2}\right)$ which is same as it is given in [2, (2.14)].

3.2.5 Average Bit Error Rate

ABER performance of a diversity communication system is defined in Section 2.3 and a general mathematical expression for the ABER is given in Equation 2.17. To obtain an expression for the ABER of a MRC receiver, the obtained expression for the PDF of γ_{mrc} in Equation 3.25 and the conditional bit error rate $p_{e,\text{coh}}(\varepsilon|\gamma)$ for different modulation schemes tabulated in Table 2.1 are used. For binary, coherent and noncoherent modulations we obtain expressions for ABER as below.

Binary Coherent Modulations

For binary coherent modulations (BPSK or BFSK), expressions for the conditional BERs $p_{e,coh}(\varepsilon|\gamma)$ can be obtained by evaluating the entries for MPSK and MFSK modulations for $M = 2$ in Table 2.1. A simplified combined expression for this conditional BER is also given in Equation 2.24. Putting

$p_{e,\text{coh}}(\varepsilon|\gamma)$ and $f_{\gamma_{mrc}}(\gamma_{mrc})$ into Equation 2.17, ABER can be given as

$$P_{e_{coh}}(\bar{\gamma}) = \frac{1}{\Gamma(L)}\left(\frac{1+q^2}{2\bar{\gamma}q}\right)^L \int_0^\infty \gamma_{mrc}^{L-1} Q\left(\sqrt{2a\gamma_{mrc}}\right) e^{-\frac{1+q^2}{2\bar{\gamma}q^2}\gamma_{mrc}} {}_1F_1\left(\frac{L}{2};L;\frac{1-q^4}{2\bar{\gamma}q^2}\gamma_{mrc}\right) d\gamma_{mrc}. \quad (3.32)$$

The integral in Equation 3.32 can be solved by modifying it applying [1, A-(8a)] (reproduced in Equation B.14) to the $Q(\cdot)$ function involved. Further, expressing the confluent hypergeometric function in series form [4, 9.14.1] (reproduced in Equation B.11), Equation 3.32 can be rewritten as

$$\begin{aligned} P_{e_{coh}}(\bar{\gamma}) &= \frac{1}{2\sqrt{\pi}\Gamma(L)}\left(\frac{1+q^2}{2\bar{\gamma}q}\right)^L \sum_{k=0}^{\infty} \frac{\left(\frac{L}{2}\right)_k}{k!\,(L)_k}\left(\frac{1-q^4}{2\bar{\gamma}q^2}\right)^k \\ &\times \int_0^\infty \gamma_{mrc}^{L+k-1} e^{-\frac{1+q^2}{2q^2\bar{\gamma}}\gamma_{mrc}} \Gamma\left(\frac{1}{2}, a\gamma_{mrc}\right) d\gamma_{mrc}. \end{aligned} \quad (3.33)$$

Integral in Equation 3.33 can be solved using [1, A-(6)] (reproduced in Equation B.13) and an expression for ABER can be obtained as

$$\begin{aligned} P_{e_{coh}}(\bar{\gamma}) &= q^{L+1}\lambda^{L+\frac{1}{2}}\sqrt{\frac{a\bar{\gamma}}{2\pi(1+q^2)}} \sum_{k=0}^{\infty} \frac{\left(\frac{L}{2}\right)_k \Gamma(L+k+\frac{1}{2})}{k!\,(L+k)!} \\ &\times \left[\lambda(1-q^2)\right]^k {}_2F_1\left(1, L+k+\frac{1}{2}; L+k+1; \lambda\right), \end{aligned} \quad (3.34)$$

where $\lambda \triangleq \frac{1+q^2}{1+q^2+2aq^2\bar{\gamma}}$. Equation 3.34 can be verified for Rayleigh fading case ($q=1$) for which it reduces to [1, (30), for $m=1$]. This verifies the correctness of the obtained analytical expression.

Binary Non-coherent Modulations

For binary noncoherent modulations, a simplified expression for the conditional BER from Table 2.1 is given in Equation 2.25. Substituting $p_{e,\text{ncoh}}(\varepsilon|\gamma)$ and $f_{\gamma_{mrc}}(\gamma_{mrc})$ into Equation 2.17, an expression for the noncoherent ABER can be given as

$$P_{e_{ncoh}}(\bar{\gamma}) = \frac{1}{2\Gamma(L)}\left(\frac{1+q^2}{2\bar{\gamma}q}\right)^L \int_0^\infty \gamma_{mrc}^{L-1} e^{-\frac{1+q^2+2a\bar{\gamma}q^2}{2\bar{\gamma}q^2}\gamma_{mrc}} {}_1F_1\left(\frac{L}{2};L;\frac{1-q^4}{2\bar{\gamma}q^2}\gamma_{mrc}\right) d\gamma_{mrc}. \quad (3.35)$$

The integral in Equation 3.35 can be solved using [4, (7.621.4)] (reproduced in Equation B.10) and [1, A-(5)] (reproduced in Equation B.12). A closed-form expression for the ABER can be obtained as

$$P_{e_{ncoh}}(\bar{\gamma}) = \frac{1}{2}\left[\frac{1+q^2}{\sqrt{(1+q^2+2\bar{\gamma}aq^2)(1+q^2+2\bar{\gamma}a)}}\right]^L \quad (3.36)$$

Equation 3.36 can be verified for Rayleigh fading case ($q = 1$) which reduces to the result in [1, for $m = 1$].

3.2.6 Upper Bound on Truncation Error

The expressions obtained for the outage probability and the ABER for coherent modulations in Equations 3.28 and 3.34 contain infinite series. In the numerical evaluation of these expressions, a finite number of terms K, of the infinite series are included. This results in a truncation error. An expression for the upper bound on the truncation error can be obtained by applying the technique discussed in [55]. Below we present error bounds for the outage probability and the ABER.

Outage Probability

The upperbound on truncating the infinite series in Equation 3.28 is derived in in Equation A.53 of Appendix. The upper bound can be given as

$$\begin{aligned}\tilde{E}_{K_{out}} \leq & \left(\frac{1+q^2}{2\bar{\gamma}_N q}\right)^L {}_1F_1\left(L+K; L+K+1; -\frac{1+q^2}{2\bar{\gamma}_N q^2}\right)\frac{\left(\frac{L}{2}\right)_K}{K!(L+K)!} \\ & \times\left(\frac{1-q^4}{2\bar{\gamma}_N q^2}\right)^K {}_2F_2\left[\begin{matrix}1 & \frac{L}{2}+K & \frac{1-q^4}{2\bar{\gamma}_N q^2} \\ K+1 & L+K+1 & \end{matrix}\right].\end{aligned} \quad (3.37)$$

ABER for Coherent Modulation

A derivation for the upper bound in the truncating error of the Equation 3.34 is shown in Equation A.56. This expression can be given as

$$\tilde{E}_{K_{ABER}} \leq \sqrt{\frac{a\bar{\gamma}}{2\pi(1+q^2)}}\frac{q^{L+1}\lambda^{L+\frac{1}{2}}\left(\frac{L}{2}\right)_K\Gamma\left(L+K+\frac{1}{2}\right)}{K!(L+K)!}$$

$$\times\left[\lambda(1-q^2)\right]^K {}_2F_1\left(1, L+K+\frac{1}{2}; L+K+1; \lambda\right)$$
$$\times {}_3F_2\left[\begin{array}{cccc} 1 & \frac{L}{2}+K & L+K+\frac{1}{2} & \lambda(1-q^2) \\ K+1 & L+K+1 & & \end{array}\right]. \quad (3.38)$$

3.2.7 Results and Discussion

Analytically obtained expressions have been numerically evaluated and plotted for illustration. Outage probability $P_{\text{out}}(\bar{\gamma}_N)$ vs. $\bar{\gamma}_N$ has been plotted in Figure 3.5 for different values of L and q. It can be observed that with the decrease in q the receiver suffers more outage for a fixed value of γ_{th} (or $\bar{\gamma}_N$ and L. Also an increase in L with fixed γ_N and q, reduces the probability of outage, as expected. Amount of fading vs. L curves have been shown in Figure 3.6 for different values of q. The figure shows that the maximum and minimum value of AF are 2 (for $L=1$ and $q=0$) and 1 (for $L=1$ and $q=1$), respectively and it decreases with increase in L. It can also be observed that the effect of q on AF is more for $L \leq 4$ and approaches fast to zero for large L, irrespective of q. ABER vs. $\bar{\gamma}$ for binary, coherent and noncoherent modulations have been shown in Figures 3.7 and 3.8, respectively. It can be observed that the ABER degrades with a decrease in q, as expected and the degradation rate can be seen to be high for $q \leq 0.5$ than otherwise. To investigate the effect of L on the ABER performance, the magnitude of the gain in SNR vs. L has been plotted in Figure 3.9 for an ABER of 10^{-3}, for CPSK and DPSK modulations. From this figure it can be seen that the gain magnitude increases with increase in L. Although the curves for CPSK is very close to DPSK at low L they are quite apart at high L. Also, in the Figure 3.9 the diversity gain at the output of the MRC receiver has been shown as a function of L. Further, the upper bound on the truncation error obtained for Equation A.56 for CPSK modulation has been plotted in Figure 3.10. It can be seen that the error bound decreases very fast with K and we observed in the numerical evaluation that a maximum of 15 terms is enough to achieve an accuracy at 7^{th} place of decimal digit of the sum.

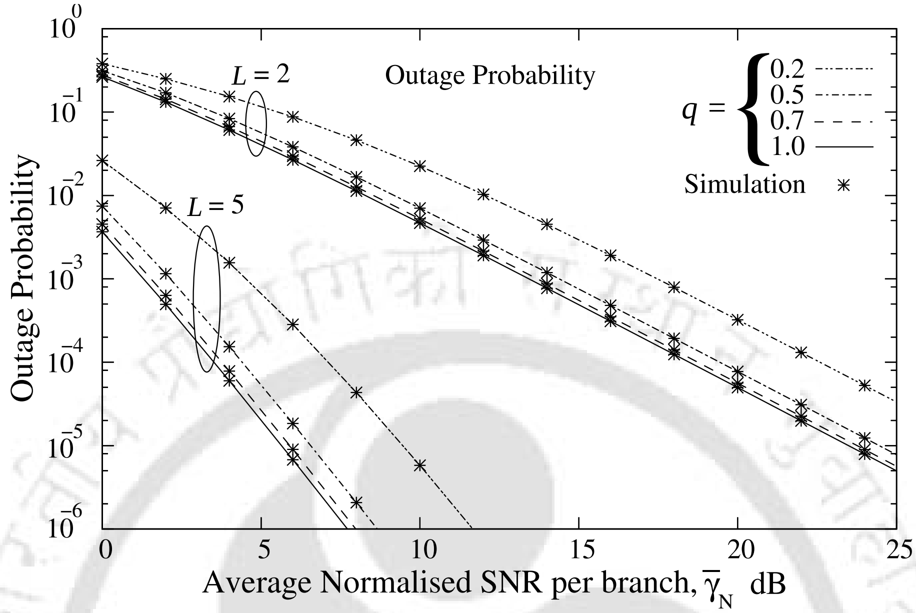

Figure 3.5: Outage probability vs. $\bar{\gamma}_N$ as a function of L and q.

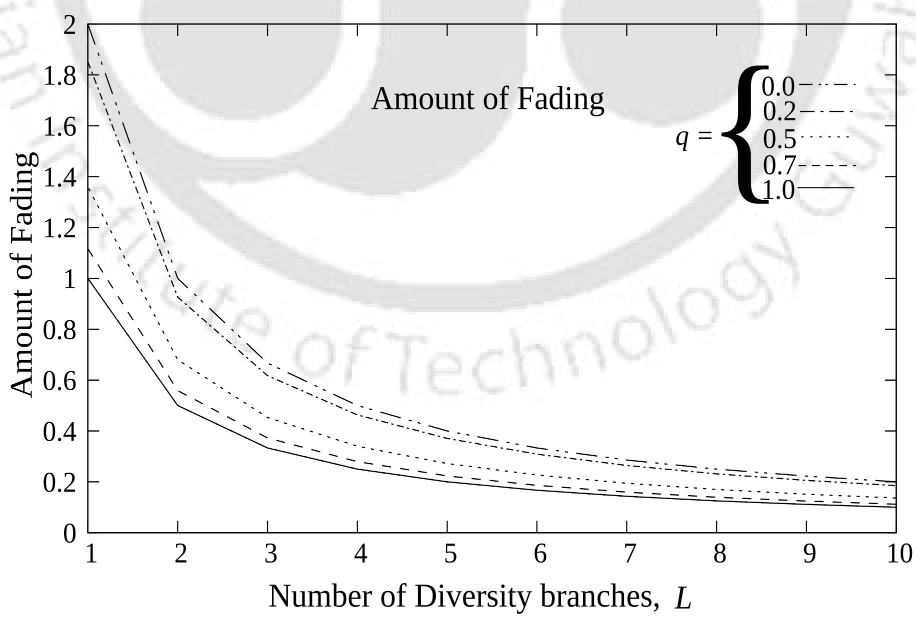

Figure 3.6: Amount of fading vs. L as a function of q.

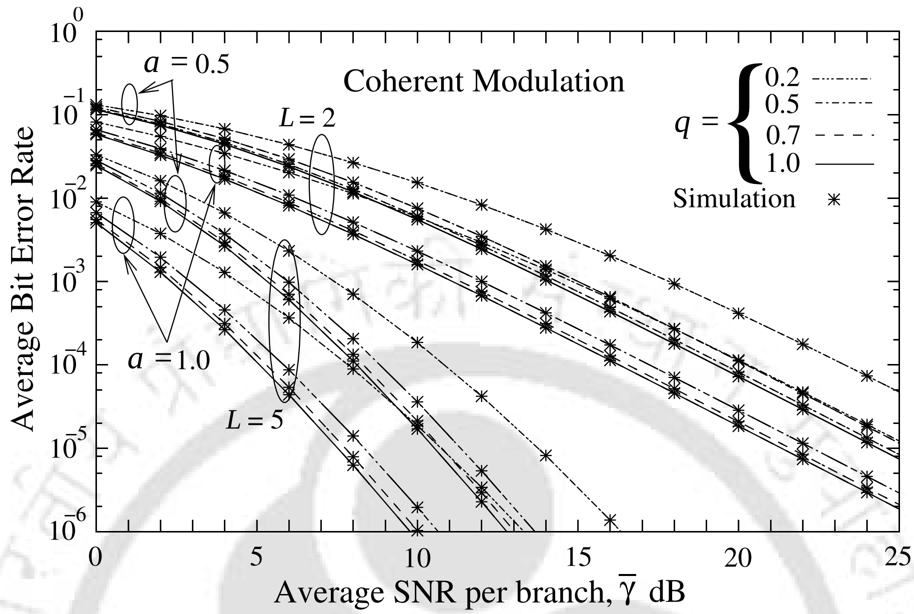

Figure 3.7: ABER vs. $\bar{\gamma}$ for CPSK ($a = 1$) and BFSK ($a = 0.5$) modulations as a function of L, q.

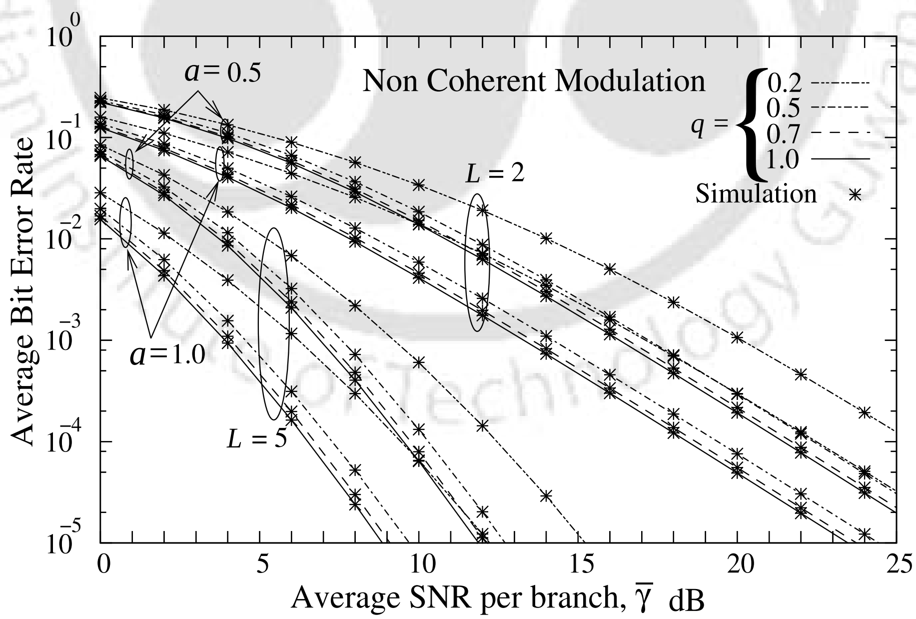

Figure 3.8: ABER vs. $\bar{\gamma}$ for DPSK ($a = 1$) and NCFSK ($a = 0.5$) modulations as a function of L and q.

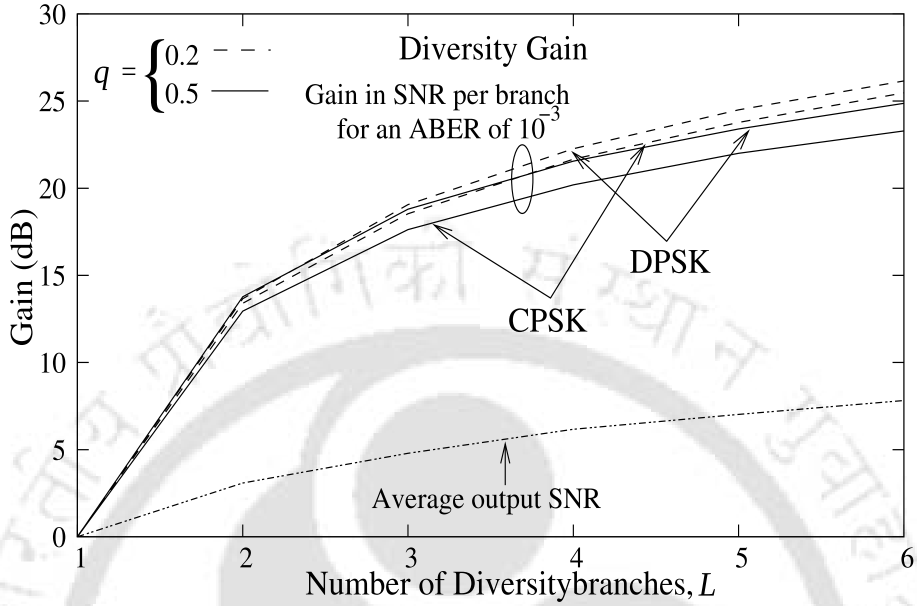

Figure 3.9: Diversity gain vs. L for average output SNR, CPSK and DPSK modulations.

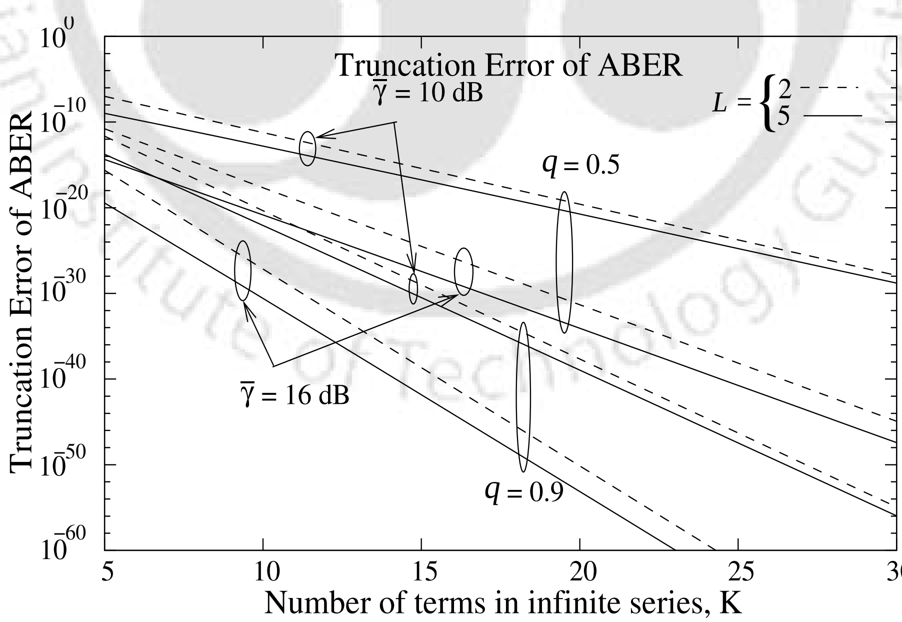

Figure 3.10: Truncation error for ABER in Equation 3.34 as a function of K.

3.3 Dual Diversity in Correlated Hoyt Fading channels

Correlation among received fading signals cannot be avoided due to reasons discussed in [1, 2]. Analysis of diversity receivers for correlated channels is relatively more complicated compared to the independent fading case. For Hoyt fading channels, some analysis are available for correlated cases in literature [32, 35, 36, 56, 57]. In this section, performance of dual -MRC, - EGC and - SC receivers are analyzed for correlated Hoyt fading channels. For MRC receiver an analysis for unequal fading parameters is also presented in addition to the equal fading parameter case. Unequal channel fading parameters may be observed in urban fading environments where diversity channels may have different characteristics [58]. In the analysis presented here the PDF based approach is used.

3.3.1 Maximal Ratio Combining Receiver

In this analysis correlation between the fading envelopes α_ls ($l = 1,2$) is assumed. A general expression for the combiner output SNR γ_{mrc} is given in Equation 3.19. It can be expressed for the dual diversity case as

$$\gamma_{mrc} = \frac{E_b}{N_0}\left(\alpha_1^2 + \alpha_2^2\right). \tag{3.39}$$

An expression for the PDF of γ_{mrc} i.e. $f_{\gamma_{mrc}}(\gamma_{mrc})$, when α_1 and α_2 are correlated with correlation coefficient ρ can be obtained using the complex Gaussian model of Hoyt RV in [13]. Using the PDF $f_{\gamma_{mrc}}(\gamma_{mrc})$, performance measures such as average output SNR, outage probability and ABER for binary, coherent and non-coherent modulations are derived.

PDF of Combiner Output Signal-to-Noise Ratio

From Equation 3.39, it can be observed that an expression for the PDF of γ_{mrc} can be obtained from the PDF of the RV $\alpha_1^2 + \alpha_2^2$. Using the complex Gaussian model for Hoyt distribution in [13], an expression for the joint CF of RVs α_1^2 and α_2^2 is derived in Appendix A.2 as given in Equation A.26. For the convenience of presentation, it is reproduced below.

$$\Phi_{\alpha_1^2,\alpha_2^2}(j\omega_1, j\omega_2) = \frac{1}{(1-\rho^2)(2\sigma_x\sigma_y)^2}\sum_{k=0}^{\infty}\sum_{t=0}^{\infty}\frac{(2k-1)!!(2t-1)!!}{k!t!\left[\left(\frac{1}{2(1-\rho^2)\sigma_x^2}+j\omega_1\right)\left(\frac{1}{2(1-\rho^2)\sigma_x^2}+j\omega_2\right)\right]^{k+\frac{1}{2}}}$$
$$\times\left[\frac{\rho}{\sqrt{8}\sigma_x^2(1-\rho^2)}\right]^{2(k+t)}\frac{1}{\left[\left(\frac{1}{2(1-\rho^2)\sigma_y^2}+j\omega_1\right)\left(\frac{1}{2(1-\rho^2)\sigma_y^2}+j\omega_2\right)\right]^{t+\frac{1}{2}}}. \quad (3.40)$$

An expression for the PDF of $\alpha^2 = \alpha_1^2 + \alpha_2^2$ can be obtained by substituting $\omega_1 = \omega_2 = \omega$ in Equation 3.40 and subsequently taking the inverse Fourier transform to the resulting expression. This can be given as

$$f_{\alpha^2}(\alpha^2) = \frac{1}{8\pi(1-\rho^2)(\sigma_x\sigma_y)^2}\sum_{k=0}^{\infty}\sum_{t=0}^{\infty}\frac{(2k-1)!!(2t-1)!!}{k!t!}\left[\frac{\rho}{\sqrt{8}\sigma_x^2(1-\rho^2)}\right]^{2(k+t)}$$
$$\times\int_{-\infty}^{\infty}\frac{e^{j\omega\alpha}}{\left(\frac{1}{2(1-\rho^2)\sigma_x^2}+j\omega\right)^{2k+1}\left(\frac{1}{2(1-\rho^2)\sigma_y^2}+j\omega\right)^{2t+1}}d\omega. \quad (3.41)$$

The integration in Equation 3.41 can be solved using [4, 3.384.8] (reproduced in Equation B.8) and hence an expression can be obtained as

$$f_{\alpha^2}(\alpha^2) = \frac{1}{(2\sigma_x\sigma_y)^2(1-\rho^2)}\sum_{k=0}^{\infty}\sum_{t=0}^{\infty}\frac{(2k-1)!!(2t-1)!!\alpha^{2(k+t)+1}e^{-\frac{1}{2(1-\rho^2)\sigma_y^2}\alpha}}{k!t!\Gamma(2(k+t+1))}$$
$$\times\left[\frac{\rho}{\sqrt{8}\sigma_x^2(1-\rho^2)}\right]^{2(k+t)}{}_1F_1\left[2k+1;2(k+t+1);\left(\frac{1}{\sigma_y^2}-\frac{1}{\sigma_x^2}\right)\frac{\alpha}{2(1-\rho^2)}\right]. \quad (3.42)$$

The combiner output SNR can be given as $\gamma_{mrc} = \frac{E_b}{N_0}\alpha^2$. Thus, the PDF of γ_{mrc} can be obtained by scaling Equation 3.42 corresponding to the multiplying factor E_b/N_0, applying the concept of transformation of RVs. For identical branch average power i.e. $\Omega_1 = \Omega_2 = \Omega$ (equivalently, $\bar{\gamma}_1 = \bar{\gamma}_2 = \bar{\gamma}$), it can be shown that $E_b/N_0 = \bar{\gamma}/(1+q^2)$ (given in Equation A.3). Substituting this relation, subsequent to the transformation of RV, an expression for $f_{\gamma_{mrc}}(\gamma_{mrc})$ can be obtained as

$$f_{\gamma_{mrc}}(\gamma_{mrc}) = \left(\frac{1+q^2}{2q\sqrt{1-\rho^2}\bar{\gamma}}\right)^2\sum_{k=0}^{\infty}\sum_{t=0}^{\infty}\frac{(2k-1)!!(2t-1)!!}{k!t!\Gamma(2(k+t+1))}\left[\frac{\rho\left(1+q^2\right)}{\sqrt{8}\left(1-\rho^2\right)\bar{\gamma}}\right]^{2(k+t)}$$

$$\times\gamma_{mrc}^{2(k+t)+1} e^{-\frac{1+q^2}{2q^2(1-\rho^2)\bar{\gamma}}\gamma_{mrc}} {}_1F_1\left\{2k+1;2(k+t+1);\frac{1-q^4}{2q^2(1-\rho^2)\bar{\gamma}}\gamma_{mrc}\right\}. \quad (3.43)$$

Average Output Signal-to-Noise Ratio

Average output SNR of the combiner for the correlated fading channels can be obtained by substituting $f_{\gamma_{mrc}}(\gamma_{mrc})$ into Equation 2.15. Subsequently, solving the integral applying the identity [4, (7.621.4)] (reproduced in Equation B.10) and simplifying an expression for $\bar{\gamma}_{mrc}$ can be obtained as

$$\begin{aligned}\bar{\gamma}_{mrc} &= \frac{\left[2q^2(1-\rho^2)\right]^2\bar{\gamma}}{1+q^2}\sum_{k=0}^{\infty}\sum_{t=0}^{\infty}\frac{(2k-1)!!(2t-1)!!\,(k+t+1)}{k!t!} \\ &\times\left(\frac{\rho q^2}{\sqrt{2}}\right)^{2(k+t)} {}_2F_1\left\{2k+1,2k+2t+3;2(k+t+1);1-q^2\right\}. \end{aligned} \quad (3.44)$$

For independent channels i.e., for $\rho = 0$, Equation 3.44 can be simplified further to $\bar{\gamma}_{mrc} = 2\bar{\gamma}$, which is as expected.

Outage Probability

Outage probability for a diversity receiver is defined in Section 2.3 and a mathematical expression for this is given in Equation 2.16. Putting $f_{\gamma_{mrc}}(\gamma_{mrc})$ from Equation 3.43 into Equation 2.16, an expression for the outage probability for correlated dual-MRC receiver can be expressed as

$$\begin{aligned}P_{\text{out}}(\gamma_{th}) &= \left(\frac{1+q^2}{2q\bar{\gamma}\sqrt{(1-\rho^2)}}\right)^2\sum_{k=0}^{\infty}\sum_{t=0}^{\infty}\frac{(2k-1)!!(2t-1)!!}{k!t!\Gamma(2(k+t+1))}\left[\frac{\rho(1+q^2)}{\sqrt{8}\bar{\gamma}(1-\rho^2)}\right]^{2(k+t)} \\ &\times\int_0^{\gamma_{th}} e^{-\frac{1+q^2}{2\bar{\gamma}(1-\rho^2)q^2}\gamma_{mrc}}\gamma_{mrc}^{2k+2t+1} {}_1F_1\left\{2k+1;2(k+t+1);\frac{1-q^4}{2q^2\bar{\gamma}(1-\rho^2)}\gamma_{mrc}\right\}d\gamma_{mrc}, \end{aligned}$$

(3.45)

where γ_{th} is the threshold value of the combiner output SNR. The integral in Equation 3.45 cannot be solved in the given form. By expressing the hypergeometric function in infinite series using [4, 9.14.1] (reproduced in Equation B.11), Equation 3.45 can rewritten as

$$P_{\text{out}}(\gamma_{th}) = \left(\frac{1+q^2}{2q\bar{\gamma}\sqrt{(1-\rho^2)}}\right)^2 \sum_{k=0}^{\infty}\sum_{t=0}^{\infty} \frac{(2k-1)!!(2t-1)!!}{k!t!} \left[\frac{\rho(1+q^2)}{\sqrt{8}\bar{\gamma}(1-\rho^2)}\right]^{2(k+t)} \times \sum_{r=0}^{\infty} \frac{(2k+1)_r}{r!\,(2k+2t+r+2)!} \left(\frac{1-q^4}{2q^2\bar{\gamma}(1-\rho^2)}\right)^r \int_0^{\gamma_{th}} \gamma_{mrc}^{2k+2t+r+1} e^{-\frac{1+q^2}{2\bar{\gamma}(1-\rho^2)q^2}\gamma_{mrc}} d\gamma_{mrc}. \tag{3.46}$$

Equation in 3.46 can be solved using [4, (3.381.1)] (reproduced in Equation B.6). Thus, an expression for the outage probability can be obtained as

$$P_{\text{out}}(\bar{\gamma}_N) = (1-\rho^2)q^2 \sum_{k=0}^{\infty}\sum_{t=0}^{\infty} \frac{(2k-1)!!(2t-1)!!}{k!t!\Gamma(2(k+t+1))} \left(\frac{\rho q^2}{\sqrt{2}}\right)^{2(k+t)} \times \sum_{r=0}^{\infty} \frac{(2k+1)_r (1-q^2)^r}{r!\,(2(k+t+1))_r} g\left(2k+2t+r+2, \frac{1+q^2}{2\bar{\gamma}_N(1-\rho^2)q^2}\right), \tag{3.47}$$

where $\bar{\gamma}_N$ is defined in Section 3.1.3.

Average Bit Error Rate

ABER for a diversity receiver is defined in Section 2.3 and an expression for ABER is given in Equation 2.17. Equation 2.17 can be evaluated using the expression for the PDF of γ_{mrc} in Equation 3.43 and the conditional BER expression $p_{e,\text{coh}}(\varepsilon|\gamma)$. Expressions for conditional BER for different digital modulation schemes are listed in Table 2.1. ABER expressions for binary, coherent and noncoherent modulations are derived below.

1. **Binary Coherent Modulations**

   A combined expression for conditional BER for coherent BPSK and BFSK modulations obtained from Table 2.1 is given in Equation 2.24. By putting $p_{e,\text{coh}}(\varepsilon|\gamma)$ from Equation 2.24 and $f_{\gamma_{mrc}}(\gamma_{mrc})$ from Equation 3.43 into Equation 2.17, the ABER expression can be given as

$$P_{e,ch}(\bar{\gamma}) = \left(\frac{1+q^2}{2q\bar{\gamma}\sqrt{(1-\rho^2)}}\right)^2 \sum_{k=0}^{\infty}\sum_{t=0}^{\infty} \frac{(2k-1)!!(2t-1)!!}{k!t!\Gamma(2(k+t+1))} \left(\frac{\rho(1+q^2)}{\sqrt{8}\bar{\gamma}(1-\rho^2)}\right)^{2(k+t)}$$

$$\int_0^\infty \gamma_{mrc}^{2k+2t+1} Q\left(\sqrt{2a\gamma_{mrc}}\right) e^{-\frac{1+q^2}{2\bar{\gamma}(1-\rho^2)q^2}\gamma_{mrc}}$$
$$ {}_1F_1\left(2k+1; 2(k+t+1); \frac{1-q^4}{2q^2\bar{\gamma}(1-\rho^2)}\gamma_{mrc}\right) d\gamma_{mrc}. \quad (3.48)$$

The integration in Equation 3.48 can be solved applying [1, A-(8a)] (reproduced in Equation B.14) and expressing the hypergeometric function in series form [4, 9.14.1] (reproduced in Equation B.11). Thus, Equation 3.48 can be rewritten as

$$\begin{aligned} P_{e,ch}(\bar{\gamma}) &= \frac{1}{8\sqrt{\pi}}\left(\frac{1+q^2}{q\bar{\gamma}\sqrt{(1-\rho^2)}}\right)^2 \sum_{k=0}^{\infty}\sum_{t=0}^{\infty} \frac{(2k-1)!!(2t-1)!!}{k!t!\Gamma(2(k+t+1))} \\ &\times \left(\frac{\rho(1+q^2)}{\sqrt{8}\bar{\gamma}(1-\rho^2)}\right)^{2(k+t)} \sum_{r=0}^{\infty} \frac{(2k+1)_r}{r!\,(2(k+t+1))_r}\left(\frac{1-q^4}{2q^2\bar{\gamma}(1-\rho^2)}\right)^r \\ &\times \int_0^\infty \gamma_{mrc}^{2k+2t+r+1} e^{-\frac{1+q^2}{2\bar{\gamma}(1-\rho^2)q^2}\gamma_{mrc}} \Gamma\left(\frac{1}{2}, a\gamma_{mrc}\right) d\gamma_{mrc}. \end{aligned} \quad (3.49)$$

Solving the above integral using [1, A-(6)] (reproduced in Equation B.13), an expression for ABER can be given

$$\begin{aligned} P_{e,ch}(\bar{\gamma}) &= \lambda^{\frac{5}{2}} q^3 \sqrt{\frac{a\bar{\gamma}(1-\rho^2)}{2\pi(1+q^2)}} \sum_{k=0}^{\infty}\sum_{t=0}^{\infty}\left(\frac{\lambda\rho q^2}{\sqrt{2}}\right)^{2k+2t} \frac{(2k-1)!!(2t-1)!!}{k!t!\Gamma(2(k+t+1))} \\ &\times \sum_{r=0}^{\infty} \frac{\Gamma\left(2k+2t+r+\frac{5}{2}\right)}{r!(2k+2t+r+2)} \frac{(2k+1)_r}{(2(k+t+1))_r}\left[\lambda(1-q^2)\right]^r \\ &\times {}_2F_1\left(1, 2k+2t+r+\frac{5}{2}; 2k+2t+r+3; \lambda\right), \end{aligned} \quad (3.50)$$

where $\lambda \triangleq (1+q^2)/\left[1+q^2+2q^2 a\bar{\gamma}(1-\rho^2)\right]$.

2. **Binary Non-coherent Modulations**

A combined expression for conditional BER for DPSK and noncoherent BFSK modulations obtained from Table 2.1 is given in Equation 2.25. By putting $p_{e,\text{coh}}(\varepsilon|\gamma)$ from Equation 2.25 and $f_{\gamma_{mrc}}(\gamma_{mrc})$ from Equation 3.43 into Equation 2.17, the ABER expression can be given as

$$P_{e,nch}(\bar{\gamma}) = \left[\frac{1+q^2}{\sqrt{8}q\bar{\gamma}\sqrt{(1-\rho^2)}}\right]^2 \sum_{k=0}^{\infty}\sum_{t=0}^{\infty} \frac{(2k-1)!!(2t-1)!!}{k!t!\Gamma(2(k+t+1))}\left[\frac{\rho(1+q^2)}{\bar{\gamma}\sqrt{8(1-\rho^2)}}\right]^{2(k+t)}$$

$$\times \int_0^\infty \gamma_{mrc}^{2k+2t+1} e^{-\left(\frac{1+q^2}{2\bar{\gamma}(1-\rho^2)q^2}+a\right)\gamma_{mrc}}$$
$$\times {}_1F_1\left(2k+1; 2(k+t+1); \frac{1-q^4}{2q^2\bar{\gamma}(1-\rho^2)}\gamma_{mrc}\right) d\gamma_{mrc} \quad (3.51)$$

Solving the integral in the above expression using [4, (7.621.4)] (reproduced in Equation B.10), an expression for noncoherent ABER can be obtained as

$$P_{e,nch}(\bar{\gamma}) = \frac{(\lambda q)^2(1-\rho^2)}{2} \sum_{k=0}^{\infty}\sum_{t=0}^{\infty} \frac{(2k-1)!!(2t-1)!!}{k!t!} \left(\frac{\lambda q^2 \rho}{\sqrt{2}}\right)^{2(k+t)}$$
$$\times {}_2F_1\left(2(k+t+1), 2k+1; 2(k+t+1); [1-q^2]\lambda\right). \quad (3.52)$$

For independent Rayleigh fading channels i.e. for $\rho = 0$ and $q = 1$, it can be verified that Equations 3.50 and 3.52 reduces to

$$\bar{p}_e(\bar{\gamma}) = \frac{3\sqrt{a\bar{\gamma}}}{16}\left(\frac{1}{1+\bar{\gamma}a}\right)^{\frac{5}{2}} {}_2F_1\left(1, \frac{5}{2}; 3; \frac{1}{1+\bar{\gamma}a}\right) \quad (3.53)$$

and

$$\bar{P}_e(\bar{\gamma}) = \frac{1}{2}\left(\frac{1}{1+a\bar{\gamma}}\right)^2, \quad (3.54)$$

respectively, as in [1, for $m = 1$ and $M = 2$].

Results and Discussion

Obtained mathematical expressions have been numerically evaluated and plotted against parameters of interest. In Figure 3.11, $P_{\text{out}}(\bar{\gamma}_N)$ vs. $\bar{\gamma}_N$ has been plotted for different values of ρ and q. The effect of branch correlation on the outage can be observed by comparing the outage values for $\rho = 0.5$ and $\rho = 0.8$ against the values for $\rho = 0$ (uncorrelated case). Clearly, with the increase in ρ the receiver suffers more outage, for any value of γ_{th}. These results can be verified against the results in [2], which is a special case of the results presented here, and is found to be matching closely. For binary, coherent and noncoherent modulations, ABER vs. $\bar{\gamma}$ curves have been plotted in Figures 3.12 and 3.13, respectively. It can be observed that the ABER performance degrades with the increase in ρ.

For the purpose of illustration and further investigation on the effect of ρ on the ABER performance, we have tabulated the excess SNR [1] required to achieve an ABER of 10^{-3}, for CPSK and DPSK modulations, in Figure 3.14. From the figure it can be observed that for CPSK modulation, the excess SNR is close to 0.5 dB for $\rho = 0.5$ whereas it is nearly 2 dB for $\rho = 0.8$, which is certainly a very high penalty. Since, the excess SNR demands more transmitter power, in power limited cases this is not a suitable option to maintain the receiver ABER performance at a desired value, when ρ varies. An alternate solution in this case could be to rely on the spatial configuration of receiving antennas so as to restrict[2] ρ at smaller values < 0.5. There can also be a trade-off between the transmitter power and the antenna configuration depending on the maximum excess SNR that the transmitter can support. For example, from Table 3.1 for the CPSK case, if the transmitter supports a maximum excess SNR of 0.5 dB, then the ABER of 10^{-3} can be maintained by the transmitter as long as $\rho \leq 0.5$ beyond which it needs to be maintained by antenna spacing. Similar conclusions can also be drawn for other modulation schemes from the expressions obtained for ABER.

In the numerical evaluation of expressions involving infinite series we have truncated them suitably so as to achieve an accuracy in ABER at least at 7^{th} place of decimal digit. In Table 3.1, we have illustrated the number of terms required to achieve this accuracy in the evaluation of Equation 3.50 as a function of $\bar{\gamma}$ and ρ. It can be observed that for $\rho = 0.5$ the maximum number of terms to be included for this accuracy is 20 only.

[1] We define 'excess SNR' as the SNR required in excess over the uncorrelated case, i.e. $\rho = 0$

[2] ρ decreases with increase of antenna separation

Table 3.1: Number of terms (N) required for an accuracy at 7^{th} place of decimal digit in the numerical evaluation of Equation 3.50.

SNR (dB)	ρ	$q = 0.5$		$q = 1$	
		N	BER	N	BER
0	0.5	26	0.0671340	5	0.0633901
	0.8	43	0.0635529	12	0.0745122
8	0.5	10	0.0061955	2	0.0045822
	0.8	16	0.0089991	4	0.0074228

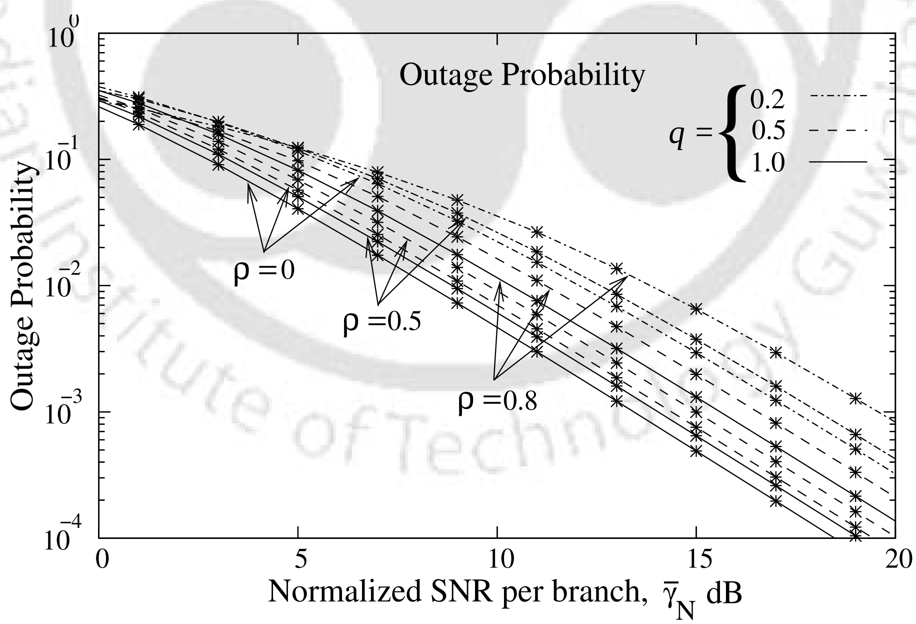

Figure 3.11: Outage probability vs. $\bar{\gamma}_N$ for correlated dual-MRC receiver.

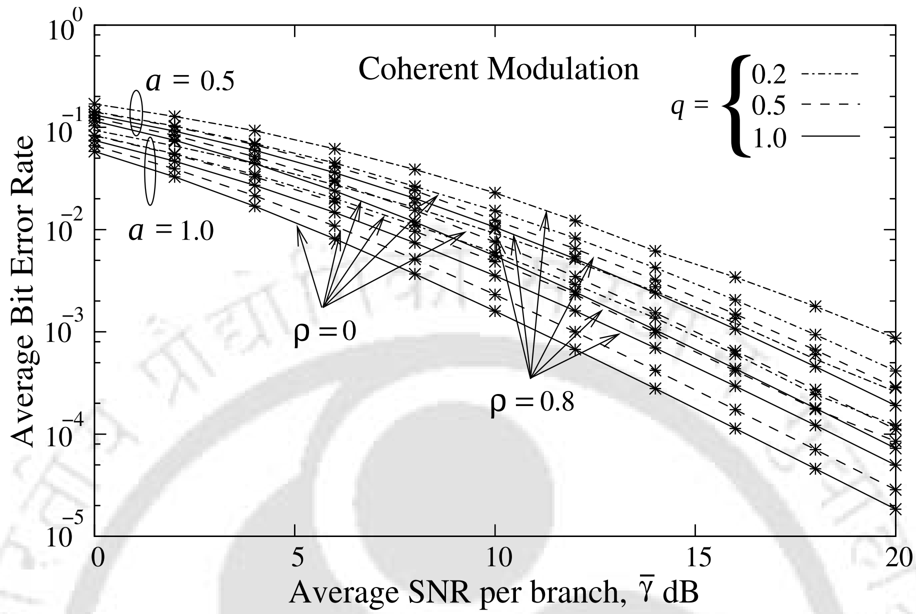

Figure 3.12: ABER vs. $\bar{\gamma}$ for correlated dual-MRC receiver with coherent modulation.

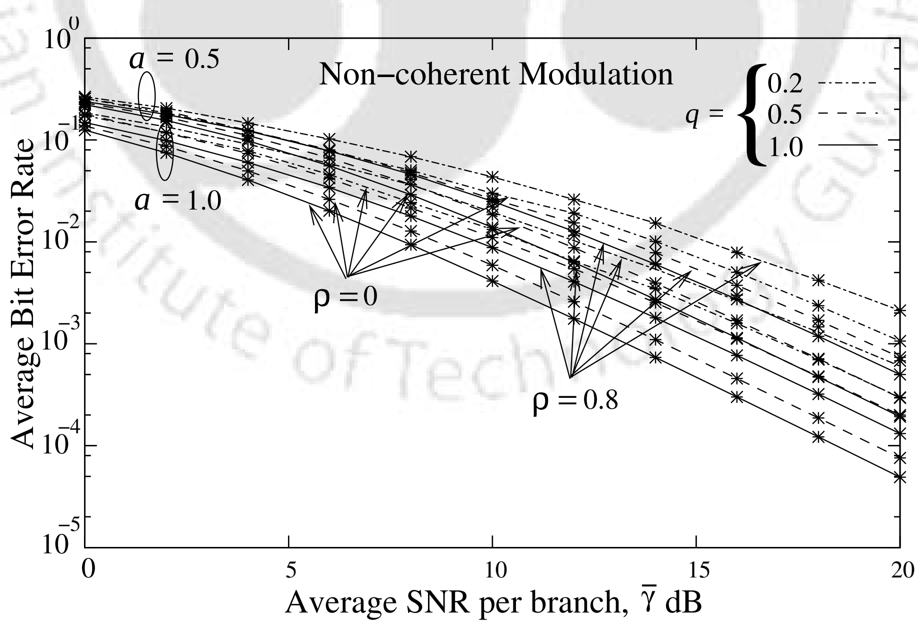

Figure 3.13: ABER vs. $\bar{\gamma}$ for correlated dual-MRC receiver with noncoherent modulation.

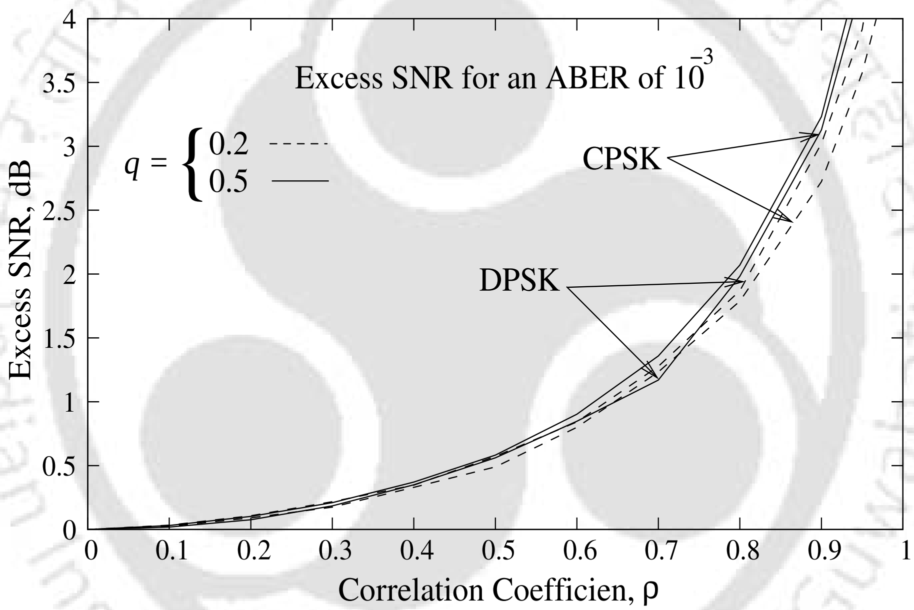

Figure 3.14: Excess SNR vs. correlation coefficient for CPSK and DPSK modulations.

3.3.2 Maximal Ratio Combining for Unequal Fading Parameters

The analysis presented in the previous section is valid for a scenario where the fading parameter q and the average input SNR $\bar{\gamma}_l$ $(l = 1,2)$ of both the diversity branches are identical. However, in practice the branch fading parameters may be different for each branch due to several reasons such as surface irregularities, and strength of the line-of-sight signal component, reported in [58] and the references therein. The branch SNRs may also be different as the channels corresponding to branches are different from each other. In this presentation we analyze the effect of unequal branch statistics and fading parameters on the receiver performance. The system here is same as considered in the previous section with nonidentical statistics for α_ls.

PDF of Output Signal-to-Noise Ratio

The approach used in the Section 3.3.1 does not yield to an expression for the PDF of $\alpha^2 = \alpha_1^2 + \alpha_2^2$ as the inverse Fourier transform is not possible in this case. So, an alternative method is used to obtain the PDF of γ_{mrc} here. It is presented below.

In MRC receiver, the PDF of the combiner output SNR γ_{mrc}, is the sum of input SNRs i.e. $\gamma_{mrc} = \gamma_1 + \gamma_2$. Using the complex Gaussian model for Hoyt RVs with unequal inphase and quadrature phase powers, an expression for the joint CF of α_l^2 and α_2^2 is derived in Equation A.35 in Appendix. Also, the correlation coefficient between α_1 and α_2 can be obtained as shown in Section A.6 of Appendix. The inverse Fourier transform of this expression which is the joint PDF of α_1^2 and α_2^2, can be given as

$$\begin{aligned} f_{\alpha_1^2,\alpha_2^2}(\alpha_1^2,\alpha_2^2) \quad = \quad & \frac{1}{4\sigma_{x_1}\sigma_{x_2}\sigma_{y_1}\sigma_{y_2}(1-\rho^2)} \sum_{k_1=0}^{\infty}\sum_{k_2=0}^{\infty} \frac{(2k_1-1)!!(2k_2-1)!!}{k_1!k_2!\,(\sigma_{x_1}\sigma_{x_2})^{2k_1}} \left[\frac{\rho\sqrt{\alpha_1\alpha_2}}{\sqrt{8}(1-\rho^2)}\right]^{2(k_1+k_2)} \\ & \times \frac{e^{-\frac{1}{2(1-\rho^2)\sigma_{y_1}^2}\alpha_1} e^{-\frac{1}{2(1-\rho^2)\sigma_{y_2}^2}\alpha_2}}{(\sigma_{y_1}\sigma_{y_2})^{2k_2}\,\Gamma^2(k_1+k_2+1)} {}_1F_1\left(k_1+\frac{1}{2};k_1+k_2+1;\frac{\sigma_{x_1}^2-\sigma_{y_1}^2}{2(1-\rho^2)\sigma_{y_1}^2\sigma_{x_1}^2}\alpha_1\right) \\ & \times {}_1F_1\left(k_1+\frac{1}{2};k_1+k_2+1;\frac{\sigma_{x_2}^2-\sigma_{y_2}^2}{2(1-\rho^2)\sigma_{y_2}^2\sigma_{x_2}^2}\alpha_2\right). \end{aligned} \tag{3.55}$$

Now, applying the concept of transformation of RVs for the multiplying factor E_b/N_0 and substituting $E_b/N_0 = \bar{\gamma}_l/(1+q_l^2)$, an expression for the joint PDF of γ_1 and γ_2 can be obtained as

$$\begin{aligned} f_{\gamma_1,\gamma_2}(\gamma_1,\gamma_2) &= \frac{(1+q_1^2)(1+q_2^2)}{4q_1q_2\bar{\gamma}_1\bar{\gamma}_2(1-\rho^2)}\sum_{k_1=0}^{\infty}\sum_{k_2=0}^{\infty}\frac{(2k_1-1)!!(2k_2-1)!!}{k_1!k_2!\Gamma^2(k_1+k_2+1)(q_1q_2)^{2k_2}} \\ &\times\left[\frac{\gamma_1\gamma_2\rho^2(1+q_1^2)(1+q_2^2)}{8\bar{\gamma}_1\bar{\gamma}_2(1-\rho^2)^2}\right]^{k_1+k_2} e^{-\frac{1}{2(1-\rho^2)}\left[\frac{1+q_1^2}{\bar{\gamma}_1q_1^2}\gamma_1+\frac{1+q_2^2}{\bar{\gamma}_2q_2^2}\gamma_2\right]} \\ &\times {}_1F_1\left(k_1+\frac{1}{2};k_1+k_2+1;\frac{(1-q_1^4)}{2\bar{\gamma}_1(1-\rho^2)q_1^2}\gamma_1\right) \\ &\times {}_1F_1\left(k_1+\frac{1}{2};k_1+k_2+1;\frac{(1-q_2^4)}{2\bar{\gamma}_2(1-\rho^2)q_2^2}\gamma_2\right). \end{aligned} \tag{3.56}$$

The PDF of γ_{mrc} i.e., the sum of γ_1 and γ_2, can be derived from Equation 3.56 using the convolution approach [59, (6.44)], and can be obtained as

$$\begin{aligned} f_{\gamma_{mrc}}(\gamma_{mrc}) &= \frac{(1+q_1^2)(1+q_2^2)}{4q_1q_2\bar{\gamma}_1\bar{\gamma}_2(1-\rho^2)}\sum_{k_1=0}^{\infty}\sum_{k_2=0}^{\infty}\frac{(2k_1-1)!!(2k_2-1)!!}{k_1!k_2!\Gamma^2(k_1+k_2+1)(q_1q_2)^{2k_2}} \\ &\times\left[\frac{\rho(1+q_1^2)(1+q_2^2)}{8\bar{\gamma}_1\bar{\gamma}_2(1-\rho^2)^2}\right]^{k_1+k_2}\int_0^{\gamma_{mrc}}[\gamma_2(\gamma_{mrc}-\gamma_2)]^{k_1+k_2}e^{-\frac{1+q_1^2}{2(1-\rho^2)\bar{\gamma}_1q_1^2}(\gamma_{mrc}-\gamma_2)} \\ &\times e^{-\frac{1+q_2^2}{2(1-\rho^2)\bar{\gamma}_2q_2^2}\gamma_2}\,{}_1F_1\left\{k_1+\frac{1}{2};k_1+k_2+1;\frac{(1-q_1^2)(1+q_1^2)}{2\bar{\gamma}_1(1-\rho^2)q_1^2}(\gamma_{mrc}-\gamma_2)\right\} \\ &\times {}_1F_1\left\{k_1+\frac{1}{2};k_1+k_2+1;\frac{(1-q_2^2)(1+q_2^2)}{2\bar{\gamma}_2(1-\rho^2)q_2^2}\gamma_2\right\}d\gamma_2. \end{aligned} \tag{3.57}$$

The hypergeometric function in Equation 3.57 can be expressed in infinite series form [4, 9.14.1] (reproduced in Equation B.11). Then, solving the resulting integral using [4, 3.383.1] (reproduced in Equation B.7), we get

$$\begin{aligned} f_{\gamma_{mrc}}(\gamma_{mrc}) &= \frac{(1+q_1^2)(1+q_2^2)}{4q_1q_2\bar{\gamma}_1\bar{\gamma}_2(1-\rho^2)}\sum_{k_1=0}^{\infty}\sum_{k_2=0}^{\infty}\sum_{k_3=0}^{\infty}\sum_{k_4=0}^{\infty}\frac{(2k_1-1)!!(2k_2-1)!!}{\left\{\prod_{i=1}^{4}k_i!\right\}[q_1q_2]^{2k_2}}\left[\frac{\rho^2(1+q_1^2)(1+q_2^2)}{8\bar{\gamma}_1\bar{\gamma}_2(1-\rho^2)^2}\right]^{k_1+k_2} \\ &\times\left[\frac{1-q_1^4}{\bar{\gamma}_1q_1^2}\right]^{k_3}\left[\frac{1-q_2^4}{\bar{\gamma}_2q_2^2}\right]^{k_4}\frac{\left(k_1+\frac{1}{2}\right)_{k_3}\left(k_1+\frac{1}{2}\right)_{k_4}\gamma_{mrc}^{2k_1+k_2+k_4+1}e^{-\frac{1+q_1^2}{2(1-\rho^2)\bar{\gamma}_1q_1^2}\gamma_{mrc}}}{[2(1-\rho^2)]^{k_3+k_4}\Gamma(2k_1+k_2+k_4+2)} \\ &\times {}_1F_1\left(k_1+k_2+k_4+1;2k_1+k_2+k_4+2;\frac{\bar{\gamma}_2q_2^2(1+q_1^2)-\bar{\gamma}_1q_1^2(1+q_2^2)}{2(1-\rho^2)\bar{\gamma}_1q_1^2\bar{\gamma}_2q_2^2}\gamma_{mrc}\right). \end{aligned} \tag{3.58}$$

Outage Probability

An expression for the outage probability of the dual MRC receiver in correlated Hoyt fading channels can be obtained by substituting $f_{\gamma_{mrc}}(\gamma_{mrc})$ from Equation 3.58 into Equation 2.16. It can be expressed as

$$P_{\text{out}}(\gamma_{th}) = \\ = \frac{(1+q_1^2)(1+q_2^2)}{4q_1q_2\bar{\gamma}_1\bar{\gamma}_2(1-\rho^2)} \sum_{k_1=0}^{\infty}\sum_{k_2=0}^{\infty}\sum_{k_3=0}^{\infty}\sum_{k_4=0}^{\infty} \frac{(2k_1-1)!!(2k_2-1)!!}{\left\{\prod_{i=1}^{4} k_i!\right\}[q_1q_2]^{2k_2}} \left[\frac{\rho^2(1+q_1^2)(1+q_2^2)}{8\bar{\gamma}_1\bar{\gamma}_2(1-\rho^2)^2}\right]^{k_1+k_2} \\ \times \left[\frac{1-q_1^4}{\bar{\gamma}_1 q_1^2}\right]^{k_3} \left[\frac{1-q_2^4}{\bar{\gamma}_2 q_2^2}\right]^{k_4} \frac{\left(k_1+\frac{1}{2}\right)_{k_3}\left(k_1+\frac{1}{2}\right)_{k_4}}{[2(1-\rho^2)]^{k_3+k_4}\Gamma(2k_1+k_2+k_4+2)} \int_0^{\gamma_{th}} \gamma_{mrc}^{2k_1+k_2+k_4+1} e^{-\frac{1+q_1^2}{2(1-\rho^2)\bar{\gamma}_1 q_1^2}\gamma_{mrc}} \\ \times {}_1F_1\left(k_1+k_2+k_4+1; 2k_1+k_2+k_4+2; \frac{\bar{\gamma}_2 q_2^2(1+q_1^2)-\bar{\gamma}_1 q_1^2(1+q_2^2)}{2(1-\rho^2)\bar{\gamma}_1 q_1^2\bar{\gamma}_2 q_2^2}\gamma_{mrc}\right) d\gamma_{mrc}. \quad (3.59)$$

The integral in Equation 3.59 can be solved by expressing the hypergeometric function in infinite series form [4, 9.14.1] (reproduced in Equation B.11) and then applying [4, (3.381.1)] (reproduced in Equation B.6). An expression for the outage probability can be obtained as

$$P_{\text{out}}(\gamma_{th}) = \frac{q_1^3(1-\rho^2)\tau}{q_2} \sum_{k_1=0}^{\infty}\sum_{k_2=0}^{\infty}\sum_{k_3=0}^{\infty}\sum_{k_4=0}^{\infty}\sum_{k_5=0}^{\infty} \frac{(2k_1-1)!!(2k_2-1)!!q_1^{4k_1+2k_2+2k_4}\tau^{k_1+k_2+k_4}}{\left\{\prod_{i=1}^{5} k_i!\right\} q_2^{2k_2+2k_4}} \\ \times \left(1-\frac{q_1^2\tau}{q_2^2}\right)^{k_5} \left(\frac{\rho^2}{2}\right)^{k_1+k_2} \frac{(1-q_1^2)^{k_3}(1-q_2^2)^{k_4}\left(k_1+\frac{1}{2}\right)_{k_3}\left(k_1+\frac{1}{2}\right)_{k_4}}{\Gamma(2k_1+k_2+k_5+2)} \\ \times \left(k_1+k_2+k_4+\frac{1}{2}\right)_{k_5} g\left(2k_1+k_2+k_5+2, \frac{1+q_1^2}{2\bar{\gamma}_1(1-\rho^2)q_1^2}\gamma_{th}\right), \quad (3.60)$$

where $\tau \triangleq \frac{\bar{\gamma}_1(1+q_2^2)}{\bar{\gamma}_2(1+q_1^2)}$.

The outage probability in Equation 3.60 is given as a function of γ_{th} and not as a function of $\bar{\gamma}_N$ as it is in Section 3.1.3. It is because in this analysis a non-identical branch fading is assumed for which it was possible to express the outage as a function of $\bar{\gamma}_N$. In the numerical evaluation, we have evaluated the outage probability by obtaining the γ_{th} for a particular value of ABER as in [1]. The average input branch SNRs can be related with the help of a decay factor δ by $\bar{\gamma}_2 = \bar{\gamma}_1 e^{-\delta}$ [2].

Average Bit Error Rate

ABER performance of a diversity communication system is defined in Section 2.3 and a general mathematical expression is given in Equation 2.17. To obtain an expression for the ABER of a correlated MRC receiver, the obtained expression for the PDF of γ_{mrc} in Equation 3.58 and an expression for the conditional BER $p_{e,\text{coh}}(\varepsilon|\gamma)$ corresponding to the employed modulation scheme are required. Expressions for the conditional BER of a communication system for different digital modulation schemes are listed in Table 2.1. Thus, we obtain the ABER expression for binary, coherent and noncoherent modulations as discussed below.

1. **Binary Coherent Modulations**

   For binary coherent modulations such as BPSK and BFSK, expressions for $p_{e,\text{coh}}(\varepsilon|\gamma)$ can be obtained from the Table 2.1 by evaluating the entries for MPSK and MFSK modulations for $M = 2$. A simplified combined expression for conditional BERs is also given in Equation 2.24. Thus, putting $p_{e,\text{coh}}(\varepsilon|\gamma)$ from Equation 2.24 and $f_{\gamma_{mrc}}(\gamma_{mrc})$ from Equation 3.58 into Equation 2.17, an expression for binary coherent ABER can be given as

$$\begin{aligned} P_{e,ch} &= \frac{(1+q_1^2)(1+q_2^2)}{4q_1q_2\bar{\gamma}_1\bar{\gamma}_2(1-\rho^2)} \sum_{k_1=0}^{\infty}\sum_{k_2=0}^{\infty}\sum_{k_3=0}^{\infty}\sum_{k_4=0}^{\infty} \frac{(2k_1-1)!!(2k_2-1)!!}{\left\{\prod_{i=1}^{4} k_i!\right\}[q_1q_2]^{2k_2}[2(1-\rho^2)]^{k_3+k_4}} \\ &\times \left(\frac{1-q_1^4}{\bar{\gamma}_1 q_1^2}\right)^{k_3}\left(\frac{1-q_2^4}{\bar{\gamma}_2 q_2^2}\right)^{k_4}\left[\frac{\rho^2(1+q_1^2)(1+q_2^2)}{8\bar{\gamma}_1\bar{\gamma}_2(1-\rho^2)^2}\right]^{k_1+k_2} \frac{(k_1+\frac{1}{2})_{k_3}(k_1+\frac{1}{2})_{k_4}}{\Gamma(2k_1+k_2+k_4+2)} \\ &\times \int_0^{\infty} \gamma_{mrc}^{2k_1+k_2+k_4+1} e^{-\frac{1+q_1^2}{2(1-\rho^2)\bar{\gamma}_1 q_1^2}\gamma_{mrc}} Q\left(\sqrt{2a\gamma_{mrc}}\right) {}_1F_1\left(k_1+k_2+k_4+1;\right. \\ &\left. \times\, 2k_1+k_2+k_4+2; \frac{\bar{\gamma}_2 q_2^2(1+q_1^2)-\bar{\gamma}_1 q_1^2(1+q_2^2)}{2(1-\rho^2)\bar{\gamma}_1 q_1^2\bar{\gamma}_2 q_2^2}\gamma_{mrc}\right) d\gamma_{mrc}. \end{aligned} \tag{3.61}$$

   The integration in Equation 3.61 can be solved using [1, A-(6), A-(8a)] (reproduced in Equations B.13 and B.14, respectively) after expressing the hypergeometric function in an infinite series [4, 9.14.1] (reproduced in Equation B.11). Thus, an expression for ABER can be obtained as

$$P_{e,ch} = \frac{\sqrt{a}\bar{\gamma}_1^{\frac{3}{2}} q_1^4 \psi}{\sqrt{2\pi\zeta} q_2 \bar{\gamma}_2 (1-\rho^2)} \sum_{k_1=0}^{\infty}\sum_{k_2=0}^{\infty}\sum_{k_3=0}^{\infty}\sum_{k_4=0}^{\infty}\sum_{k_5=0}^{\infty} \frac{(2k_1-1)!!(2k_2-1)!!\left(k_1+\frac{1}{2}\right)_{k_3}}{\left\{\prod_{i=1}^{5} k_i!\right\} q_1^{2(k_2-k_4)} q_2^{2(k_2+k_4+k_5)} \zeta^{k_3+k_5}}$$
$$\times \left(\frac{\bar{\gamma}_1 \rho^2 q_1^4 \psi}{2\bar{\gamma}_2}\right)^{k_1+k_2} \frac{\left(k_1+\frac{1}{2}\right)_{k_4} (1-q_1^4)^{k_3} (k_1+k_2+k_4+1)_{k_5}}{(2k_1+k_2+k_5+2)\Gamma(2k_1+k_2+k_5+2)} \left[\tau(1-q_2^2)\right]^{k_4}$$
$$\times \Gamma\left(2k_1+k_2+k_5+\frac{5}{2}\right)\left[(1+q_1^2)(q_2^2-q_1^2\tau)\right]^{k_5}$$
$$\times {}_2F_1\left(1, 2k_1+k_2+k_5+\frac{5}{2}; 2k_1+k_2+k_5+3; \frac{1+q_1^2}{\zeta}\right), \tag{3.62}$$

where $\zeta \triangleq 1+q_1^2+2a\bar{\gamma}_1 q_1^2(1-\rho^2)$ and $\psi \triangleq \frac{(1+q_1^2)(1+q_2^2)}{\zeta^2}$.

2. **Binary Non-coherent Modulations**

For binary noncoherent modulations, expressions for the conditional BERs can be obtained by evaluating the entries in Table 2.1 for MDPSK and NCFSK, for $M=2$. A simplified combined expression for both the modulations is given in Equation 2.25. By putting $p_{e,\text{ncoh}}(\varepsilon|\gamma)$ from Equation 2.25 and $f_{\gamma_{mrc}}(\gamma_{mrc})$ from Equation 3.58 into Equation 2.17, an expression for noncoherent ABER can be given as

$$P_{e,nch} = \frac{(1+q_1^2)(1+q_2^2)}{8q_1q_2\bar{\gamma}_1\bar{\gamma}_2(1-\rho^2)} \sum_{k_1=0}^{\infty}\sum_{k_2=0}^{\infty}\sum_{k_3=0}^{\infty}\sum_{k_4=0}^{\infty} \frac{(2k_1-1)!!(2k_2-1)!!}{[q_1q_2]^{2k_2}\left\{\prod_{i=1}^{4} k_i!\right\}}$$
$$\times \left[\frac{\rho^2(1+q_1^2)(1+q_2^2)}{8\bar{\gamma}_1\bar{\gamma}_2(1-\rho^2)^2}\right]^{k_1+k_2} \left[\frac{1-q_1^4}{\bar{\gamma}_1 q_1^2}\right]^{k_3} \left[\frac{1-q_2^4}{\bar{\gamma}_2 q_2^2}\right]^{k_4} \frac{\left(k_1+\frac{1}{2}\right)_{k_3}}{[2(1-\rho^2)]^{k_3+k_4}}$$
$$\times \frac{\left(k_1+\frac{1}{2}\right)_{k_4}}{\Gamma(2k_1+k_2+k_4+2)} \int_0^{\infty} \gamma_{mrc}^{2k_1+k_2+k_4+1} e^{-\frac{1+q_1^2+2a(1-\rho^2)\bar{\gamma}_1 q_1^2}{2(1-\rho^2)\bar{\gamma}_1 q_1^2}\gamma_{mrc}}$$
$$\times {}_1F_1\left(k_1+k_2+k_4+1; 2k_1+k_2+k_4+2; \frac{\bar{\gamma}_2 q_2^2(1+q_1^2)-\bar{\gamma}_1 q_1^2(1+q_2^2)}{2(1-\rho^2)\bar{\gamma}_1 q_1^2 \bar{\gamma}_2 q_2^2}\gamma_{mrc}\right) d\gamma_{mrc}. \tag{3.63}$$

Solving the integral in Equation 3.63 using [4, (7.621.4)] (reproduced in Equation B.10), the

ABER for binary non-coherent modulations can be obtained as

$$P_{e,nch} = \frac{\bar{\gamma}_1 q_1^3 q_2 \eta(1-\rho^2)(1+q_1^2)}{2\zeta} \sum_{k_1=0}^{\infty}\sum_{k_2=0}^{\infty}\sum_{k_3=0}^{\infty}\sum_{k_4=0}^{\infty} \frac{(2k_1-1)!!(2k_2-1)!!\left(k_1+\frac{1}{2}\right)_{k_3}}{\left\{\prod_{i=1}^{4} k_i!\right\}\zeta^{k_1}(q_1q_2)^{2k_2}}$$
$$\times\left[\frac{\rho^2\bar{\gamma}_1 q_1^4 q_2^2(1+q_1^2)\eta}{2}\right]^{k_1+k_2}\left(k_1+\frac{1}{2}\right)_{k_4}(1-q_1^4)^{k_3}\left[\bar{\gamma}_1 q_1^2(1-q_2^2)\eta\right]^{k_4} \quad (3.64)$$

where $\eta \triangleq \frac{1+q_2^2}{[\bar{\gamma}_2 q_2^2\zeta - \bar{\gamma}_2 q_2^2(1+q_1^2) - \bar{\gamma}_1 q_1^2(1+q_2^2)]}$. For $\rho = 0$ and $q = 1$, which corresponds to the independent Rayleigh fading channels, Equations 3.62 and 3.64 can be simplified to [1, (32)] and [1, (26)] for $m = 1$ and $M = 2$, respectively. This verifies the correctness of the derivation.

Results and Discussion

Obtained mathematical expressions have been numerically evaluated and plotted against parameters of interest. In the numerical evaluation, δ is the average fading power decay factor [2]. In Figures 3.15 and 3.16, $P_{\text{out}}(\gamma_{th})$ vs. $\bar{\gamma}_1$ has been plotted for different modulation schemes, for different values of ρ, q_1 and q_2, for $\delta = 0$ and $\delta = 0.5$, respectively. In these plots γ_{th} has been calculated using the formula given in [1, (43)] for an ABER of 10^{-3}. The effect of branch correlation on the outage can be observed by comparing the outage values for $\rho = 0.7$ against the values for $\rho = 0$ (i.e. uncorrelated case). Clearly, with the increase in ρ the receiver suffers more outage, for a fixed value of γ_{th} and δ. Increase in δ produces more outage in the receiver for all modulation schemes, which can be seen in the plots. These results have been verified against the results in [2], which is a special case of the results presented here, and is found to be matching closely.

For binary, coherent and non-coherent modulations, ABER vs. $\bar{\gamma}$ curves have been plotted in Figures 3.17 and 3.18, respectively. It can be observed that the ABER performance degrades with the increase in ρ and δ for both the modulation schemes presented here. In the numerical evaluation of expressions involving infinite series we have truncated them suitably so as to achieve an accuracy in ABER at least at 7^{th} place of decimal digit. In Table 3.2, we have illustrated the number of terms required to achieve this accuracy in the evaluation of Equation 3.62 as a function of $\bar{\gamma}_1$, ρ, q_1 and q_2

Table 3.2: Number of terms (N) required for an accuracy at 7^{th} place of decimal digit in the numerical evaluation of Equation 3.62 for $\delta = 0$.

$\bar{\gamma}_1$ (dB)	ρ	$q_1 = 0.5, q_2 = 0.6$		$q_1 = 0.9, q_2 = 0.8$	
		N	ABER	N	ABER
6	0.2	14	0.0102545	4	0.0084477
	0.7	16	0.0150131	4	0.0121738
12	0.2	4	0.0009440	2	0.0007164
	0.7	7	0.0015787	3	0.0012323

with $\delta = 0$.

In each figure, result obtained by Monte Carlo simulations has also been shown and it can be observed that the simulation results are in close agreement with the numerical results.

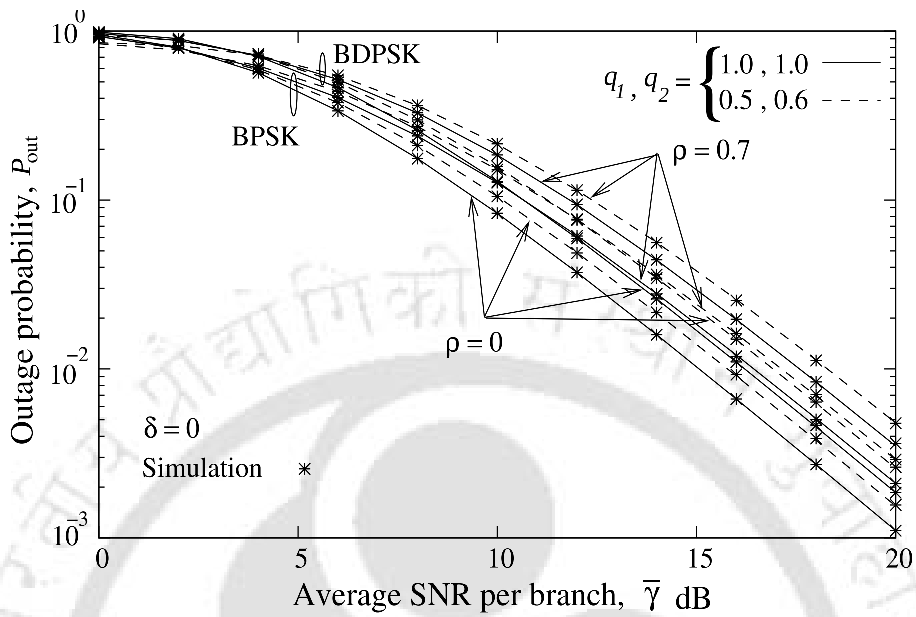

Figure 3.15: Probability of outage for an ABER of 10^{-3} and average fading power decay factor $\delta = 0$.

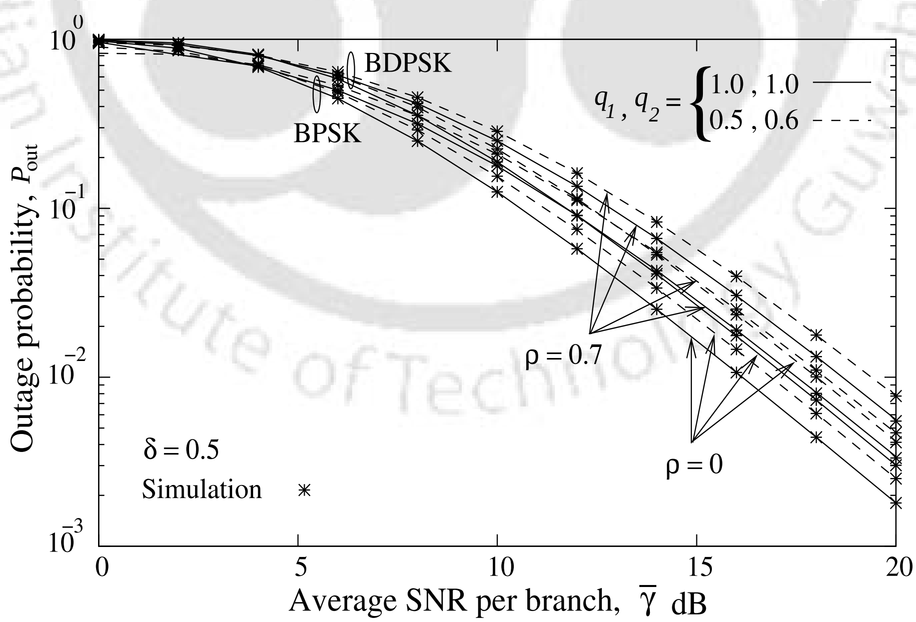

Figure 3.16: Probability of outage for an ABER of 10^{-3} and average fading power decay factor $\delta = 0.5$.

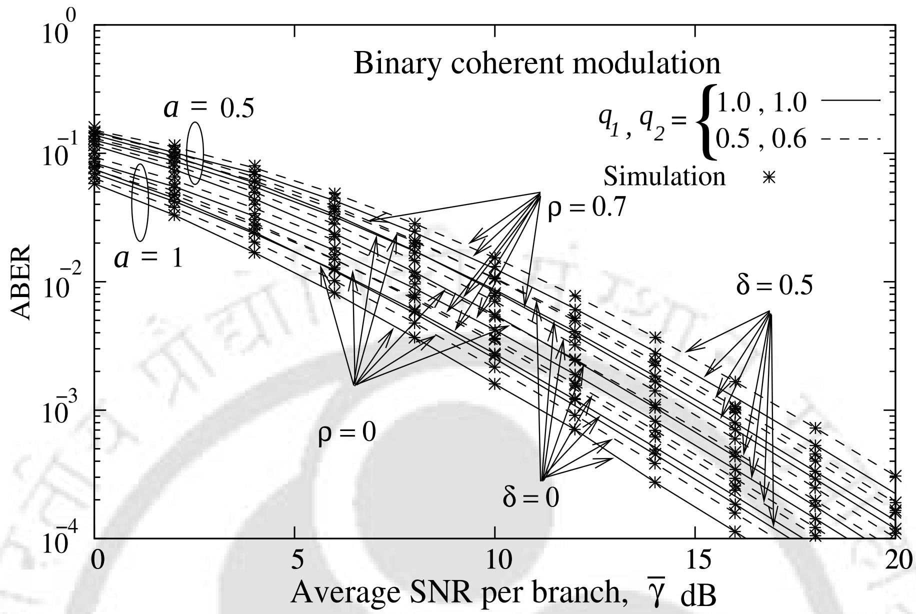

Figure 3.17: ABER vs. $\bar{\gamma}$ for correlated dual-MRC receiver with binary coherent modulations.

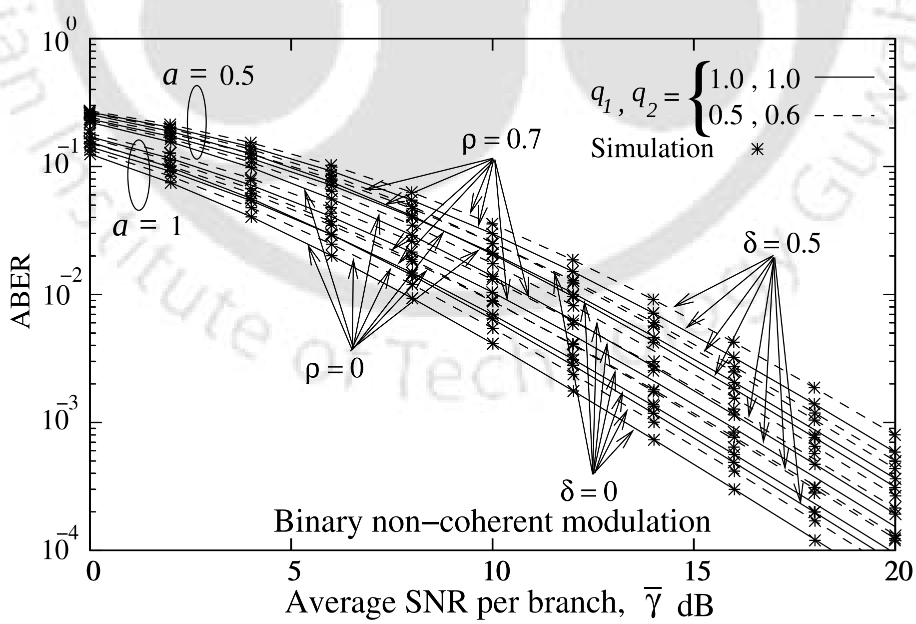

Figure 3.18: ABER vs. $\bar{\gamma}$ for correlated dual-MRC receiver with binary noncoherent modulations.

3.3.3 Equal Gain Combining Receiver

The practical importance of EGC receiver is more due to its closeness of performance to the optimum MRC receiver [3]. For Hoyt fading channels, performance of EGC receiver is presented in [17]. For dual correlated Hoyt fading channels second order statistics and outage probability performance have been presented in [32] and [36], respectively. However, the ABER is the most important performance measure for any communication system [60]. In this section, ABER performance analysis of a dual correlated EGC receiver over Hoyt fading channels is presented.

PDF of EGC Output Signal-to-Noise Ratio

A mathematical expression for the output SNR γ_{egc} of a dual EGC combiner can be given from the Equation 2.12 as $\gamma_{egc} = \frac{E_b}{2N_0}(\alpha_1+\alpha_2)^2$. An expression for the joint PDF of correlated α_1^2 and α_2^2 is derived in Appendix and is given in Equation A.29. From this PDF, an expression for the joint PDF of α_1 and α_2 can be derived by applying the concept of transformation of RVs as

$$f_{\alpha_1,\alpha_2}(\alpha_1,\alpha_2) = \frac{\alpha_1\alpha_2}{(\sigma_x\sigma_y)^2(1-\rho^2)}\sum_{k_1=0}^{\infty}\sum_{k_2=0}^{\infty}\frac{(2k_1-1)!!(2k_2-1)!!}{k_1!k_2!\Gamma^2(k_1+k_2+1)}\left[\frac{\rho\alpha_1\alpha_2}{\sigma_x^2\sqrt{8}(1-\rho^2)}\right]^{2(k_1+k_2)} \times P(\alpha_1)P(\alpha_2)e^{-\frac{(\alpha_1^2+\alpha_2^2)}{2(1-\rho^2)\sigma_y^2}}, \quad (3.65)$$

where $P(\alpha_l) \triangleq {}_1F_1\left(k_1+\frac{1}{2};k_1+k_2+1;\frac{(\sigma_x^2-\sigma_y^2)\alpha_l^2}{2(1-\rho^2)\sigma_y^2\sigma_x^2}\right)$. For $\rho=0$ and $\sigma_x=\sigma_y$, it can be shown that Equation 3.65 becomes the product of two Rayleigh PDFs, which is as expected. From Equation 3.65, an expression for the PDF of $\alpha=\alpha_1+\alpha_2$ can be obtained by using the formula [59, (6.44)] as

$$f_\alpha(\alpha) = \frac{1}{q^2(1-\rho^2)}\sum_{k_1=0}^{\infty}\sum_{k_2=0}^{\infty}\sum_{k_3=0}^{\infty}\sum_{k_4=0}^{\infty}\frac{\rho^{2(k_1+k_2)}(2k_1-1)!!(2k_2-1)!!}{\left\{\prod_{i=1}^{4}k_i!\right\}2^{3k_1+2k_2+k_4}(1-\rho^2)^{2k_1+k_2+k_4}} \times\left(\frac{1-q^2}{q^2}\right)^{k_3+k_4}\frac{\left(k_1+\frac{1}{2}\right)_{k_3}\left(k_1+\frac{1}{2}\right)_{k_4}e^{-\frac{\alpha^2}{2(1-\rho^2)q^2}}}{\Gamma^2(k_1+k_2+1)\,(k_1+k_2+1)_{k_3}\,(k_1+k_2+1)_{k_4}} \times\int_0^{\alpha}\alpha_1^{2(k_1+k_3)+1}(\alpha-\alpha_1)^{2(k_1+k_2+k_4)+1}e^{-\frac{1}{(1-\rho^2)q^2}\alpha_1^2}e^{\frac{h}{(1-\rho^2)q^2}\alpha_1}d\alpha_1. \quad (3.66)$$

Expressing the exponential terms in Equation 3.66 in infinite series [61] and applying Binomial expansion to $(\alpha - \alpha_1)^{2(k_1+k_2+k_4)+1}$ by [4, 1.111] (reproduced in Equation B.5), an expression for the PDF of α can be given as

$$\begin{aligned} f_\alpha(\alpha) &= \frac{1}{q^2(1-\rho^2)} \sum_{k_1=0}^{\infty}\sum_{k_2=0}^{\infty}\sum_{k_3=0}^{\infty}\sum_{k_4=0}^{\infty} \sum_{k_6=0}^{2(k_1+k_2+k_4)+1} (-1)^{k_6} \frac{\rho^{2k_1+2k_2}(2k_1-1)!!(2k_2-1)!!}{\left\{\prod_{i=1}^{5} k_i!\right\} 2^{3k_1+2k_2+k_4}} \\ &\times \frac{\left(k_1+\frac{1}{2}\right)_{k_3}\left(k_1+\frac{1}{2}\right)_{k_4}}{(1-\rho^2)^{2k_1+k_2+k_4}\Gamma^2(k_1+k_2+1)\,(k_1+k_2+1)_{k_3}\,(k_1+k_2+1)_{k_4}} \left(\frac{1-q^2}{q^2}\right)^{k_3+k_4} \\ &\times \binom{2(k_1+k_2+k_4)+1}{k_6} \left(\frac{1}{(1-\rho^2)q^2}\right)^{k_5} e^{-\frac{\alpha^2}{2(1-\rho^2)q^2}} \alpha^{2(k_1+k_2+k_4)+k_5+1-k_6} \\ &\times \int_0^{\alpha} \alpha_1^{2k_1+2k_3+k_5+k_6+1} e^{-\frac{\alpha_1^2}{(1-\rho^2)q^2}} d\alpha_1. \end{aligned} \tag{3.67}$$

Performing the integration in Equation 3.67 using [4, 3.381.1] (reproduced in Equation B.6), an expression for $f_\alpha(\alpha)$ can be given as

$$\begin{aligned} f_\alpha(\alpha) &= \frac{\alpha}{2} \sum_{k_1=0}^{\infty}\sum_{k_2=0}^{\infty}\sum_{k_3=0}^{\infty}\sum_{k_4=0}^{\infty}\sum_{k_5=0}^{\infty} \sum_{k_6=0}^{2k_1+2k_2+2k_4+1} (-1)^{k_6} \frac{(2k_1-1)!!(2k_2-1)!!\left(k_1+\frac{1}{2}\right)_{k_4}}{\left\{\prod_{i=1}^{5} k_i!\right\}(k_1+k_2+1)_{k_3}} \\ &\times \left(\frac{\rho q^2}{\sqrt{8}}\right)^{2(k_1+k_2)} \left(\frac{1-q^2}{2}\right)^{k_3+k_4} \frac{\left(k_1+\frac{1}{2}\right)_{k_3}(\zeta\alpha)^{2(k_1+k_2+k_4)+k_5-k_6}}{\Gamma^2(k_1+k_2+1)\,(k_1+k_2+1)_{k_4}\, e^{(\zeta\alpha)^2/2}} \\ &\times \binom{2k_1+2k_2+2k_4+1}{k_6} g\left(\frac{2k_1+2k_3+k_5+k_6+2}{2}, (\zeta\alpha)^2\right), \end{aligned} \tag{3.68}$$

where $\zeta \triangleq \frac{1}{q\sqrt{(1-\rho^2)}}$. From Equation 3.68, an expression for the PDF of $\gamma_{egc} = \alpha^2 E_b/2N_0$ can be obtained as

$$\begin{aligned} f_{\gamma_{egc}}(\gamma_{egc}) &= \frac{1+q^2}{2\bar{\gamma}} \sum_{k_1=0}^{\infty}\sum_{k_2=0}^{\infty}\sum_{k_3=0}^{\infty}\sum_{k_4=0}^{\infty}\sum_{k_5=0}^{\infty} \sum_{k_6=0}^{2k_1+2k_2+2k_4+1} (-1)^{k_6} \frac{(2k_1-1)!!(2k_2-1)!!\left(k_1+\frac{1}{2}\right)_{k_3}}{\left\{\prod_{i=1}^{5} k_i!\right\} 2^{k_3-\frac{k_5-k_6}{2}}} \\ &\times \left(\frac{\rho q^2}{2}\right)^{2k_1+2k_2} \binom{2k_1+2k_2+2k_4+1}{k_6} \frac{\left(k_1+\frac{1}{2}\right)_{k_4}(1-q^2)^{k_3+k_4} e^{-\frac{(1+q^2)\zeta^2}{\bar{\gamma}}\gamma_{egc}}}{\Gamma(k_1+k_2+k_3+1)\,\Gamma(k_1+k_2+k_4+1)} \end{aligned}$$

$$\times\left(\frac{\gamma_{egc}(1+q^2)\zeta^2}{\bar{\gamma}}\right)^{k_1+k_2+k_4+\frac{k_5-k_6}{2}} g\left(\frac{2k_1+2k_3+k_5+k_6+2}{2}, \frac{2(1+q^2)\zeta^2\gamma_{egc}}{\bar{\gamma}}\right). \tag{3.69}$$

Average Bit Error Rate

ABER performance of a diversity communication system is defined in Section 2.3 and a general mathematical expression is given in Equation 2.17. To obtain an expression for the ABER of a correlated EGC receiver, the obtained expression for the PDF of output SNR γ_{egc} in Equation 3.69 and an expression for the conditional BER $p_{e,\text{coh}}(\varepsilon|\gamma)$ corresponding to the employed modulation scheme are required. Expressions for the $p_{e,\text{coh}}(\varepsilon|\gamma)$ of a communication system for different digital modulation schemes are listed in Table 2.1. Thus, we obtain the ABER expression for binary, coherent and noncoherent modulations as discussed below.

1. **Binary Coherent Modulations**

   For binary coherent modulations such as BPSK and BFSK, expressions for $p_{e,\text{coh}}(\varepsilon|\gamma)$ can be obtained from the Table 2.1 by evaluating the entries for MPSK and MFSK modulations, for $M=2$. A simplified combined expression for both the conditional BERs is obtained and is given in Equation 2.24. Thus, putting $p_{e,\text{coh}}(\varepsilon|\gamma)$ from Equation 2.24 and $f_{\gamma_{egc}}(\gamma_{egc})$ from Equation 3.69 into Equation 2.17, an expression for ABER can be given as

$$\begin{aligned} P_{e,ch}(\bar{\gamma}) = & \frac{(1+q^2)}{2\bar{\gamma}} \sum_{k_1=0}^{\infty}\sum_{k_2=0}^{\infty}\sum_{k_3=0}^{\infty}\sum_{k_4=0}^{\infty}\sum_{k_5=0}^{\infty}\sum_{k_6=0}^{2(k_1+k_2+k_4)+1}(-1)^{k_6}\frac{(2k_1-1)!!}{\left\{\prod_{i=1}^{5}k_i!\right\}2^{2k_1+k_2-\frac{k_5-k_6}{2}}} \\ & \times\frac{(2k_2-1)!!\rho^{2k_1+2k_2}\left(1-q^2\right)^{k_3+k_4}\left(k_1+\frac{1}{2}\right)_{k_3}\left(k_1+\frac{1}{2}\right)_{k_4}q^{k_6-k_5}}{(1-\rho^2)^{k_1+k_2+k_4-k_3+\frac{k_5-k_6}{2}}\Gamma^2(k_1+k_2+1)\left(k_1+k_2+1\right)_{k_3}\left(k_1+k_2+1\right)_{k_4}} \\ & \times\binom{2(k_1+k_2+k_4)+1}{k_6}\left(\frac{1+q^2}{\bar{\gamma}}\right)^{k_1+k_2+k_4+\frac{k_5-k_6}{2}}\int_0^{\infty}\gamma_{egc}^{k_1+k_2+k_4+\frac{k_5-k_6}{2}} \\ & \times e^{-\frac{(1+q^2)}{\bar{\gamma}(1-\rho^2)q^2}\gamma_{egc}}Q\left(\sqrt{2a\gamma_{egc}}\right)g\left(k_1+k_3+\frac{k_5+k_6}{2}+1, \frac{2(1+q^2)}{(1-\rho^2)\bar{\gamma}q^2}\gamma_{egc}\right)d\gamma_{egc}. \end{aligned}$$

(3.70)

Expressing $Q(\cdot)$ function in terms of incomplete gamma function (using [1, A-(8a)]) (reproduced in Equation B.14), Equation 3.70 can be rewritten as

$$P_{e,ch}(\bar{\gamma}) = \frac{(1+q^2)}{4\sqrt{\pi}\bar{\gamma}} \sum_{k_1=0}^{\infty}\sum_{k_2=0}^{\infty}\sum_{k_3=0}^{\infty}\sum_{k_4=0}^{\infty}\sum_{k_5=0}^{\infty}\sum_{k_6=0}^{2(k_1+k_2+k_4)+1} (-1)^{k_6} \frac{(2k_1-1)!!}{\left\{\prod_{i=1}^{5} k_i!\right\} 2^{2k_1-\frac{k_5-k_6}{2}}}$$
$$\times \frac{(2k_2-1)!!\,(1-q^2)^{k_3+k_4}\,\rho^{2k_1+2k_2}\left(k_1+\frac{1}{2}\right)_{k_3}\left(k_1+\frac{1}{2}\right)_{k_4} q^{k_6-k_5}}{(1-\rho^2)^{k_1+k_2+k_4-k_3-\frac{k_6-k_5}{2}}\,\Gamma^2(k_1+k_2+1)\,(k_1+k_2+1)_{k_3}\,(k_1+k_2+1)_{k_4}}$$
$$\times \binom{2(k_1+k_2+k_4)+1}{k_6} \left(\frac{1+q^2}{\bar{\gamma}}\right)^{k_1+k_2+k_4+\frac{k_5-k_6}{2}} \int_0^{\infty} \gamma_{egc}^{k_1+k_2+k_4+\frac{k_5-k_6}{2}}$$
$$\times e^{-\frac{(1+q^2)}{\bar{\gamma}(1-\rho^2)q^2}\gamma_{egc}}\,\Gamma\left(\frac{1}{2}, a\gamma_{egc}\right) g\left(k_1+k_3+\frac{k_5+k_6}{2}+1, \frac{2(1+q^2)}{(1-\rho^2)\bar{\gamma}q^2}\gamma_{egc}\right) d\gamma_{egc}. \tag{3.71}$$

The incomplete gamma function $g(a,x)$ can be expressed in terms of confluent hypergeometric function using [5, (6.5.12)] which can further be expressed in infinite series form using [4, 9.14.1] (reproduced in Equation B.11). The resulting integral can be solved using [1, A-(6)] (reproduced in Equation B.13). Thus, an expression for the coherent ABER be obtained as

$$P_{e,ch}(\bar{\gamma}) = \frac{q^7\rho^2\psi^{\frac{9}{2}}}{(1-\rho^2)^{\frac{3}{2}}}\sqrt{\frac{a\bar{\gamma}}{\pi(1+q^2)}} \sum_{k_1=0}^{\infty}\sum_{k_2=0}^{\infty}\sum_{k_3=0}^{\infty}\sum_{k_4=0}^{\infty}\sum_{k_5=0}^{\infty}\sum_{k_6=0}^{2(k_1+k_2+k_4)+1}\sum_{k_7=0}^{\infty} (-1)^{k_6}(2k_1-1)!!$$
$$\times \frac{(2k_2-1)!!\,\Gamma\left(\frac{2k_1+2k_2+k_3+k_4+k_5+k_7+5}{2}\right)\left(k_1+\frac{1}{2}\right)_{k_3}\left(k_1+\frac{1}{2}\right)_{k_4}}{2^{k_1+k_2+k_5+k_7}\left\{\prod_{i=1}^{5} k_i!\right\}\Gamma^2(k_1+k_2+1)\,(2(k_1+k_2+k_3+1)+k_5+k_6)}$$
$$\times \frac{(1-q^2)^{k_3+k_4}\psi^{k_3+k_4+k_5+k_7}}{(k_1+k_2+1)_{k_4}(k_1+k_2+1)_{k_3}} \binom{2(k_1+k_2+k_4)+1}{k_6}$$
$$\times \frac{{}_2F_1\left(1, \frac{2k_1+2k_2+k_3+k_4+k_5+k_7+5}{2}; 2k_1+2k_2+k_3+k_4+k_5+k_7+3; 3\psi\right)}{(2k_1+2k_2+k_3+k_4+k_5+k_7+2)\left(\frac{2(k_1+k_2+k_3+2)+k_5+k_6}{2}\right)_{k_7}}, \tag{3.72}$$

where $\psi \triangleq \frac{(1+q^2)}{3(1+q^2)+a\bar{\gamma}(1-\rho^2)q^2}$.

2. **Binary Non-coherent Modulations**

For binary noncoherent modulations, the conditional BER is given in Equation 2.25. By putting $p_{e,\mathrm{ncoh}}(\varepsilon|\gamma)$ and $f_{\gamma_{egc}}(\gamma_{egc})$ from Equations 2.25 and 3.69 into Equation 2.17, an expression for noncoherent ABER can be given as

$$\begin{aligned}P_{e,nch}(\bar{\gamma}) &= \frac{1+q^2}{4\bar{\gamma}}\sum_{k_1=0}^{\infty}\sum_{k_2=0}^{\infty}\sum_{k_3=0}^{\infty}\sum_{k_4=0}^{\infty}\sum_{k_5=0}^{\infty}\sum_{k_6=0}^{2(k_1+k_2+k_4)+1}[-1]^{k_6}\frac{(2k_1-1)!!(2k_2-1)!!}{\left\{\prod_{i=1}^{5}k_i!\right\}2^{\frac{2(k_1+k_2)+k_3-(k_5-k_6)}{2}}}\\ &\times\frac{\left(1-q^2\right)^{k_3+k_4}\left(k_1+\frac{1}{2}\right)_{k_3}\left(k_1+\frac{1}{2}\right)_{k_4}}{\Gamma(k_1+k_2+k_3+1)\Gamma(k_1+k_2+k_4+1)}\left(\frac{\gamma_{egc}(1+q^2)\zeta^2}{\bar{\gamma}}\right)^{\frac{2(k_1+k_2+k_4)+k_5-k_6}{2}}\\ &\times\left(\rho q^2\right)^{2(k_1+k_2)}\begin{pmatrix}2(k_1+k_2+k_4)+1\\ k_6\end{pmatrix}\int_0^{\infty}\gamma_{egc}^{\frac{2(k_1+k_2+k_4)+k_5-k_6}{2}}e^{-\frac{(1+q^2)\zeta^2+a\bar{\gamma}}{\bar{\gamma}}\gamma_{egc}}\\ &\times g\left(\frac{2(k_1+k_2+k_3)+k_5+k_6+2}{2},\frac{2(1+q^2)\zeta^2\gamma_{egc}}{\bar{\gamma}}\right)d\gamma_{egc}. \qquad (3.73)\end{aligned}$$

The integral in the above expression can be solved using [4, (6.455.2)] (reproduced in Equation B.9). Thus, an expression for the noncoherent ABER can be obtained as

$$\begin{aligned}P_{e,nch}(\bar{\gamma}) &= q^2(1-\rho^2)\psi^2\sum_{k_1=0}^{\infty}\sum_{k_2=0}^{\infty}\sum_{k_3=0}^{\infty}\sum_{k_4=0}^{\infty}\sum_{k_5=0}^{\infty}\sum_{k_6=0}^{2(k_1+k_2+k_4)+1}(-1)^{k_6}\frac{(2k_1-1)!!(2k_2-1)!!}{\left\{\prod_{i=1}^{5}k_i!\right\}2^{k_1+k_2-k_5}}\\ &\times\frac{\Gamma(2k_1+2k_2+k_3+k_4+k_5+2)\left(k_1+\frac{1}{2}\right)_{k_3}\left(k_1+\frac{1}{2}\right)_{k_4}}{\Gamma^2(k_1+k_2+1)(k_1+k_2+1)_{k_3}(k_1+k_2+1)_{k_4}(2(k_1+k_2+k_3+1)+k_5+k_6)}\\ &\times\begin{pmatrix}2(k_1+k_2+k_4)+1\\ k_6\end{pmatrix}\left[\rho q^2\right]^{2(k_1+k_2)}\psi^{2(k_1+k_2)+k_3+k_4+k_5}\left[1-q^2\right]^{k_3+k_4}\\ &\times{}_2F_1\left(1,2k_1+2k_2+k_3+k_4+k_5+2;\frac{2(k_1+k_2+k_3+2)+k_5+k_6}{2};2\psi\right).\end{aligned}$$

(3.74)

Results and Discussion

Obtained mathematical expressions of ABER Equations 3.72 and 3.74 have been numerically evaluated and plotted for parameters of interest. For CPSK and CFSK modulations, ABER vs. $\bar{\gamma}$ curves have been plotted in Figure 3.19. As expected, ABER degrades with increase in ρ when q is kept constant. The ABER decrease with decrease in q, which indicates increase in fading severity, as expected . These numerical results are compared with the available special case results in [62] and found to be matching. The ABER plot for DPSK and NCFSK modulations are shown in Figure 3.20 and similar effect of q and ρ on the ABER performance can be observed. To compare the closeness of the ABER performance, between EGC and MRC we obtained the difference in SNR (compared Figure 3.12 with Figure 3.13) receivers to achieve a given ABER. Over a range of ABER values we found that the average difference in SNR is around 0.56 dB.

A Monte Carlo simulation of the EGC receiver has been performed and the simulation results are plotted in respective figures for coherent and non-coherent modulations. The numerical results are in close agreement with the simulation results. In addition, we have studied the effect of correlation on the excess SNR[3] required for a desired ABER and a plot is given in Figure 3.21. It can be observed that similar to MRC receiver [63], the required excess SNR is relatively small for ρ lying below 0.5 than it is otherwise. In the numerical evaluation of expressions involving infinite series we have truncated them suitably so as to achieve an accuracy at least at 6^{th} place of decimal digit. In Table 3.3, we have illustrated the number of terms (N) required to achieve an accuracy of 10^{-6} in the evaluation of Equation 3.74 as a function of $\bar{\gamma}$ and ρ.

[3] Defined in the footnote of Section 3.3.1.

Table 3.3: Number of terms (N) required for an accuracy at 6^{th} place of decimal digit in the numerical evaluation of Equation 3.74.

$\bar{\gamma}$(dB)	ρ	$q = 0.5$		$q = 1$	
		N	ABER	N	ABER
8	0	14	0.015953	11	0.011849
	0.5	15	0.018654	12	0.014372
16	0	5	0.000600	4	0.000396
	0.5	5	0.000777	4	0.000518

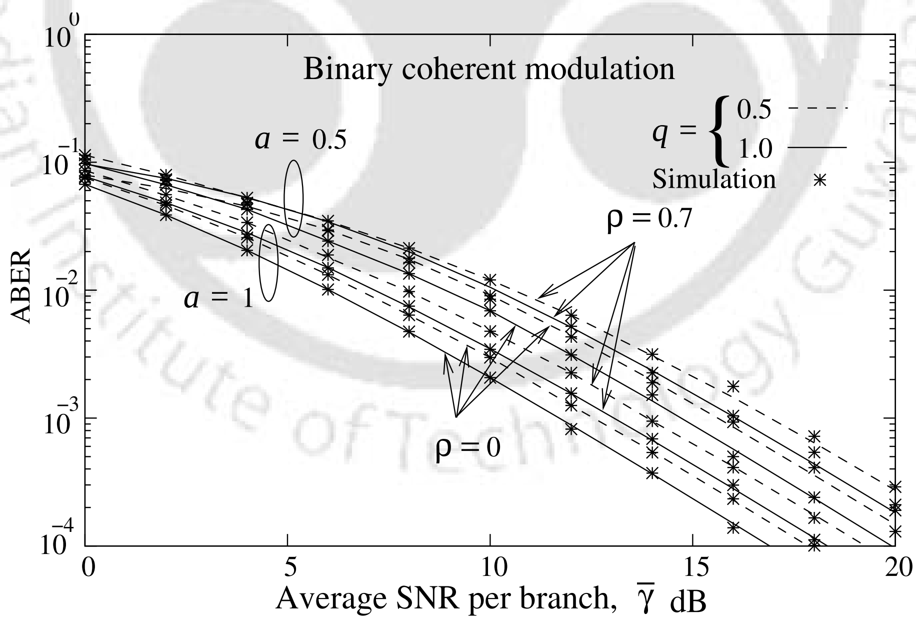

Figure 3.19: ABER vs. $\bar{\gamma}$ for EGC receiver with coherent modulations.

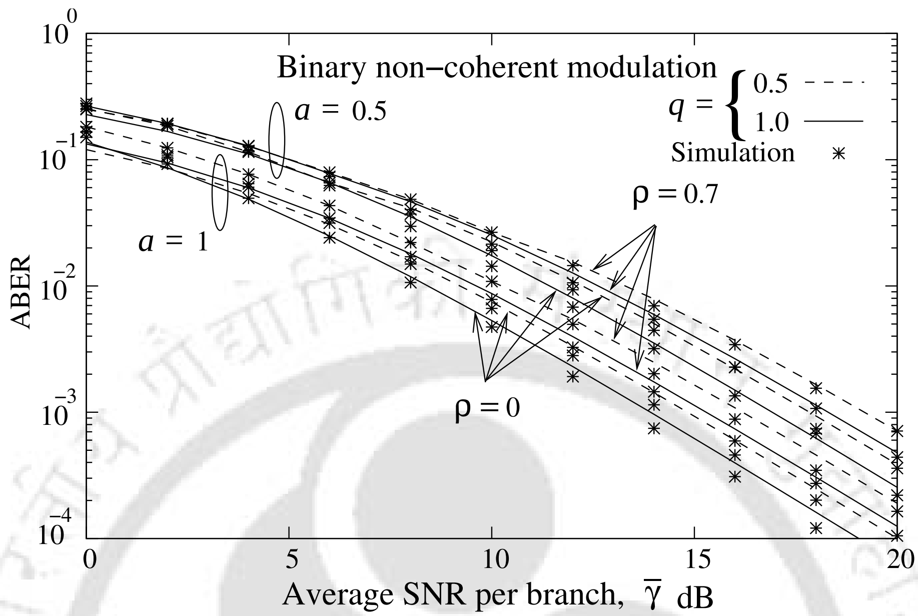

Figure 3.20: ABER vs. $\bar{\gamma}$ for EGC receiver with noncoherent modulations.

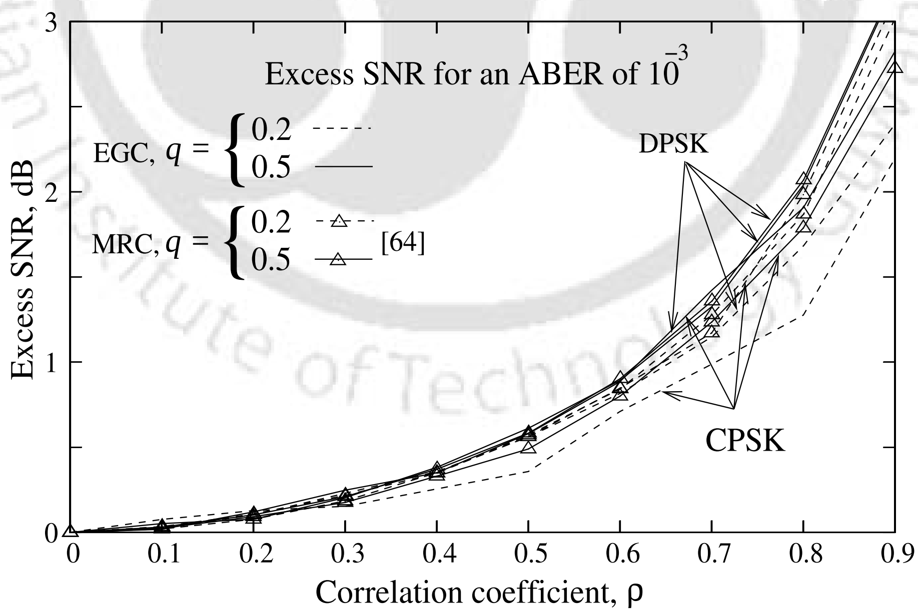

Figure 3.21: Excess SNR vs. correlation coefficient for EGC receiver for CPSK and DPSK modulations.

3.3.4 Selection Combining Receiver

Analysis of SC receiver has been presented for independent fading channels in Section 3.1. Due to the infeasibility of placing receiving antennas wide apart on mobile terminals, analysis of diversity receivers with correlated branches becomes necessary. The analysis of a SC receiver with correlated input signals requires the knowledge of the joint PDF of the correlated input signals. Below we explain analytical steps to obtain the PDF of the output SNR from the joint PDF which enables to carry out the performance analysis by the PDF based approach as given in Section 2.3.1.

PDF of Combiner Output SNR

An expression for the joint PDF of bivariate Hoyt RVs α_1 and α_2 with correlation coefficient ρ is obtained in Equation 3.65. The CDF of the output envelope α of the combiner can be obtained from this correlated joint PDF of α_1 and α_2, w.r.t. α_1 and α_2, as

$$F_\alpha(\alpha) = P(\alpha_1 \leq \alpha, \alpha_2 \leq \alpha) = \int_0^\alpha \int_0^\alpha f_{\alpha_1\alpha_2}(\alpha_1,\alpha_2)\, d\alpha_1 d\alpha_2. \tag{3.75}$$

Putting Equation 3.65 into Equation 3.75 and expressing the involved hypergeometric functions in infinite series [4, 9.14.1] (reproduced in Equation B.11), the above expression can be written as

$$\begin{aligned} F_\alpha(\alpha) = {} & \frac{1}{\sigma_x^2\sigma_y^2(1-\rho^2)} \sum_{k_1=0}^{\infty}\sum_{k_2=0}^{\infty}\sum_{k_3=0}^{\infty}\sum_{k_4=0}^{\infty} \frac{\rho^{2k_1+2k_2}(2k_1-1)!!(2k_2-1)!!}{\left\{\prod_{i=1}^{4} k_i!\right\}(\sigma_x^2(1-\rho^2))^{2k_1+2k_2+k_3+k_4}} \\ & \times \frac{\left(k_1+\frac{1}{2}\right)_{k_3}\left(k_1+\frac{1}{2}\right)_{k_4}}{2^{3k_1+3k_2+k_3+k_4}\Gamma^2(k_1+k_2+1)\,(k_1+k_2+1)_{k_3}\,(k_1+k_2+1)_{k_4}} \left(\frac{\sigma_x^2-\sigma_y^2}{\sigma_y^2}\right)^{k_3+k_4} \\ & \times \int_0^\alpha \alpha_1^{2(k_1+k_2+k_3)+1} e^{-\frac{1}{2(1-\rho^2)\sigma_y^2}\alpha_1^2} d\alpha_1 \int_0^\alpha \alpha_2^{2(k_1+k_2+k_4)+1} e^{-\frac{1}{2(1-\rho^2)\sigma_y^2}\alpha_2^2} d\alpha_2. \end{aligned} \tag{3.76}$$

Solving the integral using [4, (3.381.1)] (reproduced in Equation B.6), the above expression can be given as

$$F_\alpha(\alpha) = q^2(1-\rho^2)\sum_{k_1=0}^{\infty}\sum_{k_2=0}^{\infty}\sum_{k_3=0}^{\infty}\sum_{k_4=0}^{\infty}\frac{(2k_1-1)!!(2k_2-1)!!\left(k_1+\frac{1}{2}\right)_{k_3}\left(k_1+\frac{1}{2}\right)_{k_4}}{\left\{\prod_{i=1}^{4}k_i!\right\}\Gamma^2(k_1+k_2+1)(k_1+k_2+1)_{k_3}}$$
$$\times\left(\frac{\rho q^2}{2}\right)^{2(k_1+k_2)}\frac{\left(1-q^2\right)^{k_3+k_4}}{(k_1+k_2+1)_{k_4}}g\left(k_1+k_2+k_3+1,\frac{\alpha^2}{2q^2(1-\rho^2)}\right)$$
$$\times g\left(k_1+k_2+k_4+1,\frac{\alpha^2}{2q^2(1-\rho^2)}\right). \tag{3.77}$$

An expression for the PDF of α can be obtained by the differentiation of $F(\alpha)$ in Equation 3.77 w.r.t. α. From the relation $\gamma_{sc}=\frac{E_b}{N_0}\alpha^2$, the PDF of the combiner output SNR $f_{\gamma_{sc}}(\gamma_{sc})$ can be obtained by the transformation of RV. Putting the values of σ_x, σ_x and $\frac{E_b}{N_0}$ as discussed in Section A.1 followed by necessary algebraic manipulations, an expression for the PDF of the correlated dual-SC output SNR γ_{sc}, can be given as

$$f_{\gamma_{sc}}(\gamma_{sc}) = \frac{1+q^2}{2\pi q^2\bar{\gamma}}\sum_{k_1=0}^{\infty}\sum_{k_2=0}^{\infty}\sum_{k_3=0}^{\infty}\sum_{k_4=0}^{\infty}\frac{\rho^{2(k_1+k_2)}\zeta_1^{2k_1+2k_2+k_3+k_4}\gamma_{sc}^{2k_1+2k_2+k_3+k_4+1}e^{-\frac{2\zeta_1}{q^2}\gamma_{sc}}}{\left\{\prod_{i=1}^{4}k_i!\right\}\left(k_1+k_3+\frac{1}{2}\right)_{k_2+\frac{1}{2}}\left(k_1+k_4+\frac{1}{2}\right)_{k_2+\frac{1}{2}}}$$
$$\times\left(\frac{1-q^2}{q^2}\right)^{k_3+k_4}\left\{\frac{{}_1F_1\left(1;k_1+k_2+k_3+2;\frac{\zeta_1}{q^2}\gamma_{sc}\right)}{k_1+k_2+k_3+1}\right.$$
$$\left.+\frac{{}_1F_1\left(1;k_1+k_2+k_4+2;\frac{\zeta_1}{q^2}\gamma_{sc}\right)}{k_1+k_2+k_4+1}\right\}, \tag{3.78}$$

where $\zeta_1 \triangleq \frac{1+q^2}{2\bar{\gamma}(1-\rho^2)}$. For $\rho=0$ and $q=1$, Equation 3.78 can be shown reduces to $f_{\gamma_{sc}}(\gamma_{sc}) = \frac{2}{\bar{\gamma}}e^{-\frac{\gamma_{sc}}{\bar{\gamma}}}\left(1-e^{-\frac{\gamma_{sc}}{\bar{\gamma}}}\right)$ which is same as the result in [10, (7.60)]. Also, for independent fading channels i.e., $\rho=0$, Equation 3.78 can be simplified to the obtained expression in Equation 3.6 for $L=2$.

Upper Bound on Truncation Error

It can be observed that Equation 3.78 consists of four infinite series. In the numerical evaluation, it is practicable to include a finite number of terms for each series in the sum. This results in a truncation error of the expression. Considering equal number of terms 'K' of each infinite series in the sum, it can be shown that the truncation error thus occurs has an upper bound. This upper bound is derived in Section A.10.4 in Appendix. This expression can be given as

$$\begin{aligned} E_K \leq & \frac{2(1-\rho^2)[(1-q)\rho^2]^{2K} B^2\left(2K+\frac{1}{2}, K+\frac{1}{2}\right)}{\pi(3K+1)q^{2K+2}(K!)^4\Gamma^2(K+\frac{1}{2})} \zeta_1^{6K+2}\gamma_{sc}^{6K+1} e^{-\frac{2\zeta_1}{q^2}\gamma_{sc}} \\ & \times {}_1F_1\left[\begin{matrix} 1 & \frac{\zeta_1(1-q^2)\gamma_{sc}}{q^2} \\ K+1 & \end{matrix}\right]^2 {}_1F_1\left(1; 3K+2; \frac{\zeta_1\gamma_{sc}}{q^2}\right) {}_1F_1\left[\begin{matrix} 1 & (\rho\zeta_1\gamma_{sc})^2 \\ K+1 & \end{matrix}\right] \\ & \times {}_1F_3\left[\begin{matrix} 1 & & & (\rho\zeta_1\gamma_{sc})^2 \\ K+1 & K+\frac{1}{2} & K+\frac{1}{2} & \end{matrix}\right]. \end{aligned} \tag{3.79}$$

Moments of Output Signal-to-Noise Ratio

The definition of moment is given in Equation 3.9. Putting Equation 3.78 into Equation 3.9, an expression for the N^{th} moment of γ_{sc} can be given as

$$\begin{aligned} E[\gamma_{sc}^N] = & \frac{\zeta_1^2(1-\rho^2)}{\pi q^2} \sum_{k_1=0}^{\infty}\sum_{k_2=0}^{\infty}\sum_{k_3=0}^{\infty}\sum_{k_4=0}^{\infty} \frac{\rho^{2(k_1+k_2)}\zeta_1^{2k_1+2k_2+k_3+k_4}}{\left\{\prod_{i=1}^{4} k_i!\right\}\left(k_1+k_3+\frac{1}{2}\right)_{k_2+\frac{1}{2}}\left(k_1+k_4+\frac{1}{2}\right)_{k_2+\frac{1}{2}}} \\ & \times \left(\frac{1-q^2}{q^2}\right)^{k_3+k_4} \left\{ \frac{1}{k_1+k_2+k_4+1} \int_0^{\infty} \gamma_{sc}^{2k_1+2k_2+k_3+k_4+N+1} e^{-\frac{2\zeta_1}{q^2}\gamma_{sc}} \right. \\ & \times {}_1F_1\left(1; k_1+k_2+k_4+2; \frac{\zeta_1}{q^2}\gamma_{sc}\right) d\gamma_{sc} + \frac{1}{k_1+k_2+k_3+1} \\ & \left. \times \int_0^{\infty} \gamma_{sc}^{2k_1+2k_2+k_3+k_4+N+1} e^{-\frac{2\zeta_1}{q^2}\gamma_{sc}} {}_1F_1\left(1; k_1+k_2+k_3+2; \frac{\zeta_1}{q^2}\gamma_{sc}\right) d\gamma_{sc} \right\}. \end{aligned} \tag{3.80}$$

The integration in Equation 3.80 can be solved using [4, 7.621.4] (reproduced in Equation B.10). Thus, an expression for the N^{th} moment of the output SNR of the dual correlated SC combiner can be obtained as

$$E\left[\gamma_{sc}^{N}\right] = \frac{q^{2N+2}(1-\rho^2)}{2^{N+2}\pi\zeta_1{}^{N}} \sum_{k_1=0}^{\infty}\sum_{k_2=0}^{\infty}\sum_{k_3=0}^{\infty}\sum_{k_4=0}^{\infty} \frac{\left[\rho q^2\right]^{2(k_1+k_2)}\Gamma\left(2k_1+2k_2+k_3+k_4+N+2\right)}{\left\{\prod_{i=1}^{4}k_i!\right\}\left(k_1+k_3+\frac{1}{2}\right)_{k_2+\frac{1}{2}}\left(k_1+k_4+\frac{1}{2}\right)_{k_2+\frac{1}{2}}}$$
$$\times\left(1-q^2\right)^{k_3+k_4}\left\{\frac{{}_2F_1\left(1,2k_1+2k_2+k_3+k_4+N+2;k_1+k_2+k_4+2;\frac{1}{2}\right)}{k_1+k_2+k_4+1}\right.$$
$$\left.+\frac{{}_2F_1\left(1,2k_1+2k_2+k_3+k_4+N+2;k_1+k_2+k_3+2;\frac{1}{2}\right)}{k_1+k_2+k_3+1}\right\}. \quad (3.81)$$

It can be verified that for $\rho=0$, Equation 3.81 simplifies to Equation 3.11 with $L=2$. For $N=1$, Equation 3.81 gives $\bar{\gamma}_{\text{SC}}$, the average SNR for dual correlated SC receivers. It can be shown that for $q=1$ and $\rho=0$ i.e for Rayleigh fading case, $\bar{\gamma}_{\text{SC}}$ simplifies to [31, (12)] ($\bar{\gamma}_{\text{SC}}=\frac{3}{2}\bar{\gamma}$).

Outage Probability

The outage probability is defined in Section 2.3. Thus, substituting Equation 3.78 in Equation 2.16, an expression for the outage probability for correlated dual-SC combiner can be given as

$$P_{\text{out}}(\gamma_{th}) = \frac{\zeta_1^2(1-\rho^2)}{\pi q^2} \sum_{k_1=0}^{\infty}\sum_{k_2=0}^{\infty}\sum_{k_3=0}^{\infty}\sum_{k_4=0}^{\infty} \frac{\rho^{2(k_1+k_2)}\zeta_1^{2k_1+2k_2+k_3+k_4}}{\left\{\prod_{i=1}^{4}k_i!\right\}\left(k_1+k_3+\frac{1}{2}\right)_{k_2+\frac{1}{2}}\left(k_1+k_4+\frac{1}{2}\right)_{k_2+\frac{1}{2}}}$$
$$\times\left(\frac{1-q^2}{q^2}\right)^{k_3+k_4}\left\{\frac{\int_0^{\gamma_{th}}\gamma_{sc}^{2k_1+2k_2+k_3+k_4+1}e^{-\frac{2\zeta_1}{q^2}\gamma_{sc}}{}_1F_1\left(1;k_1+k_2+k_4+2;\frac{\zeta_1}{q^2}\gamma_{sc}\right)d\gamma_{sc}}{k_1+k_2+k_4+1}\right.$$
$$\left.+\frac{\int_0^{\gamma_{th}}\gamma_{sc}^{2k_1+2k_2+k_3+k_4+1}e^{-\frac{2\zeta_1}{q^2}\gamma_{sc}}{}_1F_1\left(1;k_1+k_2+k_3+2;\frac{\zeta_1}{q^2}\gamma_{sc}\right)d\gamma_{sc}}{k_1+k_2+k_3+1}\right\}. \quad (3.82)$$

Expressing the hypergeometric function in infinite series, the integrations in Equation 3.82 can be solved applying [4, (3.381.1)] (reproduced in Equation B.6). Thus, an expression for the outage probability can be given as

$$
\begin{aligned}
P_{\text{out}}(\gamma_{th}) \;=\;& \frac{q^2(1-\rho^2)}{4\pi}\sum_{k_1=0}^{\infty}\sum_{k_2=0}^{\infty}\sum_{k_3=0}^{\infty}\sum_{k_4=0}^{\infty}\frac{\left[\rho q^2\right]^{2(k_1+k_2)}\left(1-q^2\right)^{k_3+k_4}}{\left\{\prod_{i=1}^{4}k_i!\right\}2^{2k_1+2k_2+k_3+k_4}\left(k_1+k_3+\frac{1}{2}\right)_{k_2+\frac{1}{2}}}\\
&\times\frac{1}{\left(k_1+k_4+\frac{1}{2}\right)_{k_2+\frac{1}{2}}}\left\{\sum_{k_5=0}^{\infty}\frac{g\left(2k_1+2k_2+k_3+k_4+k_5+2,\frac{2\zeta_1}{q^2}\gamma_{th}\right)}{2^{k_5}(k_1+k_2+k_4+1)(k_1+k_2+k_4+2)_{k_5}}\right.\\
&\left.+\sum_{k_6=0}^{\infty}\frac{g\left(2k_1+2k_2+k_3+k_4+k_6+2,\frac{2\zeta_1}{q^2}\gamma_{th}\right)}{2^{k_6}(k_1+k_2+k_3+1)(k_1+k_2+k_3+2)_{k_6}}\right\}. \qquad (3.83)
\end{aligned}
$$

Average Bit Error Rate

ABER is given in Equation 2.17, which need the of PDF of γ_{sc} and the conditional bit error rate $p_{e,\text{coh}}(\varepsilon|\gamma)$ for evaluation. The conditional bit error rate (conditioned on the received SNR) for different digital modulation schemes are listed in Table 2.1. In this work, for binary coherent and noncoherent modulations, we obtain expressions for ABER.

1. **Binary Coherent Modulations**

   For binary coherent modulation i. e., BPSK and BFSK, an expression for $p_{e,\text{coh}}(\varepsilon|\gamma)$ can be obtained by evaluating the entries for MPSK and MFSK modulations in Table 2.1, for $M=2$. A simplified combined expression for this conditional BER is also given in Equation 2.24. Thus, putting $p_{e,\text{coh}}(\varepsilon|\gamma)$ from Equation 2.24 and $f_{\gamma_{sc}}(\gamma_{sc})$ from Equation 3.78 into Equation 2.17, binary coherent ABER can be given as

$$
\begin{aligned}
P_{e,ch}(\bar{\gamma}) \;=\;& \frac{\zeta_1^2(1-\rho^2)}{\pi q^2}\sum_{k_1=0}^{\infty}\sum_{k_2=0}^{\infty}\sum_{k_3=0}^{\infty}\sum_{k_4=0}^{\infty}\frac{\rho^{2(k_1+k_2)}\zeta_1^{2k_1+2k_2+k_3+k_4}\left(\frac{1-q^2}{q^2}\right)^{k_3+k_4}}{\left\{\prod_{i=1}^{4}k_i!\right\}\left(k_1+k_3+\frac{1}{2}\right)_{k_2+\frac{1}{2}}\left(k_1+k_4+\frac{1}{2}\right)_{k_2+\frac{1}{2}}}\\
&\times\left\{\frac{\int_0^{\infty}\gamma_{sc}^{2k_1+2k_2+k_3+k_4+1}Q(\sqrt{2a\gamma_{sc}})e^{-\frac{2\zeta_1}{q^2}\gamma_{sc}}{}_1F_1\left(1;k_1+k_2+k_4+2;\frac{\zeta_1}{q^2}\gamma_{sc}\right)d\gamma_{sc}}{k_1+k_2+k_4+1}\right.
\end{aligned}
$$

$$+\frac{\int_0^\infty \gamma_{sc}^{2k_1+2k_2+k_3+k_4+1} Q(\sqrt{2a\gamma_{sc}}) e_1^{-\frac{2\zeta_1}{q^2}\gamma_{sc}} F_1\left(1; k_1+k_2+k_3+2; \frac{\zeta_1}{q^2}\gamma_{sc}\right) d\gamma_{sc}}{k_1+k_2+k_3+1}\Bigg\}. \tag{3.84}$$

Expressing the hypergeometric function in infinite series [4, 9.14.1] (reproduced in Equation B.11) and $Q(\cdot)$ function in terms of incomplete gamma function (using [1, A-(8a)], reproduced in Equation B.14) the above equation can be written as

$$\begin{aligned} P_{e,ch}(\bar{\gamma}) &= \frac{\zeta_1^2(1-\rho^2)}{2q^2\pi\sqrt{\pi}} \sum_{k_1=0}^{\infty}\sum_{k_2=0}^{\infty}\sum_{k_3=0}^{\infty}\sum_{k_4=0}^{\infty} \frac{\rho^{2(k_1+k_2)}\zeta_1^{2k_1+2k_2+k_3+k_4}}{\left\{\prod_{i=1}^{4} k_i!\right\}\left(k_1+k_3+\frac{1}{2}\right)_{k_2+\frac{1}{2}}\left(k_1+k_4+\frac{1}{2}\right)_{k_2+\frac{1}{2}}} \\ &\times \left(\frac{1-q^2}{q^2}\right)^{k_3+k_4} \Bigg\{\frac{1}{k_1+k_2+k_4+1}\sum_{k_5=0}^{\infty}\left(\frac{\zeta_1}{q^2}\right)^{k_5}\frac{1}{(k_1+k_2+k_4+2)_{k_5}} \\ &\times \int_0^\infty \gamma_{sc}^{2k_1+2k_2+k_3+k_4+k_5+1} e^{-\frac{2\zeta_1}{q^2}\gamma_{sc}}\Gamma\left(\frac{1}{2}, a\gamma_{sc}\right) d\gamma_{sc} + \frac{1}{k_1+k_2+k_3+1}\sum_{k_6=0}^{\infty}\left(\frac{\zeta_1}{q^2}\right)^{k_6} \\ &\times \frac{1}{(k_1+k_2+k_3+2)_{k_6}}\int_0^\infty \gamma_{sc}^{2k_1+2k_2+k_3+k_4+k_6+1} e^{-\frac{2\zeta_1}{q^2}\gamma_{sc}}\Gamma\left(\frac{1}{2}, a\gamma_{sc}\right) d\gamma_{sc}\Bigg\}. \end{aligned} \tag{3.85}$$

Solving the integral (using [1, A-6]) (reproduced in Equation B.13), an expression for ABER can be given as

$$\begin{aligned} &P_{e,ch}(\bar{\gamma}) = \\ &= \frac{\sqrt{a}\zeta_1{}^2 q^3(1-\rho^2)}{2\pi\sqrt{\pi}(aq^2+2\zeta_1)^{\frac{5}{2}}} \sum_{k_1=0}^{\infty}\sum_{k_2=0}^{\infty}\sum_{k_3=0}^{\infty}\sum_{k_4=0}^{\infty} \frac{\left[\rho q^2\right]^{2(k_1+k_2)}(1-q^2)^{k_3+k_4}}{\left\{\prod_{i=1}^{4} k_i!\right\}\left(k_1+k_3+\frac{1}{2}\right)_{k_2+\frac{1}{2}}\left(k_1+k_4+\frac{1}{2}\right)_{k_2+\frac{1}{2}}} \\ &\times \left(\frac{\zeta_1}{aq^2+2\zeta_1}\right)^{2k_1+2k_2+k_3+k_4} \Bigg\{\sum_{k_5=0}^{\infty}\frac{\Gamma\left(2k_1+2k_2+k_3+k_4+k_5+\frac{5}{2}\right)\zeta_1^{k_5}}{(k_1+k_2+k_4+1)(k_1+k_2+k_4+2)_{k_5}} \\ &\times \frac{{}_2F_1\left(1, 2k_1+2k_2+k_3+k_4+k_5+\frac{5}{2}; 2k_1+2k_2+k_3+k_4+k_5+3; \frac{2\zeta_1}{aq^2+2\zeta_1}\right)}{(2k_1+2k_2+k_3+k_4+k_5+1)(aq^2+2\zeta_1)^{k_5}} \\ &+ \sum_{k_6=0}^{\infty}\frac{\Gamma\left(2k_1+2k_2+k_3+k_4+k_6+\frac{5}{2}\right)\zeta_1^{k_6}}{(k_1+k_2+k_3+2)_{k_6}(k_1+k_2+k_3+1)(2k_1+2k_2+k_3+k_4+k_6+2)(aq^2+2\zeta_1)^{k_6}} \end{aligned}$$

$$\times {}_2F_1\left(1, 2k_1+2k_2+k_3+k_4+k_6+\frac{5}{2};\ 2k_1+2k_2+k_3+k_4+k_6+3; \frac{2\zeta_1}{aq^2+2\zeta_1}\right)\Bigg\}. \tag{3.86}$$

It can be shown that for independent channels i.e., $\rho = 0$, Equation 3.86 simplifies to Equation 3.16 with $L = 2$.

2. **Binary Non-coherent Modulations**

As discussed in previous sections, substituting $p_{e,\text{nch}}(\varepsilon|\gamma)$ from Equation 2.25 and $f_{\gamma_{sc}}(\gamma_{sc})$ from Equation 3.78 into Equation 2.17, the ABER expression can be given as

$$\begin{aligned} P_{e,nch}(\bar{\gamma}) &= \frac{\zeta_1^2(1-\rho^2)}{2\pi q^2}\sum_{k_1=0}^{\infty}\sum_{k_2=0}^{\infty}\sum_{k_3=0}^{\infty}\sum_{k_4=0}^{\infty}\frac{\rho^{2(k_1+k_2)}\zeta_1^{2k_1+2k_2+k_3+k_4}}{\left\{\prod_{i=1}^{4}k_i!\right\}\left(k_1+k_3+\frac{1}{2}\right)_{k_2+\frac{1}{2}}} \\ &\times\frac{1}{\left(k_1+k_4+\frac{1}{2}\right)_{k_2+\frac{1}{2}}}\left[\frac{1-q^2}{q^2}\right]^{k_3+k_4}\left\{\frac{\int_0^\infty \gamma_{sc}^{2k_1+2k_2+k_3+k_4+2}e^{-\frac{2\zeta_1+aq^2}{q^2}\gamma_{sc}}}{k_1+k_2+k_4+1}\right. \\ &\times {}_1F_1\left(1; k_1+k_2+k_4+2; \frac{\zeta_1}{q^2}\gamma_{sc}\right)d\gamma_{sc}+\frac{\int_0^\infty \gamma_{sc}^{2k_1+2k_2+k_3+k_4+2}e^{-\frac{2\zeta_1+aq^2}{q^2}\gamma_{sc}}}{k_1+k_2+k_3+1} \\ &\left.\times\ {}_1F_1\left(1; k_1+k_2+k_3+2; \frac{\zeta_1}{q^2}\gamma_{sc}\right)d\gamma_{sc}\right\}. \end{aligned} \tag{3.87}$$

The integral can be solved using [4, (7.621.4)] (reproduced in Equation B.10), and the ABER expression can be obtained as

$$\begin{aligned} &P_{e,nch}(\bar{\gamma}) = \\ &= \frac{(1-\rho^2)}{2\pi}\left(\frac{q\zeta_1}{aq^2+2\zeta_1}\right)^2\sum_{k_1=0}^{\infty}\sum_{k_2=0}^{\infty}\sum_{k_3=0}^{\infty}\sum_{k_4=0}^{\infty}\frac{\rho^{2(k_1+k_2)}\Gamma(2k_1+2k_2+k_3+k_4+2)}{\left\{\prod_{i=1}^{4}k_i!\right\}\left(k_1+k_4+\frac{1}{2}\right)_{k_2+\frac{1}{2}}\left(k_1+k_3+\frac{1}{2}\right)_{k_2+\frac{1}{2}}} \\ &\times\left(\frac{q^2\zeta_1}{aq^2+2\zeta_1}\right)^{2k_1+2k_2+k_3+k_4}\left\{\frac{{}_2F_1\left(1, 2k_1+2k_2+k_3+k_4+2; k_1+k_2+k_4+2; \frac{\zeta_1}{aq^2+2\zeta_1}\right)}{k_1+k_2+k_4+1}\right. \end{aligned}$$

$$+\frac{{}_2F_1\left(1, 2k_1+2k_2+k_3+k_4+2; k_1+k_2+k_3+2; \frac{\zeta_1}{aq^2+2\zeta_1}\right)}{k_1+k_2+k_3+1}\Bigg\}\left(\frac{1-q^2}{q^2}\right)^{k_3+k_4}. \tag{3.88}$$

For independent Rayleigh fading channels i.e., $\rho = 0$ and $q = 1$, Equation 3.88 can be simplified to $P_{e,nch}(\bar{\gamma}) = \frac{1}{(2+a\bar{\gamma})(1+a\bar{\gamma})}$ as in [52, (13)].

Results and Discussion

The outage probability expression Equation 3.83, is numerically evaluated and the curves for $P_{\text{out}}(\bar{\gamma}_N)$ vs. $\bar{\gamma}_N$ are shown in Figure 3.22. In the figure, the variation in the outage probability for different values of ρ can be observed. The variation is more for $\rho \to 1$ relative to $\rho = 0$. In Figures 3.23 and 3.24, ABER vs. $\bar{\gamma}$ for coherent and noncoherent modulations are plotted, as a function of ρ and q. It can be observed that ABER increases with increase in ρ, for any value of q. The required excess SNR (The difference in SNR between the cases $\rho \neq 0$ and $\rho = 0$) vs. ρ for an ABER of 10^{-3} is also plotted in Figure 3.25, for CPSK and DPSK modulations. From this figure it can be observed that the excess SNR increases slowly for $\rho < 0.4$ but the rate of increased becomes high for $\rho > 0.4$. For example, for CPSK modulation, the excess SNR is close to 0.3 dB for $\rho = 0.4$ whereas it is nearly 2 dB for $\rho = 0.8$. It can also be observed from Figure 3.23 for $\rho = 0.8$, the ABER curve of the PSK modulation coincides with $\rho = 0$ ABER curve of FSK modulation, above the SNR of 15dB. It may be due to the high correlation which nullifies the performance advantage of PSK.

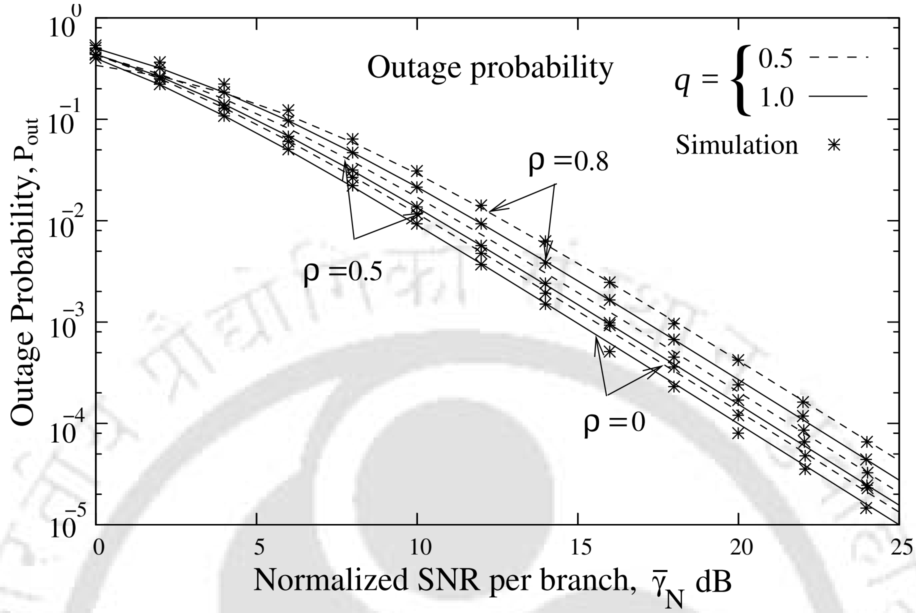

Figure 3.22: Outage probability of correlated dual-SC receiver.

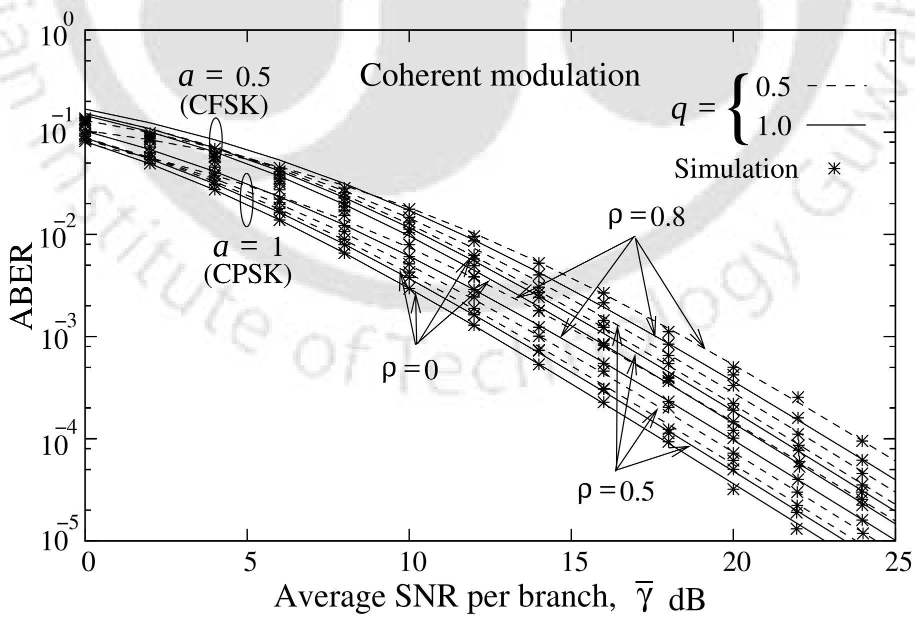

Figure 3.23: ABER of correlated dual-SC receiver for CPSK and CFSK modulations.

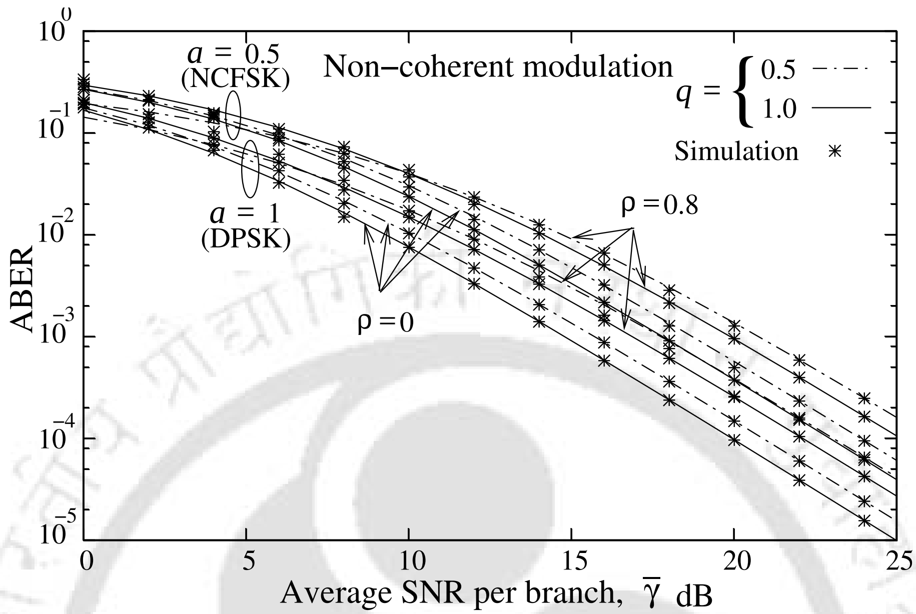

Figure 3.24: ABER of correlated dual-SC receiver for NCFSK and DPSK modulations.

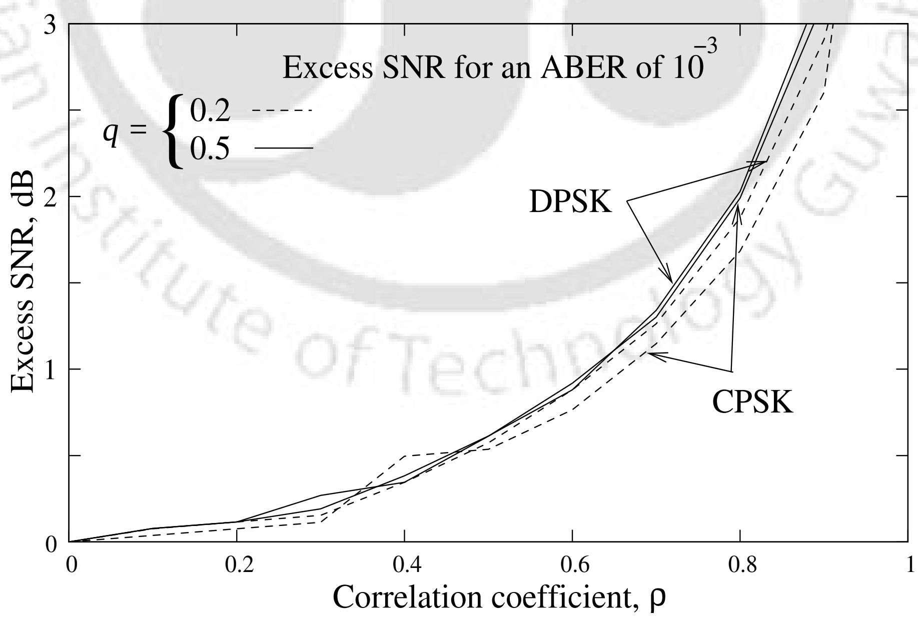

Figure 3.25: Excess SNR required for an ABER of 10^{-3} for dual-SC receiver.

3.4 Maximal Ratio Combining with Arbitrary Order Diversity

In literature on the performance evaluation of diversity receivers, an analysis for the general case of arbitrary order of diversity with arbitrary correlation is rare due to the non-availability of a suitable mathematical expression for the joint PDF of the received arbitrary number of fading amplitudes for an arbitrary correlation coefficient among them. Hence, particular cases of practical importance have been analyzed in the literature. In this section, analysis of a MRC receiver with arbitrary order of diversity with equal and exponential correlation models are presented.

3.4.1 Equal Correlation Model

In this section performance of MRC receiver is analyzed for equally correlated MRC receiver for arbitrary number of branches L. Equal or constant correlation model is discussed in Section 2.2, where the correlation coefficient $\rho_{m,n} = \rho$ for $\forall\, m \neq n$ and $1 \leq m, n \leq L$. In practice, this correlation model is observed by an array of three antennas placed on an equilateral triangle or by a closely spaced set of antennas [50]. A PDF based analysis is used to obtain expressions for different performance measures.

PDF of Combiner Output Signal-to-Noise Ratio

From Equation 3.19, the PDF of γ_{mrc} can be obtained from the knowledge of the PDF of the RV α^2, which is the sum of L Hoyt square RVs, α_l^2. As a standard approach for the derivation of the PDF of α^2, we require the joint density function or CF of α_ls. But this is not available in literature for correlated Hoyt RVs. However, using the Hoyt RV model in [13] and the expression for the sum of PDF of squared multivariate Gaussian RVs by Gurland in [64], it is possible to derive the PDF of α^2 for the special case of equally correlated α_ls. It is presented below.

From the Gaussian model of Hoyt RV in Section A.1 we can express $\alpha^2 = X^2 + Y^2$, where $X^2 (= X_1^2 + X_2^2 + \ldots + X_L^2)$ and $Y^2 (= Y_1^2 + Y_2^2 + \ldots + Y_L^2)$ are independent RVs while $X_l (Y_l)$s are correlated with correlation coefficient $\rho_{m,n}$, $1 \leq m,n \leq L$.

In [64, (4)] Gurland has presented an expression for the arithmetic mean of L equally correlated Gaussian square RVs in [64, (4)]. It is reproduced in Appendix Equation B.18 for convenience. Thus, the PDF X^2 being the sum of L correlated Gaussian square RVs, can be obtained from Equation B.18 with suitable substitutions (i.e., $\lambda = 1/2$ and $k = L$), and then performing a scaling on the PDF corresponding to the factor L. So, the PDF of X^2 can be given as

$$f_{X^2}\left(x^2\right) = \frac{x^{\frac{L}{2}-1} e^{-\frac{x}{2(1-\rho)}} {}_1F_1\left(\frac{1}{2}, \frac{L}{2}; \frac{L\rho x}{2\sigma_x^2(1-\rho)(1+(L-1)\rho)}\right)}{\left(2\sigma_x^2\right)^{\frac{L}{2}} (1-\rho)^{\frac{L-1}{2}} \Gamma(L/2) \sqrt{1+(L-1)\rho}}. \tag{3.89}$$

The PDF of Y^2, ($f_{Y^2}\left(y^2\right)$) can be obtained by substituting x by y in Equation 3.89 can be given as

$$f_{Y^2}\left(y^2\right) = \frac{y^{\frac{L}{2}-1} e^{-\frac{y}{2(1-\rho)}} {}_1F_1\left(\frac{1}{2}; \frac{L}{2}; \frac{L\rho y}{2\sigma_y^2(1-\rho)(1+(L-1)\rho)}\right)}{\left(2\sigma_y^2\right)^{\frac{L}{2}} (1-\rho)^{\frac{L-1}{2}} \Gamma(L/2) \sqrt{1+(L-1)\rho}}. \tag{3.90}$$

Since, RVs X^2 and Y^2 are independent, the PDF of $\alpha^2 = X^2 + Y^2$ can be obtained by convolving the PDFs $f_{X^2}(x^2)$ and $f_{Y^2}(y^2)$. This expression can be given as

$$\begin{aligned} f_{\alpha^2}(\alpha^2) \;=\; & \frac{e^{-\frac{\alpha}{2q^2(1-\rho)}}}{(2\sigma_x\sigma_y)^L \Gamma^2\left(\frac{L}{2}\right)(1-\rho)^{L-1}(1+(L-1)\rho)} \int_0^\alpha x^{\frac{L}{2}-1} (\alpha - x)^{\frac{L}{2}-1} e^{\frac{(1-q^2)}{2q^2(1-\rho)}x} \\ & \times {}_1F_1\left(\frac{1}{2}; \frac{L}{2}; \frac{\rho L x}{2(1-\rho)(1+(L-1)\rho)}\right) {}_1F_1\left(\frac{1}{2}; \frac{L}{2}; \frac{\rho L(\alpha - x)}{2q^2(1-\rho)(1+(L-1)\rho)}\right) dx. \end{aligned} \tag{3.91}$$

The integral in Equation 3.91 cannot be solved in this present form. Expressing the hypergeometric functions in series form [4, 9.14.1] (reproduced in Equation B.11) and solving the integration using [4, 3.383.1] (reproduced in B.7), the PDF of α^2 can be given as

$$\begin{aligned} f_{\alpha^2}(\alpha^2) \;=\; & \frac{\alpha^{L-1} e^{-\frac{\alpha}{2q^2(1-\rho)}}}{(2q)^L \pi (1-\rho)^{L-1}(1+(L-1)\rho)} \sum_{k_1=0}^{\infty}\sum_{k_2=0}^{\infty} \frac{\Gamma\left(k_1+\frac{1}{2}\right)\Gamma\left(k_2+\frac{1}{2}\right)}{k_1!k_2!q^{2k_2}\Gamma(L+k_1+k_2)} \\ & \times \left[\frac{\rho L \alpha}{2(1-\rho)(1+(L-1)\rho)}\right]^{k_1+k_2} {}_1F_1\left(\frac{L}{2}+k_1; L+k_1+k_2; \frac{1-q^2}{2q^2(1-\rho)}\alpha\right). \end{aligned} \tag{3.92}$$

The PDF of γ_{mrc} can be obtained by scaling the PDF in 3.92 by the transformation of RV corresponding to the multiplying factor (E_b/N_0). The ratio (E_b/N_0) can be expressed as $E_b/N_0 = \frac{\bar{\gamma}}{1+q^2}$

(Refer Equation A.4). Thus, the final expression for the PDF of γ_{mrc} can be written as

$$f_{\gamma_{mrc}}(\gamma_{mrc}) = \frac{(1-\rho)(q\eta')^L \gamma_{mrc}^{L-1}}{\pi[1+(L-1)\rho]} \sum_{k_1=0}^{\infty}\sum_{k_2=0}^{\infty} \frac{\Gamma\left(k_1+\frac{1}{2}\right)\Gamma\left(k_2+\frac{1}{2}\right)}{k_1!k_2!q^{2k_2}\Gamma(L+k_1+k_2)e^{\eta'\gamma_{mrc}}} \left[\frac{L\rho\eta' q^2\gamma_{mrc}}{1+(L-1)\rho}\right]^{k_1+k_2}$$
$$ {}_1F_1\left\{\frac{L}{2}+k_1; L+k_1+k_2; (1-q^2)\eta'\gamma_{mrc}\right\}, \quad (3.93)$$

where $\eta' \triangleq \frac{1+q^2}{2q^2\bar{\gamma}(1-\rho)}$.

Moments of Combiner Output Signal-to-Noise Ratio

Using Equation 3.93, the moments of the combiner output SNR γ_{mrc} can be expressed as

$$E[\gamma_{mrc}^N] = \frac{(1-\rho)(q\eta')^L}{\pi\{1+(L-1)\rho\}} \sum_{k_1=0}^{\infty}\sum_{k_2=0}^{\infty} \frac{\Gamma\left(k_1+\frac{1}{2}\right)\Gamma\left(k_2+\frac{1}{2}\right)}{k_1!k_2!q^{2k_2}\Gamma(L+k_1+k_2)} \left[\frac{L\rho\eta' q^2}{1+(L-1)\rho}\right]^{k_1+k_2}$$
$$\times \int_0^{\infty} \gamma_{mrc}^{L+N+k_1+k_2-1} e^{-\eta'\gamma_{mrc}} {}_1F_1\left\{\frac{L}{2}+k_1; L+k_1+k_2; (1-q^2)\eta'\gamma_{mrc}\right\}. \quad (3.94)$$

Solving the above integral using [4, (7.621.4)] (reproduced in Equation B.10), an expression for $E[\gamma_{mrc}^N]$ can be obtained as

$$E\left[\gamma_{mrc}^N\right] = \frac{(1-\rho)q^L}{\pi[1+(L-1)\rho]\eta'^N} \sum_{k_1=0}^{\infty}\sum_{k_2=0}^{\infty} \frac{\Gamma\left(k_1+\frac{1}{2}\right)\Gamma\left(k_2+\frac{1}{2}\right)(L+k_1+k_2)_N}{k_1!k_2!q^{2k_2}} \left(\frac{L\rho q^2}{1+(L-1)\rho}\right)^{k_1+k_2}$$
$$\times {}_2F_1\left(\frac{L}{2}+k_1, L+N+k_1+k_2; L+k_1+k_2; 1-q^2\right). \quad (3.95)$$

The average output SNR can be obtained by putting $N=1$ in Equation 3.95. It can be given as

$$\bar{\gamma}_{mrc} = \frac{q^L(1-\rho)}{\pi[1+(L-1)\rho]\eta'} \sum_{k_1=0}^{\infty}\sum_{k_2=0}^{\infty} \frac{q^{2k_1}\Gamma\left(k_1+\frac{1}{2}\right)\Gamma\left(k_2+\frac{1}{2}\right)(L+k_1+k_2)}{k_1!k_2!}$$
$$\times \left(\frac{L\rho}{1+(L-1)\rho}\right)^{k_1+k_2} {}_2F_1\left(\frac{L}{2}+k_1, L+k_1+k_2+1; L+k_1+k_2; 1-q^2\right). \quad (3.96)$$

Equation 3.96 is a general expression valid for L-MRC receiver operating in equally correlated Hoyt fading environments. For the particular case of $\rho=0$ (independent fading channels), it can be shown that Equation 3.96 reduces to $\bar{\gamma}_{mrc} = L\bar{\gamma}$, as expected.

Outage Probability

Putting $f_{\gamma_{mrc}}(\gamma_{mrc})$ from Equation 3.93 to Equation 2.16, an expression for outage probability can be expressed for a threshold γ_{th} as

$$P_{\text{out}}(\gamma_{th}) = \frac{(q\eta')^L(1-\rho)}{\pi(1+(L-1)\rho)}\sum_{k_1=0}^{\infty}\sum_{k_2=0}^{\infty}\frac{q^{2k_1}\Gamma\left(k_1+\frac{1}{2}\right)\Gamma\left(k_2+\frac{1}{2}\right)}{k_1!k_2!\Gamma(L+k_1+k_2)}\left(\frac{\rho\eta' L}{1+\rho(L-1)}\right)^{k_1+k_2}$$
$$\times\int_0^{\gamma_{th}}\gamma_{mrc}^{L+k_1+k_2-1}e^{-\eta'\gamma_{mrc}}{}_1F_1\left\{\frac{L}{2}+k_1;L+k_1+k_2;(1-q^2)\eta'\gamma_{mrc}\right\}d\gamma_{mrc}. \quad (3.97)$$

The integral in Equation 3.97 can be solved by expressing the hypergeometric function in infinite series form [4, 9.14.1] (reproduced in Equation B.11) and using [4, (3.381.1)]. An expression for the outage probability can be obtained as

$$P_{\text{out}}(\gamma_{th}) = \frac{q^L(1-\rho)}{\pi[1+(L-1)\rho]}\sum_{k_1=0}^{\infty}\sum_{k_2=0}^{\infty}\sum_{k_3=0}^{\infty}\frac{q^{2k_1}\Gamma\left(k_1+\frac{1}{2}\right)\Gamma\left(k_2+\frac{1}{2}\right)\left(\frac{L}{2}+k_1\right)_{k_3}(1-q^2)^{k_3}}{k_1!k_2!k_3!\Gamma(L+k_1+k_2+k_3)}$$
$$\times\left[\frac{\rho L}{1+(L-1)\rho}\right]^{k_1+k_2} g\left(L+k_1+k_2+k_3,\frac{1+q^2}{2q^2\bar{\gamma}_N(1-\rho)}\right). \quad (3.98)$$

Average Bit Error Rate

ABER is given in equation Equation 2.17, which need an expression for the PDF of γ_{mrc} and the conditional bit error rate $p_{e,\text{coh}}(\varepsilon|\gamma)$. The conditional bit error rate (conditioned on the received SNR) for different digital modulation schemes are listed in Table 2.1. For binary coherent and noncoherent modulations we present expressions for ABER are presented below.

1. **Binary Coherent Modulations**

   For binary coherent modulations (i.e BPSK and BFSK), the expression for the conditional BER is given in Equation 2.24. Putting $p_{e,\text{coh}}(\varepsilon|\gamma)$ and $f_{\gamma_{mrc}}(\gamma_{mrc})$ from Equations 2.24 and 3.93 into Equation 2.17, the ABER expression can be given as

$$P_{e,ch}(\bar{\gamma}) = \frac{(1-\rho)(q\eta')^L}{\pi(1+(L-1)\rho)}\sum_{k_1=0}^{\infty}\sum_{k_2=0}^{\infty}\frac{q^{2k_1}\Gamma\left(k_1+\frac{1}{2}\right)\Gamma\left(k_2+\frac{1}{2}\right)}{k_1!k_2!\Gamma(L+k_1+k_2)}\left[\frac{\rho L\eta'}{1+\rho(L-1)}\right]^{k_1+k_2}$$

$$\times \int_0^\infty \gamma_{mrc}^{L+k_1+k_2-1} Q\left(\sqrt{2a\gamma_{mrc}}\right) e^{-\eta'\gamma_{mrc}} {}_1F_1\left\{\frac{L}{2}+k_1; L+k_1+k_2; (1-q^2)\eta'\gamma_{mrc}\right\}. \tag{3.99}$$

The integral in Equation 3.99 can be solved by expressing ${}_1F_1(\cdot,\cdot;\cdot)$ in infinite series [5] and using [1, A-(6), A-(8a)] (reproduced in Equations B.13 and B.14, respectively). Thus, an expression for ABER can be given as

$$\begin{aligned} P_{e,ch}(\bar{\gamma}) &= \sqrt{\frac{a}{a+\eta'}} \frac{(1-\rho)q^L}{2\pi^{\frac{3}{2}}[1+(L-1)\rho]} \sum_{k_1=0}^{\infty}\sum_{k_2=0}^{\infty}\sum_{k_3=0}^{\infty} \frac{q^{2k_1}\Gamma\left(k_1+\frac{1}{2}\right)\Gamma\left(k_2+\frac{1}{2}\right)}{k_1!k_2!k_3!(L+k_1+k_2+k_3)!} \\ &\times \left(\frac{\eta'}{\eta'+a}\right)^{L+k_1+k_2+k_3} \Gamma(L+k_1+k_2+k_3+\frac{1}{2}) \left(\frac{L}{2}+k_1\right)_{k_3} \left[\frac{\rho L}{1+(L-1)\rho}\right]^{k_1+k_2} \\ &\times (1-q^2)^{k_3} {}_2F_1\left(1, L+k_1+k_2+k_3+\frac{1}{2}; L+k_1+k_2+k_3+1; \frac{\eta'}{a+\eta'}\right). \end{aligned} \tag{3.100}$$

2. **Binary Noncoherent Modulations**

For binary noncoherent modulations, the conditional BER is given in Equation 2.25. By putting $p_{e,\text{ncoh}}(\varepsilon|\gamma)$ and $f_{\gamma_{mrc}}(\gamma_{mrc})$ from Equations 2.25 and 3.93 into Equation 2.17, an expression of noncoherent ABER can be given as

$$\begin{aligned} P_{e,nch}(\bar{\gamma}) &= \frac{(1-\rho)(q\eta')^L}{2\pi(1+(L-1)\rho)} \sum_{k_1=0}^{\infty}\sum_{k_2=0}^{\infty} \frac{q^{2k_1}\Gamma\left(k_1+\frac{1}{2}\right)\Gamma\left(k_2+\frac{1}{2}\right)}{k_1!k_2!\Gamma(L+k_1+k_2)} \left(\frac{L\rho\eta'}{1+\rho(L-1)}\right)^{k_1+k_2} \\ &\times \int_0^\infty \gamma_{mrc}^{L+k_1+k_2-1} e^{-(\eta'+a)\gamma_{mrc}} {}_1F_1\left\{\tfrac{L}{2}+k_1; L+k_1+k_2; (1-q^2)\eta'\gamma_{mrc}\right\} d\gamma_{mrc}. \end{aligned} \tag{3.101}$$

Solving the integral in Equation 3.101 using [4, (7.621.4)], an expression for ABER can be obtained as

$$\begin{aligned} P_{e,nch}(\bar{\gamma}) &= \frac{(1-\rho)(q\eta')^L}{2\pi[1+(L-1)\rho][(a+\eta'q^2)(a+\eta')]^{\frac{L}{2}}} \sum_{k_1=0}^{\infty}\sum_{k_2=0}^{\infty} \left(\frac{q^2}{a+\eta'q^2}\right)^{k_1} \\ &\times \frac{\Gamma\left(k_1+\frac{1}{2}\right)\Gamma\left(k_2+\frac{1}{2}\right)}{k_1!k_2!(a+\eta')^{k_2}} \left[\frac{\rho\eta' L}{1+(L-1)\rho}\right]^{k_1+k_2}. \end{aligned} \tag{3.102}$$

For $\rho = 0$ and $q = 1$, i.e., for independent Rayleigh fading channels, Equations 3.100 and 3.102 simplifies to the result in [1].

Results and Discussion

Obtained mathematical expressions have been numerically evaluated and plotted against parameters of interest. Also, Monte Carlo simulations results have been included in the figures. It can be observed that the simulation results are in close agreement with the numerical results. In Figure 3.26, $P_{\text{out}}(\gamma_{th})$ vs. $\bar{\gamma}_N$ has been plotted for different values of L, ρ and q. The effect of branch correlation on the outage can be observed by comparing the outage values for $\rho = 0.8$ against the values for $\rho = 0$ (uncorrelated case). Clearly, with the increase in ρ, the receiver suffers more outage, for a fixed value of $\bar{\gamma}_N$ and L. Again, as expected, increase in L reduces the probability of outage. These results have been verified against the results in [2], which is a special case of the results presented here, and are found to be matching. For binary, coherent and non-coherent modulations, ABER vs. $\bar{\gamma}$ curves have been plotted in Figures 3.27 and 3.28, respectively. It can be observed that the ABER performance degrades with the increase in ρ. Also, for the modulation schemes under consideration, bit error rate degrades with decrease in q, as expected. The effect of number of input branches on the ABER, curves are shown as a function of L.

In the numerical evaluation of expressions involving infinite series, we have truncated them suitably by including finite number of terms N ensuring to achieve an accuracy in ABER at least at 7^{th} place of decimal digit. In Table 3.4, we have illustrated the number of terms required to achieve this accuracy in the evaluation of Equation 3.100 as a function of $\bar{\gamma}$, L and ρ for $q = 0.5$. It can be observed that for a given SNR the value of N is increasing with increase in ρ and L.

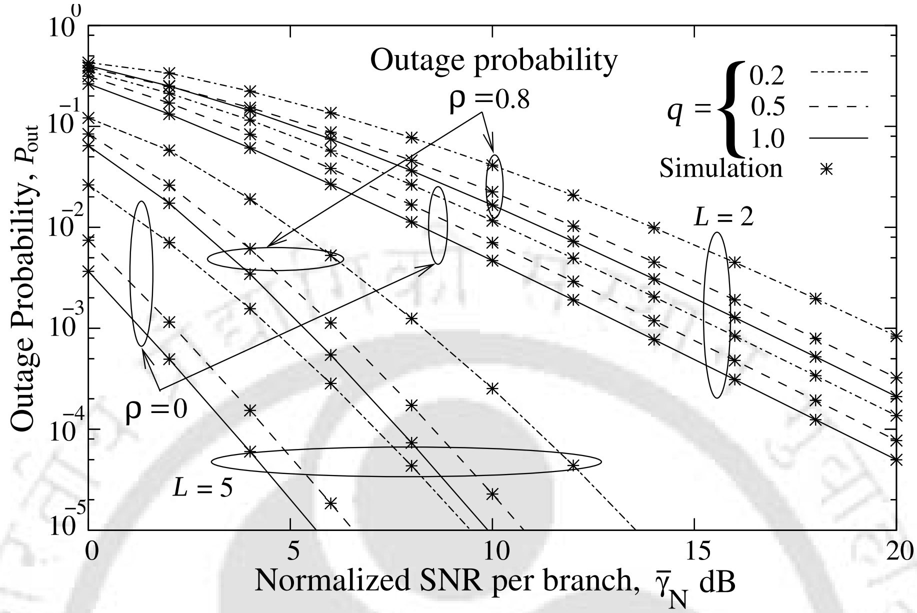

Figure 3.26: Outage probability of the L-MRC receiver with equal correlation.

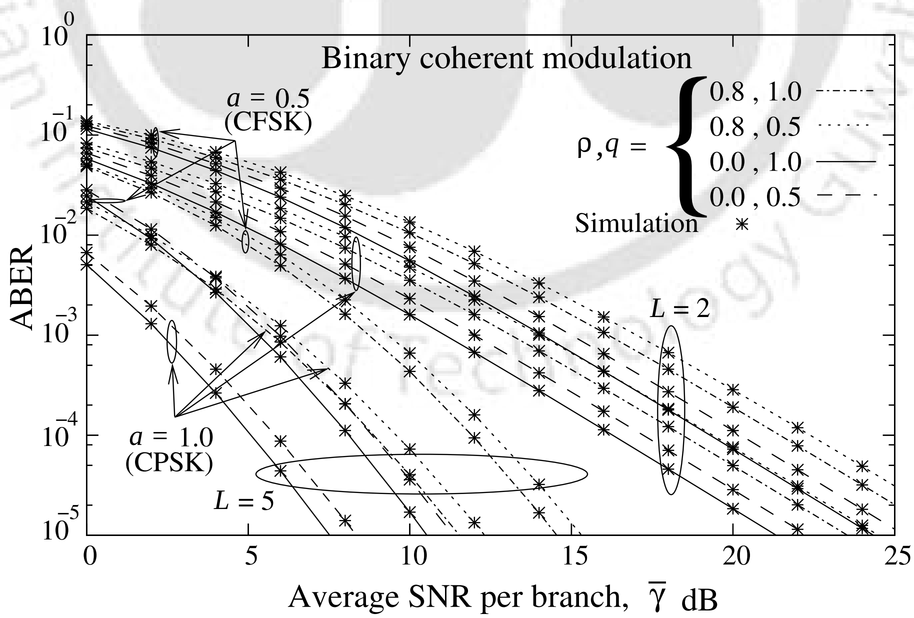

Figure 3.27: ABER vs. $\bar{\gamma}$ for L-MRC receiver with binary coherent modulations.

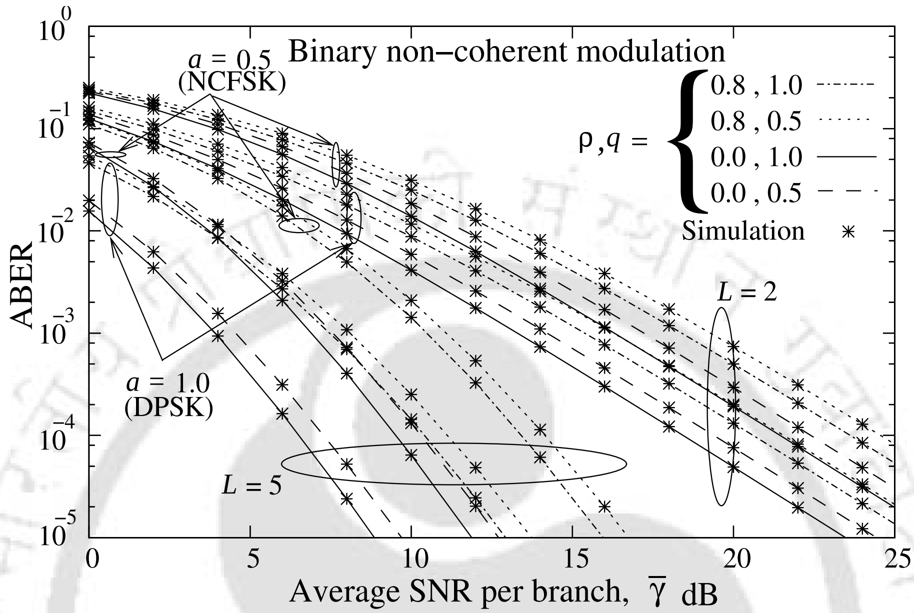

Figure 3.28: ABER vs. $\bar{\gamma}$ for L-MRC receiver with binary noncoherent modulations.

Table 3.4: Value of N for an accuracy at 7^{th} place of decimal digit in the numerical evaluation of Equation 3.100 for $q = 0.5$.

$\bar{\gamma}$ (dB)	ρ	$L = 2$		$L = 5$	
		N	ABER	N	ABER
0	0.5	33	0.0716715	34	0.0108255
	0.8	65	0.0834794	66	0.0221059
8	0.5	10	0.0062631	8	0.0000454
	0.8	18	0.0096621	16	0.0003301

3.4.2 Exponential Correlation Model

The exponential correlation, which is observed when the receiving antennas are placed in a linear array [1, 2, 51] as discussed in Section 2.2. The system model considered for analysis is similar to the previous one except that the input branch signals are exponentially correlated. An approximate closed form mathematical expression for the PDF of the combiner output SNR ($\gamma_{mrc},$) is obtained using the useful expression given in [65] with necessary modifications.

PDF of MRC Output Signal-to-Noise Ratio

In the model described for equal correlation in Section 3.4.1, it is assumed that X_l^2s (Y_l^2s) are exponentially correlated, for which the correlation matrix is given as [51] $\Sigma_{ij} = \rho^{2|i-j|}$, where

$$\rho = \frac{\mathrm{cov}(X_1, X_2)}{\sqrt{\mathrm{var}(X_1)\mathrm{var}(X_2)}}, \quad 1 \leq i, j \leq L \quad , \quad i \neq j.$$

From Equation A.18, it can be shown that the correlation matrix for α_l^2s is also $\Sigma_{ij} = \rho^{2|i-j|}$. Extending the useful formula given for exponentially correlated sum of gamma RVs in [65], (putting $r = 1/2$ and $\theta = 2\sigma_x^2$) which is discussed in section A.7, the distribution of $X = \sum_{l=1}^{L} X_l^2$ can be closely approximated by

$$f_X(x) = \left(\frac{\tau}{\sigma_x^2}\right)^{L\tau} \frac{x^{L\tau-1} e^{-\frac{\tau}{\sigma_x^2}x}}{\Gamma(L\tau)}, \tag{3.103}$$

where $\tau \triangleq \frac{L}{2\left[L+\frac{2\rho}{1-\rho}\left(L-\frac{1-\rho^L}{1-\rho}\right)\right]}$.

Similarly, the PDF of $Y = \sum_{l=1}^{L} Y_l^2$ can be given as

$$f_Y(y) = \left(\frac{\tau}{\sigma_y^2}\right)^{L\tau} \frac{y^{L\tau-1} e^{-\frac{\tau}{\sigma_y^2}y}}{\Gamma(L\tau)}. \tag{3.104}$$

Since, RVs X and Y are independent, the joint PDF of X and Y can be obtained by multiplying $f_X(x)$

and $f_Y(y)$. Thus, using the joint PDF of X and Y and [59, (6.44)], the PDF of α^2 can be written as

$$f_{\alpha^2}(\alpha^2) = \left(\frac{\tau}{\sigma_y\sigma_x}\right)^{2L\tau} \frac{e^{-\frac{\tau}{\sigma_y^2}\alpha}}{\Gamma^2(L\tau)} \int_0^{\alpha} x^{L\tau-1}(\alpha-x)^{L\tau-1} e^{\frac{\sigma_x^2-\sigma_y^2}{\sigma_y^2\sigma_x^2}\tau x} dx. \tag{3.105}$$

Solving the integral in Equation 3.105, using [4, (3.383.1)](reproduced in Appendix B.7) the simplified equation can be given as

$$f_{\alpha^2}(\alpha^2) = \left(\frac{\tau}{\sigma_y\sigma_x}\right)^{2L\tau} \frac{\alpha^{2L\tau-1} e^{-\frac{\tau}{\sigma_y^2}\alpha}}{\Gamma(2L\tau)} {}_1F_1\left(L\tau; 2L\tau; \frac{\sigma_x^2-\sigma_y^2}{\sigma_y^2\sigma_x^2}\tau\alpha\right). \tag{3.106}$$

Performing transformation of RV corresponding to the multiplying factor E_b/N_0 on Equation 3.106, the expression for the PDF of γ_{mrc} can be obtained as

$$f_{\gamma_{mrc}}(\gamma_{mrc}) = \left(\frac{N_0\tau}{\sigma_y\sigma_x E_b}\right)^{2L\tau} \frac{\gamma_{mrc}^{2L\tau-1} e^{-\frac{N_0\tau}{E_b\sigma_y^2}\gamma_{mrc}}}{\Gamma(2L\tau)} {}_1F_1\left\{L\tau; 2L\tau; \left(\frac{\sigma_x^2-\sigma_y^2}{\sigma_y^2\sigma_x^2}\right)\frac{\tau N_0}{E_b}\gamma_{mrc}\right\} \tag{3.107}$$

Putting the value of $\sigma_x = 1$, which results in $\sigma_y = q$ and $E_b/N_0 = \bar{\gamma}/(1+q^2)$ as given in Section A.4. Thus the PDF of γ_{mrc} can be finally given as

$$f_{\gamma_{mrc}}(\gamma_{mrc}) = \frac{(q\varsigma)^{2L\tau}\gamma_{mrc}^{2L\tau-1}e^{-\varsigma\gamma_{mrc}}}{\Gamma(2L\tau)} {}_1F_1\left(L\tau; 2L\tau; \varsigma(1-q^2)\gamma_{mrc}\right), \tag{3.108}$$

where $\varsigma \triangleq \frac{(1+q^2)\tau}{\bar{\gamma}q^2}$.

Moments of Combiner Output SNR

Using Equations 3.108 and 3.9, the N^{th} moment of the MRC output SNR can be given as

$$E\left[\gamma_{mrc}^N\right] = \frac{(q\varsigma)^{2L\tau}}{\Gamma(2L\tau)} \int_0^{\infty} \gamma_{mrc}^{2L\tau+N-1} e^{-\varsigma\gamma_{mrc}} {}_1F_1\left(L\tau; 2L\tau; \varsigma(1-q^2)\gamma_{mrc}\right) d\gamma_{mrc} \tag{3.109}$$

The integral in Equation 3.109 can be solved by applying [4, (7.621)]. The final expression for the N^{th} moment can be obtained as

$$E[\gamma_{mrc}^N] = \frac{q^{2L\tau}(2L\tau)_N}{\varsigma^N} {}_2F_1\left(L\tau; 2L\tau+N; 2L\tau; 1-q^2\right). \tag{3.110}$$

The average SNR at the output of the MRC, $\bar{\gamma}_{mrc}$, can be obtained from Equation 3.110 by putting $N = 1$ as

$$\bar{\gamma}_{mrc} = \frac{2L\tau q^{2L\tau}}{\varsigma} {}_2F_1\left(L\tau; 2L\tau+1; 2L\tau; 1-q^2\right). \tag{3.111}$$

Outage Probability

Putting $f_{\gamma_{mrc}}(\gamma_{mrc})$ from Equation 3.108 to Equation 2.16, the expression for the outage probability can be expressed for a threshold γ_{th} as

$$P_{\text{out}}(\gamma_{th}) = \frac{(q\varsigma)^{2L\tau}}{\Gamma(2L\tau)} \int_0^{\gamma_{th}} \gamma_{mrc}^{2L\tau-1} e^{-\varsigma\gamma_{mrc}} {}_1F_1\left(L\tau; 2L\tau; \varsigma(1-q^2)\gamma_{mrc}\right) d\gamma_{mrc}. \tag{3.112}$$

The integral in Equation 3.112 can be solved by expressing the involved hypergeometric function in infinite series form [4, 9.14.1] and then using [4, (3.381.1)] (reproduced in B.11 and B.7, respectively), the outage probability can be given as

$$P_{\text{out}}(\bar{\gamma}_N) = \frac{q^{2L\tau}}{\Gamma(2L\tau)} \sum_{t=0}^{\infty} \frac{(L\tau)_t (1-q^2)^t g(2L\tau+t, \frac{\varsigma\bar{\gamma}}{\bar{\gamma}_N})}{t!\,(2L\tau)_t}. \tag{3.113}$$

It can be shown that for $q = 1$, the Rayleigh fading channels, Equation 3.113 becomes $P_{\text{out}}(\bar{\gamma}_N) = \frac{g\left(L, \frac{\gamma_{th}}{\bar{\gamma}}\right)}{\Gamma(L)}$, which is same as the result in [1, (40), for $m = 1$]. The infinite series involved in Equation 3.113 is a convergent series and an upper bound on its truncation error is given in Equation A.65.

Average Symbol Error Rate

The ASER of a digital communication system for various M-ary modulations can be obtained by averaging the conditional SER corresponding to the modulation over the PDF of the receiver output SNR [2]. Mathematically, ASER can be given as

$$P_e(\bar{\gamma}) = \int_0^{\infty} p_e(\varepsilon|\gamma) f_{\gamma_{mrc}}(\gamma_{mrc}) d\gamma_{mrc}, \tag{3.114}$$

Table 3.5: Values of a and b for some coherent and noncoherent modulations.

b	a			
	0.5	1	$\frac{4(\sqrt{M}-1)}{\sqrt{M}}$	$\frac{M-1}{2}$
0.5	NBFSK	-	-	-
1	CBFSK/NDBPSK	-	-	NMFSK
2	-	DBPSK	-	-
$2sin^2(\pi/M)$	-	MPSK	-	-
$\frac{3}{M-1}$	-	-	Rect. QAM	-

where $p_e(\varepsilon|\gamma)$ is the conditional SER corresponding to the modulation scheme used. The conditional symbol error rate for different digital M-ary modulation schemes available in literature are given in Table 3.5. Below we obtain expression for ASER for some modulation schemes.

1. **Coherent Modulations**

For coherent modulations, the expression for the conditional BER can be given as

$$p_{e,\text{coh}}(\varepsilon|\gamma) = aQ\left(\sqrt{b\gamma_{mrc}}\right), \tag{3.115}$$

where parameters a and b are given in Table 3.5 for different modulation schemes of interest. Putting $p_{e,\text{coh}}(\varepsilon|\gamma)$ and $f_{\gamma_{mrc}}(\gamma_{mrc})$ into Equation 3.114, ASER for coherent modulation can be expressed as

$$P_{e_{coh}} = \frac{[q\varsigma]^{2L\tau}}{\Gamma(2L\tau)} \int_0^\infty \gamma_{mrc}^{2L\tau-1} e^{-\varsigma\gamma_{mrc}} Q(\sqrt{2a\gamma_{mrc}})\, {}_1F_1\left(L\tau; 2L\tau; \varsigma(1-q^2)\gamma_{mrc}\right) d\gamma_{mrc}. \tag{3.116}$$

Using [1, A-(8a)] (reproduced in Equation B.14), the $Q(\cdot)$ function can be expressed in terms of an incomplete gamma function, and the expression of ASER can be rewritten as

$$P_{e_{coh}} = \frac{1}{2\sqrt{\pi}} \frac{[q\varsigma]^{2L\tau}}{\Gamma(2L\tau)} \sum_{t=0}^{\infty} \frac{(L\tau)_t \left[\varsigma(1-q^2)\right]^t}{t!\,(2L\tau)_t} \int_0^\infty \gamma_{mrc}^{2L\tau+t-1} e^{-\varsigma\gamma_{mrc}} \Gamma\left(\tfrac{1}{2}, a\gamma_{mrc}\right) d\gamma_{mrc} \tag{3.117}$$

The integral can be solved using [1, A-(6)] (reproduced in Equations B.13). Thus, an expression for ASER can be obtained as

$$P_{e_{coh}} = \frac{a}{2}\sqrt{\frac{b}{\pi(b+\varsigma)}}\left[\frac{q\varsigma}{a+\varsigma}\right]^{2L\tau}\sum_{t=0}^{\infty}\frac{(L\tau)_t\,\Gamma\left(t+\frac{1}{2}\right)}{t!^2}\left[\frac{\varsigma(1-q^2)}{b+\varsigma}\right]^t \times {}_2F_1\left(1,t+\frac{1}{2};t+1;\frac{\varsigma}{b+\varsigma}\right). \quad (3.118)$$

2. **Noncoherent Modulations**

For noncoherent modulations, the conditional BER for MRC receiver can be given as [3]

$$p_{e,\text{nch}}(\varepsilon|\gamma) = a\exp(-b\gamma_{mrc}), \quad (3.119)$$

where the values of a and b are given in in Table 3.5. By putting $p_{e,\text{ncoh}}(\varepsilon|\gamma)$ and $f_{\gamma_{mrc}}(\gamma_{mrc})$ into Equation 3.114, an expression for the ASER for noncoherent modulations can be given as

$$P_{e_{nch}} = \frac{[q\varsigma]^{2L\tau}}{2\Gamma(2L\tau)}\int_0^{\infty}\gamma_{mrc}^{2L\tau-1}e^{-(\varsigma+a)\gamma_{mrc}}\,{}_1F_1\left(L\tau;2L\tau;\varsigma(1-q^2)\gamma_{mrc}\right)d\gamma_{mrc}. \quad (3.120)$$

Solving the integral using [4, (7.621.4)] and [1, A-(5)] (reproduced in B.10 and B.12, respectively), a closed-form expression for ASER can be obtained as

$$P_{e_{nch}} = a\left[\frac{q\varsigma}{\sqrt{(\varsigma+b)(b+\varsigma q^2)}}\right]^{2L\tau}. \quad (3.121)$$

For $q = 1$ and $\rho = 0$, can be shown that Equations 3.118 and 3.121 are matching with the result given in [1, (40)] and [1, (39)] for $m = 1$ and $\rho = 0$, respectively.

Evaluation of Truncation Error for Expressions Involving Infinite Series

The expressions obtained in Equations 3.113 and 3.118 for the outage probability and coherent ASER contain infinite series. A finite number of terms are considered for numerical evaluation of these expression, due to which a truncation error may occur. Upper bounds on truncation errors for these expressions have been derived applying the approach in [55] from which the accuracy of numerical evaluation can be verified. We present expression for the upper bound of the above two expressions.

1. **Error Bound for Outage Probability:** The error bound for Equation 3.113 is derived in Section A.10.5 in Equation A.65. It can be given as

$$E_{K_{out}} \leq \frac{q^{2L\tau}(\varsigma\gamma_{th})^{2L\tau+K}(1-q^2)^K (L\tau)_K}{K!(2L\tau+K)\Gamma(2L\tau)(2L\tau)_K} {}_1F_1(2L\tau+K;1+2L\tau+K;-\varsigma\gamma_{th}) \times {}_2F_2\left[\begin{matrix} 1 & L\tau+K & \varsigma\gamma_{th}(1-q^2) \\ K+1 & 2L\tau+K+1 & \end{matrix}\right]. \quad (3.122)$$

2. **Error Bound for ASER for Coherent Modulation:** The error bound for Equation 3.118 is derived in Section A.10.6 in Equation A.68. It can be given as

$$E_{K_{ASER}} \leq \frac{a}{2K!\phi!}\sqrt{\frac{b}{\pi}}\left[\frac{q}{a+\varsigma}\right]^{2L\tau} \frac{(L\tau)_K\Gamma\left(\phi+\frac{1}{2}\right)\varsigma^{2L\tau+K}\left(1-q^2\right)^K}{(b+\varsigma)^{K+\frac{1}{2}}} \times {}_2F_1\left(1,\phi+\frac{1}{2};\phi+1;\frac{\varsigma}{b+\varsigma}\right){}_3F_2\left[\begin{matrix} 1 & \phi+\frac{1}{2} & L\tau+K & \frac{\varsigma(1-q^2)}{b+\varsigma} \\ K+1 & \phi+1 & & \end{matrix}\right], \quad (3.123)$$

where $\phi \triangleq 2L\tau+K$.

Results and Discussion

Analytically obtained expressions have been numerically evaluated and plotted for illustration. Outage probability $P_{\text{out}}(\bar{\gamma}_N)$ vs. $\bar{\gamma}_N$ has been plotted in Figure 3.29 for different values of L, ρ and q. It can be observed that with the decrease in q the receiver suffers more outage, for a fixed value of γ_N, ρ and L, as decrease in q indicates severe fading. The outage degrades with increase in ρ for all values of L, ρ and q, for a fixed $\bar{\gamma}_N$. ASER vs. $\bar{\gamma}$ for some coherent and noncoherent modulations have been shown in Figures 3.30 and 3.31, respectively. In Figure 3.30 plot for coherent PSK has been included. From the plot of BPSK and 8PSK, it can be observed that the ASER performance degrades with a decrease in q and increase in ρ, as expected. Also ASER degrades with increase in the constellation size of the modulation scheme. In Figure 3.31 plots for noncoherent FSK has been shown, for noncoherent BFSK and 4FSK modulations. The observations are similar to the coherent modulations. From these figures one important observation is that, the effect of q is strong enough to counter the performance advantage expected out of L. In the numerical evaluation of expressions involving infinite series we have truncated them suitably to K terms so as to achieve an accuracy in outage and ASER at least at 7^{th} place of decimal digit. Further, the bound on the truncation error has been obtained for outage probability as well as for ASER. In Figure 3.32, $E_{K_{ASER}}$ vs. K has been plotted for 8PSK modulation scheme as a function of L, ρ and $\bar{\gamma}$ with $q = 0.5$. It can be observed that the error bound decreases very fast with K and a maximum of 20 terms is enough for numerical evaluation for the above accuracy.

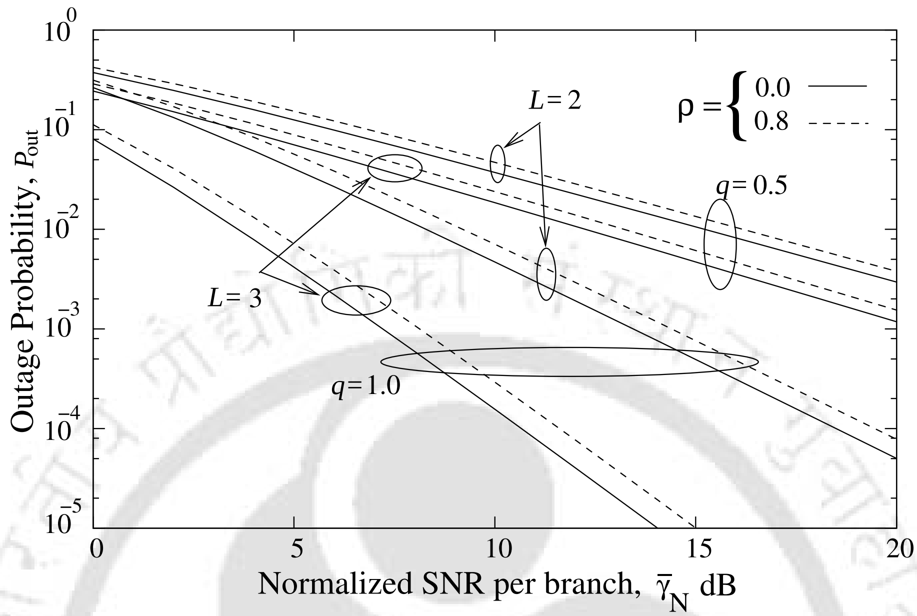

Figure 3.29: Outage probability vs. $\bar{\gamma}_N$ as a function of L and q.

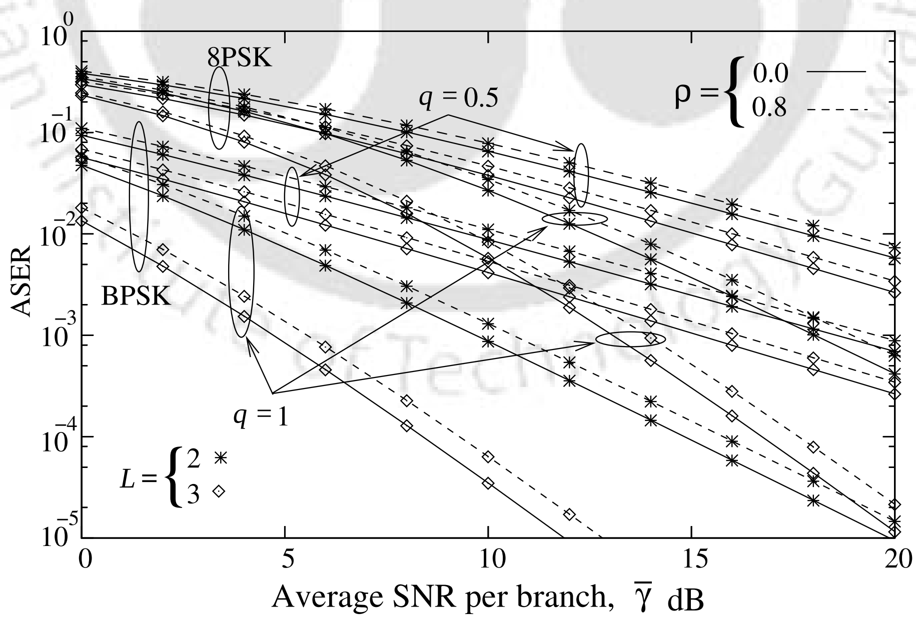

Figure 3.30: ASER vs. $\bar{\gamma}$ for some coherent modulation scheme as a function of L,ρ and q.

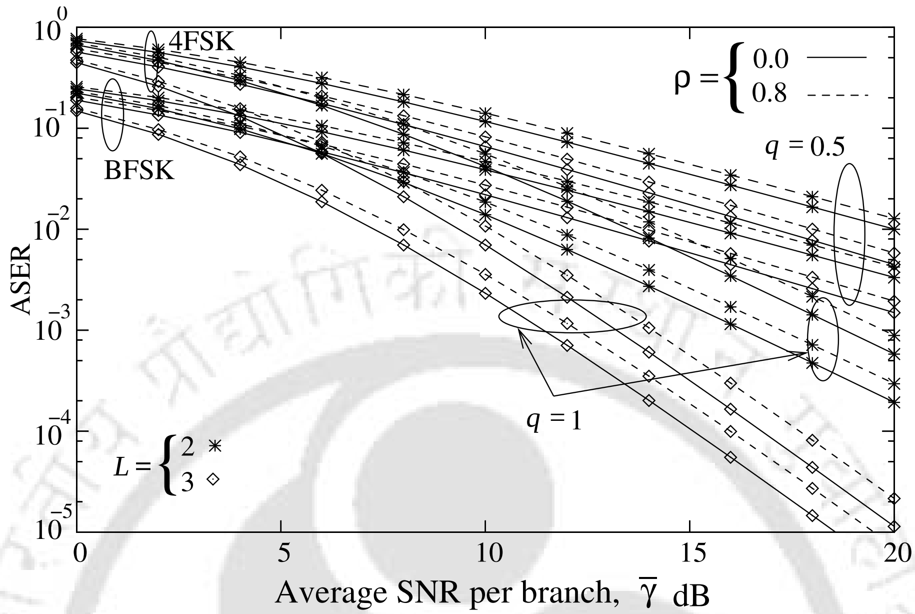

Figure 3.31: ASER vs. $\bar{\gamma}$ for some noncoherent modulation scheme as a function of L,ρ and q.

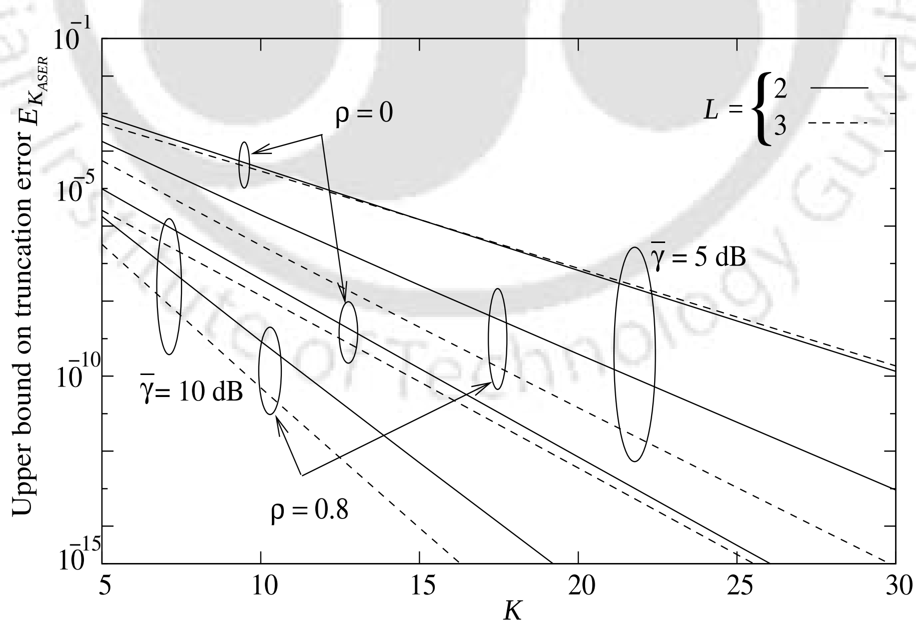

Figure 3.32: $E_{K_{ASER}}$ vs. K for 8PSK modulation scheme as a function of L,ρ and $\bar{\gamma}$ with $q = 0.5$.

Table 3.6: SNR (dB) of dual MRC, EGC and SC at an ABER of 10^{-3}.

	ρ	MRC		EGC		SC	
		$q=1$	$q=0.8$	$q=1$	$q=0.8$	$q=1$	$q=0.8$
CPSK	0	11.06	11.16	11.67	11.80	12.54	12.61
	0.7	12.38	12.51	13.02	13.15	13.84	13.99
DPSK	0	13.17	13.35	13.86	13.94	14.73	14.83
	0.7	14.6	14.73	15.2	15.32	16.16	16.23

3.5 Performance Comparison Among the Diversity Schemes

A Comparison of ABER performance of SC, EGC and MRC diversity schemes is given in Table 3.6. It is obtained for the SNR of dual correlated receivers for different values of q and ρ at an ABER of 10^{-3}. From the table it can be observed that the SNR remains almost same for fixed values of ρ and q for MRC and EGC receivers. Further, the difference in SNR between SC and EGC is more compared to the difference between MRC and EGC, as expected.

3.6 Summary

In this chapter, performance analysis of SC, EGC and MRC receivers over independent and correlated Hoyt fading channels are presented for dual and L order of diversity. Performance measures such as ASNR, outage probability and ABER have been considered. Mathematical expressions for these performance measures have been provided. Numerical and simulation results have been provided with discussion. The diversity receivers for which analyses have been provided are enumerated below.

1. Dual correlated and L independent SC receiver.
2. L independent, equally correlated and exponentially correlated MRC receiver.
3. Dual correlated MRC receiver with equal and unequal fading parameters.

4. Dual correlated EGC receiver.

Chapter 4

Performance Analysis in $\eta-\mu$ Fading Channels

A $\eta-\mu$ is a generalized fading channel model, which best fits to the experimental data with no line-of-sight path [14]. Commonly used fading channel models such as Rayleigh, Hoyt, Nakagami-*m* etc. can be realized as special cases of this model. In this section, performance parameters of L -SC and -MRC receivers are derived over $\eta-\mu$ fading channels. For SC receiver, the outage probability is obtained from the joint PDF of the input SNRs $\gamma_l|_{l=1}^{L}$, for exponential fading correlation fading models. For the MRC receiver, a PDF based approach discussed in Section 2.3.1 is used to obtain moments of the combiner output SNR γ_{mrc}, outage probability and ABER for binary, coherent and non-coherent modulations.

4.1 Selection Combining in Independent Fading Channels

Performance of an L-SC receiver is analyzed over independent η-μ fading channels using a PDF based approach discussed in Section 2.3.1. An expression for the PDF of the combiner output SNR is to be obtained in this approach. The analysis is carried out in two parts; first part deals with the derivation of an expression for the PDF of the combiner output SNR $f_{\gamma_{sc}}(\gamma_{sc})$ and in the second part using the obtained PDF expression, mathematical expression for the moment and the ABER performance are derived.

The CDF of $\eta-\mu$ distribution is known in closed form in terms of Yacoub integral [14]. A general solution of which is recently presented in [48]. But, we observed that it is difficult to used in this form to obtain the PDF of the γ_{sc}. In order to obtain desired performance measures for a general case we have obtained this CDF expression in an infinite series form using which it is possible to obtain the PDF of γ_{sc}. It is explained below.

4.1.1 PDF of Combiner Output Signal-to-Noise Ratio

An expression for the PDF of SNR in $\eta-\mu$ fading channels is given as [14]

$$f_{\gamma_l}(\gamma_l) = \frac{2\sqrt{\pi}h^{\mu}}{\Gamma(\mu)}\left[\frac{\mu}{\bar{\gamma}_l}\right]^{\mu+\frac{1}{2}}\left[\frac{\gamma_l}{H}\right]^{\mu-\frac{1}{2}} e^{-\frac{2\mu h\gamma_l}{\bar{\gamma}_l}} I_{\mu-\frac{1}{2}}\left(\frac{2\mu H\gamma_l}{\bar{\gamma}_l}\right), \tag{4.1}$$

where the parameters H, h and μ are explained in Equation 1.6. An expression for the CDF of the l^{th} branch SNR can be obtained, by integrating Equation 4.1 w. r. t. γ_l as

$$\begin{aligned} F_{\gamma_l}(\gamma_l) &= \frac{2\sqrt{\pi}h^{\mu}}{\Gamma(\mu)}\left[\frac{\mu}{\bar{\gamma}_l}\right]^{\mu+\frac{1}{2}}\left[\frac{1}{H}\right]^{\mu-\frac{1}{2}}\int_0^{\gamma_{sc}} \gamma_l^{\mu-\frac{1}{2}} e^{-\frac{2\mu h\gamma_l}{\bar{\gamma}_l}} I_{\mu-\frac{1}{2}}\left[\frac{2\mu H\gamma_l}{\bar{\gamma}_l}\right] d\gamma_l \\ &= \frac{\sqrt{\pi}}{\Gamma(\mu)}\sum_{t=0}^{\infty}\frac{H^{2t} g\left(2\mu+2t, \frac{2\mu h}{\bar{\gamma}_l}\gamma_l\right)}{t!\Gamma(\mu+t+\frac{1}{2})2^{2\mu+2t-1}h^{\mu+2t}}. \end{aligned} \tag{4.2}$$

The integration in the above expression is solved by expressing the $I_{\mu}(\cdot)$ in infinite series [54] (reproduced in Equation B.17) and using [4, (3.381.1)] (reproduced in Equation B.6). For independent and identical branch powers i.e. for $\bar{\gamma}_l = \bar{\gamma}, \forall l$, the CDF of γ_{sc} can be written as the product of L-CDFs of L branch SNRs, as

$$F_{\gamma_{sc}}(\gamma_{sc}) = P(\gamma_1 \le \gamma_{sc}, \gamma_2 \le \gamma_{sc}, \ldots, \gamma_L \le \gamma_{sc}) = \prod_{l=1}^{L} F_{\gamma_l}(\gamma_l)$$

$$= \left[\frac{\sqrt{\pi}}{\Gamma(\mu)}\sum_{t=0}^{\infty}\frac{H^{2t}g\left(2\mu+2t,\frac{2\mu h}{\bar{\gamma}}\gamma_{sc}\right)}{t!2^{2\mu+2t-1}\Gamma(\mu+t+\frac{1}{2})h^{\mu+2t}}\right]^{L}. \quad (4.3)$$

Differentiating Equation 4.3 w. r. t. γ_{sc}, the PDF of γ_{sc} can be given as

$$f_{\gamma_{sc}}(\gamma_{sc}) = \frac{2^L L\pi^{L/2}h^{L\mu}}{\Gamma^L(\mu)}\sum_{t_1=0}^{\infty}\sum_{t_2=0}^{\infty}\cdots\sum_{t_L=0}^{\infty}\frac{H^{2\sum_{i=1}^{L}t_i}\gamma_{sc}^{2(L\mu+\sum_{i=1}^{L}t_i)-1}}{\left\{\prod_{i=1}^{L}t_i!\Gamma\left(\mu+t_i+\frac{1}{2}\right)\right\}}\left(\frac{\mu}{\bar{\gamma}}\right)^{2(L\mu+\sum_{i=1}^{L}t_i)}$$
$$\times e^{-\frac{2L\mu h}{\bar{\gamma}}\gamma_{sc}}\left\{\prod_{i=1}^{L-1}\frac{{}_1F_1\left(1;2\mu+2t_i+1;\frac{2\mu h}{\bar{\gamma}}\gamma_{sc}\right)}{2\mu+2t_i}\right\}. \quad (4.4)$$

For Rayleigh fading channels, which is a special case of $\eta-\mu$ fading model ($\mu=0.5$, $\eta=1$), it can be shown that Equation 4.4 reduces to [10, (7.60)].

4.1.2 Moments of Combiner Output Signal-to-Noise Ratio

Using Equations 4.4 and 3.9, the N^{th} moment of the γ_{sc} over η-μ channels can be expressed as

$$E\left[\gamma_{sc}^{N}\right] = \frac{2^L L\pi^{L/2}h^{L\mu}}{\Gamma^L(\mu)}\sum_{t_1=0}^{\infty}\sum_{t_2=0}^{\infty}\cdots\sum_{t_L=0}^{\infty}\frac{H^{2\sum_{i=1}^{L}t_i}}{\left\{\prod_{i=1}^{L}t_i!\Gamma\left(\mu+t_i+\frac{1}{2}\right)\right\}\left\{\prod_{i=1}^{L-1}(2\mu+2t_i)\right\}}\left(\frac{\mu}{\bar{\gamma}}\right)^{2(L\mu+\sum_{i=1}^{L}t_i)}$$
$$\times\int_0^{\infty}\gamma_{sc}^{2(L\mu+\sum_{i=1}^{L}t_i)+N+1}e^{-\frac{2L\mu h}{\bar{\gamma}}\gamma_{sc}}\left\{\prod_{i=1}^{L-1}{}_1F_1\left(1;2\mu+2t_i+1;\frac{2\mu h}{\bar{\gamma}}\gamma_{sc}\right)\right\}d\gamma_{sc}. \quad (4.5)$$

The involved integration in Equation 4.5 can be solved using [3, (C.1)] (reproduced in Equation B.15) and an expression for $E[\gamma_{sc}^{N}]$ can be given as

$$E[\gamma_{sc}^{N}] =$$
$$= \frac{2^{L-N}\pi^{\frac{L}{2}}}{L^{N-1}\Gamma^L(\mu)}\left(\frac{\bar{\gamma}}{h\mu}\right)^{N}\sum_{t_1=0}^{\infty}\sum_{t_2=0}^{\infty}\cdots\sum_{t_L=0}^{\infty}\frac{\Gamma\left(N+2(L\mu+\sum_{i=1}^{L}t_i)\right)h^{L\mu-2(L\mu+\sum_{i=1}^{L}t_i)}H^{2\sum_{i=1}^{L}t_i}}{(2L)^{2(L\mu+\sum_{i=1}^{L}t_i)}\left\{\prod_{i=1}^{L-1}(2\mu+2t_i)\right\}\left\{\prod_{i=1}^{L}t_i!\Gamma\left(\mu+t_i+\frac{1}{2}\right)\right\}}$$

$$\times F_A\left(N+\lambda,\ \underbrace{1,1,\ldots,1}_{(L-1)\,\text{numbers}};\ 2\mu+2t_1+1,\ 2\mu+2t_2+1,\ldots,2\mu+2t_{L-1}+1;\underbrace{\frac{1}{L},\frac{1}{L},\ldots,\frac{1}{L}}_{(L-1)\,\text{numbers}}\right). \tag{4.6}$$

An expression for the average output SNR $\bar{\gamma}$ can be obtained from Equation 4.6, substituting $N=1$ as

$$\bar{\gamma}_{sc} = \frac{2^{L-1}\pi^{\frac{L}{2}}\bar{\gamma}h^{L\mu-1}}{\mu\Gamma^{L}(\mu)}\sum_{t_1=0}^{\infty}\sum_{t_2=0}^{\infty}\cdots\sum_{t_L=0}^{\infty}\frac{\Gamma\left(1+2(L\mu+\sum_{i=1}^{L}t_i)\right)H^{2\sum_{i=1}^{L}t_i}}{(2hL)^{2(L\mu+\sum_{i=1}^{L}t_i)}\left\{\prod_{i=1}^{L}t_i!\Gamma\left(\mu+t_i+\frac{1}{2}\right)\right\}\left\{\prod_{i=1}^{L-1}(2\mu+2t_i)\right\}}$$
$$\times F_A\left(1+2(L\mu+\sum_{i=1}^{L}t_i),\ \underbrace{1,1,\ldots,1}_{(L-1)\text{numbers}};\ 2\mu+2t_1+1,2\mu+2t_2+1,\ldots,2\mu+2t_{L-1}+1;\right.$$
$$\left.\underbrace{\frac{1}{L},\frac{1}{L},\ldots,\frac{1}{L}}_{(L-1)\text{numbers}}\right). \tag{4.7}$$

4.1.3 Average Bit Error Rate

A general expression to obtain the ABER is given in Equation 2.17 which needs the PDF of γ_{sc} and the conditional bit error rate $p_{e,\text{coh}}(\varepsilon|\gamma)$, for evaluation. The conditional bit error rate (conditioned on the received SNR) for different digital modulation schemes are listed in Table 2.1. In the work presented here, we obtain expressions for ABER for binary, coherent and noncoherent modulations as discussed below.

Binary Coherent Modulations

For binary coherent modulations (BPSK and BFSK), an expression for the conditional BER is given in Equation 2.24. Putting $p_{e,\text{coh}}(\varepsilon|\gamma)$ and $f_{\gamma_{sc}}(\gamma_{sc})$ from Equations 2.24 and 4.4 into Equation 2.17, an expression for ABER can be written as

$$P_{e_{ch}}(\bar{\gamma}) = \frac{L\left(2\sqrt{\pi}\right)^{L}}{\Gamma^{L}(\mu)}\left(\frac{\mu\sqrt{h}}{\bar{\gamma}}\right)^{2L\mu}\sum_{t_1=0}^{\infty}\sum_{t_2=0}^{\infty}\cdots\sum_{t_L=0}^{\infty}\frac{\left(\frac{H\mu}{\bar{\gamma}}\right)^{2\sum_{i=1}^{L}t_i}}{\left\{\prod_{i=1}^{L}t_i!\Gamma\left(\mu+t_i+\frac{1}{2}\right)\right\}}$$
$$\times\int_0^{\infty}Q\left(\sqrt{2a\gamma_{sc}}\right)\gamma_{sc}^{2(L\mu+\sum_{i=1}^{L}t_i)-1}e^{-\frac{2L\mu h}{\bar{\gamma}}\gamma_{sc}}\left\{\prod_{i=1}^{L-1}\frac{{}_1F_1\left(1;2\mu+2t_i+1;\frac{2\mu h}{\bar{\gamma}}\gamma_{sc}\right)}{2\mu+2t_i}\right\}d\gamma_{sc}. \tag{4.8}$$

The integral in Equation 4.8 cannot be solved in this form. Hence, expressing the hypergeometric function in Equation 4.8 in an infinite series [4, 9.14.1] (reproduced in Equation B.11) and expressing, above expression for the coherent ABER can be rewritten as

$$P_{e_{ch}}(\bar{\gamma}) = \frac{2^{L}L\pi^{L/2}}{\Gamma^{L}(\mu)}\left(\frac{\mu\sqrt{h}}{\bar{\gamma}}\right)^{2L\mu}\sum_{t_1=0}^{\infty}\sum_{t_2=0}^{\infty}\cdots\sum_{t_L=0}^{\infty}\sum_{k_1=0}^{\infty}\sum_{k_2=0}^{\infty}\cdots\sum_{k_{L-1}=0}^{\infty}\frac{(2h)^{\sum_{l=1}^{L-1}k_l}H^{2\sum_{i=1}^{L}t_i}}{\left\{\prod_{i=1}^{L}t_i!\Gamma\left(\mu+t_i+\frac{1}{2}\right)\right\}}$$
$$\times\frac{1}{\left\{\prod_{i=1}^{L-1}(2\mu+2t_i)(2\mu+2t_i+1)_{k_i}\right\}}\left(\frac{\mu}{\bar{\gamma}}\right)^{2\sum_{i=1}^{L}t_i+\sum_{l=1}^{L-1}k_l}$$
$$\times\int_0^{\infty}Q\left(\sqrt{2a\gamma_{sc}}\right)\gamma_{sc}^{2(L\mu+\sum_{i=1}^{L}t_i)+\sum_{l=1}^{L-1}k_l-1}e^{-\frac{2L\mu h}{\bar{\gamma}}\gamma_{sc}}d\gamma_{sc}. \tag{4.9}$$

The integral in Equation 4.9 can be solved after expressing the $Q(\cdot)$ function in incomplete gamma function using [1, A-(6)] (reproduced in Equations B.13) as below

$$P_{e_{ch}}(\bar{\gamma}) = \frac{\left(2\sqrt{\pi}\right)^{L-1}L}{\Gamma^{L}(\mu)}\left(\frac{\sqrt{h}\mu}{\bar{\gamma}}\right)^{2L\mu}\sum_{t_1=0}^{\infty}\sum_{t_2=0}^{\infty}\cdots\sum_{t_L=0}^{\infty}\sum_{k_1=0}^{\infty}\sum_{k_2=0}^{\infty}\cdots\sum_{k_{L-1}=0}^{\infty}\frac{(2h)^{\sum_{l=1}^{L-1}k_l}H^{2\sum_{i=1}^{L}t_i}}{\left\{\prod_{i=1}^{L}t_i!\Gamma\left(\mu+t_i+\frac{1}{2}\right)\right\}}$$
$$\times\frac{1}{\left\{\prod_{i=1}^{L-1}(2\mu+2t_i)(2\mu+2t_i+1)_{k_i}\right\}}\left(\frac{\mu}{\bar{\gamma}}\right)^{2\sum_{i=1}^{L}t_i+\sum_{l=1}^{L-1}k_l}$$

$$\times \int_0^\infty \Gamma\left(\frac{1}{2}, a\gamma_{sc}\right) \gamma_{sc}^{2L\mu+2\sum_{i=1}^{L} t_i + \sum_{l=1}^{L-1} k_l - 1} e^{-\frac{2L\mu h}{\bar{\gamma}}\gamma_{sc}} d\gamma_{sc}. \tag{4.10}$$

Solving the integral in 4.10, using [1, A-(8a)] (reproduced in Equation B.14), an expression for ABER can be obtained as

$$P_{e_{ch}}(\bar{\gamma}) =$$
$$= \sqrt{\frac{a\bar{\gamma}}{\mu}} \frac{\left(2\sqrt{\pi}\right)^{L-1} L h^{L\mu} \Phi^{2L\mu+\frac{1}{2}}}{\Gamma^L(\mu)} \sum_{t_1=0}^{\infty}\sum_{t_2=0}^{\infty}\cdots\sum_{t_L:=0}^{\infty}\sum_{k_1=0}^{\infty}\sum_{k_2=0}^{\infty}\cdots\sum_{k_{L-1}:=0}^{\infty} \frac{\Gamma\left(2L\mu+2\sum_{i=1}^{L} t_i + \sum_{l=1}^{L-1} k_l + \frac{1}{2}\right)}{\left\{\prod_{i=1}^{L} t_i! \Gamma\left(\mu+t_i+\frac{1}{2}\right)\right\}}$$
$$\times \frac{(2h)^{\sum_{l=1}^{L-1} k_l} H^{2\sum_{i=1}^{L} t_i} \Phi^{2\sum_{i=1}^{L} t_i + \sum_{l=1}^{L-1} k_l} {}_2F_1\left(1, 2L\mu+2\sum_{i=1}^{L} t_i + \sum_{l=1}^{L-1} k_l + \frac{1}{2}; 2L\mu+2\sum_{i=1}^{L} t_i + \sum_{l=1}^{L-1} k_l + 1; 2Lh\Phi\right)}{\left\{\prod_{i=1}^{L-1} (2\mu+2t_i)(2\mu+2t_i+1)_{k_i}\right\}\left(2L\mu+2\sum_{i=1}^{L} t_i + \sum_{l=1}^{L-1} k_l\right)}, \tag{4.11}$$

where $\Phi \triangleq \frac{\mu}{2L\mu h + a\bar{\gamma}}$.

Binary Non-coherent Modulations

For binary noncoherent modulations, an expression for the conditional BER is given in Equation 2.25. By putting $p_{e,\mathrm{ncoh}}(\varepsilon|\gamma)$ and $f_{\gamma_{sc}}(\gamma_{sc})$ from Equations 2.25 and 4.4 into Equation 2.17 an expression for the noncoherent ABER can be given as

$$P_{e,nch}(\bar{\gamma}) = \frac{2^{L-1} L \pi^{\frac{L}{2}}}{\Gamma^L(\mu)} \left(\frac{\sqrt{h}\mu}{\bar{\gamma}}\right)^{2L\mu} \sum_{t_1=0}^{\infty}\sum_{t_2=0}^{\infty}\cdots\sum_{t_L=0}^{\infty} \frac{\left(\frac{\mu H}{\bar{\gamma}}\right)^{2\sum_{i=1}^{L} t_i}}{\left\{\prod_{i=1}^{L} t_i! \Gamma\left(\mu+t_i+\frac{1}{2}\right)\right\}\left\{\prod_{i=1}^{L-1} 2\mu+2t_i\right\}}$$
$$\times \int_0^\infty \gamma_{sc}^{2L\mu+2\sum_{i=1}^{L} t_i - 1} e^{-\frac{2L\mu h + a\bar{\gamma}_{sc}}{\bar{\gamma}}\gamma_{sc}} \left\{\prod_{i=1}^{L-1} {}_1F_1\left(1; 2\mu+2t_i+1; \frac{2\mu h}{\bar{\gamma}}\gamma_{sc}\right)\right\} d\gamma_{sc}. \tag{4.12}$$

Solving the integral in Equation 4.12 using [3, (C.1)] (reproduced in Equation B.15) expression for the noncoherent ABER can be obtained as

$$P_{e,nch}(\bar{\gamma}) = \frac{2^{L-1}L\pi^{L/2}}{\Gamma^{L}(\mu)}\left(\sqrt{h}\Phi\right)^{2L\mu}\sum_{t_1=0}^{\infty}\sum_{t_2=0}^{\infty}\cdots\sum_{t_L=0}^{\infty}\frac{\Gamma\left(2L\mu+2\sum_{i=1}^{L}t_i\right)(\Phi H)^{2\sum_{i=1}^{L}t_i}}{\left\{\prod_{i=1}^{L}t_i!\Gamma\left(\mu+t_i+\frac{1}{2}\right)\right\}\left\{\prod_{i=1}^{L-1}2\mu+2t_i\right\}}F_A\left(2L\mu+2\sum_{i=1}^{L}t_i;\right.$$

$$\left.\underbrace{1,1,\ldots,1;}_{(L-1)\ \text{numbers}}\quad 2\mu+2t_1+1,\ldots,2\mu+2t_{L-1}+1;\quad \underbrace{2h\Phi,\ldots,2h\Phi}_{(L-1)\ \text{numbers}}\right). \tag{4.13}$$

4.1.4 Results and Discussion

ABER vs. $\bar{\gamma}$ for binary coherent and non-coherent modulations over η-μ fading channels are shown in Figures 4.1 and 4.2, respectively. The η-μ fading model is applicable to non line-of-sight fading channel communications and similar to κ-μ fading channels, here μ is also proportional to the number of multi-path clusters. So, the effect of μ on system performance is similar to κ-μ fading channels. Also, the performance is directly proportional to L for fixed, η and μ. The parameter η depends on the variance of the in-phase and the quadrature phase components of clusters. Hence, as expected, increase in η degrades the ABER performance. It can be observed from Figures 4.1 and 4.2, that for an increase in diversity order from 2 to 3 a diversity gain of 3.49 dB and 4.57 dB, respectively, can be achieved at an ABER of 10^{-4}. The corresponding values of diversity gain for non-coherent modulations are observed to be 1.23 dB and 1.89 dB, respectively. In the numerical evaluation of expressions involving infinite series, we have truncated them suitably so as to achieve an accuracy at least at 7^{th} place of decimal digit. In Table 4.1 we have illustrated the number of terms (N) required to achieve an ABER of 10^{-7} in the evaluation Equation 4.11 as a function of $\bar{\gamma}$.

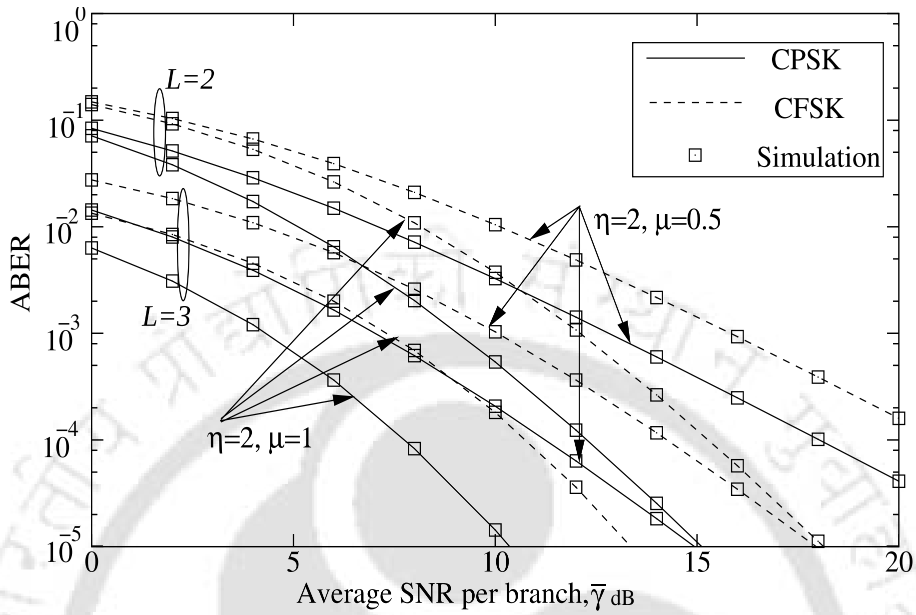

Figure 4.1: ABER vs. $\bar{\gamma}$ for SC receiver with CPSK and CFSK modulations.

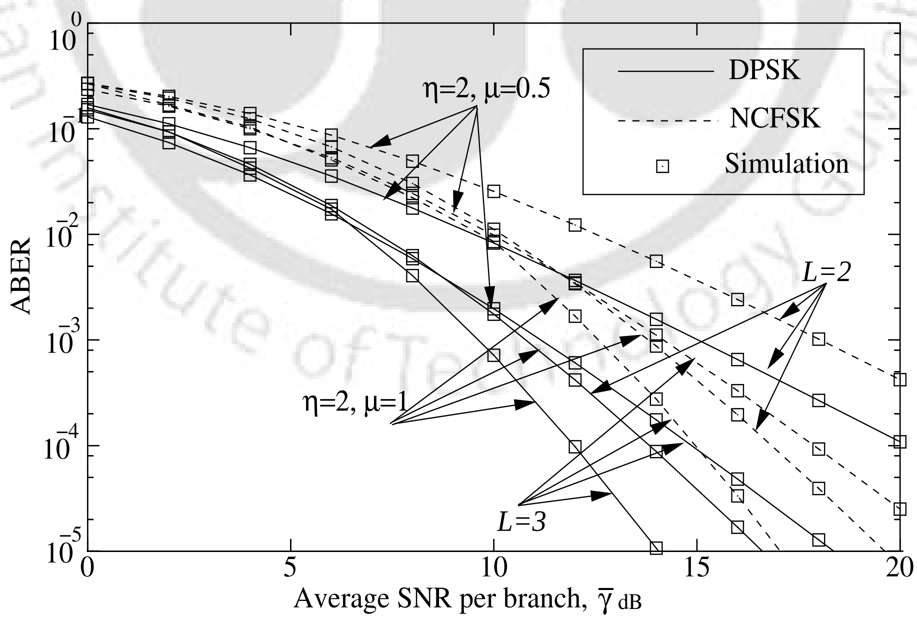

Figure 4.2: ABER vs. $\bar{\gamma}$ for SC receiver with DPSK and NCFSK modulations.

Table 4.1: Number of terms (N) required for an accuracy at 7^{th} place of decimal digit in the numerical evaluation of Equation 4.11 for $\eta = 2, \mu = 1$.

$\bar{\gamma}$ (dB)	Modulation	$L=2$		$L=3$	
		N	ABER	N	ABER
5	CPSK	6	0.0209453	8	0.0025874
	CFSK	10	0.0515436	13	0.0080392
10	CPSK	5	0.0032608	5	0.0002074
	CFSK	6	0.0104652	6	0.0010341

4.2 Selection Combining in Exponentially Correlated Channels

In this section, an expression for the outage probability of an L-SC receiver is derived for an exponentially correlated $\eta-\mu$ fading channel. An expression for the joint PDF of exponentially correlated multivariate $\eta-\mu$ RV is obtained which is further used to derive the expression for the outage probability. Monte Carlo simulation has been performed to validate the obtained mathematical expression. Numerical and simulation results are plotted and the effects of correlation, number of diversity branches and fading parameters on the outage probability of the receiver are studied.

4.2.1 Joint PDF of Exponentially Correlated $\eta-\mu$ Random Variables

From [14], $\eta-\mu$ distributed RVs Z_l ($l = 1, 2, \ldots, L$) can be modeled as $Z_l^2 = X_l^2 + Y_l^2 = \sum_{i=1}^{n} X_{l,i}{}^2 + \sum_{i=1}^{n} Y_{l,i}{}^2$, where $X_{l,i}$ and $Y_{l,i}$ are independent Gaussian RVs with zero mean and variances σ_x^2 and σ_y^2, respectively. In this representation the PDF Z_l is as given in Equation 1.6, where the fading parameter $\eta = \frac{\sigma_x{}^2}{\sigma_y{}^2}$. An expression for the joint PDF of exponentially correlated (for which the correlation matrix is given as $\Sigma_{ij} = \sqrt{\rho}^{|i-j|}$, where $\rho = \mathrm{cov}(x_1^2, x_2^2)/\sqrt{\mathrm{var}(x_1^2)\mathrm{var}(x_2^2)}, 1 \leq i, j \leq L$ and $i \neq j$) RVs X_l, can be obtained extending the useful formula given for generalized Rayleigh RVs in [66] as (Section A.9)

$$f_{X_1,X_2,\ldots,X_L}(x_1,x_2,\ldots,x_L) = \frac{x_1^{m-1}x_L^m e^{-\frac{x_L^2+x_1^2}{2\sigma_x^2(1-\rho)}-\frac{(1+\rho)}{2\sigma_x^2(1-\rho)}\sum_{k=2}^{L-1}x_k^2}}{2^{m-1}\Gamma(m)\left[\sigma_x^{2L}(1-\rho)^{L-1}\right]^m}\left\{\prod_{k=1}^{L-1}\left(\frac{\sqrt{\rho}}{\sigma_x^2(1-\rho)}\right)^{-(m-1)} \times x_k I_{m-1}\left(\frac{\sqrt{\rho}}{\sigma_x^2(1-\rho)}x_k x_{k+1}\right)\right\}, x_k \geq 0, \tag{4.14}$$

where $m=n/2$. Joint PDF of $\{X_1,X_2,\ldots,X_L\}$s obtained in Equation 4.14 cannot be used in this format as it is not possible to derive $X_l^2+Y_l^2$, to evaluate the joint PDF of exponentially correlated $\eta-\mu$ envelopes (Z_ls). Expressing the Bessel function in infinite series [4, (8.455)], Equation 4.14 can be expressed as

$$f_{X_1,X_2,\ldots,X_L}(x_1,x_2,\ldots,x_L) = \frac{2^{L(1-m)}(x_1,x_2,\ldots,x_L)^{2m-1}}{\Gamma(m)\left[\sigma_x^{2L}(1-\rho)^{L-1}\right]^m}e^{-\frac{x_L^2+x_1^2}{2\sigma_x^2(1-\rho)}-\frac{(1+\rho)}{2\sigma_x^2(1-\rho)}\sum_{k=2}^{L-1}x_k^2} \times\sum_{t_1=0}^{\infty}\sum_{t_2=0}^{\infty}\cdots\sum_{t_{L-1}=0}^{\infty}\frac{\rho^{t_1+t_2+\ldots+t_{L-1}}x_1^{2t_1}x_2^{2t_1+2t_2}\ldots x_{L-1}^{2t_{L-2}+2t_{L-1}}x_L^{2t_{L-1}}}{(\sigma_x^2(1-\rho))^{2t_1+2t_2+\ldots+2t_{L-1}}\left\{\prod_{i=1}^{L-1}4^{t_i}t_i!\Gamma(m+t_i)\right\}}. \tag{4.15}$$

Thus, the joint PDF of exponentially correlated RVs X_l^2 can be derived from Equation 4.15 as

$$f_{X_1^2,X_2^2,\ldots,X_L^2}(x_1^2,x_2^2,\ldots,x_L^2) = \frac{(x_1,x_2,\ldots,x_L)^{m-1}}{2^{Lm}\Gamma(m)\left[\sigma_x^{2L}(1-\rho)^{L-1}\right]^m}e^{-\frac{x_L+x_1}{2\sigma_x^2(1-\rho)}-\frac{(1+\rho)}{2\sigma_x^2(1-\rho)}\sum_{k=2}^{L-1}x_k} \times\sum_{t_1=0}^{\infty}\sum_{t_2=0}^{\infty}\cdots\sum_{t_{L-1}=0}^{\infty}\frac{\rho^{t_1+t_2\ldots+t_{L-1}}x_1^{t_1}x_2^{t_1+t_2}\ldots x_{L-1}^{t_{L-2}+t_{L-1}}x_L^{t_{L-1}}}{\{\sigma_x^2(1-\rho)\}^{2t_1+2t_2\ldots+2t_{L-1}}\left\{\prod_{i=1}^{L-1}4^{t_i}t_i!\Gamma(m+t_i)\right\}}. \tag{4.16}$$

An expression for the joint PDF of exponentially correlated RVs Y_l^2s can be obtained by putting y in place of x in Equation 4.16. It can be given as

$$f_{Y_1^2,Y_2^2,\ldots,Y_L^2}(y_1^2,y_2^2,\ldots,y_L^2) = \frac{(y_1\ldots y_n)^{m-1}}{2^{mL}\Gamma(m)\left[\sigma_y^{2L}(1-\rho)^{L-1}\right]^m}e^{-\frac{y_1+y_L}{2\sigma_y^2(1-\rho)}-\frac{(1+\rho)}{2\sigma_y^2(1-\rho)}\sum_{k=2}^{L-1}y_k}$$

$$\times \sum_{l_1=0}^{\infty}\sum_{l_2=0}^{\infty}\cdots\sum_{l_{L-1}=0}^{\infty}\frac{\left(\frac{\sqrt{\rho}}{\sigma_y^2(1-\rho)}\right)^{2(l_1+l_2\ldots+l_{L-1})} y_1^{l_1}y_2^{l_1+l_2}\ldots y_{L-1}^{l_{L-2}+l_{L-1}}y_L^{l_{L-1}}}{\left\{\prod_{j=1}^{L-1}4^{l_j}l_j!\Gamma(m+l_j)\right\}}. \tag{4.17}$$

Since X_l^2 and Y_l^2 are independent RVs, applying convolution operation [59, 6.44], an expression for the joint PDF of exponentially correlated RVs $Z_l^2 = X_l^2+Y_l^2$, can be derived as

$$f_{Z_1^2,Z_2^2,\ldots,Z_L^2}(z_1^2,z_2^2,\ldots,z_L^2) =$$
$$= \frac{(1-\rho)^{2m(1-L)}}{4^{Lm}\Gamma^2(m)\left[\sigma_x\sigma_y\right]^{2Lm}}\sum_{t_1=0}^{\infty}\sum_{t_2=0}^{\infty}\cdots\sum_{t_{L-1}=0}^{\infty}\sum_{l_1=0}^{\infty}\sum_{l_2=0}^{\infty}\cdots\sum_{l_{L-1}=0}^{\infty}\frac{z_1^{2m+t_1+l_1-1}B(m+t_1,m+l_1)}{\left\{\prod_{i=1}^{L-1}4^{t_i+l_i}t_i!l_i!\Gamma(m+t_i)\Gamma(m+l_i)\right\}}$$
$$\times\left(\frac{\sqrt{\rho}}{1-\rho}\right)^{2(t_T+l_T)}\frac{e^{-\frac{z_1}{2\sigma_y^2(1-\rho)}}}{\sigma_x^{4t_T}\sigma_y^{4l_T}}{}_1F_1\left(m+t_1;2m+t_1+l_1;\frac{\sigma_x^2-\sigma_y^2}{2\sigma_x^2\sigma_y^2(1-\rho)}z_1\right)$$
$$\times\left\{\prod_{k=2}^{L-1}e^{-\frac{(1+\rho)z_k}{2\sigma_y^2(1-\rho)}}\frac{B\left(m_k^t,m_k^l\right)}{z_k^{1-m_k^t-m_k^l}}{}_1F_1\left(m_k^t;m_k^t+m_k^l;\frac{\left(\sigma_x^2-\sigma_y^2\right)(1+\rho)}{2\sigma_x^2\sigma_y^2(1-\rho)}z_k\right)\right\}e^{-\frac{z_L}{2\sigma_y^2(1-\rho)}}$$
$$\times B\left(m+t_{L-1},m+l_{L-1}\right)z_L^{2m+t_{L-1}+l_{L-1}-1}{}_1F_1\left(m+t_{L-1};2m+t_{L-1}+l_{L-1};\frac{\sigma_x^2-\sigma_y^2}{2\sigma_x^2\sigma_y^2(1-\rho)}z_L\right), \tag{4.18}$$

where, $j_T \triangleq j_1+j_2\ldots+j_{L-1}$, $s_k^j \triangleq s+j_{k-1}+j_k$. The power correlation co-efficient of Z_ls can also be shown as ρ [67]. It is shown in Section A.8.

4.2.2 Outage Probability

To obtain an expression for the outage probability of a SC receiver with L input branches, the joint PDF of the input branch SNRs is required to be known. From Equation 4.18, the joint PDF of input SNRs γ_l of SC receiver can be obtained by applying the concept of RV transformation on $\gamma_l = z_l^2\frac{E_b}{N_0}$. Assuming $\sigma_y^2 = 1$ in the resulting expression, for the convenience of presentation and without loss of generality, which results in $\sigma_x^2 = \eta$ and $\frac{E_b}{N_0} = \frac{\bar{\gamma}}{2\mu(1+\eta)}$. Also, from [14] parameter $\mu = n/2$, where

n is the number of multipath cluster, hence, in this we can write m=μ. After these substitutions and some algebraic manipulations, the expression for the exponentially correlated joint PDF of γ_ls, can be given as

$$f_{\gamma_1,\gamma_2,\ldots,\gamma_L}(\gamma_1,\gamma_2,\ldots,\gamma_L) = \\ = \frac{(1-\rho)^{2\mu(1-L)}}{4^{L\mu}\Gamma^2(\mu)\eta^{L\mu}} \sum_{t_1=0}^{\infty}\sum_{t_2=0}^{\infty}\cdots\sum_{t_{L-1}=0}^{\infty}\sum_{l_1=0}^{\infty}\sum_{l_2=0}^{\infty}\cdots\sum_{l_{L-1}=0}^{\infty} \frac{B(\mu+t_1,\mu+l_1)\,{}_1F_1\left(\mu+t_1;2\mu+t_1+l_1;\lambda\gamma_1\right)}{\eta^{2t_T}\left\{\prod_{i=1}^{L-1}\left(4^{t_i+l_i}t_i!l_i!\Gamma(\mu+t_i)\Gamma(\mu+l_i)\right)\right\}} \\ \times\left(\frac{\sqrt{\rho}}{1-\rho}\right)^{2(t_T+l_T)}\xi^{2\mu+t_1+l_1}\gamma_1^{2\mu+t_1+l_1-1}e^{-\frac{\xi\gamma_1}{2(1-\rho)}}\left\{\prod_{k=2}^{L-1}\frac{B\left(\mu_k^t,\mu_k^l\right){}_1F_1\left(\mu_k^t,\mu_k^t+\mu_k^l;\lambda(1+\rho)\gamma_k\right)}{\gamma_k^{1-(\mu_k^t+\mu_k^l)}e^{\frac{\xi(1+\rho)\gamma_k}{2(1-\rho)}}\xi^{-({}_k^t\mu+{}_k^l\mu)}}\right\} \\ \times\xi^{2\mu+t_{L-1}+l_{L-1}}B\left(\mu+t_{L-1},\mu+l_{L-1}\right)\gamma_L^{2\mu+t_{L-1}+l_{L-1}-1}e^{-\frac{\xi\gamma_L}{2(1-\rho)}}{}_1F_1\left(\mu+t_{L-1};2\mu+t_{L-1}+l_{L-1};\lambda\gamma_L\right), \tag{4.19}$$

where $\lambda \triangleq \frac{\mu(\eta^2-1)}{\eta\bar{\gamma}(1-\rho)}$ and $\xi \triangleq \frac{2\mu(1+\eta)}{\bar{\gamma}}$. The joint CDF of γ_ls can be obtained by integrating Equation 4.19, w.r.t $\gamma_1,\gamma_2,\ldots,\gamma_L$. Then, expressing the hypergeometric function in infinite series [4, 9.14.1] (reproduced in Equation B.11) the CDF can be given as

$$F_{\gamma_1,\gamma_2,\ldots,\gamma_L}(\Gamma_1,\Gamma_2,\ldots,\Gamma_L) = \\ = \frac{1}{4^{L\mu}\Gamma^2(\mu)\eta^{L\mu}(1-\rho)^{2\mu(L-1)}}\sum_{t_1=0}^{\infty}\sum_{t_2=0}^{\infty}\cdots\sum_{t_{L-1}=0}^{\infty}\sum_{l_1=0}^{\infty}\sum_{l_2=0}^{\infty}\cdots\sum_{l_{L-1}=0}^{\infty}\sum_{p_1=0}^{\infty}\sum_{p_2=0}^{\infty}\cdots\sum_{p_L=0}^{\infty} \\ \times\left(\frac{\sqrt{\rho}}{1-\rho}\right)^{2(t_T+l_T)}\frac{B(\mu+t_1,\mu+l_1)(\mu+t_1)_{p_1}\xi^{2\mu+t_1+l_1}\lambda^{p_1}}{p_1!\left\{\prod_{i=1}^{L-1}\left(4^{t_i+l_i}t_i!l_i!\Gamma(\mu+t_i)\Gamma(\mu+l_i)\right)\right\}}\int_0^{\Gamma_1}\gamma_1^{2\mu+t_1+l_1+p_1-1}e^{-\frac{\xi\gamma_1}{2(1-\rho)}}d\gamma \\ \times_1\left\{\prod_{k=2}^{L-1}\frac{\xi^{\mu_k^t+\mu_k^l}\left(\mu_k^t\right)_{p_1}B\left(\mu_k^t,\mu_k^l\right)(\lambda(1+\rho))^{p_k}}{\left(\mu_k^t+\mu_k^l\right)_{p_k}\eta^{2t_T}(2\mu+t_1+l_1)_{p_1}p_k!}\int_0^{\Gamma_k}e^{-\frac{\xi(1+\rho)\gamma_k}{2(1-\rho)}}\gamma_k^{\mu_k^t+\mu_k^l+p_k-1}d\gamma_k\right\}\xi^{2\mu+t_{L-1}+l_{L-1}}\lambda^{p_L} \\ \times\frac{(\mu+t_{L-1})_{p_L}B(\mu+t_{L-1},\mu+l_{L-1})}{p_L!(2\mu+t_{L-1}+l_{L-1})_{p_L}}\int_0^{\Gamma_L}e^{-\frac{\xi\gamma_L}{2(1-\rho)}}\gamma_L^{2\mu+t_{L-1}+l_{L-1}+p_L-1}d\gamma_L. \tag{4.20}$$

Solving the integral using [4, 3.381.1] (reproduced in Equation B.7), the CDF can be expressed as

$$F_{\gamma_1,\gamma_2,\ldots,\gamma_L}(\Gamma_1,\Gamma_2,\ldots,\Gamma_L) =$$

$$
\begin{aligned}
&= \frac{1}{4^{\mu(L-2)}\Gamma^2(\mu)\,\eta^{L\mu}(1-\rho)^{2\mu(L-3)}}\sum_{t_1=0}^{\infty}\sum_{t_2=0}^{\infty}\cdots\sum_{t_{L-1}=0}^{\infty}\sum_{l_1=0}^{\infty}\sum_{l_2=0}^{\infty}\cdots\sum_{l_{L-1}=0}^{\infty}\sum_{p_1=0}^{\infty}\sum_{p_2=0}^{\infty}\cdots\sum_{p_L=0}^{\infty}\\
&\times\frac{2^{t_1+l_1+t_{L-1}+l_{L-1}}(\eta-1)^{p_1+p_L}(1-\rho)^{t_{L-1}+l_{L-1}+t_1+l_1-2(t_T+l_T)}\,g\left(2\mu+t_1+l_1+p_1,\frac{\xi\Gamma_1}{2(1-\rho)}\right)}{p_1!p_L!\Gamma(2\mu+t_1+l_1+p_1)\,\eta^{2t_T+p_T+p_L}\left\{\prod_{i=1}^{L-1}\left(4^{t_i+l_i}t_i!l_i!\Gamma(\mu+t_i)\Gamma(\mu+l_i)\right)\right\}}\\
&\times\left\{\prod_{k=2}^{L-1}\frac{2^{\mu_k^t+\mu_k^l}\Gamma\left(\mu_k^t+p_k\right)\Gamma\left(\mu_k^l\right)(\eta-1)^{p_k}}{p_k!\Gamma\left(\mu_k^t+\mu_k^l+p_k\right)}\left(\frac{1-\rho}{1+\rho}\right)^{\mu_k^t+\mu_k^l}g\left({}_k^t\mu+{}_k^l\mu+p_k,\frac{\xi(1+\rho)\Gamma_k}{2(1-\rho)}\right)\right\}\\
&\times\frac{\rho^{t_T+l_T}\Gamma(\mu+l_1)\Gamma(\mu+t_1+p_1)\Gamma(\mu+t_{L-1})\Gamma(\mu+t_{L-1}+p_L)}{\Gamma(2\mu+t_{L-1}+l_{L-1}+p_L)}\\
&\times g\left(2\mu+t_{L-1}+l_{L-1}+p_L,\frac{\xi\Gamma_L}{2(1-\rho)}\right).
\end{aligned}
\tag{4.21}
$$

Mathematically, outage probability can be expressed as $P_{\text{out}}(\gamma_{th}) = F_{\gamma_{sc}}(\gamma_{th})$. For the SC receiver, an expression for the $P_{\text{out}}(\gamma_{th})$ can be obtained by evaluating Equation 4.21 at $\gamma_i = \gamma_{th}, \forall i$. The final expression can be given as

$$
\begin{aligned}
&P_{\text{out}}(\gamma_N) =\\
&= \frac{1}{4^{\mu(L-2)}\Gamma^2(\mu)\,\eta^{L\mu}(1-\rho)^{2\mu(L-3)}}\sum_{t_1=0}^{\infty}\sum_{t_2=0}^{\infty}\cdots\sum_{t_{L-1}=0}^{\infty}\sum_{l_1=0}^{\infty}\sum_{l_2=0}^{\infty}\cdots\sum_{l_{L-1}=0}^{\infty}\sum_{p_1=0}^{\infty}\sum_{p_2=0}^{\infty}\cdots\sum_{p_L=0}^{\infty}\\
&\times\frac{2^{t_1+l_1+t_{L-1}+l_{L-1}}(\eta-1)^{p_1+p_L}(1-\rho)^{t_{L-1}+l_{L-1}+t_1+l_1-2(t_T+l_T)}\,g\left(2\mu+t_1+l_1+p_1,\frac{\xi\bar{\gamma}}{2\bar{\gamma}_N(1-\rho)}\right)}{p_1!p_L!\Gamma(2\mu+t_1+l_1+p_1)\,\eta^{2t_T+p_T+p_L}\left\{\prod_{i=1}^{L-1}\left(4^{t_i+l_i}t_i!l_i!\Gamma(\mu+t_i)\Gamma(\mu+l_i)\right)\right\}}\\
&\times\left\{\prod_{k=2}^{L-1}\frac{2^{\mu_k^t+\mu_k^l}\Gamma\left(\mu_k^t+p_k\right)\Gamma\left(\mu_k^l\right)(\eta-1)^{p_k}}{p_k!\Gamma\left(\mu_k^t+\mu_k^l+p_k\right)}\left(\frac{1-\rho}{1+\rho}\right)^{\mu_k^t+\mu_k^l}g\left({}_k^t\mu+{}_k^l\mu+p_k,\frac{\xi(1+\rho)\bar{\gamma}}{2\bar{\gamma}_N(1-\rho)}\right)\right\}\\
&\times\frac{\rho^{t_T+l_T}\Gamma(\mu+l_1)\Gamma(\mu+t_1+p_1)\Gamma(\mu+t_{L-1})\Gamma(\mu+t_{L-1}+p_L)}{\Gamma(2\mu+t_{L-1}+l_{L-1}+p_L)}\\
&\times g\left(2\mu+t_{L-1}+l_{L-1}+p_L,\frac{\xi\bar{\gamma}}{2\bar{\gamma}_N(1-\rho)}\right).
\end{aligned}
\tag{4.22}
$$

4.2.3 Results and Discussion

The expression for the outage probability given in Equation 4.22 has been numerically evaluated and plotted for illustration. In Figure 4.3, $P_{\text{out}}(\bar{\gamma}_N)$ vs. $\bar{\gamma}_N$ has been plotted for different values of

η, μ, ρ and L. As described in Section 1.2 η is the ratio of power (variance) between the inphase and quadrature phase components of the channel (Format 1). Hence, increase in η means a poor channel and as expected it can be observed that the probability of outage is high for higher value of η in Figure 4.3. Increase in μ indicates more number of clusters, hence, a better channel. This can be seen from the outage probability in Figure 4.3. The outage probability degrades with increase in ρ for all values of η, μ and L, for a fixed $\bar{\gamma}_N$. We observed that the for fixed η and μ the outage probability is small for $L=2$ with $\rho=0$ compared to $L=3$ and $\rho=0.8$ for lower $\bar{\gamma}_N$. The crossover point for $\mu=0.5$ and $\eta=0.75$ is at $\bar{\gamma}_N=12$dB and is increasing with increase in μ. Hence, an important conclusion can be drawn from these observation is that it is better to go for a lower order diversity with sufficient antenna spacing instead of higher order diversity in space and power limited scenario. To validate the obtained results, the outage probability has been also obtained by Monte Carlo simulation. Simulation results are also shown in Figure 4.3. It can be been observed that the numerical results are in close agreement with the simulation results. In the numerical evaluation, an accuracy at least at 7^{th} place of decimal digit has been maintained by suitably truncating the infinite series in Equation 4.22 to finite number of terms.

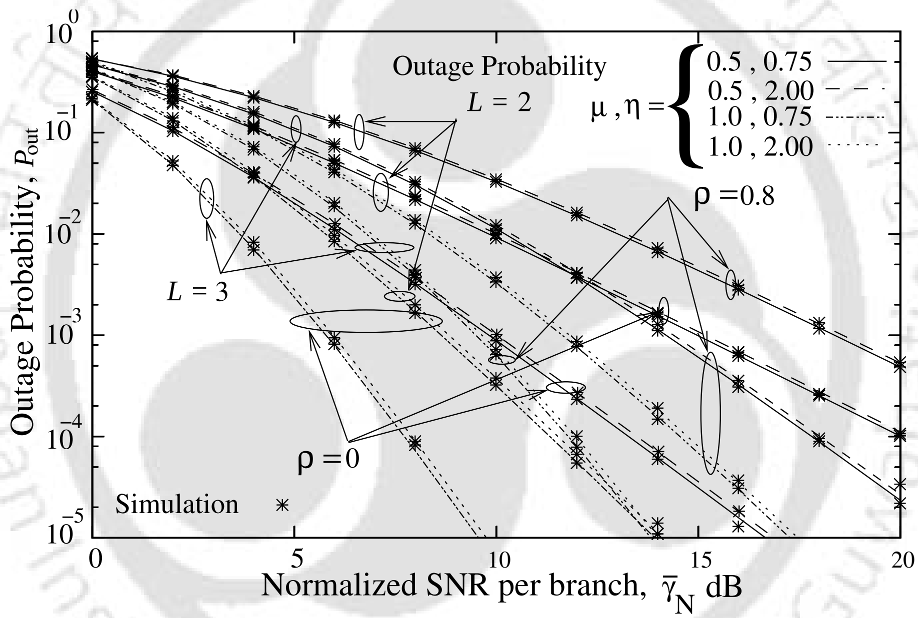

Figure 4.3: Outage probability of SC receiver in exponentially correlated $\eta - \mu$ fading channels.

4.3 Maximal Ratio Combining Receiver in Equally Correlated Fading Channels

For L correlated MRC receiver, performance measures like outage probability, moments and ABER for coherent and nocoherent modulations are obtained for equal correlation model discussed in Section 2.2. For MRC receiver it is mentioned in Section 2.1.2 that the PDF of output SNR is the sum of all input branch SNRs. From this relation, by obtaining the sum of equally correlated $\eta-\mu$ square RV, it is possible to obtain the PDF of the output SNR. The approach is explained below.

4.3.1 PDF of Combiner Output SNR

For a MRC receiver, the PDF of output SNR, γ_{mrc} can be obtained by obtaining the PDF of combiner output envelope α. From input envelopes α_ls $(l=1,2,\ldots,L)$, α can be obtained from the relation $\alpha^2=\alpha_1^2+\alpha_2^2+\ldots+\alpha_L^2$, from which an expression for the PDF of output SNR γ_{mrc} can be obtained by a scaling it corresponding to the factor (E_b/N_0). As a standard approach to obtain the PDF of α^2, the joint density function of α_ls is required. But it is not available for correlated $\eta-\mu$ RVs in literature. However, using the $\eta-\mu$ RV model in [14] and the expression for the sum of PDF of squared multivariate Gaussian RVs by Gurland in [64], it is possible to derive the PDF of α^2 for the special case of equally correlated α_ls. It is presented as below.

The $\eta-\mu$ RV model explained in Section 1.2 is considered here with envelopes are equally correlated with correlation coefficient ρ. From the $\eta-\mu$ RV model in [14], we can express $\alpha^2=X^2+Y^2$, where $X^2=\sum_{i=1}^{n}X_{1i}{}^2+\sum_{i=1}^{n}X_{2i}{}^2+\ldots+\sum_{i=1}^{n}X_{Li}{}^2$ and $Y^2=\sum_{i=1}^{n}Y_{1i}{}^2+\sum_{i=1}^{n}Y_{2i}{}^2+\ldots+\sum_{i=1}^{n}Y_{Li}{}^2$ are independent RVs while X_{li} (Y_{li})s are correlated with correlation coefficient $\rho_{mi,ki}$, $1\le m,k\le L$ and $1\le i\le n$. The method described for Hoyt fading channels in Section 3.4.1 can be extended to obtained the PDF of RV X^2 (by increasing the number of Gaussian RV) and the expression can be given as

$$f_{X^2}\left(x^2\right)=\frac{x^{\frac{Ln}{2}-1}e^{-\frac{x}{2\sigma_x^2(1-\rho)}}{}_1F_1\left(\frac{n}{2};\frac{Ln}{2};\frac{\rho Lx}{2\sigma_x^2(1-\rho)(1+(L-1)\rho)}\right)}{\Gamma\left(\frac{Ln}{2}\right)\left(2\sigma_x^2\right)^{\frac{Ln}{2}}(1-\rho)^{\frac{n(L-1)}{2}}(1+(L-1)\rho)^{\frac{n}{2}}}. \tag{4.23}$$

Similarly, $f_{Y^2}\left(y^2\right)$ can be obtained by substituting x by y in Equation 4.23 as

$$f_{y^2}(y^2)=\frac{y^{\frac{Ln}{2}-1}e^{-\frac{y}{2\sigma_y^2(1-\rho)}}{}_1F_1\left(\frac{n}{2};\frac{Ln}{2};\frac{\rho Ly}{2\sigma_y^2(1-\rho)(1+(L-1)\rho)}\right)}{\Gamma\left(\frac{Ln}{2}\right)\left(2\sigma_y^2\right)^{\frac{Ln}{2}}(1-\rho)^{\frac{n(L-1)}{2}}(1+(L-1)\rho)^{\frac{n}{2}}}. \tag{4.24}$$

Since, RVs X^2 and Y^2 are independent the PDF of the RV $\alpha^2=X^2+Y^2$ can be obtained by convolving the PDFs $f_{X^2}(x^2)$ and $f_{Y^2}(y^2)$ which can be obtained as

$$\begin{aligned} f_{\alpha^2}(\alpha^2) &= \frac{1}{(2\sigma_x\sigma_y)^{Ln}\Gamma^2\left(\frac{nL}{2}\right)(1-\rho)^{n(L-1)}[1+(L-1)\rho]^n}e^{-\frac{\alpha}{2\sigma_y^2(1-\rho)}} \\ &\times\int_0^{\alpha}x^{\frac{L}{2}n-1}(\alpha-x)^{\frac{L}{2}n-1}e^{\frac{\sigma_x^2-\sigma_y^2}{2\sigma_x^2\sigma_y^2(1-\rho)}x}{}_1F_1\left(\frac{n}{2};\frac{nL}{2};\frac{\rho Lx}{2\sigma_x^2(1-\rho)(1+(L-1)\rho)}\right) \\ &\times{}_1F_1\left(\frac{n}{2};\frac{nL}{2};\frac{\rho L(\alpha-x)}{2\sigma_y^2(1-\rho)(1+(L-1)\rho)}\right)dx. \end{aligned} \tag{4.25}$$

Expressing hypergeometric functions in Equation 4.25 infinite series [4, 9.14.1] (reproduced in Equation B.11) we can rewrite it as

$$\begin{aligned} f_{\alpha^2}(\alpha^2) &= \frac{e^{-\frac{\alpha}{2\sigma_y^2(1-\rho)}}}{(2\sigma_x\sigma_y)^{Ln}(1-\rho)^{n(L-1)}(1+\rho(L-1))^n\Gamma^2\left(\frac{Ln}{2}\right)}\sum_{t_1=0}^{\infty}\sum_{t_2=0}^{\infty}\frac{\left(\frac{n}{2}\right)_{t_1}\left(\frac{n}{2}\right)_{t_2}}{t_1!t_2!\sigma_x^{2t_1}\sigma_y^{2t_2}\left(\frac{nL}{2}\right)_{t_1}\left(\frac{nL}{2}\right)_{t_2}} \\ &\times\left[\frac{\rho L}{2(1-\rho)(1+(L-1)\rho)}\right]^{t_1+t_2}\int_0^{\alpha}x^{\frac{Ln}{2}+t_1-1}(\alpha-x)^{\frac{Ln}{2}+t_2-1}e^{\frac{\sigma_x^2-\sigma_y^2}{2\sigma_x^2\sigma_y^2(1-\rho)}x}dx. \end{aligned} \tag{4.26}$$

Performing the above integration we get

$$\begin{aligned} f_{\alpha^2}(\alpha^2) &= \frac{e^{-\frac{\alpha}{2\sigma_y^2(1-\rho)}}}{(2\sigma_x\sigma_y)^{Ln}(1-\rho)^{n(L-1)}(1+\rho(L-1))^n\Gamma^2\left(\frac{Ln}{2}\right)}\sum_{t_1=0}^{\infty}\sum_{t_2=0}^{\infty}\frac{\left(\frac{n}{2}\right)_{t_1}\left(\frac{n}{2}\right)_{t_2}}{t_1!t_2!} \\ &\times\left[\frac{\rho L}{2(1-\rho)(1+(L-1)\rho)}\right]^{t_1+t_2}\frac{B\left(\frac{L}{2}n+t_2,\frac{L}{2}n+t_1\right)\alpha^{Ln+t_1+t_2-1}}{\sigma_x^{2t_1}\sigma_y^{2t_2}\left(\frac{nL}{2}\right)_{t_1}\left(\frac{nL}{2}\right)_{t_2}} \\ &\times{}_1F_1\left(\frac{L}{2}n+t_1;Ln+t_1+t_2;\frac{\sigma_x^2-\sigma_y^2}{2\sigma_x^2\sigma_y^2(1-\rho)}\alpha\right). \end{aligned} \tag{4.27}$$

The PDF of γ_{mrc} can be obtained by scaling Equation 4.27 (applying concept of transformation of RV) by the multiplying factor (E_b/N_0). The obtained expression can be further simplified by assuming $\sigma_y^2 = 1$ as explained in Section . Also, relation between n and μ is given in Section as $\mu = n/2$. Thus, finally the PDF of γ_{mrc} can be expressed as

$$\begin{aligned} f_{\gamma_{mrc}}(\gamma_{mrc}) &= \frac{1}{(1-\rho)^{2(L\mu-\mu)}[1+(L-1)\rho]^{2\mu}} \left[\frac{\mu(1+\eta)}{\bar{\gamma}\sqrt{\eta}}\right]^{2L\mu} \sum_{t_1=0}^{\infty}\sum_{t_2=0}^{\infty} \frac{(\mu)_{t_1}(\mu)_{t_2}}{t_1!t_2!\eta^{t_1}} \\ &\times \left[\frac{L\rho\mu(1+\eta)}{\bar{\gamma}(1-\rho)(1+(L-1)\rho)}\right]^{t_1+t_2} \frac{\gamma_{mrc}^{2L\mu+t_1+t_2-1} e^{-\frac{\mu(1+\eta)}{\bar{\gamma}(1-\rho)}\gamma_{mrc}}}{\Gamma(2L\mu+t_1+t_2)} \\ &\times {}_1F_1\left(L\mu+t_1; 2L\mu+t_1+t_2; \frac{\mu(\eta^2-1)}{\eta(1-\rho)\bar{\gamma}}\gamma_{mrc}\right). \end{aligned} \quad (4.28)$$

Upper Bound on Truncation Error

The error bound for Equation 4.28 is derive in Section A.10.7 in Equation A.72. It can be given as

$$\begin{aligned} E_K &\leq \frac{\Gamma^2(\mu+K)\Im^{2(L\mu+K)}(1-\rho)^{2\mu}(L\rho\gamma_{mrc})^{2K}}{\Gamma(2(L\mu+K))K!^2\Gamma^2(\mu)\eta^{L\mu+K}} \gamma_{mrc}^{2L\mu-1} e^{-\frac{\mu(1+\eta)}{\bar{\gamma}(1-\rho)}\gamma_{mrc}} \\ &\times {}_1F_1\left(L\mu+K; 2(L\mu+K); \frac{\mu(\eta^2-1)}{\eta(1-\rho)\bar{\gamma}}\gamma_{mrc}\right) \\ &\times {}_2F_2\left[\begin{matrix} 1 & \mu+K & \frac{L\rho\gamma_{mrc}\Im}{\eta} \\ K+1 & L\mu+K & \end{matrix}\right] {}_2F_2\left[\begin{matrix} 1 & \mu+K & L\rho\gamma_{mrc}\Im \\ K+1 & L\mu+K & \end{matrix}\right], \end{aligned} \quad (4.29)$$

where $\Im \triangleq \frac{\mu(1+\eta)}{\bar{\gamma}(1-\rho)(1+(L-1)\rho)}$.

4.3.2 Moments of the Combiner Output SNR

The moments associated with the γ_{mrc} can be expressed as $E[\gamma_{mrc}^N] = \int_0^\infty \gamma_{mrc}^N f_{\gamma_{mrc}}(\gamma_{mrc}) d\gamma_{mrc}$. Putting Equation 4.28 in it we obtain

$$\begin{aligned} E\left[\gamma^N\right] &= \frac{1}{(1-\rho)^{2(L\mu-\mu)}[1+(L-1)\rho]^{2\mu}} \left[\frac{\mu(1+\eta)}{\bar{\gamma}\sqrt{\eta}}\right]^{2L\mu} \sum_{t_1=0}^{\infty}\sum_{t_2=0}^{\infty} \frac{(\mu)_{t_1}}{t_1!} \\ &\times \frac{(\mu)_{t_2}}{t_2!\eta^{t_1}\Gamma(2L\mu+t_1+t_2)} \left[\frac{L\rho\mu(1+\eta)}{\bar{\gamma}(1-\rho)(1+(L-1)\rho)}\right]^{t_1+t_2} \int_0^\infty \gamma_{mrc}^{2L\mu+N+t_1+t_2-1} \end{aligned}$$

$$\times e^{-\frac{\mu(1+\eta)}{\bar{\gamma}(1-\rho)}\gamma_{mrc}} {}_1F_1\left(L\mu+t_1;2L\mu+t_1+t_2;\frac{\mu(\eta^2-1)}{\eta(1-\rho)\bar{\gamma}}\gamma_{mrc}\right)d\gamma_{mrc}. \quad (4.30)$$

Solving the integral (using [4, (7.621.4)], reproduced in B.10), the N^{th} moment can be obtained as

$$E\left[\gamma_{mrc}^N\right] = \frac{1}{\eta^{L\mu}}\left[\frac{1-\rho}{1+(L-1)\rho}\right]^{2\mu}\sum_{t_1=0}^{\infty}\sum_{t_2=0}^{\infty}\frac{(\mu)_{t_1}(\mu)_{t_2}\Gamma(2L\mu+N+t_1+t_2)}{t_1!t_2!\eta^{t_1}\Gamma(2L\mu+t_1+t_2)}\left[\frac{L\rho}{1+(L-1)\rho}\right]^{t_1+t_2}$$
$$\times\left[\frac{\bar{\gamma}(1-\rho)}{\mu(1+\eta)}\right]^N {}_2F_1\left(L\mu+t_1,2L\mu+N+t_1+t_2;2L\mu+t_1+t_2;\frac{\eta-1}{\eta}\right). \quad (4.31)$$

The average value of the combiner output SNR can be obtained, by putting $N=1$ in Equation 4.31, as

$$\bar{\gamma} = \frac{1}{\eta^{L\mu}}\left[\frac{1-\rho}{1+(L-1)\rho}\right]^{2\mu}\sum_{t_1=0}^{\infty}\sum_{t_2=0}^{\infty}\frac{(\mu)_{t_1}(\mu)_{t_2}\Gamma(2L\mu+t_1+t_2+1)}{t_1!t_2!\eta^{t_1}\Gamma(2L\mu+t_1+t_2)}\left[\frac{L\rho}{1+(L-1)\rho}\right]^{t_1+t_2}$$
$$\times\frac{\bar{\gamma}(1-\rho)}{\mu(1+\eta)}{}_2F_1\left(L\mu+t_1,2L\mu+t_1+t_2+1;2L\mu+t_1+t_2;\frac{\eta-1}{\eta}\right). \quad (4.32)$$

4.3.3 Outage Probability

Putting $f_{\gamma_{mrc}}(\gamma_{mrc})$ from Equation 4.28 to Equation 2.16, the expression for the outage probability after expressing the hypergeometric function in series form [4, 9.14.1] (reproduced in Equation B.11) can be expressed for a threshold γ_{th} as

$$P_{\text{out}}(\gamma_{th}) = \frac{\left[\frac{\mu(1+\eta)}{\bar{\gamma}\sqrt{\eta}}\right]^{2L\mu}}{(1-\rho)^{2(L\mu-\mu)}[1+(L-1)\rho]^{2\mu}}\sum_{t_1=0}^{\infty}\sum_{t_2=0}^{\infty}\sum_{t_3=0}^{\infty}\frac{(\mu)_{t_1}(\mu)_{t_2}(L\mu+t_1)_{t_3}}{t_1!t_2!t_3!\eta^{t_1}\Gamma(2L\mu+t_1+t_2+t_3)}$$
$$\times\left[\frac{\mu(1+\eta)}{(1-\rho)\bar{\gamma}}\right]^{t_1+t_2+t_3}\left[\frac{L\rho}{1+(L-1)\rho}\right]^{t_1+t_2}\left[\frac{\mu(\eta-1)}{\eta}\right]^{t_3}\int_0^{\gamma_{th}}\gamma_{mrc}^{2L\mu+\lambda+t_1+t_2-1}$$
$$\times e^{-\frac{\mu(1+\eta)}{\bar{\gamma}(1-\rho)}\gamma_{mrc}}d\gamma_{mrc} \quad (4.33)$$

The integral in the above expression can be solved by using [4, (3.381.1)] (reproduced in Equation B.6). The final expression for the outage probability can be obtained as

$$P_{\text{out}}(\gamma_N) = \frac{1}{\eta^{L\mu}}\left[\frac{1-\rho}{1+(L-1)\rho}\right]^{2\mu}\sum_{t_1=0}^{\infty}\sum_{t_2=0}^{\infty}\sum_{t_3=0}^{\infty}\frac{(\mu)_{t_1}(\mu)_{t_2}(L\mu+t_1)_{t_3}}{t_1!t_2!t_3!\Gamma(2L\mu+t_1+t_2+t_3)}$$

$$\times\frac{(\eta-1)^{t_3}}{\eta^{t_1+t_3}}\left[\frac{L\rho}{1+(L-1)\rho}\right]^{t_1+t_2} g\left(2L\mu+t_1+t_2+t_3,\frac{\mu(1+\eta)}{\bar{\gamma}_N(1-\rho)}\right). \quad (4.34)$$

4.3.4 Average Bit Error Rate

ABER is given in equation Equation 2.17, which need the of PDF of γ_{mrc} and the conditional bit error rate $p_{e,\mathrm{coh}}(\varepsilon|\gamma)$ for evaluation. The conditional bit error rate (conditioned on the received SNR) for different digital modulation schemes are listed in Table 2.1. In this work, for binary coherent and noncoherent modulations, we obtain expressions for ABER.

1. **Binary Coherent Modulations**

For binary coherent modulation i. e. BPSK and BFSK, an expression for $p_{e,\mathrm{coh}}(\varepsilon|\gamma)$ can be obtained by evaluating the entries for MPSK and MFSK modulations in Table 2.1, for $M=2$. A simplified combined expression for this conditional BER is also given in Equation 2.24. Thus, putting $p_{e,\mathrm{coh}}(\varepsilon|\gamma)$ from Equation 2.24 and $f_{\gamma_{mrc}}(\gamma_{mrc})$ from Equation 4.28 into Equation 2.17, binary coherent ABER can be given as

$$\begin{aligned}P_{e,ch}(\bar{\gamma}) &= \frac{1}{(1-\rho)^{2(L\mu-\mu)}[1+(L-1)\rho]^{2\mu}}\left[\frac{\mu(1+\eta)}{\bar{\gamma}\sqrt{\eta}}\right]^{2L\mu}\sum_{t_1=0}^{\infty}\sum_{t_2=0}^{\infty}\frac{(\mu)_{t_1}(\mu)_{t_2}}{t_1!t_2!\eta^{t_1}\Gamma(2L\mu+\lambda)}\\ &\times\left[\frac{L\rho\mu(1+\eta)}{\bar{\gamma}(1-\rho)(1+(L-1)\rho)}\right]^{t_1+t_2}\int_0^{\infty}Q\left(\sqrt{2a\gamma_{mrc}}\right)\gamma_{mrc}^{2L\mu+t_1+t_2-1}e^{-\frac{\mu(1+\eta)}{\bar{\gamma}(1-\rho)}\gamma_{mrc}}\\ &\times{}_1F_1\left(L\mu+t_1;2L\mu+t_1+t_2;\frac{\mu(\eta^2-1)}{\eta(1-\rho)\bar{\gamma}}\gamma_{mrc}\right)d\gamma_{mrc}. \end{aligned} \quad (4.35)$$

Expressing ${}_1F_1(\cdot,\cdot;\cdot)$ in infinite series [5] and $Q(\cdot)$ function in incomplete gamma function (using [1, A-(6)], reproduced in Equations B.13) Equation 4.35 can be rewritten as

$$\begin{aligned}P_{e,ch}(\bar{\gamma}) &= \frac{1}{2\sqrt{\pi}(1-\rho)^{2(L\mu-\mu)}[1+(L-1)\rho]^{2\mu}}\left[\frac{\mu(1+\eta)}{\bar{\gamma}\sqrt{\eta}}\right]^{2L\mu}\sum_{t_1=0}^{\infty}\sum_{t_2=0}^{\infty}\sum_{t_3=0}^{\infty}\frac{(\mu)_{t_1}(\mu)_{t_2}}{t_1!t_2!t_3!}\\ &\times\frac{(L\mu+t_1)_{t_3}}{\eta^{t_1}\Gamma(2L\mu+t_1+t_2+t_3)}\left[\frac{\mu(1+\eta)}{(1-\rho)\bar{\gamma}}\right]^{t_1+t_2+t_3}\left[\frac{L\rho}{1+(L-1)\rho}\right]^{t_1+t_2}\left[\frac{\eta-1}{\eta}\right]^{t_3}\\ &\times\int_0^{\infty}\gamma_{mrc}^{2L\mu+t_1+t_2+t_3-1}\Gamma\left(\frac{1}{2},a\gamma_{mrc}\right)e^{-\frac{\mu(1+\eta)}{\bar{\gamma}(1-\rho)}\gamma_{mrc}}d\gamma_{mrc}. \end{aligned} \quad (4.36)$$

Using [1, A-(8a)] (reproduced in Equation B.14), the above integration can be solved and an expression for ABER can be given as

$$
\begin{aligned}
P_{e,ch}(\bar{\gamma}) \;=\;& \frac{1}{2}\sqrt{\frac{a\bar{\gamma}(1-\rho)}{\pi\mu(1+\eta)}}\frac{\zeta^{2L\mu+\frac{1}{2}}}{\eta^{2L\mu}}\left[\frac{1-\rho}{1+(L-1)\rho}\right]^{2\mu}\sum_{t_1=0}^{\infty}\sum_{t_2=0}^{\infty}\sum_{t_3=0}^{\infty}\frac{(\mu)_{t_1}(\mu)_{t_2}}{t_1!t_2!t_3!\eta^{t_1}} \\
&\times\frac{\Gamma\left(2L\mu+t_1+t_2+t_3+\frac{1}{2}\right)(L\mu+t_1)_{t_3}\zeta^{t_1+t_2+t_3}}{(2L\mu+t_1+t_2+t_3)!}\left[\frac{L\rho}{1+(L-1)\rho}\right]^{t_1+t_2}\left[\frac{\eta-1}{\eta}\right]^{t_3} \\
&\times{}_2F_1\left(1,2L\mu+t_1+t_2+t_3+\frac{1}{2};2L\mu+t_1+t_2+t_3+1;\zeta\right), \qquad (4.37)
\end{aligned}
$$

where $\zeta \triangleq \frac{\mu(1+\eta)}{a\bar{\gamma}(1-\rho)+\mu(1+\eta)}$.

2. **Binary Non-coherent Modulations**

For binary noncoherent modulations, the conditional BER is given in Equation 2.25. By putting $p_{e,\text{ncoh}}(\varepsilon|\gamma)$ and $f_{\gamma_{mrc}}(\gamma_{mrc})$ from Equations 2.25 and 4.28, into Equation 2.17 an expression for noncoherent ABER can be given as

$$
\begin{aligned}
P_{e,nch}(\bar{\gamma}) \;=\;& \frac{1}{2}\left[\frac{1-\rho}{1+(L-1)\rho}\right]^{2\mu}\left[\frac{\mu(1+\eta)}{\bar{\gamma}(1-\rho)\sqrt{\eta}}\right]^{2L\mu}\sum_{t_1=0}^{\infty}\sum_{t_2=0}^{\infty}\frac{(\mu)_{t_1}(\mu)_{t_2}}{t_1!t_2!\Gamma(2L\mu+t_1+t_2)} \\
&\times\frac{1}{\eta^{t_1}}\left[\frac{L\rho\mu(1+\eta)}{\bar{\gamma}(1-\rho)(1+(L-1)\rho)}\right]^{t_1+t_2}\int_0^{\infty}\gamma_{mrc}^{2L\mu+t_1+t_2-1}e^{-\frac{\mu(1+\eta)+a\bar{\gamma}(1-\rho)}{\bar{\gamma}(1-\rho)}\gamma_{mrc}} \\
&\times{}_1F_1\left(L\mu+t_1;2L\mu+t_1+t_2;\frac{\mu(\eta^2-1)}{\eta(1-\rho)\bar{\gamma}}\gamma_{mrc}\right)d\gamma_{mrc}. \qquad (4.38)
\end{aligned}
$$

Solving the integral (using [4, (7.621.4)], reproduced in B.10), an expression for ABER can be obtained as

$$
\begin{aligned}
P_{e,nch}(\bar{\gamma}) \;=\;& \frac{1}{2}\left[\frac{1-\rho}{1+(L-1)\rho}\right]^{2\mu}\left[\frac{\zeta^2}{\eta-(\eta-1)\zeta}\right]^{L\mu}\sum_{t_1=0}^{\infty}\sum_{t_2=0}^{\infty}\frac{(\mu)_{t_1}(\mu)_{t_2}}{t_1!t_2![\eta-(\eta-1)\zeta]^{t_1}} \\
&\times\left[\frac{L\rho\zeta}{1+(L-1)\rho}\right]^{t_1+t_2}. \qquad (4.39)
\end{aligned}
$$

For $\rho=0$ and $q=1$, i.e., for independent Rayleigh channels, Equations 4.37 and 4.39 simplify to the results in [1].

4.3.5 Results and Discussion

Obtained mathematical expressions have been numerically evaluated and plotted against parameters of interest for. In Figure 4.4, $P_{\text{out}}(\bar{\gamma}_N)$ vs. $\bar{\gamma}_N$ has been plotted for different values of L, ρ, η and μ. The effect of branch correlation on the outage can be observed by comparing the outage values for $\rho = 0.8$ against the values for $\rho = 0$ (uncorrelated case). Clearly, with the increase in ρ the receiver suffers more outage, for a fixed value of $\bar{\gamma}_N$, L and fading parameters η and μ. Again as expected, increase in L reduces the probability of outage. These results have been verified against the results in [1], which is a special case of the results presented here, and are found to be matching. For CFSK and NCFSK modulations, ABER vs. $\bar{\gamma}$ curves have been plotted in Figures 4.5 and 4.6, respectively. It can be observed that the ABER performance degrades with the increase in ρ with constant L and fading parameters η and μ. Increases in parameter μ indicates more number of clusters in the fading model and as expected gives better performance, whereas increases in η increases the difference of variance between in-phase and quadrature phase components and hence, degrades ABER performance. To show the effect of number of input branches on the ABER, curves are shown as a function of L. A Monte Carlo simulation of the EGC receiver under analysis has been performed and simulation results have been plotted in the respective figures. In Figure 4.7 we have plotted the upper bound of truncation error for $f_{\gamma_{mrc}}(\gamma_{mrc})$. It can observed from the figure that, as the number of turns and/or average input SNR increases the accuracy in the sum is very high. In the numerical evaluation of expressions involving infinite series we have truncated them suitably by including finite number of terms ensuring to achieve an accuracy in ABER at least at 7^{th} place of decimal digit.

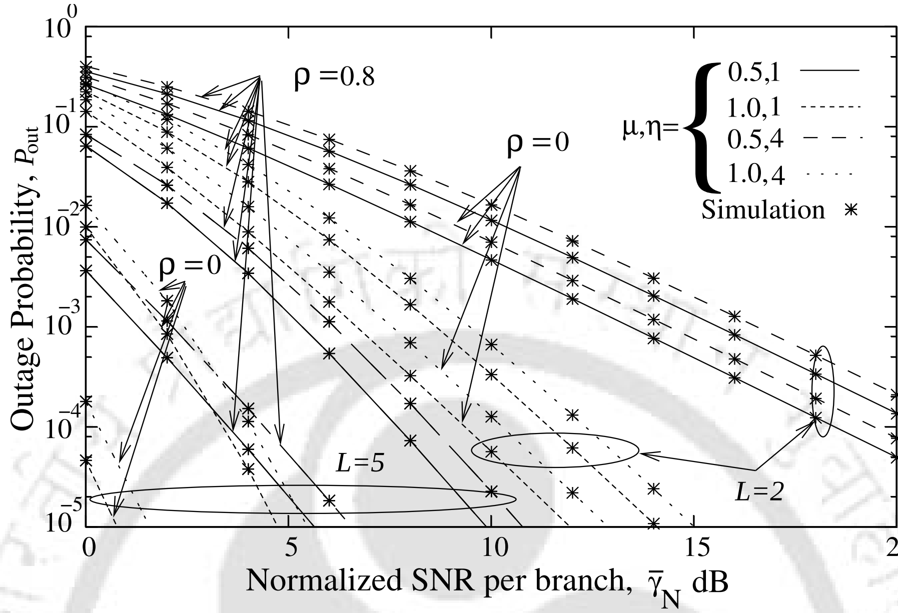

Figure 4.4: Outage probability of the L-MRC receiver with equal correlation.

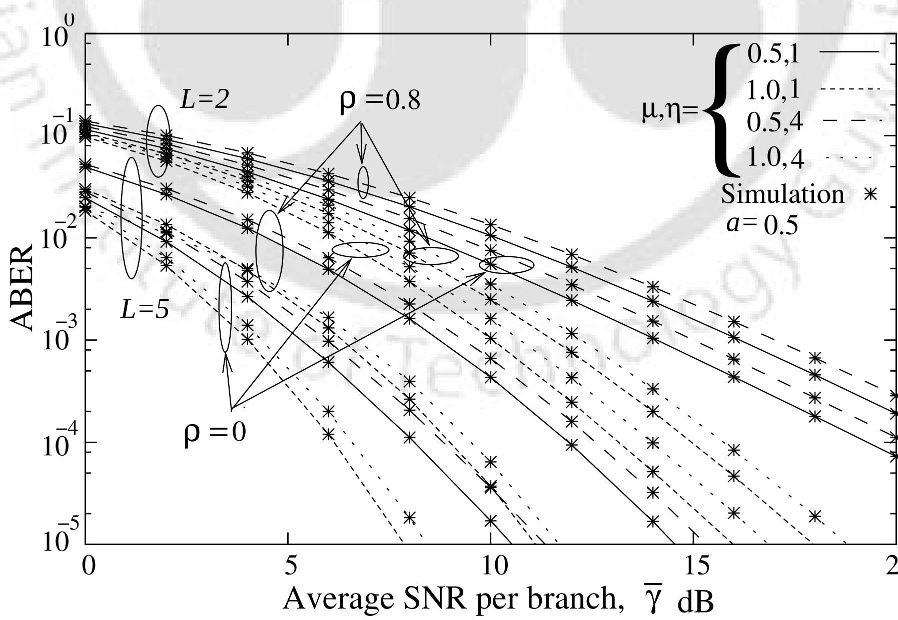

Figure 4.5: ABER of L-MRC receiver with equal correlations for binary coherent modulations.

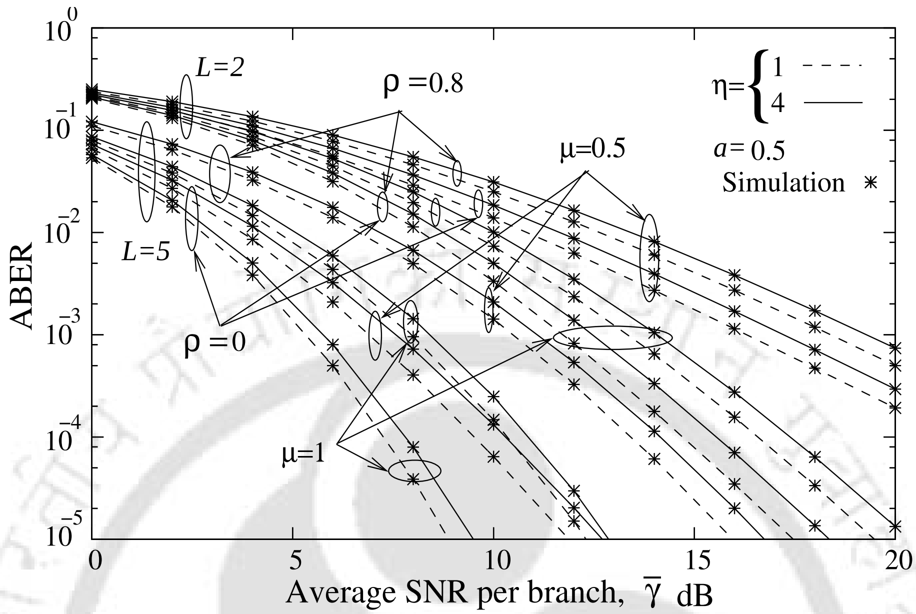

Figure 4.6: ABER of L-MRC receiver with equal correlations for binary noncoherent modulations.

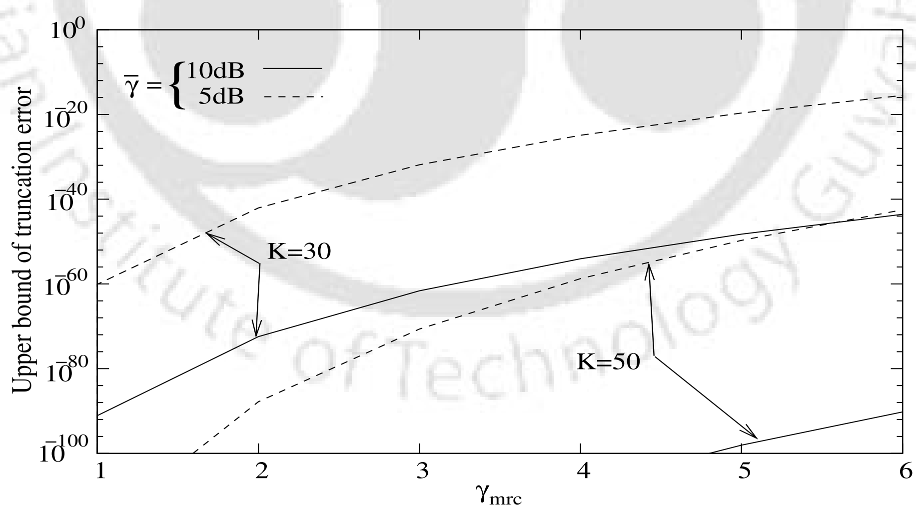

Figure 4.7: Upper bound of truncation error of Equation 4.28 for $\eta = 0.5$, $\mu = 1$ and $\rho = 0.8$.

4.4 Summary

In this chapter, we derived the PDF of output SNR and the expressions of performance measures over $\eta-\mu$ fading channels for

1. L independent SC receiver.

2. L exponentially correlated SC receiver.

3. L equally correlated MRC receiver.

Chapter 5

Performance Analysis in $\kappa-\mu$ Fading Channels

5.1 Independent Fading Channels

Performance of an L-SC receiver has been analyzed over η-μ fading channels. A PDF based approach discussed in Section 2.3.1 is used to obtain moments of the SC receiver output signal-to-noise ratio and ABER for binary, coherent and non-coherent modulations. Simulation results have been presented to validate the obtained mathematical expressions.

5.1.1 PDF of Combiner Output Signal-to-Noise Ratio

The PDF of combiner output SNR γ_{sc}, which is essential to evaluate the performances of receiver in PDF based approach. The CDF of $\kappa-\mu$ distribution is known in closed form in terms of Marcum Q function [14]. But we observed that this expression cannot be used in this form for our purpose as it is difficult to integrate the Marcum Q function. In order to obtain performance measures for a general case we have obtained this CDF expression in series form using which it is possible to obtain PDF of γ_{sc}. It is explained below.

In a L-branch SC receiver, the PDF of fading envelope α_l at the l^{th} branch is distributed according to the $\kappa-\mu$ distribution as given in Equation 1.8. In the same branch, PDF of SNR γ_l can be given from [14] as

$$f_{\gamma_l}(\gamma_l) = \frac{\mu(1+\kappa)^{\frac{\mu+1}{2}}\gamma_l^{\frac{\mu-1}{2}}e^{-\frac{\mu(1+\kappa)\gamma_l}{\bar{\gamma}_l}}}{\kappa^{\frac{\mu-1}{2}}\bar{\gamma}_l^{\frac{\mu+1}{2}}e^{\mu\kappa}} I_{\mu-1}\left(2\mu\sqrt{\frac{\kappa(1+\kappa)\gamma_l}{\bar{\gamma}_l}}\right). \tag{5.1}$$

From Equation 5.1, the CDF of γ_l can be obtained by integrating Equation 5.1 w.r.t. γ_l as

$$F_{\gamma_l}(\gamma_l) = \frac{\mu(1+\kappa)^{\frac{\mu+1}{2}}}{\kappa^{\frac{\mu-1}{2}}e^{\mu\kappa}\bar{\gamma}_l^{\frac{\mu+1}{2}}}\int_0^{\gamma_{sc}}\gamma_l^{\frac{\mu-1}{2}}e^{-\frac{\mu(1+\kappa)\gamma_l}{\bar{\gamma}_l}} I_{\mu-1}\left(2\mu\sqrt{\frac{\kappa(1+\kappa)\gamma_l}{\bar{\gamma}_l}}\right)d\gamma_l. \tag{5.2}$$

Expressing the involved Bessel function in Equation 5.2 in infinite series using [54] (reproduced in Equation B.17) we can rewrite the CDF of γ_l as

$$F_{\gamma_l}(\gamma_l) = \left[\frac{\mu(1+\kappa)}{\bar{\gamma}_l}\right]^{\mu}\frac{1}{e^{\mu\kappa}}\sum_{t=0}^{\infty}\frac{1}{t!\Gamma(\mu+t)}\left[\frac{\mu^2\kappa(1+\kappa)}{\bar{\gamma}_l}\right]^t\int_0^{\gamma_{sc}}\gamma_l^{\mu+t-1}e^{-\frac{\mu(1+\kappa)\gamma_l}{\bar{\gamma}_l}}d\gamma_l. \tag{5.3}$$

The integration in Equation 5.3 can be solved using [4, (3.381.1)] (reproduced in Equation B.7), and CDF of γ_l can be given as

$$F_{\gamma_l}(\gamma_l) = \frac{1}{e^{\mu\kappa}}\sum_{t=0}^{\infty}\frac{(\kappa\mu)^t}{t!\Gamma(\mu+t)}g\left(\mu+t,\frac{\mu(1+\kappa)}{\bar{\gamma}_l}\gamma_l\right). \tag{5.4}$$

Thus, assuming input signals are statistically independent and $\bar{\gamma}_l = \bar{\gamma}$, $\forall l$, the CDF of SNR at the output of SC receiver can be written as the product of CDFs of all L received SNRs. It can be given as

$$F_{\gamma_{sc}}(\gamma_{sc}) = \left[\frac{1}{e^{\mu\kappa}}\sum_{t=0}^{\infty}\frac{(\kappa\mu)^t}{t!\Gamma(\mu+t)}g\left(\mu+t,\frac{\mu(1+\kappa)}{\bar{\gamma}}\gamma_{sc}\right)\right]^L. \tag{5.5}$$

Now differentiating Equation 5.5 w. r. t. γ_{sc} using [5, (6.5.25)] (reproduced in Equation B.2), the PDF of the SNR at the output of the SC can be given as

$$f_{\gamma_{sc}}(\gamma_{sc}) = \frac{L}{e^{L\mu\kappa}}\left[\frac{\mu(1+\kappa)\gamma_{sc}}{\bar{\gamma}}\right]^{L\mu}\sum_{t_1=0}^{\infty}\sum_{t_2=0}^{\infty}\cdots\sum_{t_L=0}^{\infty}\frac{1}{\left\{\prod_{i=1}^{L}t_i!\Gamma(\mu+t_i)\right\}}\left[\frac{\kappa\mu^2(1+\kappa)}{\bar{\gamma}}\right]^{\sum_{i=1}^{L}t_i}$$
$$\times\gamma_{sc}^{\sum_{i=1}^{L}t_i-1}e^{-\frac{L\mu(1+\kappa)}{\bar{\gamma}}\gamma_{sc}}\left\{\prod_{i=1}^{L-1}\frac{{}_1F_1\left(1;\mu+t_i+1;\frac{\mu(1+\kappa)}{\bar{\gamma}}\gamma_{sc}\right)}{\mu+t_i}\right\}. \quad (5.6)$$

For $\mu=1$ and $\kappa\to0$ (Rayleigh fading case), it can be shown that Equation 5.6 reduces to [10, (7.60)].

5.1.2 Moments of Combiner Output Signal-to-Noise Ratio

Using Equations 5.6 and 3.9, the N^{th} moment of γ_{sc} can be expressed as

$$E[\gamma_{sc}^N] = \int_0^{\infty}\gamma_{sc}^N f_{\gamma_{sc}}(\gamma_{sc})d\gamma_{sc}, \quad (5.7)$$

Putting $f_{\gamma_{sc}}(\gamma_{sc})$ from Equation 5.6 into Equation 5.7 we obtain

$$E[\gamma_{sc}^N] = \frac{L}{e^{L\mu\kappa}}\left[\frac{\mu(1+\kappa)}{\bar{\gamma}_l}\right]^{L\mu}\sum_{t_1=0}^{\infty}\sum_{t_2=0}^{\infty}\cdots\sum_{t_L=0}^{\infty}\frac{1}{\left\{\prod_{i=1}^{L}t_i!\Gamma(\mu+t_i)\right\}\left\{\prod_{i=1}^{L-1}\mu+t_i\right\}}\left(\frac{\kappa\mu^2(1+\kappa)}{\bar{\gamma}_l}\right)^{\sum_{i=1}^{L}t_i}$$
$$\times\int_0^{\infty}\gamma_{sc}^{L\mu+\sum_{i=1}^{L}t_i+N-1}e^{-\frac{L\mu(1+\kappa)}{\bar{\gamma}_l}\gamma_{sc}}\left\{\prod_{i=1}^{L-1}{}_1F_1\left(1,\mu+t_i+1,\frac{\mu(1+\kappa)}{\bar{\gamma}_l}\gamma_{sc}\right)\right\}d\gamma_{sc}. \quad (5.8)$$

The integral in equation 5.8 can be solved using [3, (C.1)] (reproduced in Equation B.15) and the final expression can be given as

$$E[\gamma_{sc}^N] = \frac{1}{L^{L\mu+N-1}e^{L\mu\kappa}}\left[\frac{\bar{\gamma}}{\mu(1+\kappa)}\right]^N\sum_{t_1=0}^{\infty}\sum_{t_2=0}^{\infty}\cdots\sum_{t_L=0}^{\infty}\frac{[L\kappa\mu]^{\sum_{i=1}^{L}t_i}\Gamma\left(N+L\mu+\sum_{i=1}^{L}t_i\right)}{\left\{\prod_{i=1}^{L}t_i!\Gamma(\mu+t_i)\right\}\left\{\prod_{i=1}^{L-1}\mu+t_i\right\}}$$

$$\times F_A\left(N+L\mu+\sum_{i=1}^{L}t_i;\quad \underbrace{1,\ldots,1;}_{(L-1)\text{numbers}}\quad \mu+t_1+1,\ldots,\mu+t_{L-1}+1;\quad \underbrace{\frac{1}{L},\ldots,\frac{1}{L}}_{(L-1)\text{numbers}} \right). \tag{5.9}$$

The average SNR at the output of the SC can be obtained from Equation 5.9, by substituting $N=1$ in it as

$$\bar{\gamma}_{\text{out}} = \frac{\bar{\gamma}}{\mu(1+\kappa)L^{L\mu}e^{L\mu\kappa}}\sum_{t_1=0}^{\infty}\sum_{t_2=0}^{\infty}\cdots\sum_{t_L=0}^{\infty}\frac{[L\kappa\mu]^{\sum_{i=1}^{L}t_i}\Gamma\left(L\mu+1+\sum_{i=1}^{L}t_i\right)}{\left\{\prod_{i=1}^{L}t_i!\Gamma(\mu+t_i)\right\}\left\{\prod_{i=1}^{L-1}\mu+t_i\right\}}$$
$$\times F_A\left(L\mu+1+\sum_{i=1}^{L}t_i;\quad \underbrace{1,\ldots,1;}_{(L-1)\text{numbers}}\quad \mu+t_1+1,\ldots,\mu+t_{L-1}+1;\quad \underbrace{\frac{1}{L},\ldots,\frac{1}{L}}_{(L-1)\text{numbers}} \right). \tag{5.10}$$

5.1.3 Average Bit Error Rate

A general expression to obtain the ABER is given in Equation 2.17 which needs the PDF of γ_{sc} and the conditional bit error rate $p_{e,\text{coh}}(\varepsilon|\gamma)$, for evaluation. The conditional bit error rate (conditioned on the received SNR) for different digital modulation schemes are listed in Table 2.1. In the work presented here, we obtain expressions for ABER for binary, coherent and noncoherent modulations as discussed below.

1. **Binary Coherent Modulations**

   For binary coherent modulations BPSK and BFSK, the expression for the conditional BER is given in Equation 2.24. Putting $p_{e,\text{coh}}(\varepsilon|\gamma)$ and $f_{\gamma_{sc}}(\gamma_{sc})$ from Equations 2.24 and 5.6 into

Equation 2.17, binary coherent ABER can be given as

$$P_{e,ch}(\bar{\gamma}) = \frac{L}{e^{L\mu\kappa}}\left(\frac{\mu(1+\kappa)}{\bar{\gamma}}\right)^{L\mu}\sum_{t_1=0}^{\infty}\sum_{t_2=0}^{\infty}\cdots\sum_{t_L=0}^{\infty}\frac{1}{\left\{\prod_{i=1}^{L}t_i!\Gamma(\mu+t_i)\right\}\left\{\prod_{i=1}^{L-1}\mu+t_i\right\}}$$
$$\times\left(\frac{\kappa\mu^2(1+\kappa)}{\bar{\gamma}}\right)^{\sum_{i=1}^{L}t_i}\int_0^{\infty}e^{-\frac{L\mu(1+\kappa)}{\bar{\gamma}}\gamma_{sc}}\gamma_{sc}^{L\mu+\sum_{i=1}^{L}t_i-1}Q\left(\sqrt{2a\gamma_{sc}}\right)$$
$$\times\left\{\prod_{i=1}^{L-1}{}_1F_1\left(1,\mu+t_i+1,\frac{\mu(1+\kappa)}{\bar{\gamma}}\gamma_{sc}\right)\right\}d\gamma_{sc}. \tag{5.11}$$

The integral in Equation 5.11 cannot be solved in the present form. Using [1, A-(6)] (reproduced in Equations B.13) we can write the $Q(\cdot)$ function in incomplete gamma function and thus Equation 5.11 can be rewritten as

$$P_{e,ch}(\bar{\gamma}) = \frac{L}{2\sqrt{\pi}e^{L\mu\kappa}}\left(\frac{\mu(1+\kappa)}{\bar{\gamma}}\right)^{L\mu}\sum_{t_1=0}^{\infty}\sum_{t_2=0}^{\infty}\cdots\sum_{t_L=0}^{\infty}\frac{1}{\left\{\prod_{i=1}^{L}t_i!\Gamma(\mu+t_i)\right\}\left\{\prod_{i=1}^{L-1}\mu+t_i\right\}}$$
$$\times\left(\frac{\kappa\mu^2(1+\kappa)}{\bar{\gamma}}\right)^{\sum_{i=1}^{L}t_i}\int_0^{\infty}\gamma_{sc}^{L\mu+\sum_{i=1}^{L}t_i-1}\Gamma\left(\frac{1}{2},a\gamma_{sc}\right)e^{-\frac{L\mu(1+\kappa)}{\bar{\gamma}}\gamma_{sc}}$$
$$\times\left\{\prod_{i=1}^{L-1}{}_1F_1\left(1,\mu+t_i+1,\frac{\mu(1+\kappa)}{\bar{\gamma}}\gamma_{sc}\right)\right\}d\gamma_{sc} \tag{5.12}$$

The integration in 5.12 can be simplified by writing the hypergeometric function in infinite series using [5] as

$$P_{e,ch}(\bar{\gamma}) = \frac{L}{2\sqrt{\pi}e^{L\mu\kappa}}\left(\frac{\mu(1+\kappa)}{\bar{\gamma}}\right)^{L\mu}\sum_{t_1=0}^{\infty}\sum_{t_2=0}^{\infty}\cdots\sum_{t_L=0}^{\infty}\sum_{k_1=0}^{\infty}\sum_{k_2=0}^{\infty}\cdots\sum_{k_{L-1}=0}^{\infty}\frac{[\kappa\mu]^{\sum_{i=1}^{L}t_i}}{\left\{\prod_{i=1}^{L}t_i!\Gamma(\mu+t_i)\right\}}$$
$$\times\frac{1}{\left\{\prod_{i=1}^{L-1}(\mu+t_i)\,(\mu+t_i+1)_{k_i}\right\}}\left(\frac{\mu(1+\kappa)}{\bar{\gamma}}\right)^{\sum_{i=1}^{L}t_i+\sum_{i=1}^{L-1}k_i}\int_0^{\infty}\gamma_{sc}^{L\mu+\sum_{i=1}^{L}t_i+\sum_{i=1}^{L-1}k_i-1}$$
$$\times e^{-\frac{L\mu(1+\kappa)}{\bar{\gamma}}\gamma_{sc}}\Gamma\left(\frac{1}{2},a\gamma_{sc}\right)d\gamma_{sc}. \tag{5.13}$$

Solving the integral in Equation 5.13 using [1, A-(8a)] (reproduced in Equation B.14), an expression for ABER can be obtained as

$$P_{e,ch}(\bar{\gamma}) = \frac{L}{2e^{L\mu\kappa}}\sqrt{\frac{a\bar{\gamma}\beta}{\pi\mu(1+\kappa)}}\sum_{t_1=0}^{\infty}\sum_{t_2=0}^{\infty}\cdots\sum_{t_L=0}^{\infty}\sum_{k_1=0}^{\infty}\sum_{k_2=0}^{\infty}\cdots\sum_{k_{L-1}=0}^{\infty}\frac{\beta^{\zeta}\Gamma\left(\zeta+\frac{1}{2}\right)[\kappa\mu]^{\sum_{i=1}^{L}t_i}}{\zeta\left\{\prod_{i=1}^{L}t_i!\Gamma(\mu+t_i)\right\}}$$
$$\times\frac{1}{\left\{\prod_{i=1}^{L-1}(\mu+t_i)(\mu+t_i+1)_{k_i}\right\}}\,{}_2F_1\left(1,\zeta+\frac{1}{2};\zeta+1;L\beta\right), \tag{5.14}$$

where $\zeta \triangleq L\mu+\sum_{i=1}^{L}t_i+\sum_{i=1}^{L-1}k_i$ and $\beta \triangleq \frac{\mu(1+\kappa)}{a\bar{\gamma}+L\mu(1+\kappa)}$.

2. **Binary Non-coherent Modulations**

For binary noncoherent modulations (NCFSK and DPSK), the conditional BER is given in Equation 2.25. By putting $p_{e,\mathrm{ncoh}}(\varepsilon|\gamma)$ and $f_{\gamma_{sc}}(\gamma_{sc})$ from Equations 2.25 and 5.6 into Equation 2.17, an expression for noncoherent ABER can be given as

$$P_{e,nch}(\bar{\gamma}) = \frac{L}{2e^{L\mu\kappa}}\left(\frac{\mu(1+\kappa)}{\bar{\gamma}}\right)^{L\mu}\sum_{t_1=0}^{\infty}\sum_{t_2=0}^{\infty}\cdots\sum_{t_L=0}^{\infty}\frac{\left(\frac{\kappa\mu^2(1+\kappa)}{\bar{\gamma}}\right)^{\sum_{i=1}^{L}t_i}}{\left\{\prod_{i=1}^{L}t_i!\Gamma(\mu+t_i)\right\}\left\{\prod_{i=1}^{L-1}\mu+t_i\right\}}$$
$$\times\int_0^{\infty}\gamma_{sc}^{L\mu+\sum_{i=1}^{L}t_i-1}e^{-\frac{L\mu(1+\kappa)+a\bar{\gamma}}{\bar{\gamma}}\gamma_{sc}}\left\{\prod_{i=1}^{L-1}{}_1F_1\left(1,\mu+t_i+1,\frac{\mu(1+\kappa)}{\bar{\gamma}}\gamma_{sc}\right)\right\}d\gamma_{sc}. \tag{5.15}$$

Solving the integral (using [3, (C.1)], given in Equation B.15 in Appendix), an expression for ABER can be obtained as

$$P_{e,nch}(\bar{\gamma}) = \frac{L\beta^{L\mu}}{2e^{L\mu\kappa}}\sum_{t_1=0}^{\infty}\sum_{t_2=0}^{\infty}\cdots\sum_{t_L=0}^{\infty}\frac{\Gamma\left(L\mu+\sum_{i=1}^{L}t_i\right)[\kappa\mu\beta]^{\sum_{i=1}^{L}t_i}}{\left\{\prod_{i=1}^{L}t_i!\Gamma(\mu+t_i)\right\}\left\{\prod_{i=1}^{L-1}\mu+t_i\right\}}F_A\Bigg(L\mu+\sum_{i=1}^{L}t_i;\ \underbrace{1,1,\ldots,1}_{(L-1)\text{numbers}};$$
$$\mu+t_1+1,\mu+t_2+1,\ldots,\mu+t_{L-1}+1;\ \underbrace{\beta,\ldots,\beta}_{(L-1)\text{numbers}}\Bigg). \tag{5.16}$$

Table 5.1: Number of terms (N) required for an accuracy at 7^{th} place of decimal digit in the numerical evaluation of Equation 5.14 for $\kappa = 0.55, \mu = 2$.

$\bar{\gamma}$ (dB)	Modulation	$L=2$		$L=3$	
		N	ABER	N	ABER
5	CPSK	13	0.0160112	16	0.0121210
	CFSK	19	0.0593464	15	0.0604053
10	CPSK	10	0.0006925	10	0.0001977
	CFSK	12	0.0052614	13	0.0029356

5.1.4 Results and discussion

Analytically obtained expressions have been numerically evaluated and plotted for parameters of interest. For κ-μ fading channels, ABER vs. $\bar{\gamma}$ for binary coherent and non-coherent modulations have been shown in Figures 5.1 and 5.2, respectively. As expected, the performance is directly proportional to the diversity order L for given values of κ and μ. The κ-μ model is applied for line-of-sight fading communications and the parameter κ indicates the power of the dominant component. Hence, the ABER performance improves with the increase in κ for fixed values of L and μ. The parameters μ is the real extension of number of clusters n [14]. As expected, the increase in parameter μ improves the performance of the system. In the numerical evaluation of expressions involving infinite series, we have truncated them suitably so as to achieve an accuracy at least at 7^{th} place of decimal digit. In Tables 5.1 we have illustrated the number of terms (N) required to achieve an ABER of 10^{-7} in the evaluation of Equation 5.14 as a function of $\bar{\gamma}$.

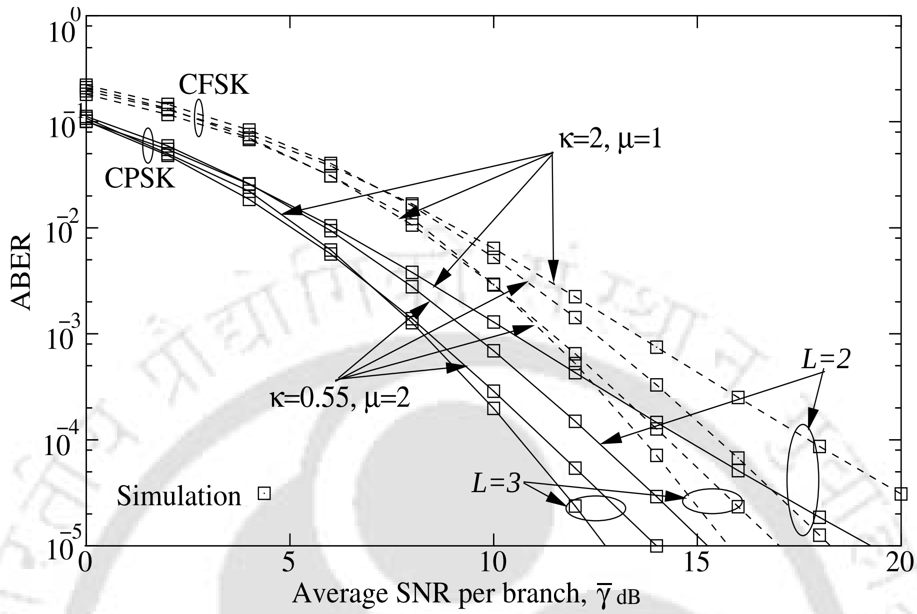

Figure 5.1: ABER vs. $\bar{\gamma}$ for SC receiver with CPSK and CFSK modulations.

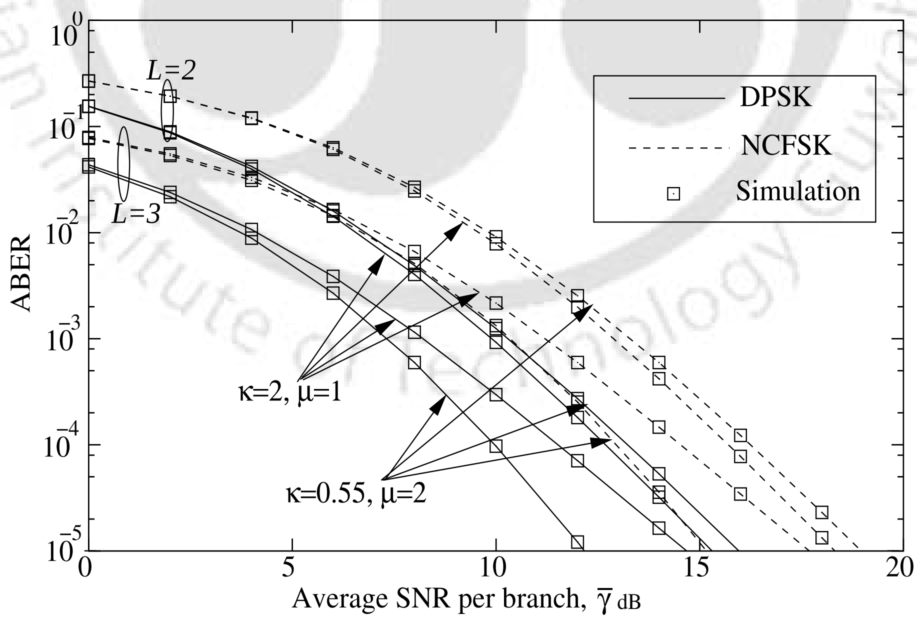

Figure 5.2: ABER vs. $\bar{\gamma}$ for SC receiver with DPSK and NCFSK modulations.

5.2 Summary

In this chapter, we have derived the PDF of output SNR and the expressions of performance measures over $\kappa - \mu$ fading channels for L independent SC receiver.

Chapter 6

Conclusions and Future Work

Performance of SC, EGC and MRC diversity receivers are analyzed over Hoyt, $\eta-\mu$ and $\kappa-\mu$ fading channels. Focusing on the analytical approach, mathematical expressions for various performance measures such as ASNR, outage probability and ABER/ASER of diversity receivers have been obtained. The PDF based analytical approach has been preferred in all analyses for these performance measures, wherever possible. It is stressed to analyze diversity receivers with arbitrary order of diversity with correlated fading channels since these cases are encountered frequently in the field deployment of diversity receivers. The mathematically obtained performance parameter expressions are numerically evaluated, plotted and the the effect of different parameters on the receiver performance is studied. Numerically obtained results have been compared with the Monte Carlo simulations results and have been found to be closely matching. The obtained expressions have been verified with the available published results which are special cases of the problems under analysis. Receiver systems with the particular configurations analyzed are enumerated below.

i) Expression of PDF of output SNR for independent fading channels:

(a) L-MRC receiver over Hoyt fading channels.

(b) L-SC receivers over Hoyt fading channels.

(c) L-SC receivers over $\eta-\mu$ fading channels.

(d) L-SC receivers over $\kappa-\mu$ fading channels.

ii) Expression of PDF of output SNR for correlated fading channels:

(a) L-MRC receiver over equally correlated Hoyt fading channels.

(b) Dual EGC receivers over Hoyt fading channels.

(c) Dual SC receivers over Hoyt fading channels.

(d) L-MRC receiver over equally correlated $\eta-\mu$ fading channels.

The obtained expressions for performance measures are obtained in terms of Gamma, incomplete Gamma, Beta, Bessel and Hypergeometric functions. Numerical expressions have been numerically evaluated using software packages like MATLAB and MATHEMATICA. In some analysis the obtained expressions are in the form of infinite series. These series have been truncated suitably by including finite number of terms ensuring to achieve an accuracy in ABER at least at 7^{th} place of decimal digit. Also wherever possible, we have derived expressions for upper bound on truncation errors.

6.1 Future Work

A few research problems that can be taken up for analysis are enumerated below:.

- Performance of L-MRC receivers over correlated Hoyt fading channels with arbitrary fading parameter
- Performance of L -EGC, SC receivers over correlated Hoyt fading channels
- Performance of L -EGC, SC receivers over correlated $\eta-\mu$ fading channels
- Performance of diversity receivers over correlated $\kappa-\mu$ fading channels

Appendix A

A.1 Complex Gaussian Model of Hoyt Random Variables

The complex Gaussian model of Hoyt RV $\alpha_l = |Z_l|$ for l^{th} $(l = 1, 2, \ldots, L)$ branch can be given as [13]

$$Z_l = X_l + jY_l, \qquad l = 1, 2, \ldots, L \tag{A.1}$$

where $j = \sqrt{-1}$, $X_l \sim N\left(0, \sigma_{x_l}^2\right)$ and $Y_l \sim N\left(0, \sigma_{y_l}^2\right)$. In this representation, the Hoyt RV $\alpha_l = |Z_l|$ has the PDF given in Equation 1.3. For the convenience of presentation but without loss of generality, we assume $\sigma_{x_l} = 1$, this result $\sigma_{y_l} = q$. Assuming $\sigma_{x_l}^2 = \sigma_x^2$ and $\sigma_{y_l}^2 = \sigma_y^2 \; \forall \; l$, from Equation A.1, we can obtain $\Omega_l = E\left[\alpha_l^2\right] = 1 + q^2$ hence, $\Omega_l = \Omega \forall \; l$. Substituting this value of Ω_l in Equation 1.3 and expressing $I_0(\cdot)$ in terms of confluent hypergeometric function [54], Equation 1.3 can be rewritten as

$$f_{\alpha_l}(\alpha_l) = \frac{\alpha_l e^{-\frac{1}{2q^2}\alpha_l^2}}{q} {}_1F_1\left(\tfrac{1}{2}; 1; \tfrac{1-q^2}{2q^2}\alpha_l^2\right). \tag{A.2}$$

For equal branch average power i.e. $\Omega_1 = \Omega_2 = \ldots = \Omega_L = \Omega$ (equivalently, for $\bar{\gamma}_1 = \bar{\gamma}_2 = \ldots = \bar{\gamma}_L = \bar{\gamma}$), E_b/N_0 can be expressed in terms of the fading parameter q as

$$\bar{\gamma} = \Omega \frac{E_b}{N_0} = (1 + q^2) \frac{E_b}{N_0}. \tag{A.3}$$

Thus,

$$\frac{E_b}{N_0} = \frac{\bar{\gamma}}{(1+q^2)}. \tag{A.4}$$

A.2 Characteristic Function of Sum of Hoyt Square RVs

In the mathematical model of Hoyt RVs in [13] i.e. $\alpha_l^2 = X_l^2 + Y_l^2$ the RVs $X_l \sim N\left(0, \sigma_x^2\right)$ and $Y_l \sim N\left(0, \sigma_y^2\right)$ are independent. So the joint CF of α_l^2 can be given as

$$\Phi_{\alpha_1^2,\alpha_1^2,\ldots,\alpha_L^2}(j\omega_1, j\omega_2, \ldots, j\omega_L) = \Phi_{X_1^2,X_2^2,\ldots,X_L^2}(j\omega_1, j\omega_2, \ldots, j\omega_L)\Phi_{Y_1^2,Y_2^2,\ldots,Y_L^2}(j\omega_1, j\omega_2, \ldots, j\omega_L), \tag{A.5}$$

the notation for $\Phi_{h_1,h_2,\ldots,h_L}(j\omega_1, j\omega_2, \ldots, j\omega_L)$ is the joint CF of RVs $h_l, h_2, \ldots, h_L$.

An expression for $\Phi_{X_1^2,X_2^2,\ldots,X_L^2}(j\omega_1, j\omega_1, \ldots, j\omega_L)$ can be derived as shown below:

From the PDF of X_l, performing transformation of random variable operation, PDF of a X_l^2 can be obtained as

$$f_{X_l^2}(x_l^2) = \frac{1}{\sqrt{2\pi\sigma_x^2 x_l}} e^{-\frac{x_l}{2\sigma_x^2}}. \tag{A.6}$$

From Equation A.6 CF of X_l^2 can be obtained as

$$\phi_{X_l^2}(j\omega_l) = E[e^{j\omega_l x_l}] = \frac{1}{(2\pi\sigma_x^2)^{1/2}} \int_0^\infty \frac{1}{\sqrt{x_l}} e^{-\left(\frac{1}{2\sigma_x^2}+j\omega_l\right)x_l} dx_l. \tag{A.7}$$

Performing the integration we obtain

$$\phi_{X_l^2}(j\omega_l) = \frac{1}{\sqrt{2\sigma_x^2\left(\frac{1}{2\sigma_x^2} + j\omega_l\right)}}. \tag{A.8}$$

Since X_ls are independent their joint CF is the product of individual CFs, hence

$$\phi_{X_1^2,X_2^2,\ldots,X_L^2}(j\omega_1, j\omega_2, \ldots, j\omega_L) = \frac{1}{(2\sigma_x^2)^{L/2}} \prod_{i=1}^{L} \frac{1}{\sqrt{\left(\frac{1}{2\sigma_x^2} + j\omega_i\right)}}. \tag{A.9}$$

Similarly the joint CF of RVs $Y_1^2, Y_2^2, \ldots, Y_L^2$ can be obtained as

$$\phi_{Y_1^2,Y_2^2,\ldots,Y_L^2}(j\omega_1, j\omega_2, \ldots, j\omega_L) = \frac{1}{(2\sigma_y^2)^{L/2}} \prod_{i=1}^{L} \frac{1}{\sqrt{\left(\frac{1}{2\sigma_y^2} + j\omega_i\right)}}. \tag{A.10}$$

Hence, the joint CF in Equation A.5 can be obtained as

$$\Phi_{\alpha_1^2,\alpha_2^2,\ldots,\alpha_L^2}(j\omega_1, j\omega_2, \ldots, j\omega_L) = \frac{1}{(2\sigma_x\sigma_y)^L} \prod_{i=1}^{L} \frac{1}{\sqrt{\left(\frac{1}{2\sigma_x^2} + j\omega_i\right)\left(\frac{1}{2\sigma_y^2} + j\omega_i\right)}}. \tag{A.11}$$

A.3 Joint Characteristic Function of Dual Correlated Hoyt RVs

Hoyt fading model is given in [13], where α_l^2 is given as

$$\alpha_l^2 = X_l^2 + Y_l^2, \qquad l = 1, 2, \tag{A.12}$$

where X_l, Y_l are independent zero mean Gaussian RVs with variances σ_x^2 and σ_y^2, respectively. In this representation the Hoyt RV α_l has the PDF given in Equation 1.3, where the fading parameter $q = \frac{\sigma_y}{\sigma_x}$. In this analysis to simplify the analysis procedure, we assume $\sigma_x^2 = 1$ resulting in $\sigma_y^2 = q^2$. However, this representation is not affecting the generality of the fading channel.

When $X_1(Y_1)$ and $X_2(Y_2)$ are correlated with correlation coefficient ρ, it can be shown that RVs α_1 and α_2 are also correlated with correlation coefficient ρ. In complex form Hoyt RV can be modeled as $Z_l = X_l + jY_l$, where α_l=$|Z_l|$ and the correlation coefficient between Z_1 and Z_2 can be written as,

$$\rho_{Z_1,Z_2} = \frac{E\left[(Z_1 - \bar{Z}_1)(Z_2 - \bar{Z}_2)^*\right]}{\sqrt{Var(Z_1)Var(Z_2)}} = \frac{E[Z_1 Z_2^*]}{\sigma_x^2 + \sigma_y^2}, \tag{A.13}$$

where $\bar{Z}_l$ represents the mean and from definition it can be shown to be zero. The variance of α_l can be derived as

$$\begin{aligned} Var(Z_l) = \quad & E(Z_l^2) - [E(Z_l)]^2 \\ = \quad & E(Z_l Z_l^*) - 0 \end{aligned} \tag{A.14}$$

$$
\begin{aligned}
&= E(X_l^2 + Y_l^2) \\
&= \sigma_x^2 + \sigma_y^2.
\end{aligned}
$$

Hence we can write

$$
\rho = \frac{E\left[(X_1 - \bar{X}_1)(X_2 - \bar{X}_2)\right]}{\sqrt{Var(X_1)Var(X_2)}} = \frac{E[X_1X_2]}{\sigma_x^2} \tag{A.15}
$$

$$
E[X_1X_2] = \sigma_x^2\rho.
$$

Similarly,

$$
E[Y_1Y_2] = \sigma_y^2\rho. \tag{A.16}
$$

Now we can write $E(\alpha_l\alpha_l^*)$ as,

$$
\begin{aligned}
E[\alpha_1\alpha_2^*] &= E[(X_1 + jY_1)(X_2 - jY_2)] \\
&= E[X_1X_2 + Y_1Y_2 + j(Y_1X_2 - X_1Y_2)] \\
&= E[X_1X_2 + Y_1Y_2] = E[X_1X_2] + E[Y_1Y_2] \\
&= \rho\sigma_x^2 + \rho\sigma_y^2 = \rho[\sigma_x^2 + \sigma_y^2].
\end{aligned} \tag{A.17}
$$

Applying values of $E[Z_1Z_2^*]$ from Equation A.17 to Equation A.13,

$$
\rho_{Z_1,Z_2} = \frac{\rho[\sigma_x^2 + \sigma_y^2]}{\sigma_x^2 + \sigma_y^2} = \rho. \tag{A.18}
$$

Joint Characteristic Function

From the model given in Equation A.12 α^2 can be written in terms of square Gaussian distribution as

$$
\alpha^2 = X_1^2 + X_2^2 + Y_1^2 + Y_2^2. \tag{A.19}
$$

Since, RV X_l^2 and Y_l^2 are independent from Equation A.12 the joint CF of RVs α_1^2 and α_2^2 can be obtained by multiplying joint CF of X_l^2 and Y_l^2 as

$$\Phi_{\alpha_1^2,\alpha_2^2}(j\omega_1, j\omega_2) = \Phi_{X_1^2,X_2^2}(j\omega_1, j\omega_2)\Phi_{Y_1^2,Y_2^2}(j\omega_1, j\omega_2), \tag{A.20}$$

where $\Phi_{h_l,g_l}(h_l, g_l)$ is the joint CF of h_l and g_l. The joint density function of the correlated Gaussian distribution X_1 and X_2 with variance σ_x^2 is given in [59] as

$$f_{X_1X_2}(x_1,x_2) = \frac{1}{2\pi\sigma_x^2\sqrt{1-\rho^2}} e^{-\frac{X_1^2-2\rho X_1X_2+X_2^2}{2(1-\rho^2)\sigma_x^2}}. \tag{A.21}$$

Performing the operation of transformation of RV in Equation A.21 joint PDF of X_1^2 and X_2^2 can be written as

$$f_{X_1^2X_2^2}(x_1^2x_2^2) = \frac{1}{4\pi\sigma_x^2\sqrt{1-\rho^2}\sqrt{x_1x_2}}\left[e^{-\frac{x_1-2\rho\sqrt{x_1x_2}+x_2}{2(1-\rho^2)\sigma_x^2}} + e^{-\frac{x_1+2\rho\sqrt{x_1x_2}+x_2}{2(1-\rho^2)\sigma_x^2}}\right]. \tag{A.22}$$

From Equation A.22 the joint CF of X_1^2 and X_2^2 can be given as

$$\begin{aligned}\Phi_{X_1^2X_2^2}(j\omega_1, j\omega_2) \quad &= \quad \frac{1}{4\pi\sigma_x^2\sqrt{1-\rho^2}}\int_0^\infty\int_0^\infty \frac{1}{\sqrt{x_1x_2}}\left[e^{-\frac{x_1-2\rho\sqrt{x_1x_2}+x_2}{2(1-\rho^2)\sigma_x^2}} + e^{-\frac{x_1+2\rho\sqrt{x_1x_2}+x_2}{2(1-\rho^2)\sigma_x^2}}\right]\\ &\quad \times e^{-jx_1\omega_1}e^{-jx_2\omega_2}dx_1dx_2.\end{aligned} \tag{A.23}$$

Solving the integration in Equation A.23 $\Phi_{x_1^2x_2^2}(j\omega_1, j\omega_2)$ can be written as

$$\begin{aligned}\Phi_{x_1^2x_2^2}(j\omega_1, j\omega_2) \quad &= \quad \frac{1}{2\sigma_x^2\sqrt{1-\rho^2}}\sum_{k=0}^{\infty}\frac{\rho^{2k}(2k-1)!!}{k!8^k(1-\rho^2)^{2k}\sigma_x^{4k}\left(\frac{1}{2(1-\rho^2)\sigma_x^2}+j\omega_1\right)^{k+\frac{1}{2}}}\\ &\quad \times\frac{1}{\left(\frac{1}{2(1-\rho^2)\sigma_x^2}+j\omega_2\right)^{k+\frac{1}{2}}}.\end{aligned} \tag{A.24}$$

Similarly joint CF of Y_1^2 and Y_2^2, $\Phi_{Y_1^2,Y_2^2}(j\omega_1, j\omega_2)$ can be obtained as

$$\Phi_{Y_1^2Y_2^2}(j\omega_1, j\omega_2) \quad = \quad \frac{1}{2\sigma_y^2\sqrt{1-\rho^2}}\sum_{t=0}^{\infty}\frac{\rho^{2t}(2t-1)!!}{t!8^t(1-\rho^2)^{2t}\sigma_y^{4t}\left(\frac{1}{2(1-\rho^2)\sigma_y^2}+j\omega_1\right)^{t+\frac{1}{2}}}$$

$$\times \frac{1}{\left(\frac{1}{2(1-\rho^2)\sigma_y^2} + j\omega_2\right)^{t+\frac{1}{2}}}. \quad \text{(A.25)}$$

Thus, the joint CF in Equation A.20 can be present as

$$\begin{aligned}\Phi_{\alpha_1^2,\alpha_2^2}(j\omega_1, j\omega_2) &= \frac{1}{4\sigma_x^2\sigma_y^2(1-\rho^2)} \sum_{k=0}^{\infty}\sum_{t=0}^{\infty} \frac{1}{k!t!} \left(\frac{\rho}{\sqrt{8}\sigma_x^2(1-\rho^2)}\right)^{\lambda_1} \frac{(2k-1)!!(2t-1)!!}{\left(\frac{1}{2(1-\rho^2)\sigma_x^2} + j\omega_1\right)^{k+1/2}} \\ &\times \frac{1}{\left(\frac{1}{2(1-\rho^2)\sigma_x^2} + j\omega_2\right)^{k+1/2} \left[\left(\frac{1}{2(1-\rho^2)\sigma_y^2} + j\omega_1\right)\left(\frac{1}{2(1-\rho^2)\sigma_y^2} + j\omega_2\right)\right]^{t+1/2}},\end{aligned} \quad \text{(A.26)}$$

where for the convenience of presentation we have used $\lambda_1 \triangleq 2(k+t)$.

A.4 Joint PDF of Dual correlated Hoyt RV

In Equation A.26, the joint CF of Hoyt square RVs α_1^2 and α_2^2 is given as

$$\begin{aligned}\Phi_{\alpha_1^2,\alpha_2^2}(j\omega_1, j\omega_2) &= \frac{1}{4\sigma_x^2\sigma_y^2(1-\rho^2)} \sum_{k_1=0}^{\infty}\sum_{k_2=0}^{\infty} \frac{(2k_1-1)!!(2k_2-1)!!}{k_1!k_2!\left[\sigma_x^2\right]^{2k_1}\left[\sigma_y^2\right]^{2k_2} 8^{\lambda_{12}}} \\ &\times \frac{\rho^{2\lambda_{12}}}{(1-\rho^2)^{2\lambda_{12}}\left(F(x,1)F(x,2)\right)^{k_1+\frac{1}{2}}\left(F(y,1)F(y,2)\right)^{k_2+\frac{1}{2}}},\end{aligned} \quad \text{(A.27)}$$

where $\lambda_{st} \triangleq (k_s + k_{s+1} + \cdots + k_t)$, $t > s$, $s > r$ and $F(z,i) \triangleq \frac{1}{2(1-\rho^2)\sigma_z^2} + j\omega_i$. By taking the inverse Fourier transform of Equation A.27 the joint PDF of α_1^2, α_2^2 can be given as

$$\begin{aligned}f_{\alpha_1^2,\alpha_2^2}(\alpha_1^2, \alpha_2^2) &= \frac{1}{4\sigma_x^2\sigma_y^2(1-\rho^2)} \sum_{k_1=0}^{\infty}\sum_{k_2=0}^{\infty} \frac{\rho^{2\lambda_{12}}(2k_1-1)!!}{k_1!k_2!8^{\lambda_{12}}(1-\rho^2)^{2\lambda_{12}}} \\ &\times \frac{(2k_2-1)!!}{4\pi^2(\sigma_x^2)^{2k_1}(\sigma_y^2)^{2k_2}} \int_{-\infty}^{\infty} \frac{1}{(F(x,1))^{k_1+\frac{1}{2}}(F(y,1))^{k_2+\frac{1}{2}}} e^{j\omega_1 s_1} d\omega_1 \\ &\times \int_{-\infty}^{\infty} \frac{1}{(F(x,2))^{k_1+\frac{1}{2}}(F(y,2))^{k_2+\frac{1}{2}}} e^{j\omega_2 s_2} d\omega_2.\end{aligned} \quad \text{(A.28)}$$

The integration in Equation A.28 can be solved using [4, (3.384.8)] and an expression for the joint PDF of α_1^2 and α_2^2 can be obtained as

$$\begin{aligned} f_{\alpha_1^2\alpha_2^2}(\alpha_1^2\alpha_2^2) &= \frac{1}{4\sigma_x^2\sigma_y^2(1-\rho^2)}\sum_{k_1=0}^{\infty}\sum_{k_2=0}^{\infty}\frac{\rho^{2\lambda_{12}}(2k_1-1)!!(2k_2-1)!!}{k_1!k_2!8^{\lambda_{12}}(1-\rho^2)^{2\lambda_{12}}\sigma_x^{4\lambda_{12}}} \\ &\times\frac{e^{-\frac{\alpha_1}{2(1-\rho^2)\sigma_y^2}}}{\Gamma^2(\lambda_{12}+1)}\alpha_1^{k+t}{}_1F_1\left(k_1+\tfrac{1}{2};\lambda_{12}+1;\left(\frac{\sigma_x^2-\sigma_y^2}{2(1-\rho^2)\sigma_x^2\sigma_y^2}\right)\alpha_1\right) \\ &\times e^{-\frac{\alpha_2}{2(1-\rho^2)\sigma_y^2}}\alpha_2^{k+t}{}_1F_1\left(k_1+\tfrac{1}{2};\lambda_{12}+1;\left(\frac{\sigma_x^2-\sigma_y^2}{2(1-\rho^2)\sigma_x^2\sigma_y^2}\right)\alpha_2\right). \qquad \text{(A.29)} \end{aligned}$$

A.5 Characteristic Function of Hoyt RV with Unequal q

From Equation A.20 the joint CF of bivariate RVs α_1^2 and α_2^2 can be obtained as by obtaining the joint CF of square Gaussian random variable.

Joint density function of correlated bivariate Gaussian RVs X_1 and X_2 is given in [59, 6.23] as

$$f_{X_1X_2}(x_1,x_2) = \frac{1}{2\pi\sigma_{x_1}\sigma_{x_2}\sqrt{1-\rho^2}}e^{-\frac{1}{2(1-\rho^2)}\left(\frac{X_1^2}{\sigma_{x_1}^2}-\frac{2\rho X_1X_2}{\sigma_{x_1}\sigma_{x_2}}+\frac{X_2^2}{\sigma_{x_2}^2}\right)}. \qquad \text{(A.30)}$$

Performing transformation of random variable in Equation A.30 the joint PDF of X_1^2, X_2^2 can be obtained as

$$f_{X_1^2,X_2^2}(x_1^2,x_2^2) = \frac{e^{-\frac{1}{2(1-\rho^2)}\left(\frac{x_1}{\sigma_{x_1}^2}-\frac{2\rho\sqrt{x_1x_2}}{\sigma_{x_1}\sigma_{x_2}}+\frac{x_2}{\sigma_{x_2}^2}\right)}+e^{-\frac{1}{2(1-\rho^2)}\left(\frac{x_1}{\sigma_{x_1}^2}+\frac{2\rho\sqrt{x_1x_2}}{\sigma_{x_1}\sigma_{x_2}}+\frac{x_2}{\sigma_{x_2}^2}\right)}}{4\pi\sqrt{\sigma_{x_1}^2\sigma_{x_2}^2x_1x_2(1-\rho^2)}}. \qquad \text{(A.31)}$$

From Equation A.31 the joint CF of X_1^2, X_2^2 can be given as

$$\begin{aligned} \Phi_{X_1^2,X_2^2}(j\omega_1, j\omega_2) &= \frac{1}{2\pi\sigma_{x_1}\sigma_{x_2}\sqrt{1-\rho^2}}\int_0^{\infty}\frac{1}{2\sqrt{x_2}}\left(\int_0^{\infty}\frac{1}{\sqrt{x_1}}e^{-\frac{1}{2(1-\rho^2)}\left(\frac{x_1}{\sigma_{x_1}^2}-\frac{2\rho\sqrt{x_1x_2}}{\sigma_{x_1}\sigma_{x_2}}\right)}\right. \\ &\left.\times\, e^{-jx_1\omega_1}dx_1+\int_0^{\infty}\frac{1}{\sqrt{x_1}}e^{-\frac{1}{2(1-\rho^2)}\left(\frac{x_1}{\sigma_{x_1}^2}+\frac{2\rho\sqrt{x_1x_2}}{\sigma_{x_1}\sigma_{x_2}}\right)}e^{-jx_1\omega_1}dx_1\right) \\ &\times e^{-\frac{x_2}{2(1-\rho^2)\sigma_{x_2}^2}}e^{-jx_2\omega_2}dx_2. \qquad \text{(A.32)} \end{aligned}$$

Solving the integration in Equation A.32 $\Phi_{X_1^2,X_2^2}(j\omega_1, j\omega_2)$ can be expressed as

$$\begin{aligned}\Phi_{X_1^2,X_2^2}(j\omega_1, j\omega_2) &= \frac{1}{2\sigma_{x_1}\sigma_{x_2}\sqrt{1-\rho^2}}\sum_{k=0}^{\infty}\frac{\rho^{2k}(2k-1)!!}{k!\left(2\sqrt{2}\sigma_{x_1}\sigma_{x_2}(1-\rho^2)\right)^{2k}} \\ &\times\frac{1}{\left(\frac{1}{2(1-\rho^2)\sigma_{x_1}^2}+j\omega_1\right)^{k+\frac{1}{2}}\left(\frac{1}{2(1-\rho^2)\sigma_{x_2}^2}+j\omega_2\right)^{k+\frac{1}{2}}}. \end{aligned} \quad (A.33)$$

Similarly $\Phi_{Y_1^2,Y_2^2}(j\omega_1, j\omega_2)$ can be derived as

$$\begin{aligned}\Phi_{Y_1^2,Y_2^2}(j\omega_1, j\omega_2) &= \frac{1}{2\sigma_{y_1}\sigma_{y_2}\sqrt{1-\rho^2}}\sum_{k=0}^{\infty}\frac{\rho^{2k}(2k-1)!!}{k!\left(2\sqrt{2}\sigma_{y_1}\sigma_{y_2}(1-\rho^2)\right)^{2k}} \\ &\times\frac{1}{\left(\frac{1}{2(1-\rho^2)\sigma_{y_1}^2}+j\omega_1\right)^{k+\frac{1}{2}}\left(\frac{1}{2(1-\rho^2)\sigma_{y_2}^2}+j\omega_2\right)^{k+\frac{1}{2}}}. \end{aligned} \quad (A.34)$$

Thus, from Equation A.20 the joint CF of α_1^2, α_2^2 can be expressed as

$$\begin{aligned}\Phi_{\alpha_1^2,\alpha_2^2}(j\omega_1, j\omega_2) &= \frac{1}{4\sigma_{x_1}\sigma_{x_2}\sigma_{y_1}\sigma_{y_2}(1-\rho^2)}\sum_{k_1=0}^{\infty}\sum_{k_2=0}^{\infty}\frac{(2k_1-1)!!(2k_2-1)!!}{k_1!k_2!\left[\sigma_{x_1}\sigma_{x_2}\right]^{2k_1}\left[\sigma_{y_1}\sigma_{y_2}\right]^{2k_2}8^{\lambda_{12}}} \\ &\times\frac{\rho^{2\lambda_{12}}}{(1-\rho^2)^{2\lambda_{12}}\left(F(x,1)F(x,2)\right)^{k_1+\frac{1}{2}}\left(F(y,1)F(y,2)\right)^{k_2+\frac{1}{2}}}, \end{aligned} \quad (A.35)$$

where for the convenience of presentation we define the terms as given below:

$$\begin{aligned}F(z,i) &\triangleq \frac{1}{2(1-\rho^2)\sigma_{z_i}^2}+j\omega_i \\ \lambda_{mn} &\triangleq (k_m+k_{m+1}+\cdots+k_n), n > m.\end{aligned}$$

A.6 Correlation Coefficient of Hoyt RV with Unequal q

Hoyt fading model is described Section 3.3.1 in terms of square Gaussian distribution, where X_l and Y_l are independent zero mean Gaussian RVs with variances $\sigma_{x_l}^2$ and $\sigma_{y_l}^2$. With this the fading parameter of l^{th} branch can be given as $q_l = \frac{\sigma_{y_l}}{\sigma_{x_l}}$.

Again assuming $X_1(Y_1)$ and $X_2(Y_2)$ are correlated with correlation coefficient ρ, the correlation coefficient between RVs α_1 and α_2 can be given as

$$\rho_{\alpha_1,\alpha_2} = \frac{E\left[(\alpha_1-\bar{\alpha}_1)(\alpha_2-\bar{\alpha}_2)^*\right]}{\sqrt{Var(\alpha_1)Var(\alpha_2)}} = \frac{E[\alpha_1\alpha_2^*]}{\sqrt{\left(\sigma_{x_1}^2+\sigma_{y_1}^2\right)\left(\sigma_{x_2}^2+\sigma_{y_2}^2\right)}}. \tag{A.36}$$

Now, $E[\alpha_1\alpha_2^*]$ can be given as

$$E[\alpha_1\alpha_2^*] = E[(X_1+jY_1)(X_2-jY_2)] = E[X_1X_2]+E[Y_1Y_2]. \tag{A.37}$$

From the definition of correlation coefficient $E[X_1X_2]$ and $E[Y_1Y_2]$ can be evaluated as $\rho\sigma_{x_1}\sigma_{x_2}$ and $\rho\sigma_{y_1}\sigma_{y_2}$, respectively. Putting these values $\rho_{\alpha_1\alpha_2}$ can be obtained as

$$\rho_{\alpha_1\alpha_2} = \frac{\rho\left(1+q_1q_2\right)}{\sqrt{\left(1+q_1^2\right)\left(1+q_2^2\right)}}. \tag{A.38}$$

A.7 PDF of Sum of Exponentially Correlated Gamma RVs

Let the PDF of RVs X_is (i=1, 2, ..., n) are given by

$$f(x_i) = \left[\Gamma(r)\theta^r\right]^{-1} e^{-x_i/\theta} x_i^{r-1}. \tag{A.39}$$

In [65], it is given that, the approximate sum of exponentially correlated RVs X_is can be obtained by replacing r and θ by r_n and θ_n, respectively, where r_n and θ_n are given as

$$r_n = \left\{n^2/\left[n+\tfrac{2\rho}{1-\rho}\left(n-\tfrac{1-\rho^n}{1-\rho}\right)\right]\right\} r, \tag{A.40}$$

and

$$\theta_n = \left\{\left[n+\tfrac{2\rho}{1-\rho}\left(n-\tfrac{1-\rho^n}{1-\rho}\right)\right]/n\right\}\theta. \tag{A.41}$$

A.8 Power Correlation Coefficient of $\eta-\mu$ RVs

From the model of $\eta-\mu$ RV given in section the power correlation coefficient can be given as

$$\upsilon = \frac{Cov[z_1^2 z_2^2]}{\sqrt{Var[z_1^2]Var[z_2^2]}}. \tag{A.42}$$

In this correlation model we are assuming that the Gaussian RVs X_ls (Y_ls) are correlated with a power correlation coefficient ρ. Hence, using [67, (15)] the variance of Z_1^2, Z_2^2 can be given as

$$Var[Z_1^2] = Var[Z_2^2] = 2n(\sigma_x^4+\sigma_y^4). \tag{A.43}$$

The covariance of $Cov[z_1^2 z_2^2]$ can be obtained form [67, (18)] as

$$Cov[Z_1^2 Z_2^2] = 2\rho n(\sigma_x^4+\sigma_y^4). \tag{A.44}$$

Therefore, using Equations A.43 and A.44 it can be shown that $\upsilon = \rho$.

A.9 Joint PDF of Generalized Rayleigh RV

For p-dimensional column vectors $Y_1, Y_2, \ldots, Y_n$ which are independent and identically normally distributed with mean zero and positive definite covariance matrix M. Let $W = M^{-1} = (w_{kk'})_{1\le k,k'\le p}$ have the property that $w_{kk'} = 0$ for $|k-k'| > 1$. Let r_k be the norm of the n-dimensional vector X_k composed of k^{th} component of Y_j. Let $R = \{r_1, r_2, \ldots, r_p\}$ be the p-dimensional vector of norms. Then the frequency function $g(R)$ of R is

$$\begin{aligned} g(R) &= \frac{|W|^{n/2}}{2^{(n-1)/2}\Gamma(n/2)} r_1^{(n-1)/2} r_p^{n/2} \exp\left(-w_{pp} r_p^2/2\right) \left\{ \prod_{k=1}^{p-1} \left|w_{k,k+1}\right|^{-(n-1)/2} r_k \right. \\ &\quad \left. \times \exp\left(-w_{kk} r_k^2/2\right) I_{(n-1)/2}\left(\left|w_{k,k+1}\right| r_k r_{k+1}\right) \right\} \qquad r_k \ge 0, 1 \le k \le p. \end{aligned} \tag{A.45}$$

A.10 Upper Bound on Truncation Error

A.10.1 Equation 3.6

The PDF of the γ_{SC} is in the form of infinite series. Hence to test the convergence of Equation 3.6 we have obtained an upper bound of error on truncation following a similar approach in [55]. Considering only K terms are used in the evaluation of PDF, the error involved in the PDF can be written as

$$\begin{aligned} E_K &= \frac{Lq^{L-2}(1+q^2)}{2\bar{\gamma}} e^{-\frac{L(1+q^2)}{2\bar{\gamma}q^2}\gamma_{SC}} \left(\frac{\gamma_{SC}(1+q^2)}{2\bar{\gamma}q^2}\right)^{L-1} \sum_{t=K}^{\infty} \frac{\left(\frac{1}{2}\right)_t}{(t!)^2} \left(\frac{\gamma_{SC}(1-q^4)}{2\bar{\gamma}q^2}\right)^t \\ &\times \left[\sum_{k=K}^{\infty} \frac{\left(\frac{1}{2}\right)_k}{(k!)^2(k+1)} \left(\frac{\gamma_{SC}(1-q^4)}{2\bar{\gamma}q^2}\right)^k {}_1F_1\left(1; k+2; \frac{1+q^2}{2\bar{\gamma}q^2}\gamma_{SC}\right)\right]^{L-1}. \end{aligned} \quad (A.46)$$

The above expression can be rewritten as

$$\begin{aligned} E_K &= \frac{Lq^{L-2}(1+q^2)}{2\bar{\gamma}} e^{-\frac{L(1+q^2)}{2\bar{\gamma}q^2}\gamma_{SC}} \left(\frac{\gamma_{SC}(1+q^2)}{2\bar{\gamma}q^2}\right)^{L-1} \sum_{t=K}^{\infty} \frac{\left(\frac{1}{2}\right)_t}{(t!)^2} \left(\frac{\gamma_{SC}(1-q^4)}{2\bar{\gamma}q^2}\right)^t \\ &\times \left[\sum_{k=K}^{\infty} \frac{\left(\frac{1}{2}\right)_k}{(k!)^2(k+1)} \left(\frac{\gamma_{SC}(1-q^4)}{2\bar{\gamma}q^2}\right)^k e^{\frac{1+q^2}{2\bar{\gamma}q^2}\gamma_{SC}} {}_1F_1\left(k+1; k+2; -\frac{1+q^2}{2\bar{\gamma}q^2}\gamma_{SC}\right)\right]^{L-1} \end{aligned} \quad (A.47)$$

The hypergeometric function involved in Equation A.47 is in the form of ${}_1F_1(r; 1+r; -z)$, can be shown to be monotonically decreasing over all positive values of r and z. Hence the upper bound on truncation error can be written as

$$\begin{aligned} E_K &\leq \frac{Lq^{L-2}(1+q^2)}{2\bar{\gamma}} e^{-\frac{L(1+q^2)}{2\bar{\gamma}q^2}\gamma_{SC}} \left[\frac{\gamma_{SC}(1+q^2)}{2\bar{\gamma}q^2}\right]^{L-1} \left[e^{\frac{1+q^2}{2\bar{\gamma}q^2}\gamma_{SC}} {}_1F_1\left(K+1; K+2; -\frac{1+q^2}{2\bar{\gamma}q^2}\gamma_{SC}\right)\right]^{L-1} \\ &\times \left[\sum_{k=K}^{\infty} \frac{\left(\frac{1}{2}\right)_k}{(k!)^2(k+1)} \left(\frac{\gamma_{SC}(1-q^4)}{2\bar{\gamma}q^2}\right)^k\right]^{L-1} \sum_{t=K}^{\infty} \frac{\left(\frac{1}{2}\right)_t}{(t!)^2} \left(\frac{\gamma_{SC}(1-q^4)}{2\bar{\gamma}q^2}\right)^t. \end{aligned} \quad (A.48)$$

Equation A.48 can be simplified to

$$\begin{aligned} E_K &\leq \frac{Lq^{L-2}(1+q^2)}{2\bar{\gamma}} e^{-\frac{L(1+q^2)}{2\bar{\gamma}q^2}\gamma_{SC}} \left[\frac{\gamma_{SC}(1+q^2)}{2\bar{\gamma}q^2}\right]^{L-1} \left[e^{\frac{1+q^2}{2\bar{\gamma}q^2}\gamma_{SC}} {}_1F_1\left(K+1; K+2; -\frac{1+q^2}{2\bar{\gamma}q^2}\gamma_{SC}\right)\right]^{L-1} \\ &\times \left[\frac{\left(\frac{1}{2}\right)_K}{(K!)^2(K+1)} \left(\frac{\gamma_{SC}(1-q^4)}{2\bar{\gamma}q^2}\right)^K + \frac{\left(\frac{1}{2}\right)_{K+1}}{(K+1!)^2(K+2)} \left(\frac{\gamma_{SC}(1-q^4)}{2\bar{\gamma}q^2}\right)^{K+1} + \ldots + \infty\right]^{L-1} \end{aligned}$$

$$\times\left[\frac{\left(\frac{1}{2}\right)_K}{(K!)^2}\left(\frac{\gamma_{SC}(1-q^4)}{2\bar{\gamma}q^2}\right)^K+\frac{\left(\frac{1}{2}\right)_{K+1}}{(K+1!)^2}\left(\frac{\gamma_{SC}(1-q^4)}{2\bar{\gamma}q^2}\right)^{K+1}+\ldots+\infty\right]. \quad \text{(A.49)}$$

After some algebraic manipulations Equation A.49 can be simplified to

$$E_K \leq \frac{Lq^{L-2}(1+q^2)\left[\left(\frac{1}{2}\right)_K\right]^L}{2\bar{\gamma}(K+1)^{L-1}(K!)^{2L}}e^{-\frac{(1+q^2)}{2\bar{\gamma}q^2}\gamma_{SC}}\left[\frac{\gamma_{SC}(1-q^4)}{2\bar{\gamma}q^2}\right]^{LK}{}_1F_1\left(K+1,K+2,-\frac{1+q^2}{2\bar{\gamma}q^2}\gamma_{SC}\right)^{L-1}$$
$$\times\left[\frac{\gamma_{SC}(1+q^2)}{2\bar{\gamma}q^2}\right]^{L-1}{}_3F_3\left[\begin{matrix}1 & \frac{1}{2}+K & K+1 & \frac{\gamma_{SC}(1-q^4)}{2\bar{\gamma}q^2}\\ K+1 & K+1 & K+2 & \end{matrix}\right]^{L-1}$$
$$\times{}_2F_2\left[\begin{matrix}1 & \frac{1}{2}+K & \frac{\gamma_{SC}(1-q^4)}{2\bar{\gamma}q^2}\\ K+1 & K+1 & \end{matrix}\right]. \quad \text{(A.50)}$$

A.10.2 Equation 3.28

The error in truncating Equation 3.28 can be given as

$$\tilde{E}_{K_{out}} = \left(\frac{1+q^2}{2\bar{\gamma}_N q}\right)^L\sum_{k=K}^{\infty}\frac{\left(\frac{L}{2}\right)_k}{(L+k)!k!}\left(\frac{1-q^4}{2\bar{\gamma}_N q^2}\right)^k{}_1F_1\left(L+k;L+k+1;-\frac{1+q^2}{2\bar{\gamma}_N q^2}\right). \quad \text{(A.51)}$$

The hypergeometric function involved in Equation A.51 which is in the form of ${}_1F_1(r;1+r;-z)$, where $r=L+k$ and $z=\frac{1+q^2}{2\bar{\gamma}_N q^2}$ can be shown to be monotonically decreasing over all positive values of r and z. Thus, Equation A.51 can be upper bounded by

$$E_{K_{out}} \leq \left(\frac{1+q^2}{2\bar{\gamma}_N q}\right)^L{}_1F_1\left(L+K;L+K+1;-\frac{1+q^2}{2\bar{\gamma}_N q^2}\right)\sum_{k=K}^{\infty}\frac{\left(\frac{L}{2}\right)_k}{k!\,(L+k)!}\left(\frac{1-q^4}{2\bar{\gamma}_N q^2}\right)^k. \quad \text{(A.52)}$$

After some algebraic manipulation Equation A.52 can shown to be

$$\tilde{E}_{K_{out}} \leq \left(\frac{1+q^2}{2\bar{\gamma}_N q}\right)^L{}_1F_1\left(L+K;L+K+1;-\frac{1+q^2}{2\bar{\gamma}_N q^2}\right)\frac{\left(\frac{L}{2}\right)_K}{K!(L+K)!}$$
$$\times\left(\frac{1-q^4}{2\bar{\gamma}_N q^2}\right)^K{}_2F_2\left[\begin{matrix}1 & \frac{L}{2}+K & \frac{1-q^4}{2\bar{\gamma}_N q^2}\\ K+1 & L+K+1 & \end{matrix}\right]. \quad \text{(A.53)}$$

A.10.3 Equation 3.34

Similarly, error on the truncation of Equation 3.34 for coherent ABER can be expressed as

$$\begin{aligned}\tilde{E}_{K_{ABER}} &= \sqrt{\frac{a\bar{\gamma}}{2\pi(1+q^2)}}\frac{q^{L+1}\lambda^{L+\frac{1}{2}}}{\Gamma(L)}\sum_{k=K}^{\infty}\frac{\left(\frac{L}{2}\right)_k\Gamma(L+k+\frac{1}{2})}{k!(L+k)\,(L)_k}\left(\lambda(1-q^2)\right)^k \\ &\times {}_2F_1\left(1,L+k+\frac{1}{2};L+k+1;\lambda\right), \end{aligned} \tag{A.54}$$

where $\lambda \triangleq \frac{1+q^2}{1+q^2+2aq^2\bar{\gamma}}$. The hypergeometric function involved in Equation A.54 can be shown to be monotonically decreasing over all values of k, hence error can be upper bounded as

$$\begin{aligned}\tilde{E}_{K_{ABER}} &\leq \sqrt{\frac{a\bar{\gamma}}{2\pi(1+q^2)}}\frac{q^{L+1}\lambda^{L+\frac{1}{2}}}{\Gamma(L)}{}_2F_1\left(1,L+K+\frac{1}{2};L+K+1;\lambda\right)\sum_{k=K}^{\infty}\frac{\Gamma(L+k+\frac{1}{2})\left(\frac{L}{2}\right)_k}{k!(L+k)\,(L)_k} \\ &\times\left[\lambda(1-q^2)\right]^k. \end{aligned} \tag{A.55}$$

After some algebraic manipulation, the infinite expression given in Equation A.55 can be expressed in terms of generalized hypergeometric function. The final expression for the upper bound on error can be given as

$$\begin{aligned}\tilde{E}_{K_{ABER}} &\leq \sqrt{\frac{a\bar{\gamma}}{2\pi(1+q^2)}}\frac{q^{L+1}\lambda^{L+\frac{1}{2}}\left(\frac{L}{2}\right)_K\Gamma\left(L+K+\frac{1}{2}\right)}{K!(L+K)!} \\ &\times\left[\lambda(1-q^2)\right]^K {}_2F_1\left(1,L+K+\frac{1}{2};L+K+1;\lambda\right) \\ &\times {}_3F_2\left[\begin{matrix}1 & \frac{L}{2}+K & L+K+\frac{1}{2} & \lambda(1-q^2) \\ K+1 & L+K+1 & & \end{matrix}\right]. \end{aligned} \tag{A.56}$$

A.10.4 Equation 3.78

Since the expression of output SNR contains infinite series we have obtained an expression for upper bound on truncation error considering a finite K terms in the evaluation of infinite series present in Equation 3.78. After some algebraic manipulation the expression due to the truncation of infinite series can be written as

$$E_K = \frac{\zeta_1^2(1-\rho^2)}{q^2}\sum_{k_1=K}^{\infty}\sum_{k_2=K}^{\infty}\sum_{k_3=K}^{\infty}\sum_{k_4=K}^{\infty}\frac{\rho^{2\lambda_{12}}\zeta_1^{\lambda_{12}+\lambda_{14}}B\left(k_1+k_3+\frac{1}{2},k_2+\frac{1}{2}\right)}{\left\{\prod_{i=1}^{4}k_i!\right\}\Gamma^2(1/2)\Gamma^2(k_2+1/2)}$$
$$\times B\left(k_1+k_4+\frac{1}{2},k_2+\frac{1}{2}\right)\gamma_{sc}^{\lambda_{12}+\lambda_{14}+1}e^{-\frac{2\zeta_1}{q^2}\gamma_{sc}}\left(\frac{1-q^2}{q^2}\right)^{\lambda_{34}}\left\{\frac{{}_1F_1\left(1;\lambda_{12}+k_4+2;\frac{\zeta_1}{q^2}\gamma_{sc}\right)}{\lambda_{12}+k_4+1}\right.$$
$$\left.+\frac{{}_1F_1\left(1;\lambda_{13}+2;\frac{\zeta_1}{q^2}\gamma_{sc}\right)}{\lambda_{13}+1}\right\}. \tag{A.57}$$

Modifying above expression using [5, 13.1.27] we can write

$$E_K = \frac{\zeta_1^2(1-\rho^2)}{q^2}\sum_{k_1=K}^{\infty}\sum_{k_2=K}^{\infty}\sum_{k_3=K}^{\infty}\sum_{k_4=K}^{\infty}\frac{\rho^{2\lambda_{12}}\zeta_1^{\lambda_{12}+\lambda_{14}}B\left(k_1+k_3+\frac{1}{2},k_2+\frac{1}{2}\right)}{\left\{\prod_{i=1}^{4}k_i!\right\}\Gamma^2(1/2)\Gamma^2(k_2+1/2)}$$
$$\times B\left(k_1+k_4+\frac{1}{2},k_2+\frac{1}{2}\right)\gamma_{sc}^{\lambda_{12}+\lambda_{14}+1}e^{-\frac{\zeta_1}{q^2}\gamma_{sc}}\left(\frac{1-q^2}{q^2}\right)^{\lambda_{34}}$$
$$\times\left\{\frac{{}_1F_1\left(\lambda_{12}+k_4+1;\lambda_{12}+k_4+2;-\frac{\zeta_1}{q^2}\gamma_{sc}\right)}{\lambda_{12}+k_4+1}+\frac{{}_1F_1\left(\lambda_{13}+1;\lambda_{13}+2;-\frac{\zeta_1}{q^2}\gamma_{sc}\right)}{\lambda_{13}+1}\right\} \tag{A.58}$$

The term

$$B\left(k_1+k_3+\tfrac{1}{2},k_2+\tfrac{1}{2}\right),\quad B\left(k_1+k_4+\tfrac{1}{2},k_2+\tfrac{1}{2}\right)\quad and$$
$$\left\{\frac{{}_1F_1\left(\lambda_{12}+k_4+1;\lambda_{12}+k_4+2;-\frac{\zeta_1}{q^2}\gamma_{sc}\right)}{\lambda_{12}+k_4+1}+\frac{{}_1F_1\left(\lambda_{13}+1;\lambda_{13}+2;-\frac{\zeta_1}{q^2}\gamma_{sc}\right)}{\lambda_{13}+1}\right\}$$

are monotonically decreasing with positive values of k_i ($i=1,2,3,4$). Hence an upper bound on truncation error can be written as

$$E \leq \frac{\zeta_1^2(1-\rho^2)\gamma_{sc}}{q^2\Gamma^2(1/2)}\left\{\frac{{}_1F_1\left(3K+;3K+2;-\frac{\zeta_1}{q^2}\gamma_{sc}\right)}{3K+1}+\frac{{}_1F_1\left(3K+1;3K+2;-\frac{\zeta_1}{q^2}\gamma_{sc}\right)}{3K+1}\right\}$$
$$\times B\left(2K+\tfrac{1}{2},K+\tfrac{1}{2}\right)B\left(2K+\tfrac{1}{2},K+\tfrac{1}{2}\right)e^{-\frac{\zeta_1}{q^2}\gamma_{sc}}\sum_{k_1=K}^{\infty}\frac{(\rho\zeta_1\gamma_{sc})^{2k_1}}{k_1!}\sum_{k_2=K}^{\infty}\frac{(\rho\zeta_1\gamma_{sc})^{2k_2}}{k_2!\Gamma^2(k_2+1/2)}$$
$$\times\sum_{k_3=K}^{\infty}\frac{1}{k_3!}\left(\frac{1-q^2}{q^2}\zeta_1\gamma_{sc}\right)^{k_3}\sum_{k_4=K}^{\infty}\frac{1}{k_4!}\left(\frac{1-q^2}{q^2}\zeta_1\gamma_{sc}\right)^{k_4}. \tag{A.59}$$

Finally arranging the series in terms of hypergeometric function an expression of upper bound on truncation error can be given as

$$\begin{aligned} E &\leq \frac{2\zeta_1^2(1-\rho^2)B^2\left(2K+\frac{1}{2},K+\frac{1}{2}\right)(\rho\zeta_1\gamma_{sc})^{4K}{}_1F_1\left(3K+1;3K+2;-\frac{\zeta_1}{q^2}\gamma_{sc}\right)}{(K!)^4\Gamma^2(K+1/2)q^2\Gamma^2(1/2)(3K+1)}\gamma_{sc}e^{-\frac{\zeta_1}{q^2}\gamma_{sc}} \\ &\times\left(\frac{(1-q^2)\zeta_1\gamma_{sc}}{q^2}\right)^{2K}{}_1F_1\left[\begin{matrix}1 & (\rho\zeta_1\gamma_{sc})^2 \\ K+1 & \end{matrix}\right]{}_1F_1\left[\begin{matrix}1 & \frac{1-q^2}{q^2}\zeta_1\gamma_{sc} \\ K+1 & \end{matrix}\right]^2 \\ &\times{}_1F_3\left[\begin{matrix}1 & & & (\rho\zeta_1\gamma_{sc})^2 \\ K+1 & K+.5 & K+.5 & \end{matrix}\right]. \end{aligned} \tag{A.60}$$

A.10.5 Equation 3.113

Expressing the incomplete gamma function in terms of confluent hypergeometric function (using [5, (6.5.12)]), Equation 3.113 can be rewritten as

$$P_{\text{out}}(\gamma_{th}) = \frac{q^{2L\tau}}{\Gamma(2L\tau)}\sum_{t=0}^{\infty}\frac{(L\tau)_t(1-q^2)^t(\varsigma\gamma_{th})^{2L\tau+t}e^{-\varsigma\gamma_{th}}}{t!(2L\tau)_t(2L\tau+t)}{}_1F_1(1;1+2L\tau+t;\varsigma\gamma_{th}). \tag{A.61}$$

Considering K number of terms in the evaluation of infinite series, the error can be expressed as

$$E_{K_{out}} = \frac{(q\varsigma\gamma_{th})^{2L\tau}e^{-\varsigma\gamma_{th}}}{\Gamma(2L\tau)}\sum_{t=K}^{\infty}\frac{(L\tau)_t(\varsigma\gamma_{th}(1-q^2))^t}{t!(2L\tau)_t(2L\tau+t)}{}_1F_1(1;2L\tau+t+1;\varsigma\gamma_{th}). \tag{A.62}$$

Using [5, 13.1.27] an expression for the upper bound on truncation error can be written as

$$E_{K_{out}} = \frac{(q\varsigma\gamma_{th})^{2L\tau}}{\Gamma(2L\tau)}\sum_{t=K}^{\infty}\frac{(L\tau)_t(\varsigma\gamma_{th}(1-q^2))^t}{t!(2L\tau)_t(2L\tau+t)}{}_1F_1(2L\tau+t;2L\tau+t+1;-\varsigma\gamma_{th}). \tag{A.63}$$

The hypergeometric function involved in Equation A.62 can be shown to be monotonically decreasing over all positive values of $(2L\tau+t)$. Thus, Equation A.62 can be upper bounded as

$$\begin{aligned} E_{K_{out}} &\leq \frac{q^{2L\tau}(\varsigma\gamma_{th})^{2L\tau+K}(1-q^2)^K(L\tau)_K}{K!(2L\tau+K)\Gamma(2L\tau)(2L\tau)_K}{}_1F_1(2L\tau+K;1+2L\tau+K;-\varsigma\gamma_{th}) \\ &\times\sum_{t=K}^{\infty}\frac{(L\tau)_t\left[\varsigma\gamma_{th}(1-q^2)\right]^t}{t!(2L\tau+t)(2L\tau)_t}. \end{aligned} \tag{A.64}$$

After some algebraic manipulation the above expression can be shown to be

$$E_{K_{out}} \leq \frac{q^{2L\tau}(\varsigma\gamma_{th})^{2L\tau+K}(1-q^2)^K (L\tau)_K}{K!(2L\tau+K)\Gamma(2L\tau)(2L\tau)_K} {}_1F_1(2L\tau+K;1+2L\tau+K;-\varsigma\gamma_{th}) \times {}_2F_2\left[\begin{array}{ccc} 1 & L\tau+K & \varsigma\gamma_{th}(1-q^2) \\ K+1 & 2L\tau+K+1 & \end{array}\right]. \quad (A.65)$$

A.10.6 Equation 3.118

From Equation 3.118, the truncation error of ASER can be written as

$$E_{K_{ASER}} = \frac{a}{2}\sqrt{\frac{b}{\pi(b+\varsigma)}}\left[\frac{q\varsigma}{a+\varsigma}\right]^{2L\tau}\sum_{t=K}^{\infty}\frac{(L\tau)_t(2L\tau+t)_{\frac{1}{2}}}{t!(2L\tau+t)}\left[\frac{\varsigma(1-q^2)}{b+\varsigma}\right]^t \times {}_2F_1\left(1,2L\tau+t+\frac{1}{2};2L\tau+t+1;\frac{\varsigma}{b+\varsigma}\right). \quad (A.66)$$

The hypergeometric function involved in Equation 3.118 can be shown to be monotonically decreasing, hence the error can be upper bounded as

$$E_{K_{ASER}} \leq \frac{a}{2K!(2L\tau+K)}\sqrt{\frac{b}{\pi(b+\varsigma)}}\left[\frac{q}{a+\varsigma}\right]^{2L\tau}{}_2F_1\left(1,2L\tau+K+\frac{1}{2};2L\tau+K+1;\frac{\varsigma}{b+\varsigma}\right) \times \varsigma^{2L\tau+K}(L\tau)_K(2L\tau+K)_{\frac{1}{2}}\left[\frac{1-q^2}{b+\varsigma}\right]^K\sum_{t=K}^{\infty}\frac{(L\tau)_t(2L\tau+t)_{\frac{1}{2}}}{t!(2L\tau+t)}\left[\frac{\varsigma(1-q^2)}{b+\varsigma}\right]^t. \quad (A.67)$$

After some algebraic manipulation the above expression can be shown to be

$$E_{K_{ASER}} \leq \frac{a}{2K!\phi!}\sqrt{\frac{b}{\pi}}\left[\frac{q}{a+\varsigma}\right]^{2L\tau}\frac{(L\tau)_K\Gamma\left(\phi+\frac{1}{2}\right)\varsigma^{2L\tau+K}\left(1-q^2\right)^K}{(b+\varsigma)^{K+\frac{1}{2}}}{}_2F_1\left(1,\phi+\frac{1}{2};\phi+1;\frac{\varsigma}{b+\varsigma}\right) \times {}_3F_2\left[\begin{array}{cccc} 1 & \phi+\frac{1}{2} & L\tau+K & \frac{\varsigma(1-q^2)}{b+\varsigma} \\ K+1 & \phi+1 & & \end{array}\right], \quad (A.68)$$

where $\phi \triangleq 2L\tau+K$.

A.10.7 Equation 4.28

The mathematical expressions obtained for the PDF of output SNR γ_{mrc} Equation 4.28 is in the form of an infinite series. An expression for upper bound of error on for the PDF of output SNR considering a finite number (K) of terms in the infinite series, following an approach in [55] can be given as

$$E_K = \left[\frac{(1-\rho)}{(1+(L-1)\rho)}\right]^{2\mu}\left[\frac{\mu(1+\eta)}{\bar{\gamma}(1-\rho)\sqrt{\eta}}\right]^{2L\mu}\sum_{t_1=K}^{\infty}\sum_{t_2=K}^{\infty}\frac{(\mu)_{t_1}(\mu)_{t_2}\gamma_{mrc}^{2L\mu+t_1+t_2-1}e^{-\frac{\mu(1+\eta)}{\bar{\gamma}(1-\rho)}\gamma_{mrc}}}{t_1!t_2!\eta^{t_1}\Gamma(2L\mu+t_1+t_2)} \times\left[\frac{L\rho\mu(1+\eta)}{\bar{\gamma}(1-\rho)(1+(L-1)\rho)}\right]^{t_1+t_2}{}_1F_1\left(L\mu+t_1;2L\mu+t_1+t_2;\frac{\mu(\eta^2-1)}{\eta(1-\rho)\bar{\gamma}}\gamma_{mrc}\right). \quad (A.69)$$

After some algebraic manipulation the expression can also be written as

$$E_K = \left[\frac{(1-\rho)}{(1+(L-1)\rho)}\right]^{2\mu}\left[\frac{\mu(1+\eta)}{\bar{\gamma}(1-\rho)\sqrt{\eta}}\right]^{2L\mu}\frac{\gamma_{mrc}^{2L\mu-1}e^{-\frac{\mu(1+\eta)}{\bar{\gamma}(1-\rho)}\gamma_{mrc}}}{\Gamma^2(\mu)}\sum_{t_1=K}^{\infty}\sum_{t_2=K}^{\infty} \times\frac{\Gamma(\mu+t_1)\Gamma(\mu+t_2)B(L\mu+t_1,L\mu+t_2)}{t_1!t_2!\Gamma(L\mu+t_1)\Gamma(L\mu+t_2)\eta^{t_1}}\left[\frac{L\rho\mu(1+\eta)\gamma_{mrc}}{\bar{\gamma}(1-\rho)(1+(L-1)\rho)}\right]^{t_1+t_2} \times{}_1F_1\left(L\mu+t_1;2L\mu+t_1+t_2;\frac{\mu(\eta^2-1)}{\eta(1-\rho)\bar{\gamma}}\gamma_{mrc}\right). \quad (A.70)$$

Even for moderate average input SNR it can be shown that $\frac{\mu(\eta^2-1)}{\eta(1-\rho)\bar{\gamma}}\gamma_{mrc} \leq 1$ for which it can be shown that the value of confluent hypergeometric function monotonically decreasing over all positive values of t_1 and t_2, hence an expression for upper bound on truncation can be written as

$$E_K \leq \left[\frac{(1-\rho)}{(1+(L-1)\rho)}\right]^{2\mu}\left[\frac{\mu(1+\eta)}{\bar{\gamma}(1-\rho)\sqrt{\eta}}\right]^{2L\mu}\frac{\gamma_{mrc}^{2L\mu-1}e^{-\frac{\mu(1+\eta)}{\bar{\gamma}(1-\rho)}\gamma_{mrc}}B(L\mu+K,L\mu+K)}{\Gamma^2(\mu)} {}_1F_1\left(L\mu+K;2L\mu+2K;\frac{\mu(\eta^2-1)}{\eta(1-\rho)\bar{\gamma}}\gamma_{mrc}\right)\sum_{t_1=K}^{\infty}\frac{\Gamma(\mu+t_1)}{t_1!\Gamma(L\mu+t_1)}\left[\frac{L\rho\mu(1+\eta)\gamma_{mrc}}{\eta\bar{\gamma}(1-\rho)(1+(L-1)\rho)}\right]^{t_1} \times\sum_{t_2=K}^{\infty}\frac{\Gamma(\mu+t_2)}{t_2!\Gamma(L\mu+t_2)}\left[\frac{L\rho\mu(1+\eta)\gamma_{mrc}}{\bar{\gamma}(1-\rho)(1+(L-1)\rho)}\right]^{t_2}. \quad (A.71)$$

Writing the series in terms of hypergeometric functions an expression of truncation on upper bound can be given as

$$\begin{aligned} E_K \quad &\leq \quad \frac{\Gamma^2(\mu+K)\gamma_{mrc}^{2L\mu-1} e^{-\frac{\mu(1+\eta)}{\bar{\gamma}(1-\rho)}\gamma_{mrc}} \Im^{2\delta}(1-\rho)^{2\mu}}{\Gamma(2\delta)(L\rho\gamma_{mrc})^{-2K} K!^2 \Gamma^2(\mu)\eta^{\delta}} {}_1F_1\left(\delta; 2\delta; \frac{\mu(\eta^2-1)}{\eta(1-\rho)\bar{\gamma}}\gamma_{mrc}\right) \\ &\times {}_2F_2\left[\begin{array}{ccc} 1 & \mu+K & \frac{L\rho\gamma_{mrc}\Im}{\eta} \\ K+1 & \delta & \end{array}\right] {}_2F_2\left[\begin{array}{ccc} 1 & \mu+K & L\rho\gamma_{mrc}\Im \\ K+1 & \delta & \end{array}\right], \end{aligned} \tag{A.72}$$

where $\delta \triangleq L\mu+K$ and $\Im \triangleq \frac{\mu(1+\eta)}{\bar{\gamma}(1-\rho)(1+(L-1)\rho)}$.

Appendix B

List of Formulas

1.

$$g(a,x) = a^{-1}x^a e^{-x}M(1,1+a,x) = a^{-1}x^a M(a,1+a,-x) \tag{B.1}$$

2.

$$\frac{\partial g(a,x)}{\partial x} = -\frac{\partial \Gamma(a,x)}{\partial x} = x^{a-1}e^{-x} \tag{B.2}$$

3.

$$I_v(z) = \left(\frac{z}{2}\right)^v \sum_{k=0}^{\infty} \frac{\left(z^2/2\right)^k}{k!\Gamma(v+k+1)} \tag{B.3}$$

4.

$$M(a,b,z) = e^z M(b-a,b,-z) \tag{B.4}$$

5.

$$(a+x)^n = \sum_{k=0}^{n} \begin{pmatrix} n \\ k \end{pmatrix} x^k a^{n-k} \tag{B.5}$$

6.

$$\int_0^u x^{v-1} e^{-\mu x} dx = \mu^{-v} g(v, \mu u) \qquad [\mathrm{Re}v > 0] \tag{B.6}$$

7.

$$\int_0^u x^{v-1}(u-x)^{\mu-1} e^{\beta x} dx = B(\mu, v) u^{u+v-1} {}_1F_1(v, \mu+v; \beta u) \qquad [\mathrm{Re}\mu > 0, \mathrm{Re}v > 0]. \tag{B.7}$$

8.

$$\begin{aligned}&\int_{-\infty}^{\infty} (\beta+ix)^{-\mu}(\gamma+ix)^{-v} e^{-ipx} dx = 0 \quad for \quad p > 0;\\ &= \frac{2\pi e^{-\gamma p}(-p)^{\mu+v-1}}{\Gamma(\mu+v)} {}_1F_1(\mu; \mu+v; (\beta-\gamma)p) \quad for \quad p < 0;\\ &[\mathrm{Re}\beta > 0, \mathrm{Re}\gamma > 0, \mathrm{Re}(\mu+v) > 1]\end{aligned} \tag{B.8}$$

9.

$$\begin{aligned}&\int_0^{\infty} x^{\mu-1} e^{-\beta x} g(v, \alpha x) dx = \frac{\alpha^v \Gamma(\mu+v)}{v(\alpha+\beta)^{\mu+v}} {}_2F_1\left(1, \mu+v; v+1; \frac{\alpha}{\alpha+\beta}\right)\\ &[\mathrm{Re}(\alpha+\beta) > 0, \mathrm{Re}\beta > 0, \mathrm{Re}(\mu+v) > 0].\end{aligned} \tag{B.9}$$

10.

$$\begin{aligned}&\int_0^{\infty} e^{-st} t^{b-1} {}_1F_1(a, c, kt) dt = \Gamma(b) s^{-b} F(a, b; c; ks^{-1}) \quad [|s| > |k|]\\ &= \Gamma(b)(s-k)^{-b} F\left(c-a, b; c; \frac{k}{k-s}\right) \quad [|s-k| > |k|]\\ &[\mathrm{Re}b > 0, \mathrm{Re}S > \max(0, \mathrm{Re}k)]\end{aligned} \tag{B.10}$$

11.

$${}_pF_q(\alpha_1, \alpha_2, \ldots, \alpha_p; \beta_1, \beta_2, \ldots, \beta_q; z) = \sum_{k=0}^{\infty} \frac{(\alpha_1)_k (\alpha_2)_k \ldots (\alpha_p)_k}{(\beta_1)_k (\beta_2)_k \ldots (\beta_q)_k k!} z^k \tag{B.11}$$

12.

$$ {}_2F_1\left(a,b;b;z\right) = (1-z)^{-a} \tag{B.12} $$

13.

$$ \int_0^\infty x^{s-1}e^{-\beta x}\Gamma(a,x)dx = \frac{\Gamma(s+a)_2F_1\left(1,s+a;s+1;\frac{\beta}{1+\beta}\right)}{s(1+\beta)^{s+a}}, \mathrm{Re}(\beta), \mathrm{Re}(s) > 0 \tag{B.13} $$

14.

$$ Q(\sqrt{2ax}) = \frac{1}{2\sqrt{\pi}}\Gamma\left(\tfrac{1}{2}, ax\right) \tag{B.14} $$

15.

$$ \begin{aligned} &\int_0^\infty x^{v-1}e^{-bx}\prod_{k=1}^{n} {}_1F_1\left(a_k;b_k;c_kx\right)dx \\ &= b^{-v}\Gamma(v)F_A\left(v;a_1,\ldots,a_n;b_1,\ldots,b_n;\frac{c_1}{b},\ldots,\frac{c_n}{b}\right) \\ &\left[b_k > 0, v > 0, \sum c_k < b\right]. \end{aligned} \tag{B.15} $$

16.

$$ F_A\left(\alpha;\beta_1,\ldots,\beta_n;\gamma_1,\ldots,\gamma_n;z_1,\ldots,z_n\right) = \sum_{m_1=0}^{\infty}\sum_{m_2=0}^{\infty}\cdots\sum_{m_n=0}^{\infty}\frac{(\alpha)_{m_1+\ldots+m_n}(\beta)_{m_1}\ldots(\beta)_{m_n}}{(\gamma)_{m_1}\ldots(\gamma)_{m_n}m_1!\ldots m_n!} \times z_1^{m_1}\ldots z_n^{m_n} \tag{B.16} $$

17.

$$ I_v(z) = \frac{z^v}{2^v e^z\Gamma(v+1)} {}_1F_1\left(v+\tfrac{1}{2};2v+1;2z\right) \tag{B.17} $$

18.

$$ p(x) = \frac{1}{c}x^{k\lambda-1}\exp\left[\frac{-kx}{\theta(1-\rho)}\right] {}_1F_1\left(\lambda, k\lambda, \frac{\rho k^2 x}{\theta(1-\rho)(1-\rho+\rho k)}\right), \tag{B.18} $$

where, $c = (\theta/k)^{\lambda k}(1-\rho)^{\lambda(k-1)}(1-\rho+\rho k)^{\lambda}\Gamma(\lambda k)$

Bibliography

[1] V. A. Aalo. Performance of maximal-ratio diversity systems in a correlated Nakagami-fading environment. *IEEE Trans. Commun.*, 43(8):2360–2369, Aug. 1995.

[2] M. K. Simon and M.'-S'. Alouini. *Digital Communication over Fading Channels*. John Wiley & Sons, Inc., 2005.

[3] A. Annamalai, C. Tellambura, and V.K. Bhargava. Equal-gain diversity receiver performance in wireless channels. *IEEE Trans. Commun.*, 48(10):1732–1745, Oct. 2000.

[4] I. S. Gradshteyn and I. M. Ryzhik. *Table of Integrals, Series, and Products*. New York: Academic, 6 edition, 2000.

[5] M. Abramowitrz and I. A. Stegun. *Handbook of Mathematical Funcitons With Formulas, Graphs, and Mathematical tables*. New York: Dover, 9 edition, 1972.

[6] G. L. Stuber. *Principles of Mobile Communications*. Norwell MA: Kluwer Academic Publishers, 1996.

[7] D. Brennan. Linear diversity combining techniques. *Proc. IRE*, 47:1075–1102, Jun. 1959.

[8] John G. Proakis. *Digital Communications*. McGraw Hill, 2004.

[9] John G. Proakis and M. Salehi. *Fundamentals of Communication Systems*. Pearson education, 2005.

[10] T. S. Rappaport. *Wireless Communications Principles and Practice*. Prentice Hall, Inc., 2002.

[11] R. S. Hoyt. Probability functions for the modulus and angle of the normal complex variate. *Bell. Syst. Tech. J*, 26:318–359, 1947.

[12] N. Youssef, C. X. Wang, and M. Patzold. A study on second order statistics of Nakagami-Hoyt mobile fading channels. *IEEE Trans. Veh. Technol.*, 54(4):1159–1265, Jul. 2005.

[13] G. Fraidenraich, O. Lévêque, and J.M. Cioffi. On the MIMO channel capacity for the dual and asymptotic cases over Hoyt channels. *IEEE Commun. Lett.*, 11(1):31–33, Jan. 2007.

[14] M.D. Yacoub. The $\kappa-\mu$ distribution and the $\eta-\mu$ distribution. *Antennas and Propagation Magazine, IEEE*, 49(1):68–81, Feb. 2007.

[15] M.D. Yacoub. The $\eta-\mu$ distribution: a general fading distribution. In *IEEE VTS-Fall VTC 2000. 52nd*, volume 2, pages 872–877, 2000.

[16] M.D. Yacoub. The $\kappa-\mu$ distribution: a general fading distribution. In *Vehicular Technology Conference, 2001. VTC 2001 Fall. IEEE VTS 54th*, volume 3, pages 1427–1431, 2001.

[17] A. Baid, H. Fadnavis, and P. R. Sahu. Performance of a predetection EGC receiver in Hoyt fading channels for arbitrary number of branches. *IEEE Commun. Lett.*, 12(9):627–629, Sep. 2008.

[18] R.M. Radaydeh and M.M. Matalgah. Average BER analysis for M -ary FSK signals in Nakagami-*q* (Hoyt) fading with noncoherent diversity combining. *IEEE Trans. Veh. Technol.*, 57(4):2257–2267, Jul. 2008.

[19] R. M. Radaydeh. Average error performance of M-ary modulation schemes in Nakagami-*q* (Hoyt) fading channels. *IEEE Commun. Lett.*, 11(3):255–257, Mar. 2007.

[20] I. Korn and J. P. Fonseka. M-CPM with MRC diversity in Rician-, Hoyt-, and Nakagami-fading channels. *IEEE Trans. Veh. Technol.*, 50:1182–1189, Jul. 2001.

[21] T. Q. Duong, H. Shin, and E. K. Hong. Error probability of binary and M-ary signals with spatial diversity in Nakagami-q (Hoyt) fading channels. *Eurasip Journal on Wireless Commun. and Networking*, 4:1–8, Oct. 2007.

[22] J. Cheng and T. Berger. Capacity of Nakagami-q (Hoyt) fading channels with channel side information. In *Communication Technology Proceedings, 2003. ICCT 2003. International Conference on*, volume 2, pages 1915–1918, Apr. 2003.

[23] S. Khatalin and J. P. Fonseka. On the channel capacity in Rician and Hoyt fading environments with MRC diversity. *IEEE Trans. Veh. Technol.*, 55:137–141, Jan. 2006.

[24] G. A. Ropokis, A. A. Rontogiannis, and P. T. Mathiopoulos. Performance analysis of orthogonal space time block coding over Hoyt fading channels. In *Proc. Globecom 2007*, pages 3416 – 3420, Nov. 2007.

[25] G. A. Ropokis, A. A. Rontogiannis, and P. T. Mathiopoulos. Quadratic forms in normal RVs: theory and applications to OSTBC over Hoyt fading channels. *IEEE Trans. Wireless Commun.*, pages 5009–5019, Dec. 2008.

[26] X. Feng, Y. Dian-Wu, and Q. F. Zhou. Performance analysis of orthogonal space-time block codes over Nakagami-q (Hoyt) fading channels. In *IEEE ICC 2008*, pages 3966–3970, May. 2008.

[27] Young-Chai Ko, M.-S. Alouini, and M.K. Simon. Average SNR of dual selection combining over correlated Nakagami-m fading channels. *IEEE Commun. Lett.*, 4(1):12–14, Jan. 2000.

[28] N.C. Sagias, G.K. Karagiannidis, D.A. Zogas, P.T. Mathiopoulos, and G.S. Tombras. Performance analysis of dual selection diversity in correlated Weibull fading channels. *IEEE Trans. Commun.*, 52(7):1063–1067, Jul. 2004.

[29] Y. Chen and C. Tellambura. Distribution functions of selection combiner output in equally correlated Rayleigh, Rician, and Nakagami-*m* fading channels. *IEEE Trans. Commun.*, 52(11):1948–1956, Nov. 2004.

[30] Yunxia Chen and C. Tellambura. Performance analysis of three-branch selection combining over arbitrarily correlated Rayleigh-fading channels. *IEEE Trans. Wireless Commun.*, 4(3):861–865, May. 2005.

[31] J. Reig, L. Rubio, and V. M. Rodrigo Pe narrocha. Performance of dual selection combiners over correlated Nakagami-*m* fading with different fading parameters. *IEEE Trans. Commun.*, 54(9):1527–1532, Sep. 2006.

[32] G. Fraidenraich, J.C.S. Santos Filho, and M.D. Yacoub. Second-order statistics of maximal-ratio and equal-gain combining in Hoyt fading. *IEEE Commun. Lett.*, 9(1):19–21, Jan. 2005.

[33] N. Youssef, W. Elbahri, M. Patzold, and S. Elasmi. On the crossing statistics of phase processes and random FM noise in Nakagami-*q* mobile fading channels. *IEEE Trans. Wireless Commun.*, 4(1):24 – 29, Jan. 2005.

[34] G. Fraidenraich, M.D. Yacoub, J.R. Mendes, and J.C.S.S. Filho. Second-order statistics for diversity-combining of non-identical correlated Hoyt signals. *IEEE Trans. Commun.*, 56(2):183–185, Feb. 2008.

[35] R. de Souza and M.D. Yacoub. Bivariate Nakagami-*q* (Hoyt) distribution. In *Communications, 2009. ICC ’09. IEEE International Conference on*, pages 1–5, Jun. 2009.

[36] R.A.A. de Souza and M.D. Yacoub. Maximal-ratio and equal-gain combining in Hoyt (Nakagami-q) fading. In *Vehicular Technology Conference, 2009. VTC Spring 2009. IEEE 69th*, pages 1–5, Apr. 2009.

[37] M. S. Alouini, Ali Abdi, and Mostafa Kaveh. Sum of gamma variates and performance of wireless communication systems over Nakagami fading channels. *IEEE Trans. Veh. Technol.*, 50(6):1471–1480, Nov. 2001.

[38] Kasun T. Hemachandra and Norman C. Beaulieu. Simple expressions for the SER of dual MRC in correlated Nakagami-q (Hoyt) fading. *IEEE Commun. Lett.*, 14(8):743–745, Aug. 2010.

[39] M. Milisic, M. Hamza, and M. Hadzialic. Outage and symbol error probability performance of L-branch maximal-ratio combiner for generalized $\kappa-\mu$ fading. In *50th International Symposium ELMAR, Zadar, Croatia*, pages 10–12, Sep. 2008.

[40] M. Milisic, M. Hamza, N. Behlilovic, and M. Hadzialic. Symbol error probability performance of L-branch maximal-ratio combiner for generalized $\eta-\mu$ fading. In *IEEE VTC Conf. 2009*, pages 1–5, Apr. 2009.

[41] K. Peppas, F. Lazarakis, A. Alexandridis, and K. Dangakis. Error performance of digital modulation schemes with MRC diversity reception over $\eta-\mu$ fading channels. *IEEE Trans. Wireless Commun.*, 8(10):4974 –4980, Oct. 2009.

[42] D.B. da Costa, M.D. Yacoub, and G. Fraidenraich. Second-order statistics for the envelope and phase of $\eta-\mu$ generalized fading channels. In *Telecommunications Symposium, 2006 International*, pages 923–928, Sep. 2006.

[43] D.B. da Costa and M.D. Yacoub. On the second order statistics of $\eta-\mu$ fading channels in diversity systems. In *Microwave and Optoelectronics Conference, 2007. IMOC 2007. SBMO/IEEE MTT-S International*, pages 799–803, Nov. 2007.

[44] D.B. da Costa, J.C. Silveira Santos Filho, M.D. Yacoub, and G. Fraidenraich. Second-order statistics of $\eta-\mu$ fading channels: theory and applications. *IEEE Trans. Wireless Commun.*, 7(3):819–824, Mar. 2008.

[45] D. B. da Costa and M. D. Yacoub. Accurate closed-form approximations to the sum of generalized random variables and applications in the performance analysis of diversity systems. *IEEE Trans. Commun.*, 57(5):1271–1274, may. 2009.

[46] N.Y. Ermolova. Useful integrals for performance evaluation of communication systems in generalised $\eta-\mu$ and $\kappa-\mu$ fading channels. *IET Commun.*, 3(2):303 –308, Feb. 2009.

[47] N. Ermolova. Moment generating functions of the generalized $\eta-\mu$ and $\kappa-\mu$ distributions and their applications to performance evaluations of communication systems. *IEEE Commun. Lett.*, 12(7):502 –504, Jul. 2008.

[48] David Morales-Jiménez and José F.Paris. Outage probability analysis for $\eta-\mu$ fading channels. *IEEE Commun. Lett.*, 14(6):521–523, Jun. 2010.

[49] Q.T. Zhang. Probability of error for equal gain combining over rayleigh channels: some closed-form solutions,.

[50] G. C. Alexandropoulos, N. C. Sagias, F. I. Lazarakis, and K. Berberidis. New results for the multivariate Nakagami-*m* fading model with arbitrary correlation matrix and applications. *IEEE Trans. Wireless Commun.*, 8(1):245–255, Jan. 2009.

[51] G.K. Karagiannidis, D.A. Zogas, and S.A. Kotsopoulos. On the multivariate Nakagami-*m* distribution with exponential correlation. *IEEE Trans. Commun.*, 51(8):1240–1244, Aug. 2003.

[52] R. Sannegowda and V. Aalo. Performance of selection diversity systems in a Nakagami fading environment. In *Southeastcon '94. 'Creative Technology Transfer - A Global Affair'., Proceedings of the 1994 IEEE*, pages 190–195, Apr. 1994.

[53] M.K. Simon and M. Alouini. A unified approach to the performance analysis of digital communication over generalized fading channels. *Proceedings of the IEEE*, 86(9):1860–1877, Sep. 1998.

[54] http://functions.wolfram.com/03.02.26.0003.01.

[55] C.C. Tan and N.C. Beaulieu. Infinite series representations of the bivariate Rayleigh and Nakagami-*m* distributions. *IEEE Trans. Commun.*, 45(10):1159–1161, Oct. 1997.

[56] M. Zeribi, N. Youssef, and F. Choubani. Fading correlation and its effect on the second order statistics of MRC diversity for Hoyt mobile radio channels. In *Electronics, Circuits and Systems, 2005. ICECS 2005. 12th IEEE International Conference on*, pages 1 –4, 11-14 2005.

[57] J.R. Mendes, M.D. Yacoub, and G. Fraidenraich. Closed-form generalized power correlation coefficient of the Hoyt fading signal. *IEEE Commun. Lett.*, 10(2):94 –96, Feb. 2006.

[58] P. Patel, P.R. Sahu, and A.K. Chaturvedi. ABER of dual predetection EGC in correlated Nakagami-*m* fading channels with arbitrary *m*. *IEEE Commun. Lett.*, 12(7):487–489, Jul. 2008.

[59] A. Papoulis and U. Pillai. *Probability, Random Variables and Stochastic Processes*. McGraw-Hill: New York, 4 edition, 2002.

[60] Gifford, W. M., Win, M. Z., and Chiani M. Jul. Diversity with practical channel estimation. *IEEE Trans. Wireless Commun.*, 4(4):1935–1947, Apr. 2005.

[61] http://functions.wolfram.com/01.03.06.0002.01.

[62] G. K. Karagiannidis, D. A. Zogas, and S. A. Kotsopoulos. BER performance of dual predetection EGC in correlative Nakagami-*m* fading. *IEEE Trans. Commun.*, 52(1):51–54, Jan. 2004.

[63] R. Subadar and P.R. Sahu. Performance analysis of dual MRC receiver in correlated Hoyt fading channels. *IEEE Commun. Lett.*, 13(6):405–407, Jun. 2009.

[64] John Gurland. Distribution of the maximum of the arithmetic mean of correlated random variables. *Annals of Math. Statistics*, 26(2):294–300, 1955.

[65] Samuel Kotz and John W. Adams. Distribution of sum of identically distributed exponentially correlated gamma variables. *Annals of Math. Statistics*, 35(1):277–283, 1964.

[66] L. E. Blumenson and K. S. Miller. Properties of generalized Rayleigh distributions. *Ann. Math. Statist.*, 34:903–910, 1963.

[67] J.R. Mendes and M.D. Yacoub. Power correlation coefficient of a general fading model. pages 497 – 502, Jul. 2005.

List of Publications

Journal Publications

1. Subadar, R. and Sahu P. R., "Performance of dual MRC receiver in correlated Hoyt fading channels," *IEEE Commun. Lett.* vol. 13, no. 6, pp. 405-407, June 2009.

2. Reddy, T., Subadar R. and Sahu, P. R., "Outage probability of SC receiver over exponentially correlated *K* fading channels," *IEEE Commun. Lett.* vol. 14, no. 2, pp. 118-120, Feb 2010.

3. Subadar, R. and Sahu P. R., "Performance of *L*-independent and dual correlated selection combiner in Hoyt fading channels," Accepted for publication in *IEEE Trans. on Commun.*

4. Subadar, R. and Sahu P. R., "Performance of *L*-MRC receiver over equally correlated Hoyt fading channels," Accepted for publication in *IETE Journal of Research.*

5. Subadar, R. and Sahu P. R., "Performance of *L*-MRC receiver over equally correlated $\eta-\mu$ fading channels," Accepted for publication in *IEEE Trans. on Wireless Commun.*

Conference Publications

1. Subadar, R., Dadheech, H. and Sahu, P. R. , "Performance Analysis of Dual MRC Receiver in Correlated Hoyt Fading Channels with Non-Identical Fading Parameters," *India Conference (INDICON)*, Dec. 2009.

2. Subadar, R., Reddy, T. and Sahu, P. R., "Performance of *L*-SC receiver over κ-μ and η-μ fading channels" *IEEE, ICC2010*, Capetown, May. 2010.

3. Subadar, R. and Sahu, P. R., "Performance of L-MRC receiver over independent Hoyt fading channels," *National Conference on Communications (NCC)*, Jan. 2010.

4. Reddy, T., Subadar, R. and Sahu, P. R., "Outage probability of selection combiner over exponentially correlated Weibull-gamma fading channels for arbitrary number of branches," *National Conference on Communications (NCC)*, Jan. 2010.